An optical fibre point temperature sensor for investigation of 3,4-methylenedioxymethamphetamine (MDMA, ‘ecstasy’) induced hyperthermia in the rat brain

Stefan Tyrone Musolino (BHlthSc(Hons))

Discipline of Pharmacology, Department of Medical Sciences, Adelaide Medical School

Faculty of Health and Medical Sciences

The University of Adelaide

A thesis submitted for the degree of Doctor of Philosophy

In the School of Medicine

August 2019

Table of Contents

List of Figures

List of Tables

Thesis Abstract

3,4-methylenedioxymehtamphetamine (MDMA, ‘ecstasy’) is an illegal stimulant drug that can produce life-threatening hyperthermia following consumption in humans. Administration of MDMA also produces similar effects in experimental animals and it can lead to death usually through multi-organ failure, and vasogenic brain oedema. Despite the danger acute MDMA-induced hyperthermia poses, current treatments for these adverse effects in a clinical setting are limited and do not address hyperthermia’s central origins. Due to ethical reasons, the investigation of these MDMA-induced changes in humans are restricted, therefore animal models are relied on to investigate the real-time thermoregulatory effects of MDMA and their underlying pharmacological mechanisms. This being considered, it is important to investigate MDMAs adverse effects in animals and potential pharmacological therapeutics using advantageous techniques in order to effectively relate these findings from animals to humans.

The aim of this thesis was to develop a novel portable optical fibre temperature sensor for the monitoring of brain temperature in awake freely-moving rats, and to use this sensor in conjunction with radiotelemetry to investigate the effects of MDMA on thermoregulation and its related physiological parameters. We also aimed to investigate the brain hyperthermia-attenuating effects of the tetracycline antibiotic drug minocycline, as well as its effects on body temperature, heart rate, and locomotor activity.

The first part of this thesis aimed at optimizing a portable optical fibre temperature sensor based on rare-earth thermometry for long-term temperature measurements *in vivo*. Initial *in vitro* tests revealed measurement instabilities in the original configuration and therefore changes were made to the optical equipment aimed at increasing its long-term stability. The susceptibility of the previous probe to signal bend-loss and breakage during animal movement following

MDMA administration was also reduced through numerous physical changes to the sensor design.

The second study aimed to provide proof-of-concept for this portable optical fibre-tip sensor capable of recording brain temperature in conscious freely-moving rats. This study was successful in demonstrating that accurate and spatially precise brain temperature recordings could be performed by the probe while utilising a portable optical setup. These brain temperature measurements also showed a good correlation with body temperature recorded with radiotelemetry throughout the experiment.

The third study made further improvements to the probe structure which increased probe durability, reusability and ease of use for *in vivo* experiments. These changes significantly increased experimental throughput and reduced time and resource costs associated with probe fabrication. Brain temperature measurements made with this probe showed that MDMA (10 mg/kg) induced a significant hyperthermia in the brains of Sprague-Dawley rats.

The fourth study looked at the effects of MDMA administered at differing ambient temperatures, as well as the hyperthermia attenuating effects of minocycline. Administration of MDMA (10 mg/kg) induced both a significant hypothermia and hyperthermia when administered at normal, and high ambient temperature respectively, and significantly increased heart rate, and locomotor activity irrespective of environmental conditions. Pretreatment with minocycline (50 mg/kg) was able to significantly attenuate MDMA-induced brain and body hyperthermia at high ambient temperature and reduce MDMA-induced increases in heart rate and locomotor activity.

In conclusion, we have developed and validated an optical fibre point temperature sensor based on rare-earth thermometry that accurately records rat brain temperature *in vivo.* We also combined optical fibre brain temperature measurements with body temperature monitoring to

investigate the thermoregulatory, and physiological effects of MDMA and minocycline in freely-moving rats.

Declaration

I certify that this work contains no material which has been accepted for the award of any other degree or diploma in my name, in any university or other tertiary institution and, to the best of my knowledge and belief, contains no material previously published or written by another person, except where due reference has been made in the text. In addition, I certify that no part of this work will, in the future, be used in a submission in my name, for any other degree or diploma in any university or other tertiary institution without the prior approval of the University of Adelaide and where applicable, any partner institution responsible for the joint-award of this degree. I acknowledge that copyright of published works contained within this thesis resides with the copyright holder(s) of those works. I also give permission for the digital version of my thesis to be made available on the web, via the University's digital research repository, the Library Search and also through web search engines, unless permission has been granted by the University to restrict access for a period of time. I acknowledge the support I have received for my research through the provision of an Australian Government Research Training Program Scholarship.

X

Stefan Musolino

Acknowledgements

Supervisors

I would like to sincerely thank my supervisors Dr Abdallah Salem, Professor Mark Hutchinson, and Dr Erik Schartner for allowing me to undertake this project. Their constant encouragement and support have really driven me to complete my PhD. Their guidance and patience with me over these long years is greatly appreciated and I do not think I could have asked for better supervisors. Special thanks to Dr Erik Schartner who helped make the physics aspects of this project "so simple, even a biologist could understand it." So appreciative, really couldn't articulate support that I collected. Amazingly supportive supervisor.

Co-authors

Thanks also to my co-authors: Professor Tanya Monro, Dr Georgios Tsiminis, Professor Rob Mclaughlin, Professor Heike Ebendorff-Heidepriem, Dr Jiawen Li, Mr Bryden Quirk, and Mr Rodney Kirk. Without their efforts I would not have been able to present my findings to the wider scientific community.

Fellow students in Pharmacology

Thank you to my fellow students in pharmacology: Rong Hu, Dylan Marsh, Helena Van-Schalkwyk, Rachael Farrington, Susan Britza, Jacob Thomas, Jake Gordon, Duy Vo, Hellen Victory, and Sukanya Das for all the, coffees, conversations, and other outings that helped to make these last few years of academic struggles bearable and even fun.

Staff Members in Pharmacology

Thanks to all the friendly staff members in pharmacology: Professor Andrew Somogyi, Associate Professor Linda Gowing, Dr Scott Smid, Dr Femke Buisman-Pjilman, Dr Janet

Coller, Dr Ian Musgrave, and Dr Dan Barratt for making the pharmacology department a warm and welcoming place to work.

Family and Friends

I would like to thank my parents Gary and Grace Musolino, my brother Tyrone Musolino for their support throughout my PhD, and for sitting through my oral presentations to settle my pre-conference nerves. I would also like to give a heartfelt thankyou to my partner Georgia Oates and our dog Jaxon (Jack boi, Ratson, Rat boy, Mr. Whiskers, Dog) for their emotional support and understanding throughout my PhD. Their constant positivity and encouragement made it possible for me to continue with my PhD struggle especially through the hard times.

Financial Support

The research presented in this thesis would have been impossible without the financial support from the ARC through the Centre of Excellence for Nanoscale Biophotonics, and the Faculty of Health Sciences Divisional PhD Scholarship. The opportunities to present my work at many national pharmacology conferences were generously supported by the ASCEPT student travel grant.

Abbreviations, prefixes, and symbols

5-HT	5-hydroxytryptamine/serotonin
5-HTT	serotonin transporter
6-OHDA	6-hydroxydopamine
AII	angiotensin II
ACh	acetylcholine
ADH	anti-diuretic hormone
AMPT	α-methyl-p-tyrosine
C_{max}	maximum concentration
CNS	central nervous system
COMT	catechol-*O*-methyltransferase
COX-2	cyclo-oxygenase-2
CSF	cerebrospinal fluid
CT	computed tomography
CYP	cytochrome P450
DA	dopamine
DAMP	dextroamphetamine
DATs	dopamine transporters
EMI	electromagnetic interference
Er^{3+}	erbium ion
FBG	fibre Bragg grating
FIR	fluorescence intensity ratio
HHA	3,4-dihydroxyamphetamine
HHMA	3,4-dihydroxymethamphetamine
HMA	3-methoxy,4-hydroxyamphetamine
HMMA	4-hydroxy-3-methoxymethamphetamine
HR	heart rate
IL-1β	interleukin-1β
IL-1RA	interleukin-1 receptor antagonist
IL-6	interleukin-6

i.p.	intraperitoneal
LMA	locomotor activity
LPS	lipopolysaccharide
MAO	monoamine oxidase
MDA	3,4-methelenedioxyamphetamine
MDEA	3,4-methylenedioxyethamphetamine
MDMA/ecstasy	3,4-methylenedioxymethamphetamine
MM	multimode
mPGES-1	prostaglandin-E synthase
MPTP	1-methyl-4-phenyl-1,2,3,6-tetrahydropyridine
MR	magnetic resonance
MRI	magnetic resonance imaging
NA	noradrenaline
NAT	noradrenaline transporter
NF-κB	nuclear factor kappaB
NIR	near-infrared
PGE_2	prostaglandin-E_2
$PGF_{-2}\alpha$	prostaglandin-F2α
PM	polarisation maintaining
PMA	para-methoxyamphetamine
SART	sustained attention to response test
s.c.	subcutaneous
SD	Sprague-Dawley
SM	single mode
SSRA	selective serotonin releasing agent
SSRI	selective serotonin reuptake inhibitor
TBI	traumatic brain injury
TNF-α	tumor necrosis factor-α
TPH	tryptophan hydroxylase
UHNA	ultra-high numerical aperture

VMAT	vesicular monoamine transporter
WGM	whispering gallery mode techniques
Yb^{3+}	ytterbium ion

Chapter 1 - Research Background

3,4-methylenedioxymethamphetamine (MDMA, 'ecstasy') is an amphetamine derivative drug used worldwide in raves and night clubs. MDMA has the tendency to be viewed as a less harmful substance when compared to alleged 'hard' drugs, such as cocaine and heroin, due to its stimulant, and positive mood enhancing effects, in addition to its perceived lack of acute side effects. However, in some users, MDMA administration can result in fatality. Hyperthermia is the most severe acute consequence of MDMA; however, it is hard to predict when this severe and sometimes fatal adverse effect will occur. Fatal case reports of MDMA users show varied MDMA plasma concentrations following drug administration (Gowing et al., 2002, Caldicott et al., 2003), and animal studies report that there are many contributing behavioural, and environmental factors that can exacerbate the hyperthermic response (Malberg and Seiden, 1998, Brown and Kiyatkin, 2004, Ridge et al., 2019). The hyperthermic response in the brain is the most severe adverse effect of MDMA administration as it can lead to deleterious effects in the brain including neuronal cell damage (Kiyatkin, 2010), disruption of the blood-brain barrier and brain oedema (Kiyatkin et al., 2007, Kiyatkin and Sharma, 2009, Kiyatkin et al., 2014, Kiyatkin et al., 2016), and is likely responsible for the exacerbation of monoamine system neurotoxicity (Broening et al., 1995, Malberg and Seiden, 1998, O'Shea et al., 2005, Li et al., 2019). Despite the potential dangers that MDMA administration poses, emergency room strategies to manage these serious adverse effects are limited. Current emergency techniques to counteract MDMA-induced hyperthermia include simple whole body cooling, fluid replacement, anaesthesia, and muscle relaxants in extreme cases of hyperpyrexia (Hall and Henry, 2006, Grunau et al., 2010). Considering these limited options, there is a pressing need for effective pharmacotherapy to treat MDMA-induced hyperthermia in a clinical setting. In order to investigate the adverse effects of MDMA, as well as the potential

pharmacotherapies for attenuating MDMA-induced hyperthermia, animal models of drug-induced hyperthermia are essential. However, there are some deficiencies apparent in previous animal studies investigating MDMA-induced hyperthermia related to choice of observed parameters and methodological approaches to temperature measurement. Until recently, MDMA's effects on brain temperature remained relatively unexplored compared to its effects in the body, even though it has since been revealed that the most severe and damaging temperature effects of MDMA occur in the brain (Brown and Kiyatkin, 2004, Kiyatkin et al., 2014). In addition to this, many previous studies relied on rectal or ear temperature measurements to record MDMA-induced core temperature change, which have since been shown to lead to stress-induced increases in core temperature (Gordon, 1990, Bae et al., 2007). Even studies measuring brain temperature have utilised thermocouple electrodes to record MDMA-induced brain temperature changes, which while effective, lack the many advantages provided by more modern techniques such as optical fibre-based sensing methods (Lee, 2003). We therefore decided to develop a new method to examine the thermoregulatory and physiological effects of MDMA using an optical fibre brain temperature sensor, and implanted telemetry device in freely-moving rats.

The first aim of this project was to develop and validate an optical fibre-based point brain temperature sensor suitable for *in vivo* use outside of a conventional optics laboratory. Following this successful proof-of-concept, the second main aim was to investigate the thermoregulatory and physiological effects of MDMA, as well as the brain hyperthermia-attenuating effects of the tetracycline-derivative drug minocycline, previously shown to attenuate MDMA-induced increases in core body temperature. The approach involved a sequence of *in vitro* and *in vivo* optical fibre probe trials to optimise the new method, as well as many subsequent sequential improvements before it was reliable for use in MDMA-treated

rats. This sensor along with the implanted telemetry devices were then used to investigate the thermoregulatory, and physiological effects of MDMA and minocycline in the brain and body under differing environmental conditions.

1.1 Historical origins of 3,4-Methylenedioxymethamphetamine (MDMA, "ecstasy")

MDMA was first synthesised by Merck, a German Pharmaceutical company in 1912 (Freudenmann et al., 2006). In the 1950's it was studied by the US army along with other mescaline analogues in five animal models, however, this work was not published until much later (Hardman et al., 1973). The psychoactive properties of the drug in humans were published soon after this (Anderson et al., 1978). MDMA started to be used recreationally throughout the 1970's by small numbers of people, however after its classification as a Schedule 1 drug in 1985 its use increased following its increased publicity (Parrott, 2001). It has since become more popular since the 1980's as a party drug at "rave" or "dance" parties under the name "ecstasy". The name ecstasy often refers to MDMA, a ring substituted amphetamine derivative related to the hallucinogenic compound mescaline (Hardman et al., 1973, Kamien et al., 1986) through chemical structure, and is closely related to methamphetamine, a psychomotor stimulant (Kamien et al., 1986). These compounds contain structural modifications such as methoxy group at various positions on the benzene ring and varying lengths and branching of the side chain leading to differences in their pharmacological activity (Hardman et al., 1973). Although the majority of ecstasy tablets contain MDMA, they can often contain other related chemicals (Fig. 1.1) such as 3,4-methelenedioxyamphetamine (MDA), 3,4-methylenedioxyethamphetamine (MDEA), para-methoxyamphetamine (PMA) as well as other types of drugs like ephedrine, salicylates and painkillers (Cole et al., 2002).

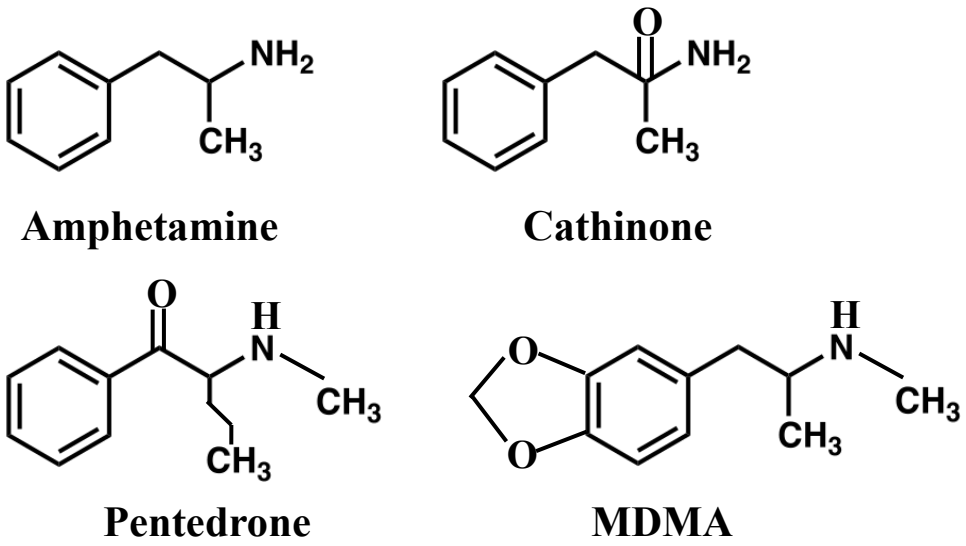

Figure 1.1: Chemical structures of MDMA and related amphetamine derivatives.

1.2 Prevalence of MDMA use

MDMA is a drug commonly used by adolescents and young adults. Published studies report that 6.5% of young adults in high school have reported at least one use of the substance (Johnston et al., 2007), with its increased use in universities and college campuses well documented (Strote et al., 2002). According to Australia's national drug household survey (2016), the most commonly used illegal drugs that were used at least once in the past 12 months were cannabis (10.4%), cocaine (2.5%), ecstasy (2.2%) and meth/amphetamines (1.4%) (Australian Institute of Health and Welfare, 2017). Historically, Oceania has reported high levels of ecstasy use compared to the rest of the world, and more recent reports show that estimated past-year prevalence rates for the drug's use in the region are still among the highest in the world (United Nations, 2018). In 2016, increased use of the drug was reported in New Zealand, whereas Australia saw the past-year use of the drug among the population aged 14 or older fall from 2.5% in 2013, to 2.2% (approximately 400,000) in 2016 (Fig. 1.2) (Australian Institute of Health and Welfare, 2017). However, within this same demographic, 11.2% (2.2 million) reported using ecstasy in their life time, 6.4% had the opportunity to use ecstasy in the

past 12 months, 7.0% of people in their twenties had recently used ecstasy, and the average age of people trying ecstasy for the first time was 21.7 years old (Australian Institute of Health and Welfare, 2017).

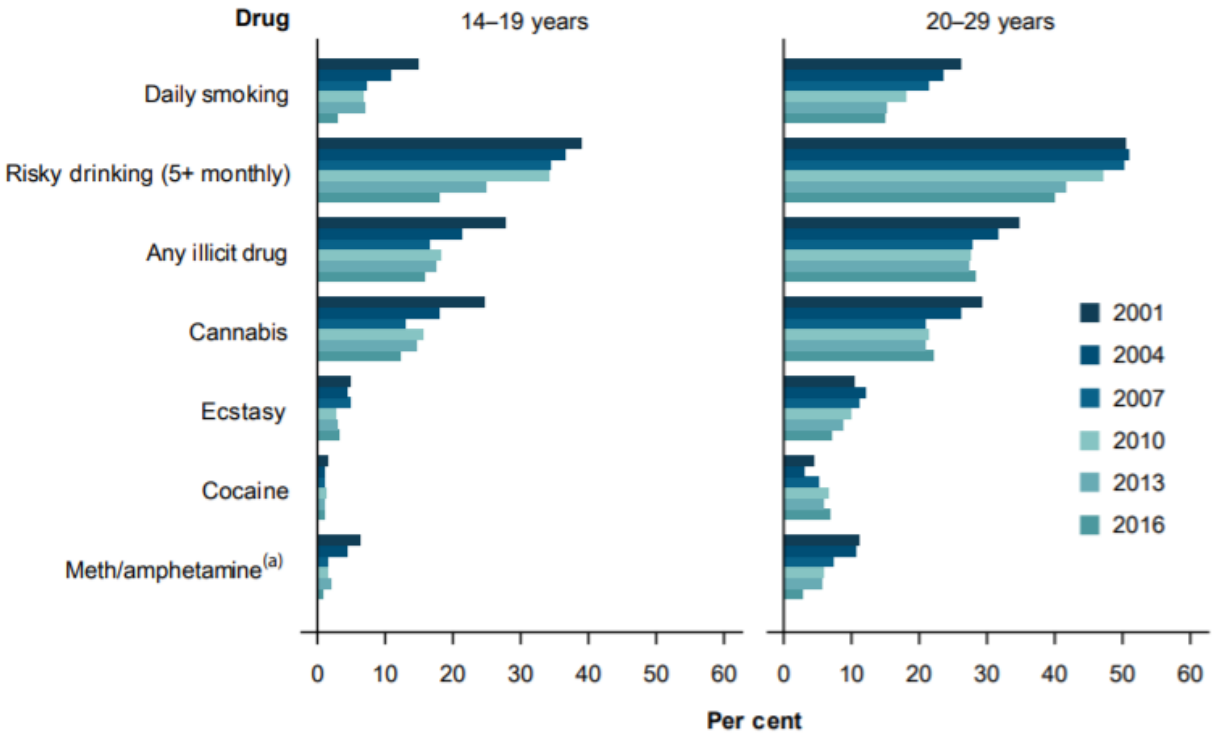

Figure 1.2: Australian drug-taking behaviours, people aged 14-26, 2001-2016 (%). Derived from Australian Institute of Health and Welfare (2017).

1.3 Effects of MDMA in Humans

1.3.1 Desirable effects

The desirable psychological effects of MDMA are responsible for ecstasy use in humans as shown in Table 1. After MDMA administration humans have reported feelings of euphoria, increased sense of closeness with others, reduction of negative thoughts, happiness, increased energy, calmness, relaxation, as well as heightened perception of senses (Green et al., 2003, Baylen and Rosenberg, 2006, Davison and Parrott, 1997). It is used as a recreational drug as it is perceived by its users as relatively safe. It is primarily ingested in pill form and thus is not

associated with the unpleasant aspects of 'hard' intravenous drugs such as heroin. The drug has a low potential for dependence and addiction and is not usually associated with aggressive or violent behaviour, which is commonplace for other recreational drugs (Degenhardt et al., 2010).

Psychological effects on-MDMA	**Percentage of subjects reporting effect**
Happy	100
Exhilarated	100
Warm and Friendly	100
Increased perception of sound	100
Increased perception of touch	95
Increased perception of colour	85
Full of energy	95
Calm and relaxed	80
Talkative	80
Distorted Vision	65
Hallucinations	60
Confused thought	50

Table 1.1: Self-reported psychological effects on-MDMA. Derived from Davison and Parrott (1997).

1.3.2 Acute adverse effects

The recreational use of ecstasy has many adverse side effects. It can cause motor and muscular problems like hyperactivity, muscle ache, tension, and jaw clenching as well as complications such as elevated blood pressure and heart rate (HR), nausea, chills, sweating and hyperthermia (Green et al., 2003, McCann et al., 1996, Davison and Parrott, 1997). Evidence suggests that risk of adverse side effects is low (Byard et al., 1998), however the events are unpredictable and heavily influenced and exacerbated by a wide range of factors that increase the chance of death or morbidity (Gowing et al., 2002, Williamson et al., 1997). Hyperthermia is the major adverse effect of acute MDMA toxicity, which can lead to death due to cardiac arrhythmias, acute renal failure, rhabdomyolysis, brain oedema and disseminated intravascular coagulation (Lyles and Cadet, 2003). Hyperthermia occurs when the body's thermoregulatory mechanisms are overwhelmed by excessive metabolic production of heat, excessive environmental heat, or

impaired heat dissipation (Rusyniak and Sprague, 2005, Simon, 1993). When a change in core body temperature occurs, many autonomic processes are initiated, mostly via signals from the hypothalamus. Autonomic responses to increased body temperature include sweating and cutaneous vasodilation (Rusyniak and Sprague, 2005, Sessler, 1997). In hyperthermic states, the temperature set-point of the hypothalamus is normal, however the peripheral mechanisms are unable to maintain body temperature that matches the set-point (Simon, 1993). This differs from fever as fever occurs when the hypothalamic set-point is increased due to the action of circulating pyrogenic cytokines, causing peripheral mechanisms to conserve and generate heat until body temperatures rise to the new set-point (Dinarello et al., 1988). An ecstasy overdose victim presents with symptoms like those described as "serotonin syndrome" due to an excess of serotonin (5-hydroxytryptamine; 5-HT) in the synapse, which is associated with drugs that affect the 5-HT system (Sun-Edelstein et al., 2008). Symptoms such as hyperactivity, confusion and jaw clenching are considered normal effects of ecstasy, however some users develop the more serious complication of hyperthermia.

1.3.3 Long-term adverse effects

In addition to the acute adverse effects associated with MDMA, there are many long-term problems associated with its continued use. Users report feelings of lethargy, irritability, moodiness, insomnia, paranoia and depression in the days following MDMA use (Davison and Parrott, 1997, Green et al., 2003). It has been suggested that MDMA use could lead to the development of depression due to long-term depletion of 5-HT that has been observed in both humans and animals (Malberg and Seiden, 1998, McCann et al., 1998, Wang et al., 2004). Studies have shown that ecstasy users have reduced serotonin transporter (5HTT) levels, an indicator for loss of 5-HT neurons (McCann et al., 1998, Reneman et al., 2002a, Reneman et al., 2002b). There is also a history of long-term cognitive impairment problems associated with ecstasy use (Parrott and Lasky, 1998, Fox et al., 2001). In a study conducted in individuals with

low exposure to other recreational drugs, MDMA users displayed deficits in mental processing speed and impulsivity compared to non-users (Halpern et al., 2004). Another group found that MDMA users showed higher impulsivity and lower decision making performance compared to cannabis users and non-drug users (Quednow et al., 2007), as well as memory deficits compared to the same control groups (Quednow et al., 2006).

1.4 Mechanisms of action of MDMA

The mechanisms of action of MDMA are currently not fully understood, however it is well known to have a stimulant effect. MDMA acutely increases extracellular concentrations of neurotransmitters such as 5-HT, dopamine (DA), noradrenaline (NA), and acetylcholine (ACh) in the central nervous system (CNS), as well as having direct agonist action on pre- and postsynaptic receptors for these neurotransmitters (Cole and Sumnall, 2003). MDMA increases neurotransmitter concentration in the brain in several ways (Fig. 1.3). It acts as a competitive reuptake inhibitor at vesicular and plasma membrane reuptake transporters, and reverses their action so high amounts of neurotransmitter (5-HT, DA, NA) are left lingering in the synaptic cleft (Cole and Sumnall, 2003, Miller, 2011). After entering the neuron, MDMA also enhances the release of monoamines from storage vesicles via a carrier-mediated mechanism after entering vesicles through vesicular monoamine transporters (VMAT) (Partilla et al., 2006). MDMA also inhibits tryptophan hydroxylase (TPH) through sulphydryl oxidation to decrease the synthesis of 5-HT and contribute to long-term serotonin depletion (Nishisawa et al., 1999, Kuhn and Geddes, 2000, Schmid and Kehne, 1990). MDMA inhibits monoamine oxidase (MAO), which is involved in breaking down these monoamines resulting in increased monoamine binding at postsynaptic receptors (Leonardi and Azmitia, 1994). As previously mentioned, MDMA works to increase release of NA (Rothman et al., 2001), which potentiates NA-induced smooth muscle contraction (Al-Sahli et al., 2001), as well as dopamine which is

likely responsible for amphetamine-like psychostimulant effects of MDMA (Green et al., 2003, Beardsley et al., 1986). It elicits brain release of ACh (Acquas et al., 2001, Fischer et al., 2000) as well as acutely increases hormones such as cortisol (Connor et al., 1999), oxytocin, and vasopressin (Forsling et al., 2002), which may be involved in psychological and psychomotor stimulant effects of MDMA. MDMA also causes pronounced changes in immune function such as reducing numbers of circulating lymphocytes, reducing T-cell proliferation and immunoglobin production, and increases in cytokine production and release (Connor et al., 1998, Connor et al., 2000, House et al., 1995).

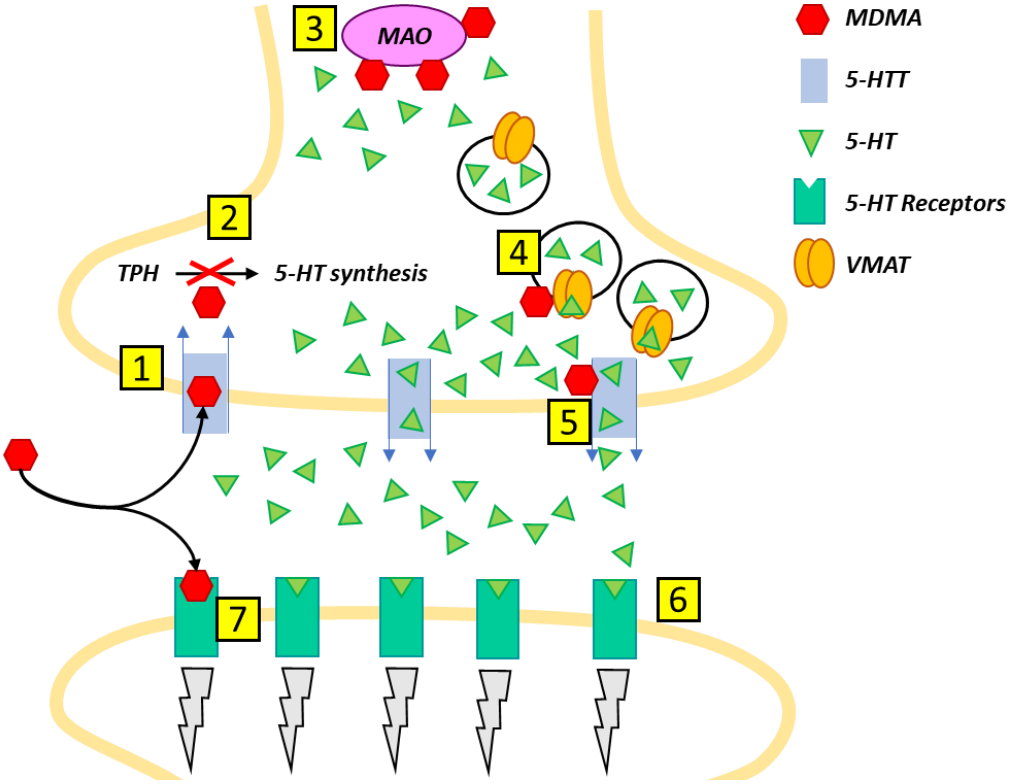

Figure 1.3: Diagrammatic representation of the main pharmacological effects of MDMA at the neuronal serotonergic terminal and synapse. 1) MDMA enters the neuron via monoamine transporters (5-HTT) acting as a substrate and produces competitive reuptake inhibition. 2) MDMA inhibits TPH, the rate limiting enzyme for 5-HT synthesis resulting in long-term depletion of 5-HT. 3) MAO, the enzyme responsible for 5-HT degradation is partially inhibited by MDMA. 4) MDMA produces an acute and rapid release of 5-HT from storage vesicles entering through VMAT and releasing vesicular stores via a carrier-mediated exchange mechanism. 5) MDMA promotes rapid release of intracellular 5-HT via reversal of 5-HTT activity. 6) MDMA administration results in increased serotonin binding and 5-HT receptor activity. 7) MDMA agonist activity on post-synaptic receptors.

1.5 Pharmacokinetics of MDMA

1.5.1 Humans

MDMA is usually taken orally and is sold in the form of tablets or capsules featuring various designs and colours. MDMA is produced in a racemic mixture where the S(+) isomer of MDMA (80-120 mg effective dose) is more potent causing euphoria and a number of other desirable effects compared to its R(-) isomer (300 mg effective dose), which predominantly causes its mescaline-like effects (Fantegrossi et al., 2003, De la Torre et al., 2004, Parrott, 2004). However, the dose and purity of 'ecstasy' tablets containing MDMA may differ between batches, and some batches may not contain MDMA at all, but rather be a mix of similar substances such as MDA, MDEA, or PMA (Parrott, 2004, Capela et al., 2009). One tablet of MDMA contains on average 80-150 mg of MDMA (Green et al., 2003) however, this can range as high as 245 mg per tablet (Morefield et al., 2011). It is common for users to consume 1-2 tablets over a short period of time (Parrott, 2001), however, there have been reports of users consuming in excess of 5 or 10 tablets (Morefield et al., 2011).

Following oral consumption, MDMA is absorbed from the gastrointestinal tract into the bloodstream. The onset of MDMA's effects usually takes between 20 to 60 min to occur, with peak effects occurring between 60 to 90 min after drug consumption. The acute effects of MDMA last for several hours following initial drug administration (Green et al., 2003). Following oral ingestion of MDMA by humans (50-125 mg), its maximum plasma concentration (C_{max}) appears at approximately 2 hours with a half-life of 8 hours (De la Torre et al., 2004). Elimination of MDMA after a single dose occurs approximately 40 hours after administration and its elimination half-life is approximately 8-9 hours, significantly lower than other stimulant drugs such as methamphetamine (10-12 hours) and amphetamine (12-15 hours) at similar doses (De la Torre et al., 2004). Plasma and brain concentrations of MDMA are not

proportional to administration of an increased dose of drug. These non-linear pharmacokinetics can be explained by saturation of MDMA's metabolism at high doses, as well as the interaction between metabolites of MDMA with enzymes involved in its own metabolic pathways (De la Torre et al., 2004, De la Torre et al., 2000). Therefore, saturation of MDMA metabolism can occur after the repeated administration of MDMA and can cause fatal MDMA intoxication.

1.5.2 Animals

There is a wealth of pharmacodynamic data demonstrating the effects of MDMA in animals, however, there are fewer studies concerning MDMA pharmacokinetics (Chu et al., 1996, Baumann et al., 2009, Concheiro et al., 2014), and even fewer related to the relationship between pharmacodynamics and pharmacokinetics (Chu et al., 1996). Studies on MDMA pharmacokinetics undertaken in animals are crucial to help improve our understanding and interpretation of animal based MDMA studies, and how they relate to the drugs' effects in humans. A study by Baumann et al., (2009) investigated how different dose and route of administration affected MDMA pharmacokinetics in rats. They demonstrated that a low oral dose of MDMA (2 mg/kg) produced low MDMA concentrations, whereas high dose (10 mg/kg) intraperitoneal (i.p.) administration produced high concentrations of MDMA (Baumann et al., 2009). The half-life of the drug was 45 min in rats given 2 mg/kg orally, significantly shorter than the half-life in humans of about 7-9 hours (De la Torre et al., 2000). The higher dose of MDMA (10 mg/kg) had a half-life of 1 hour, suggesting that a longer time for drug elimination occurs at higher doses and when administered intraperitoneally. This study also found that low dose MDMA (2 mg/kg) produced plasma C_{max} values of ~200 ng/ml. Similar studies demonstrated that MDMA doses of 2.5 mg/kg administered subcutaneously (s.c.), and 3 mg/kg administered i.p. resulted in C_{max} of 164 ng/ml and 300 ng/ml respectively, results comparable to humans given recreational doses (1.3 – 1.7 mg/kg) under controlled

conditions (De la Torre et al., 2000). Similar to Baumann et al., (2009), a 1 hour half-life of MDMA was found at low dose (2.5 mg/kg, s.c.), still significantly reduced compared to human drug consumption (De la Torre et al., 2000). Like humans, rats have non-linear MDMA pharmacokinetics with MDMA concentrations in the rat brain increasing non-linearly with dose (Chu et al., 1996). High dose MDMA (10 mg/kg, s.c.) was found to increase plasma MDMA concentrations in Sprague-Dawley rats 10-fold compared to low dose MDMA (2.5 mg/kg, s.c.), while in the same animals the MDMA metabolites (±)-3,4-dihydroxymethamphetamine (HHMA) and (±)-4-hydroxy-3-methoxymethamphetamine (HMMA) saw only a 2-fold increase (Concheiro et al., 2014). This is thought to be due to metabolic inhibition of MDMA at high doses (Concheiro et al., 2014).

1.5.3 Metabolism

The pharmacological effects of MDMA in humans and animals can be complicated by the extensive hepatic metabolism it undergoes after the drug is absorbed and distributed throughout the body. There are two main pathways (Fig. 1.4) that are involved in the metabolism of MDMA once it reaches the liver (Maurer et al., 2000, De la Torre et al., 2004). In the first pathway, MDMA undergoes *O*-demethylation by cytochrome P450 (CYP) CYP2D6, 1A2, 2B6 and 3A4 in humans, and by CYP2D1 and 3A2 in rats, to form HHMA, which undergoes *O*-methylation to form HMMA by catechol-*O*-methyltransferase (COMT) (Concheiro et al., 2014). Within the second pathway, MDMA undergoes *N*-demethylation by CYP2B6, 1A2, and 2D6 in humans, and CYP1A2 and 2D1 in rats, to form MDA, which is then *O*-demethylated in a similar fashion to MDMA to form 3,4-dihydroxyamphetamine (HHA), which is then subsequently metabolised by COMT to form 3-methoxy,4-hydroxyamphetamine (HMA) (Concheiro et al., 2014). The HHMA and HHA metabolites of MDMA and MDA undergo conjugation with glutathione and the resulting conjugates are thought to contribute to the long-

term neurotoxic effects of MDMA (Green et al., 2003, de la Torre and Farré, 2004, Capela et al., 2009). Metabolites such as HHA, and HMA have been shown to induce 5-HT toxicity in rats when administered subcutaneously, and the metabolites 5-(GSH)-α-MeDA, 5-(NAC)-α-MeDA, 5-(NAC)-*N*-Me-α-MeDA, and 2,5-(GSH)-α-MeDA were demonstrated to cause long-term 5-HT neurotoxicity in rats when undergoing direct intra-striatal administration (Capela et al., 2009). The elimination of MDMA occurs when the hydroxylated metabolites of MDMA are excreted in the urine as glucuronide and sulphate conjugates. The main differences between human and rat metabolism of MDMA involves the specific CYP isoforms involved in each species' metabolism, the shorter MDMA and metabolite half-life in rats, as well as the propensity for rats to form more MDA than in humans, and the formation of glucuronide-conjugated metabolites predominating in rats (Maurer et al., 2000, De la Torre et al., 2004). Metabolic differences between species are a major limitation when attempting to extrapolate data from animal models to humans. Extrapolation of results from animal models to humans implies that the metabolic disposition of MDMA among the species is similar and that the metabolic disposition is comparable (de la Torre and Farré, 2004). However, there are numerous differences in MDMA metabolism between rats and humans. *N*-demethylation of MDMA to MDA is the main metabolic pathway in rats compared to *O*-demethylenation of MDMA to HHMA in humans (De la Torre et al., 2004) resulting in differing production rates of HHMA and HMMA between rats and humans. This is relevant as thioether adducts with quinones formed from autooxidation of the MDMA metabolites HHMA and HHA are the most likely chemical species involved in 5-HT neurotoxicity as previously stated (de la Torre and Farré, 2004, Capela et al., 2009). Furthermore, differences in enzyme kinetics and enzyme inhibition between rats and humans suggests that each species experiences different rates of formation for neurotoxic metabolites (Bowyer et al., 2003, Bogaards et al., 2000). The inconsistencies between species regarding metabolic disposition, and non-linear kinetics within

the main metabolic pathways limits allometric scaling across animal models, and complicates the extrapolation of results to human studies.

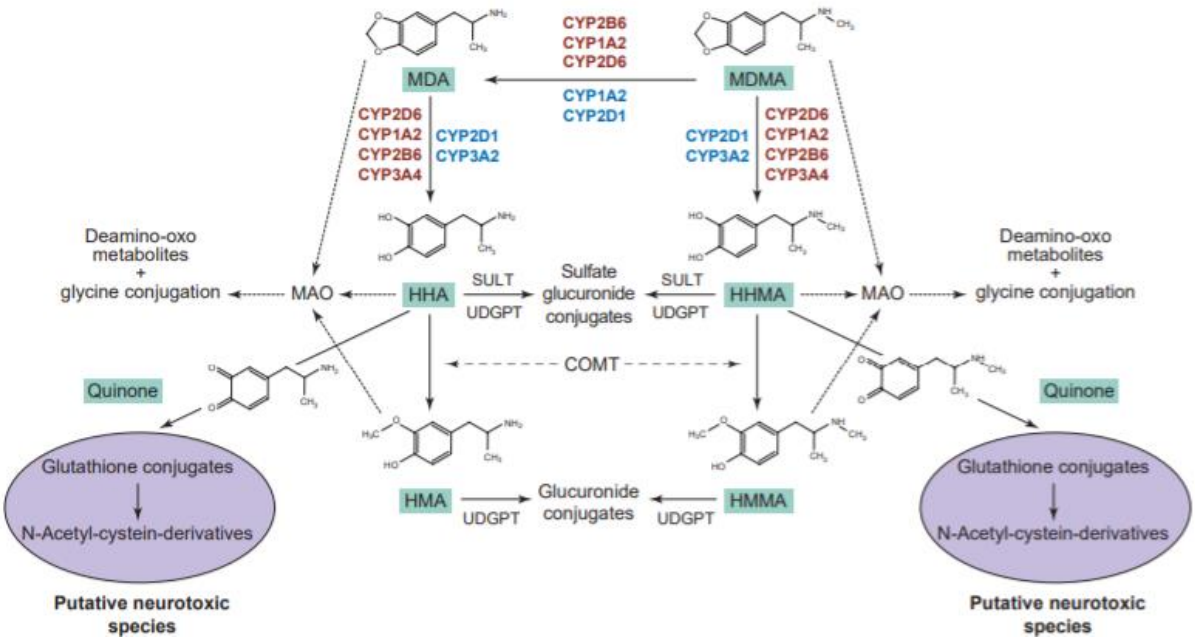

Figure 1.4: Pathways involved in the metabolism of MDMA in rats and humans. The CYP450 enzymes involved in rats are coloured blue, the enzymes involved in humans are coloured red. Derived from de la Torre and Farre (2004).

1.6 Effects of MDMA in animals

1.6.1 Disruption of thermoregulation

Previous animal studies have used systemic doses of 10-15 mg/kg MDMA to produce consistent changes (including both increases and decreases) in body temperature, neurotransmitter release, behaviour, and a wide range of other physiological parameters without causing fatalities (Daws et al., 2000, Freezer et al., 2005, Stanley et al., 2007, Anderson et al., 2011). The drug doses used in these studies results in similar MDMA plasma concentrations observed in humans, thus making the results in animals comparable to recreational human usage (Colado et al., 1995, Chu et al., 1996, Green et al., 2003).

Hyperthermia is the major acute effect of MDMA administration and can last several hours following drug use. Previous findings have demonstrated hyperthermia (+1-2 °C) in response to MDMA with temperatures peaking between 40-60 min after systemic MDMA administration (Malberg et al., 1996, Mechan et al., 2002, Orio et al., 2010, Anderson et al., 2011). Like human MDMA use, animals studies have shown that the degree of MDMA-induced hyperthermia is affected by environmental factors such as ambient temperature, social interaction, and diminished heat dissipation (Dafters and Lynch, 1998, Malberg and Seiden, 1998, Brown and Kiyatkin, 2004). Dafters and Lynch (1998) demonstrated that MDMA (10-15 mg/kg) resulted in significant body temperature increases (+2.3 °C) at normal ambient temperature (22 °C), however, significant body temperature decreases (-2.7 °C) were observed at an ambient temperature of 17 °C. Malberg and Seiden (1998) showed that higher doses of MDMA (20-40 mg/kg) resulted in hyperthermia at ambient temperatures between 28-30 °C, whereas hypothermia was observed between 20-22 °C. Brown and Kiyatkin (2004) found that when administered under quiet resting conditions, MDMA (9 mg/kg) caused no significant increases in brain or body temperature, however, significant temperature increases in both the brain and body were seen during male-female social interaction, during jugular vein occlusion, and when administered at a high ambient temperature of 29 °C. This study also found that brain areas showed consistently faster temperature increases and to greater elevations (+0.4 - 0.8 °C) when compared to the body under warm environmental conditions (Brown and Kiyatkin, 2004). This suggests that physiological mechanisms of drug-induced metabolic neural activation (Gordon et al., 1991, Quate et al., 2004, Darvesh et al., 2002) and diminished heat dissipation (Brown and Kiyatkin, 2004, Kiyatkin et al., 2014, Nybo et al., 2002) result in increased intra-brain heat production, which can be viewed as the primary cause of brain hyperthermia, and a contributor to a delayed and weaker body hyperthermia (Brown and Kiyatkin, 2004).

Neurotransmitters that contribute most to MDMA-induced hyperthermia have long been the subject of debate. It is well-known that MDMA-induced hyperthermia involves release of 5-HT (Freezer et al., 2005, Stanley et al., 2007), however DA release has also been implicated in the hyperthermic response (Mechan et al., 2002, Blessing et al., 2003). Several studies have used 5-HT and DA uptake inhibitors and receptor antagonists to investigate these neurotransmitters' contribution to the hyperthermic response, however, these studies produced variable results. Mechan et al. (2002) demonstrated that a dose of 12.5 mg/kg at normal ambient temperature produced a significant increase in rectal temperature. They also demonstrated that pretreatment of animals with several 5-HT receptor antagonists and uptake inhibitors prior to MDMA administration failed to significantly attenuate this hyperthermic response. In contrast, pretreatment with the DA D_1 receptor antagonist SCH 23390 (0.3-2 mg/kg) was effective in preventing these observed increases in body temperature. Other microdialysis studies have also shown that increases in extracellular 5-HT have no association with increases in body temperature (Freezer et al., 2005, Stanley et al., 2007). They have also shown that administration of 5-HT uptake inhibitors, such as fluoxetine, block increases in extracellular 5-HT but have no effect on hyperthermia (Schmidt et al., 1990, Berger et al., 1992, Malberg et al., 1996). In contrast, Malberg et al. (1996) reported that pretreatment with 6 mg/kg of the 5-HT_{2A} receptor antagonist ketanserin, and 75 mg/kg of the tyrosine hydroxylase inhibitor α-methyl-p-tyrosine (AMPT) was successful in preventing the hyperthermic effects of a much higher 40 mg/kg dose of MDMA at normal ambient temperature. Blessing and Seaman (2003) showed that activation of post-synaptic 5-HT_{2A} receptors caused cutaneous vasoconstriction and hyperthermia in both rats and rabbits (Blessing and Seaman, 2003), whereas activation of inhibitory presynaptic 5-HT_{1A} receptors lead to vasodilation and decreases in body temperature (Ootsuka and Blessing, 2003). This group also demonstrated that MDMA's temperature effects work via a vasoactive mechanism (Blessing et al., 2003). They found that administration of 10

mg/kg MDMA induced increases in body temperature of between 1.5-2 °C, which was accompanied by a 50% decrease in tail artery blood flow, indicating vasoconstriction. Administration of clozapine, an antipsychotic agent with antagonistic action at DA D_4 receptors and action at several 5-HT and muscarinic receptors, reversed both the temperature and vasoconstrictive effects of MDMA, and promoted increased blood flow. More recent work has identified peripheral vasoconstriction as a critical mechanism underlying the activity and state-dependent potentiation of MDMA-induced brain hyperthermia under different environmental conditions (Kiyatkin et al., 2014). These results, although variable, suggest that both 5-HT and DA play a role in the thermoregulatory effects of MDMA.

In addition to neurotransmitters, microglial activation and pro-inflammatory cytokines such as interleukin-1β (IL-1β), interleukin-6 (IL-6), and tumor necrosis factor-α (TNF-α) are known to increase body temperature by acting directly or indirectly in the brain. IL-1β, in particular, is known to be involved in the development of hyperthermia in response to exogenous pyrogens such as lipopolysaccharide (Klir et al., 1994), turpentine (Luheshi et al., 1997), and leptin (Luheshi et al., 1999). Furthermore, administration of the interleukin-1 receptor antagonist (IL-1RA) inhibits the rise in temperature caused by these inflammatory stimuli in experimental animals. It has been demonstrated that immediately after administration of MDMA, an acute increase in IL-1β concentration is observed in the hypothalamus and frontal cortex, peaking at 3 h post-MDMA administration (Orio et al., 2004, O'Shea et al., 2005). However, Orio et al. (2004) demonstrated that IL-1β release is likely a consequence of MDMA-induced hyperthermia rather than its cause. Their results displayed a clear dissociation between hyperthermia and IL-1β release with marked hyperthermia visible within the first 20 min of MDMA administration (Colado et al., 1993), peaking at 60 min, compared to IL-1β release, which peaked 3 h post-MDMA. Furthermore, interleukin-1 receptor antibodies did not modify peak hyperthermia following MDMA administration, and abolishment of hyperthermia by

maintaining animals at low ambient temperature (4 °C) resulted in reduced IL-1β release (Orio et al., 2004). Inhibition of microglial activation and IL-1β release by the cannabinoid CB2 receptor agonist JWH-015 has also been shown to have no effect on the acute hyperthermic response (Torres et al., 2010). Contrary to these findings however, O'Shea et al. (2005) showed that pretreatment with an intracerebroventricular injection of IL-1β 30 min prior to MDMA (12.5 mg/kg) increased the temperature response to MDMA. Administration of IL-1β in control animals treated with saline also produced an increase in rectal temperature compared with vehicle-treated controls (O'Shea et al., 2005). Thermoregulation is known to be affected by changes in both neural, and neuroinflammatory pathways. Therefore, it is likely that MDMA-induced variations in both neurotransmitter and pro-inflammatory cytokine concentrations contribute to its disruptive thermoregulatory effects.

1.6.2 Behavioural effects

In addition to hyperthermia, activation of serotonergic, dopaminergic, and noradrenergic pathways by MDMA differentially associated with specific behaviours. MDMA produces acute 'serotonin syndrome' in animals, which is most likely attributed to increases in extracellular 5-HT levels in multiple brain regions. Serotonin syndrome is characterised by hyperactivity, head-weaving, fore-paw treading, piloerection, proptosis, penile erection, ejaculation, salivation, and defecation (Spanos and Yamamoto, 1989). Administration of MAO inhibitors, L-tryptophan (Grahame-Smith, 1971b), non-selective 5-HT agonists (Grahame-Smith, 1971a), and 5-HT_{1A} agonists (Goodwin and Green, 1985) have been shown to produce this syndrome, thus highlighting the importance of increased 5-HT activity on MDMA-induced behavioural changes.

In contrast, activation of the dopaminergic system has been linked to increases in locomotor activity (LMA) and stereotypical gnawing (Robinson and Becker, 1986, Bankson and

Cunningham, 2001, Yamamoto and Spanos, 1988). MDMA administration causes dose-dependent increases in spontaneous LMA and this behavioural change occurs immediately after drug administration (Dafters, 1994). MDMA has been shown to produce a release of dopamine both *in vitro* (Stone et al., 1986) and *in vivo* (Yamamoto and Spanos, 1988) and its release has been paralleled with the time-course of hyperlocomotion in rats (Spanos and Yamamoto, 1989). However, lesions of the mesolimbic DA system have been shown to be associated with only partial attenuation of MDMA-induced hyperlocomotion (Gold et al., 1989), and 5-HT release alone is insufficient to increase LMA (Aulakh et al., 1988). Therefore an interaction between DA and 5-HT may underlie MDMA-induced hyperlocomotion (Bankson and Cunningham, 2001). Kehne et al (1996) showed that the dose-dependent increase in LMA was attenuated by pretreatment with the 5-HT_{2A} receptor antagonist MDL 100907 (Kehne et al., 1996). Callaway et al (1990) found similar reductions in MDMA-induced hyperlocomotion using the 5-HT uptake inhibitor fluoxetine (Callaway et al., 1990). This suggests that 5-HT mediated DA release, as well as direct 5-HT receptor agonist activity are involved in MDMA-induced increases in LMA.

Increases in extracellular NA have also been linked to the behavioural effects associated with MDMA use. These effects include emotional excitation, anxiety, as well as blissful state, and the experience of unity (Hysek et al., 2011). The magnitude of subjective effects caused by MDMA in humans correlates with its potency to release NA (Rothman et al., 2001). This is supported by results showing that inhibition of the noradrenaline transporter (NAT) reversed the acute cognitive effects of MDMA in rhesus monkeys (Verrico et al., 2008). Similar results were replicated in humans with NAT inhibitors attenuating the subjective response to both MDMA (Hysek et al., 2011), and D-amphetamine (Sofuoglu et al., 2009).

1.6.3 Cardiovascular effects

Administration of MDMA in rats produces cardiovascular changes, in addition to variations in brain and body temperatures and LMA that are consistent with its effects on monoamine pathways in the brain (Green et al., 2003, Bexis and Docherty, 2006, Jaehne et al., 2008). The cardiovascular response to ambient temperature is closely related to core temperature and is a mechanism for heat production in rats (Chambers et al., 2000). Therefore, increases in HR, and other cardiovascular parameters such as blood pressure, may provide indication for increases in heat production and impairment of thermoregulation in animals (Gordon et al., 1991, Jaehne et al., 2011). Acute MDMA administration produces cardiac stimulation, tachycardia, and arrhythmia (Gordon et al., 1991) whilst also facilitating vasoconstriction in rats and rabbits (Fitzgerald and Reid, 1994, Pedersen and Blessing, 2001). These cardiovascular effects may potentially be caused by the actions of MDMA displacing NA from adrenergic nerve terminals (Fitzgerald and Reid, 1993) and its subsequent effect on adrenoreceptors. MDMA users have been reported to display increased plasma catecholamine levels, potentially due to noradrenergic hyperactivity (Stuerenburg et al., 2002). MDMA has also been shown to have direct agonist action on peripheral (Lavelle et al., 1999) and central α_1 and α_2 adrenoreceptors both *in vitro* and *in vivo* (McDaid and Docherty, 2001) and may also competitively block the NA transporter to increase extracellular NA concentrations (Al-Sahli et al., 2001). Studies show that agonist action at α_1 and α_2 adrenoreceptors contribute to MDMA's blood pressure effects in rats (McDaid and Docherty, 2001, Rajamani et al., 2001) with the α_{2A} receptor involved with its hyperthermic response in mice (Bexis and Docherty, 2005). These cardiovascular changes are compounded by increased renin and angiotensin II (AII) production induced by MDMA (Burns et al., 1996). In addition to its own vasoconstrictive effects, AII promotes aldosterone release from the adrenal cortex leading to increases in blood pressure. Furthermore, MDMA causes hyponatremia by increasing secretion of anti-diuretic hormone

(ADH) which also has moderate vasoconstrictive effects (Bora et al., 2016, Irvine et al., 2006). It is compounded by the excessive intake of hypotonic liquid accompanied by hyperthermia in MDMA users (Bora et al., 2016). Hyponatremia, in addition to previously described vascular changes, are a primary contributor to the potentially deadly adverse effects associated with human MDMA use such as intracerebral haemorrhage and brain oedema (Fitzgerald and Reid, 1994, Wolff et al., 2006). Interestingly, MDMA reportedly does not alter 5-HT induced aortic contraction (Cannon et al., 2001, Murphy et al., 2002). However, the selective serotonin releasing agents (SSRA) 4-methylthioamphetamine and 4-methylthiomethamphetamine are potent inhibitors of 5-HT mediated vascular contraction (Murphy et al., 2002). Neurotoxic MDMA regimens have also been shown to alter cardiovascular function through actions on both descending peripheral and central 5-HT pathways (O'Cain et al., 2000) indicating that cardiovascular changes induced by MDMA are partially 5-HT-mediated.

1.6.4 Long-term effects

Like human MDMA use, chronic MDMA administration in animals has been linked to the long-term depletion of 5-HT, and other serotonergic components in the brain. It has been shown to lead to serotonergic problems in the brain such as a decrease in tryptophan hydroxylase (Stone et al., 1988), 5-HT and 5-HIAA (Schmidt et al., 1986, Clemens et al., 2004, Callaghan et al., 2006, Wang et al., 2004), a loss of 5-HT uptake sites (Battaglia et al., 1988), 5-HT terminal degeneration (O'Hearn et al., 1988), reduction of 5-HTT binding (Green et al., 2003), and impairment of 5-HT function (Hatzidimitriou et al., 1999). Callaghan et al (2006) demonstrated that MDMA (10-20 mg/kg) caused significant reductions in cortical 5-HTT binding, 5-HT content, and 5-HIAA concentrations in rats two weeks after repeated drug administration. Wang et al (2004) showed similar results after two weeks of repeated administration with MDMA (7.5 mg/kg) resulting in a 50% reduction in 5-HT concentration

across multiple brain areas. Clemens et al (2004) used albino Wistar rats to demonstrate that MDMA (5 mg/kg) had similar neurotoxic effects on 5-HT systems for as long as seven weeks after an initial two days of repeated drug administration.

The long-term neurotoxic effects of MDMA can be exacerbated when administered at high ambient temperature resulting in hyperthermia. Broening et al (1995) administered MDMA (20 or 40 mg/kg) to rats aged 40-70 days at varying ambient temperatures. Rats displayed a significant hyperthermia at ambient temperatures of 25 and 30 °C, and showed larger decreases in cortical 5-HT one week after drug administration. Malberg and Seiden (1998) displayed similar findings when MDMA (20 and 40 mg/kg) was administered at different ambient temperatures. Rats administered MDMA at ambient temperatures between 26-30 °C showed greater increases in body temperature as well as significant decreases in cortical 5-HT concentrations two weeks after drug administration compared to rats administered MDMA at 20-22 °C. It has been suggested that hyperthermia's influence on serotonergic neurotoxicity has been linked to dopamine receptor activity (Malberg et al., 1996, Malberg and Seiden, 1998, Yuan et al., 2002, Yuan et al., 2001). However, MDMA has been shown to induce increased concentrations of both 5-HT and DA in the nucleus accumbens at an ambient temperature of 30 °C compared to 20 °C (O'Shea et al., 2005), therefore 5-HT receptor activity is likely also implicated in this increased severity. Low ambient temperature has been shown to have a protective effect on MDMA-induced reductions in brain 5-HT levels. MDMA administration at ambient temperatures of 10 °C and 22 °C resulted in decreases in core body temperature and either no, or smaller decreases in brain 5-HT concentrations compared to those treated at higher ambient temperatures (Broening et al., 1995, Malberg et al., 1996). In contrast to this, other studies have found that pretreatment with drugs such as fluoxetine and mazindol protected against 5-HT neurotoxicity without attenuating MDMA-induced hyperthermia (Shankaran and

Gudelsky, 1999, Falk et al., 2002), suggesting that a mechanism unrelated to hyperthermia is responsible for the increased severity of 5-HT neurotoxicity.

1.7 Conventional methodological approaches to assess MDMA temperature effects in animals

Previous studies have utilised many different methods to determine the thermoregulatory, neurochemical and physiological effects of MDMA within animal models. However, the different methods used to monitor these effects have produced many confounding results that make data comparison between these studies difficult and translational relevance to human MDMA use hard to assess. These contradictory results are summarised in Table 1.2. The results of this table clearly outline the importance of the selected materials and methodology, especially when examining the thermoregulatory effects of MDMA.

References and MDMA Dose	Animal/Strain	Ambient Temp	Parameters measured, method, and result			
			Core body temp	**Brain temp**	**Neurochemical**	**Physiological**
Brown and Kiyatkin (2004) 9 mg/kg i.p.	Rat Male Long-Evans	29 °C	↑ 3.7 °C (thermocouple)	↑ 4.5 °C (thermocouple)	Not recorded	Not recorded
Colado et al. (1995) 10 mg/kg i.p.	Rat Male Dark Agouti	21°C	↑ 1.0 °C (rectal probe)	Not recorded	↓ 5-HT 40% (long term)	Not recorded
Freezer et al. (2005) 10 mg/kg i.p.	Rat Male Sprague-Dawley	22 °C	↑ 1.8 °C (aural thermometer)	Not recorded	↑ 5-HT 600% (microdialysis)	Behaviour score 3-3.5
Anderson et al. (2011) 10 mg/kg i.p.	Rat Male Sprague-Dawley	22 °C	↑ 2.5 °C (rectal probe)	Not recorded	IL-1β ns (P>0.05) (ELISA)	Behaviour score 2-3
Daws et al. (2000) 10 mg/kg i.p.	Rat Male Sprague-Dawley	30 °C	↑ 0.5 °C (telemetry)	Not recorded	↑ DA release (chronoamperometry)	LMA to 250 counts (telemetry)
Jaehne et al. (2005) 10 mg/kg i.p.)	Rat Male Sprague-Dawley	30 °C	↑ 3.5 °C (telemetry)	Not recorded	Not recorded	HR 450 bpm LMA 1000 counts/min (telemetry)
Stanley et al. (2007) 10 mg/kg i.p.	Rat Male Sprague-Dawley	30 °C	↑ 1.5 °C (rectal probe)	Not recorded	↑ 5-HT 375% (microdialysis)	Behaviour score 3-4
Orio et al. (2010) 12.5 mg/kg i.p.	Rat Male Dark Agouti	21 °C	↑ ~2.0 °C (rectal probe)	Not recorded	↓ 5-HT uptake sites 50% ([3H]paroxetine binding) IL-1β 3 pg/mg protein (ELISA)	Not recorded
Bexis and Docherty (2006) 20 mg/kg s.c.	Rat Male Wistar	22 °C	↓ 2.0 °C (telemetry)	Not recorded	Not recorded	20 mmHg MAP (telemetry)
Zhang et al. (2006) 3 x 10 mg/kg s.c.	Mouse Male Balb/c	22 °C	↑ ~2.7 °C (rectal probe)	Not recorded	↓ 5-HT 60% ↓ DA 40% (microdialysis) ↑ microglial activation (Mac1-IHC)	Not recorded
Gordon et al. (1991) 30 mg/kg s.c.	Rat Male Long-Evans	30 °C	↑ 3.0 °C (rectal probe)	Not recorded	Not recorded	LMA 350 units/60 min (Doppler system)

Table 1.2: Brief summary of several MDMA studies.

1.7.1 Rectal probes

Rectal temperature measurement has been used in the past to assess the effects of MDMA on core body temperature (Stanley et al., 2007, Colado et al., 1995, Zhang et al., 2006, Anderson et al., 2011, Orio et al., 2010, Gordon et al., 1991). Rectal temperature is usually measured from thermistor probes inserted 5-9 cm into the rectum (Poole and Stephenson, 1977). For continuous temperature measurement rats are often placed in a restraining device (Feldberg and Saxena, 1975) or an enclosure small enough to restrict their movement (Stoner, 1971), however for intermittent measurements, animals are allowed to move freely around their enclosure except when restrained to permit insertion of the probe. Although this method seems advantageous requiring no surgery prior to experiments to permit temperature measurements, the need for restraint offers a profound disadvantage as it has been shown to interfere with normal thermoregulation (Martin and Papp, 1979, Frankel, 1959). The requirement for constant handling and repeated insertion of the rectal probe into the rectum can also produce stress-induced increases in body temperature (Gordon, 1990), brain temperature (Bae et al., 2007), as well as effects on HR, blood pressure, and LMA (Guiol et al., 1992, Van Den Buuse, 1994, Irvine et al., 1997). This may contribute to conflicting reports of the effect of MDMA on core body temperature in studies using rectal thermometers. For example, when core body temperature was measured with a rectal probe at normal ambient temperature, core temperature increased in response to MDMA (Anderson et al., 2011, Orio et al., 2010, Colado et al., 1995). Contrary to this, when measured with non-restrictive methods such as radio telemetry, core body temperature decreased at normal ambient temperature (22 ^{o}C) (Bexis and Docherty, 2006), a result consistent with previous studies reporting hypothermia at low or normal ambient room temperature (Malberg and Seiden, 1998). Elimination of restraint and stress-inducing probe insertion from the recording procedure reduces the confounding effects on body temperature (Clement et al., 1989, Dilsaver et al., 1990) as well as HR, blood pressure, and

LMA (Irvine et al., 1997, Guiol et al., 1992, Van Den Buuse, 1994, Gegout-Pottie et al., 1999). Previous studies have shown core body temperature measurement in rats using rectal probes and thermosensor telemetry produce qualitatively similar, but quantitatively different results (Dilsaver et al., 1990). This has led to more recent research utilising telemetric sensors for the continuous monitoring of core body temperature, as well as other physiological parameters in free-moving animals (Bexis and Docherty, 2005, Jaehne et al., 2005, Bexis and Docherty, 2006).

1.7.2 Radiotelemetry

Telemetry was first used in an ecology study in 1959 (LeMunyan et al., 1959), however since this time, telemetry transmitters have been enhanced to be smaller, and more durable with longer life expectancies. These transmitters were initially used only to monitor core body temperature, however, since then, this technique has evolved to measure numerous physiological and behavioural parameters including cardiovascular (Rubenson et al., 1984), LMA (Clement et al., 1989), and HR variables (Gordon et al., 1991). They can be used to gather physiological data in awake, freely-moving animals without the need for restraint or restrictive caging to perform temperature measurements. Instead, an implantable transmitter is used to transmit data to a receiver consolidation matrix linked to a computer equipped with data acquisition software (Fig. 1.5) (Guiol et al., 1992, Rodsiri et al., 2011). These transmitters are surgically implanted prior to experimentation and when activated can continuously transmit data via radio signals to the nearby receiver, which is then collected by a data acquisition program running on a nearby computer. As mentioned previously, this technique has been used in the past to assess the effects of MDMA in animal models (Bexis and Docherty, 2005, Jaehne et al., 2005, Daws et al., 2000, Bexis and Docherty, 2006). Bexis et al. (2006) found that a high dose of MDMA (20 mg/kg, s.c.) at normal ambient temperature resulted in a prolonged

hypothermic response (Bexis and Docherty, 2006). At high ambient temperature (30 ºC), Daws et al. (2000) found that a modest dose of MDMA (10mg/kg, i.p.) caused a slight increase in core body temperature and LMA (Daws et al., 2000). Jaehne et al. (2005) found that the same dose of MDMA caused a more prolonged and intense increase in core body temperature and LMA, as well as an increase in HR when administered at high ambient temperature (Jaehne et al., 2005), however, methodological differences regarding animal confinement during core temperature measurements could explain the differences between these studies. Although the effects of MDMA on core body temperature have been studied extensively in the past, the temperature effects of MDMA in the brain have only been investigated within the last two decades (Kiyatkin et al., 2002, Brown and Kiyatkin, 2004).

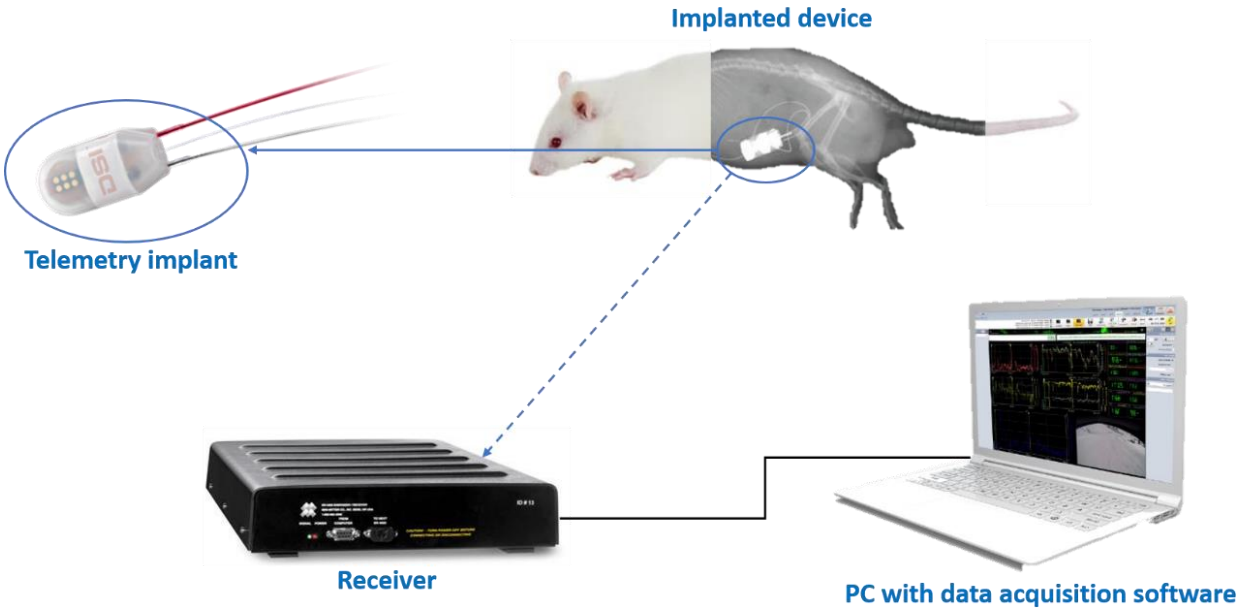

Figure 1.5: Diagram of radiotelemetry technique setup.

1.7.3 Thermocouples

The majority of studies concerned with MDMA-induced hyperthermia have historically focused exclusively on MDMA's effect on body temperature (Gordon et al., 1991, Colado et al., 1995, Malberg et al., 1996, Malberg and Seiden, 1998, Daws et al., 2000, Bexis et al.,

2004, Orio et al., 2010). However, more recent studies show that brain tissue increases at a faster rate and to greater magnitude than muscle tissue in response to MDMA, and that brain hyperthermia may contribute to a delayed and weaker hyperthermia in the body (Brown and Kiyatkin, 2004). These changes in brain and muscle temperature were demonstrated using thermocouples to perform *in vivo* brain temperature monitoring (Kiyatkin, 2013). Thermocouples are conventional temperature probes that consist of two dissimilar metallic wires connected at one end creating a junction where temperature is measured. A unique voltage is produced at a given temperature and this voltage can then be measured and interpreted by a thermocouple thermometer. Thermocouples are usually inexpensive with good accuracy (~1 °C) and have relatively short response times. However, this strongly depends on probe diameter, and can be much shorter than 1 second (Schena et al., 2016). In addition to brain temperature monitoring, thermocouples have been previously utilised to perform temperature measurements during a variety of thermal ablation procedures for tumour treatment (Saccomandi et al., 2013). However, during these procedures, substantial thermocouple measurement error occur for two main reasons: 1) direct absorption of light by the metallic wires during laser ablation, and sonication during high-intensity focused ultrasound can result in substantial temperature overestimation (Banerjee and Dasgupta, 2010, Manns et al., 1998); and 2) the high heat conductivity of the metallic wires can cause temperature overestimation at low temperatures, or underestimation at high temperatures (Rivens et al., 2007). The metallic wires can also potentially cause significant image artefacts in computed tomography (CT) or magnetic resonance (MR) guided thermal procedures (Schena et al., 2016). These thermal ablation procedures occur at extreme temperatures selected to cause death in tumorous cells, therefore these temperature artefacts would be unlikely to occur over the biologically relevant range between 35-45 °C. For example, Brown and Kiyatkin (2004) utilised copper-constantan thermocouples to show that

MDMA administration induced hyperthermia in both the brain and body that was exacerbated by numerous environmental conditions (Brown and Kiyatkin, 2004). Although thermocouples can be used to provide a means of localised temperature measurement within the brain, the method is not without its limitations. Optical fibre sensors are an attractive and advantageous alternative to traditional temperature measurement techniques devoid of many of the limitations present in traditional electrical sensors.

1.8 Optical Fibres

1.8.1 Background

Transmission of light through optical fibres plays a large role in our everyday lives. Optical fibres permit transmission of light over long distances and have many applications in telecommunications, computer networking, and power transmission in situations where metallic conductors present in conventional electrical systems are undesirable. Optical fibres operate based on the principle of total internal reflection. The core of an optical fibre has a higher refractive index than the surrounding fibre cladding, therefore light entering the fibre is reflected back into the core to propagate along its length as opposed to 'leaking' out into the periphery (Addanki et al., 2018). Approximately 40 years have passed since the manufacture of the first optical fibres (Powell, 1974, Sheem and Giallorenzi, 1979, Hocker, 1979) and they have since been developed for a wide range of applications (Fig 1.6) due to their inherent advantages such as low cost, small size, and increased durability. One of these applications is optical fibre sensors. Optical fibre sensors have many advantages when compared to conventional measurement techniques. These include immunity to electromagnetic interference (EMI), lightweight, small size, high sensitivity, large bandwidth, ease in signal light transmission, as well as the ability to provide multiplexed or distributed sensing (Lee, 2003, Wade et al., 2003, Grattan and Meggitt, 1995). Optical fibres have found use in the

security and chemical industry, as well as in aircraft manufacture for temperature, pressure, fluid, and acceleration monitoring (Taylor and Cardimona, 2008, Addanki et al., 2018). They have also seen use for numerous biological sensing applications (Samset et al., 2001, Yoo et al., 2010, Webb et al., 2000, Tosi et al., 2016, Fajkus et al., 2017). However, despite their numerous advantages, only a limited number of optical fibre sensing techniques that have been successfully commercialised (Lee, 2003, Grattan and Meggitt, 1995, Culshaw and Dakin, 1989). In many fields of application, optical fibres compete with mature, conventional techniques that are already well established within their field, and their installation cannot occur without the development of new infrastructure. To appeal to users already accustomed and comfortable with these technologies, the superiority of optical fibres needs to be made clear. Ideally, high performance sensor systems should be available at a reasonable price in the form of complete systems including detection and signal-processing electronics to increase their appeal and ease of use (Lee, 2003).

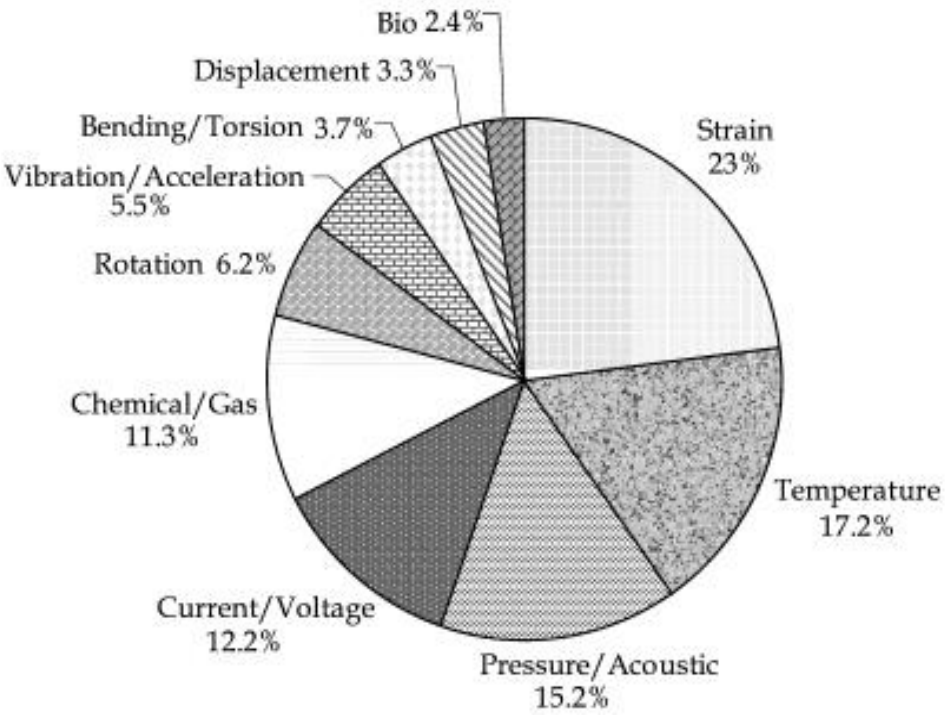

Figure 1.6: Distribution of OFS-15 papers according to measurands. Derived from Lee (2003).

1.8.2 Optical fibre temperature sensors

Temperature sensors make up a large portion of commercially available optical sensors and present an attractive alternative to conventional temperature measurement techniques for operation in thermally, chemically, and electromagnetically hazardous environments (Dos Santos et al., 1998). Fibre optic temperature sensors have previously found use in several different industries such as telecommunications and aerospace (Selker et al., 2006, Taylor and Cardimona, 2008, Bhatia, 1999), however, since the late 1990's, they have also reached maturity as a sensing technology for biomedical applications (Tosi et al., 2018). Ongoing research in the field of optical fibre-based temperature sensors has focused on improving accuracy and measurement range, as well as reducing cost. There are many different techniques used to perform temperature sensing utilizing optical fibres, with the most common being fibre Bragg gratings (FBG) (Rai, 2007), however techniques such as long-period gratings and whispering gallery modes (WGM) have also been used (Guan et al, 2006, Lee and Nishii, 1998). These techniques have found use within structural health monitoring applications, however for temperature measurements requiring high resolution with high spatial precision, these methods are not ideal. Some examples of the temperature range, sensitivity, response time, and resolution of these techniques is given in Table 1.3. FBG show a relatively low response to temperature, which limits their resolution (Rao, 1997). Long-period gratings require long fibre lengths to obtain good sensitivity, limiting spatial resolution (Lee and Nishii, 1998). WGM techniques are typically sensitive to changes in local refractive index making separation of the temperature from environmental changes challenging (Guan et al., 2006). Other methods for grating fabrication that can provide good sensitivity with good spatial precision (Guan et al., 2006) require complex fabrication techniques making them difficult to expand to commercial applications due to their high cost.

OFS	Sensitivity	Resolution	Range	Response time
Fluorescence	0.5 μs $^{o}C^{-1}$	± 0.5 °C	20-80 °C	a
FBG	27 pm $^{o}C^{-1}$	0.1 °C	20-80 °C	100 ms
FPI	0.19 nm $^{o}C^{-1}$	0.34 °C	25-80 °C	67 °C/sb
Rayleigh scattering	10 pm $^{o}C^{-1}$	0.1 °C	20-46 °C	1 s
LPG	62.9 nm $^{o}C^{-1}$	0.005 °C	20-100 °C	100 ms

a No information available. b This is the rate of temperature change that the sensor can measure, rather than the response time.

Table 1.3: Summary of key parameters of numerous types of optical fibre temperature sensors. Derived from Correia et al. (2018).

1.8.3 Fluorescence Temperature Measurement

One promising alternative method for temperature measurement utilising optical fibres involves rare-earth absorption and fluorescence monitoring. Rare-earth ions have been of interest for use in optical fibre temperature sensors because their absorption and emission properties depend on temperature (Berthou and Jörgensen, 1990, Dos Santos et al., 1998, Maciel et al., 1995). Rare-earth metals suitable for these temperature sensing applications have been studied extensively (Berthou and Jörgensen, 1990, Dos Santos et al., 1998, Maciel et al., 1995, Wade et al., 1999, Rai et al., 2006, Rai and Rai, 2007). Materials deemed suitable for temperature sensing all contain pairs of energy levels where small separations in the order of the thermal energy is seen. The principle of these sensors is based on the temperature-dependent nature of light emitted from rare-earth ions. As temperature changes, populations in the energy level pairs change as the ions undergo thermal excitation to a higher energy state. By monitoring the upconversion emission from these ions, the temperature of the host medium can be discerned (Wade et al., 2003). Temperature sensors based on fluorescence have been used for many years and historically they made use of the temperature dependence of

fluorescence decay time (Grattan et al., 1987, Augousti et al., 1988). However, sensors based on this principle have a temperature resolution no better than a few degrees (Berthou and Jörgensen, 1990), making them impractical for biological applications requiring high precision.

Fluorescence signal processing is greatly simplified if temperature information can be given as the ratio of two light intensities rather than requiring a time-resolved measurement. This is the basis for the fluorescence intensity ratio (FIR) principle. In order for this principle to apply, the ratio must be an inherent function of temperature alone, and the same ratio of optical signals must be conveyed down the fibre regardless of disruptions in transmission of light along the fibre (Berthou and Jörgensen, 1990). These conditions are satisfied by the rare-earth ion erbium. The first condition is satisfied by the $^2H_{11/12}$ and $^4S_{3/2}$ levels of erbium that fluoresce at approximately 520 and 550 nm respectively (Berthou and Jörgensen, 1990). This pair of excited levels are close enough to each other to be thermally linked, which allows the $^2H_{11/12}$ level to be populated by the $^4S_{3/2}$ level during thermal agitation (Fig. 1.7), therefore temperature can be expressed as a ratio of the two light intensities at approximately 520 and 550 nm (Dos Santos et al., 1998, Berthou and Jörgensen, 1990, Maciel et al., 1995). The second condition is also satisfied here as fibre bends, and the fluctuations these cause to the spectral loss curve of the fibre, only amount to a shift in signal amplitude. The power ratio remains unaffected and therefore temperature information can still be discerned (Berthou and Jörgensen, 1990).

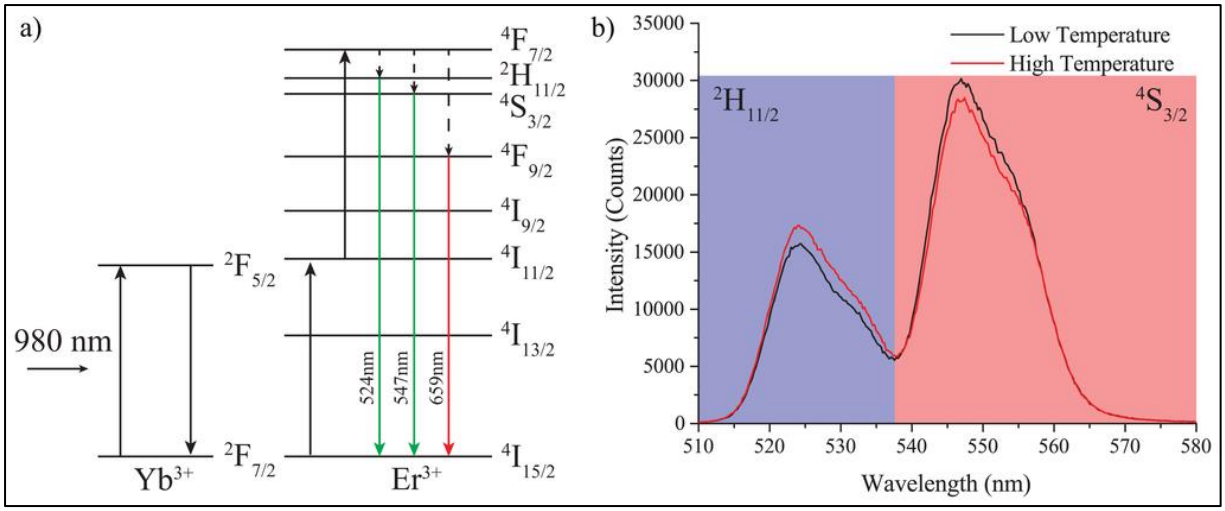

Figure 1.7: (**a**) Erbium and ytterbium energy level diagram detailing energy absorption required to reach higher energy excited states. (**b**) Example erbium ytterbium spectra for the two measured fluorescence signals. The two bands recorded to measure the fluorescence intensity are shaded in red and blue. Both low (23 °C, black) and high (39 °C, red) temperature emission spectra are shown, demonstrating the variation in the emission ratio of the two bands with changing temperature. Derived from Schartner and Monro (2014).

Erbium doped temperature sensors based on this principle have been explored in the past. For example, Berthou and Jörgensen (1990) found an almost linear temperature dependence of fluorescence in optical fibres doped with 1% erbium under the excitation of a 488 nm argon laser. They also showed that co-doping the glass with a sensitizer, in this case ytterbium, dramatically reduced the excitation power requirements compared to erbium alone. Ytterbium ions (Yb^{3+}) can be used as sensitisers due to their large absorption cross section compared to the weaker absorption of erbium ions (Er^{3+}). This greatly reduces the excitation power required to generate a given fluorescence signal (Desirena et al., 2008, Jakutis et al., 2010, Schartner and Monro, 2014). This finding is important considering the increased cost, reduced lifetime, and practicality issues a source of high excitation power would present, as well as the hazard it would pose to living cells if used to perform sensing in biological tissue samples. Yb^{3+} absorbs the near-infrared (NIR) radiation of the laser at 980 nm and transfers this energy to the acceptor Er^{3+} according to the equation:

$$Yb^{3+}(^2F_{5/2}) + Er^{3+}(^4 I_{15/2}) \rightarrow Yb^{3+}(^2F_{7/2}) + Er^{3+}(^4I_{11/2})$$ (Desirena et al., 2008).

As Er^{3+} relaxes to its ground state it releases this absorbed energy as green photons at approximately 524 nm and 547 nm (Schartner and Monro, 2014) (Fig. 1.7). As stated previously, the temperature of the host medium can be expressed as the ratio of these two light intensities.

1.8.4 Biomedical application of optical fibre temperature sensors

Temperature is a key vital sign and a routinely monitored parameter in all clinical settings. Although the requirements of temperature sensors are application dependent, a range of 35-45 °C with a resolution of 0.1 °C is required for the majority of applications (Teunissen et al., 2011). As mentioned previously, optical fibre sensors can be employed to measure temperature when requiring a temperature sensor immune to EMI or when electrical insulation is required (Mignani and Baldini, 1996, Christensen, 1988) such as during magnetic resonance imaging (MRI) or radio frequency treatment (Christensen, 1988, Dziuda et al., 2013, Su et al., 2017, Correia et al., 2018). Also, thanks to their constitution, usually glass or polymer, they are not prone to temperature overestimation caused by light absorption and have low heat conductivity compared to conventional thermocouple probes (Schena et al., 2016). Although commercial optical fibre temperature sensors are readily available, there are few examples of their use in animals and humans *in vivo* (Schena et al., 2016). Samset et al. (2001) measured temperature distribution with multiplexed FBG sensors to validate 3D temperature maps during cryo-surgery in porcine livers (Samset et al., 2001). Yoo et al. (2010) proposed respiration sensors for respiratory monitoring during an MRI scan and reported two types of non-invasive sensor. The first, a nasal-cavity attached sensor capable of measuring temperature variation of air-flow, and the second, an abdomen-attached sensor capable of measuring abdominal circumference change (Yoo et al., 2010). Webb et al. (2000) performed *in vivo* trials with a

FBG temperature sensor on diseased livers and healthy kidneys in rabbits undergoing hyperthermia (Webb et al., 2000). A key advantage of biomedical temperature sensing using optical fibres is their potential for multiplexed sensing when combined with other optical sensing techniques. The combination of multiple sensors within the same network enables the measurement of multiple parameters within the one system without requiring the implantation of additional sensing equipment. Tosi et al (2016) described an optical fibre sensor for intra-tissue pressure and temperature measurement in liver tissue undergoing laser ablation. Li et al (2018) described a miniaturized single-fibre-based imaging and sensing probe capable of simultaneous optical coherence tomography imaging and temperature sensing. Fajkus et al (2017) also described a multiplexed system for the measurement of body temperature, HR, and respiratory rate. The system was tested on 10 human volunteers and displayed good correlation with conventional measurement techniques. Although optical fibre sensors present numerous advantages over conventional technology, the crucial challenge for researchers in this field is to increase academic and clinician awareness about their ability to overcome the drawbacks related to the use of traditional electrical sensors. This could lead to their increased use in biomedical studies to investigate multiple parameters in locations where previously it may have been impossible or impractical to do so. Their implementation would also be a large improvement on conventional assays in many research areas, such as brain thermorecording during MDMA-induced hyperthermia using thermocouple electrodes.

1.9 Current strategies for treatment of MDMA-induced hyperthermia

The difficulty in treating MDMA-induced hyperthermia comes from the complex central and peripheral effects that the drug has on pathways involved in thermoregulation. MDMA deregulates heat accumulation in the brain by increasing the release of, and preventing the re-uptake of key neurotransmitters (Colado et al., 1995, Green et al., 2004). The accumulation of

these neurotransmitters can lead to an increase in noradrenergic signalling that contributes to the peripheral effects of MDMA by affecting cutaneous vasoconstriction, blood flow, and tissue thermogenesis (Pedersen and Blessing, 2001, Docherty and Green, 2010). As mentioned previously, complications arising from MDMA-induced hyperthermia can be life-threatening. Pharmacological treatment strategies to manage this hyperthermic response have been studied extensively animal models (Kiyatkin et al., 2016, Mechan et al., 2002, Nash et al., 1988, Freezer et al., 2005, Anderson et al., 2011), however, these treatments have not been systematically evaluated in the emergency room setting as hyperthermic complications are relatively rare. However, placebo-controlled studies have been conducted, which can inform us of mechanisms underlying MDMA-induced hyperthermia in humans, and the effects of potential future pharmacological interventions.

Surveys of drug-related emergency department admissions show that intravenous fluid replacement, and patient sedation with benzodiazepines are the most effective first response in patients presenting with acute drug-induced hyperthermia (Halpern et al., 2011). External cooling techniques such as fanning, icepacks, ice baths, and cooling blankets are also important for continued management of hyperthermia (Hall and Henry, 2006). The muscle relaxant drug dantrolene has also been used in extreme cases of hyperpyrexia (Grunau et al., 2010), however it does not work to inhibit the thermogenic effects of MDMA nor the pharmacological mechanisms of MDMA-induced hyperthermia in the brain (Rusyniak et al., 2004). Peripherally acting adrenergic receptor antagonists have proven to be useful in reversing increased temperatures induced by MDMA. Blockade of α-adrenoreceptors in human subjects was shown to reduce temperature, and blood pressure increases induced by MDMA (Hysek et al., 2013a). Furthermore, a combined α- and β- receptor blockade was also shown to reduce these MDMA-induced increases in humans (Hysek et al., 2012, Hysek et al., 2013b), and these results were also found in experimental animals (Kiyatkin et al., 2016). Kiyatkin et al. (2016) also

demonstrated that drugs acting centrally, such as the 5-HT_{2A} receptor antagonist clozapine, had greater hypothermic effects in the brain and body of rats when compared to peripherally acting adrenoreceptor antagonists (Kiyatkin et al., 2016). In humans, the centrally acting 5-HT_{2A} receptor antagonist ketanserin reduced MDMA-induced increases in body temperature (Liechti et al., 2000b), similar to previous results reported in animals (Nash et al., 1988). Furthermore, pretreatment with the selective NA reuptake inhibitor reboxetine attenuated MDMA-induced increases in body temperature in humans (Hysek et al., 2011), and pre-clinical data has shown that D_1 receptor antagonists could possibly contribute to the attenuation of MDMA-induced hyperthermia (Mechan et al., 2002), however this has not yet been evaluated in humans. Despite the wealth of human and animal data advocating the efficacy of both central and peripherally acting pharmacological interventions for MDMA-induced hyperthermia, there are some risks associated with their use (Liechti et al., 2000a, Hysek et al., 2010, Lange et al., 1990), and many have not undergone testing in clinical trials. Considering this, the current pharmacological strategies for treatment of MDMA-induced hyperthermia are limited. Therefore, there is a clear need for a pharmacological intervention for attenuating MDMA-induced hyperthermia in an emergency room setting.

1.10 Minocycline

1.10.1 History of origins

Since their discovery in the 1940's, tetracyclines have undergone many molecular modifications to enhance their antibacterial activity, tissue absorption and half-life (Stirling et al., 2004). The antibiotic properties of tetracyclines were initially described in the late 1940's, however more recently numerous studies have focused on their non-antibiotic properties as they have displayed a variety of biological actions independent of their antimicrobial activity. Minocycline (Fig. 1.8) is a second-generation tetracycline derivative with better

pharmacokinetic profile than first generation tetracyclines. When administered orally, it is rapidly and completely absorbed with a long half-life, good tissue penetration, and an almost complete bioavailability (Garrido-Mesa et al., 2013, Klein and Cunha, 1995). Minocycline is a highly lipophilic molecule that can pass through the blood-brain barrier (Brogden et al., 1975) and accumulate in the cerebrospinal fluid (CSF) and CNS (Kielian et al., 2007), enabling its use to treat many CNS diseases (Wang et al., 2003, Yong et al., 2004). It has been shown to provide neuroprotection from a wide range of neurodegenerative diseases including brain ischemia (Yrjänheikki et al., 1998), spinal cord injury (Stirling et al., 2004), and dopamine neurotoxicity caused by 6-hydroxydopamine (6-OHDA) and 1-methyl-4-phenyl-1,2,3,6-tetrahydropyridine (MPTP) (Du et al., 2001).

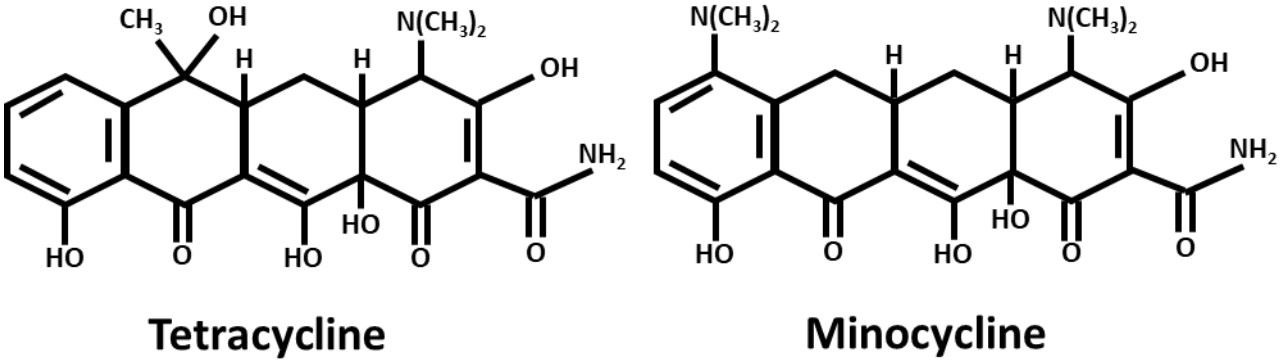

Figure 1.8: Chemical structure of minocycline and its parent, tetracycline.

1.10.2 Mechanisms of action of minocycline

Neuroprotective effects provided by minocycline are known to be related to its antioxidant, anti-inflammatory, and inhibitory glutamatergic effects not unrelated to its well-known anti-microbial properties (Dean et al., 2012). Minocycline causes an inhibition of microglial activation (Kim et al., 2009, Yrjänheikki et al., 1998, Dean et al., 2012) and release of subsequent cytotoxic substances. A high repeated dosing regimen of minocycline (90 mg/kg i.p. day 1, 45 mg/kg i.p. day 2-3) was shown to reduce IL-1β levels following traumatic brain injury (TBI) in mice (Homsi et al., 2009), and also in rats treated with MDMA (12.5 mg/kg,

i.p.) (Orio et al., 2010). Minocycline also reduces prostaglandin-E_2 (PGE_2) and inhibits cyclo-oxygenase-2 (COX-2) in a dose-dependent manner within murine microglia (Kim et al., 2004). It has also been shown to reduce prostaglandin-F2α ($PGF_{-2}\alpha$) and PGE_2 production induced by lipopolysaccharide (LPS) in primary rat microglial cells via down-regulation of microsomal prostaglandin-E synthase (mPGES-1) (Silva Bastos et al., 2011). Minocycline administration reduces TNF-α levels in the brain following administration of 3-nitropropionic acid in rats (Ahuja et al., 2008, Levkovitz et al., 2010). These neuroinflammatory markers have been previously linked to subsequent neurotoxicity of monoamine pathways in the brain of animals (Orio et al., 2010). There is also evidence to support the role of reduced glutamate excitotoxicity, reduced oxidative stress, and augmented neurogenesis in the mechanisms of action of minocycline (Fig. 1.9) (Dean et al., 2012). Minocycline's protective neuro-anti-inflammatory effects, as well as its direct effects within monoamine systems in the brain, have been described in both animal and human models of illegal drug use (Zhang et al., 2006, Orio et al., 2010, Sofuoglu et al., 2011).

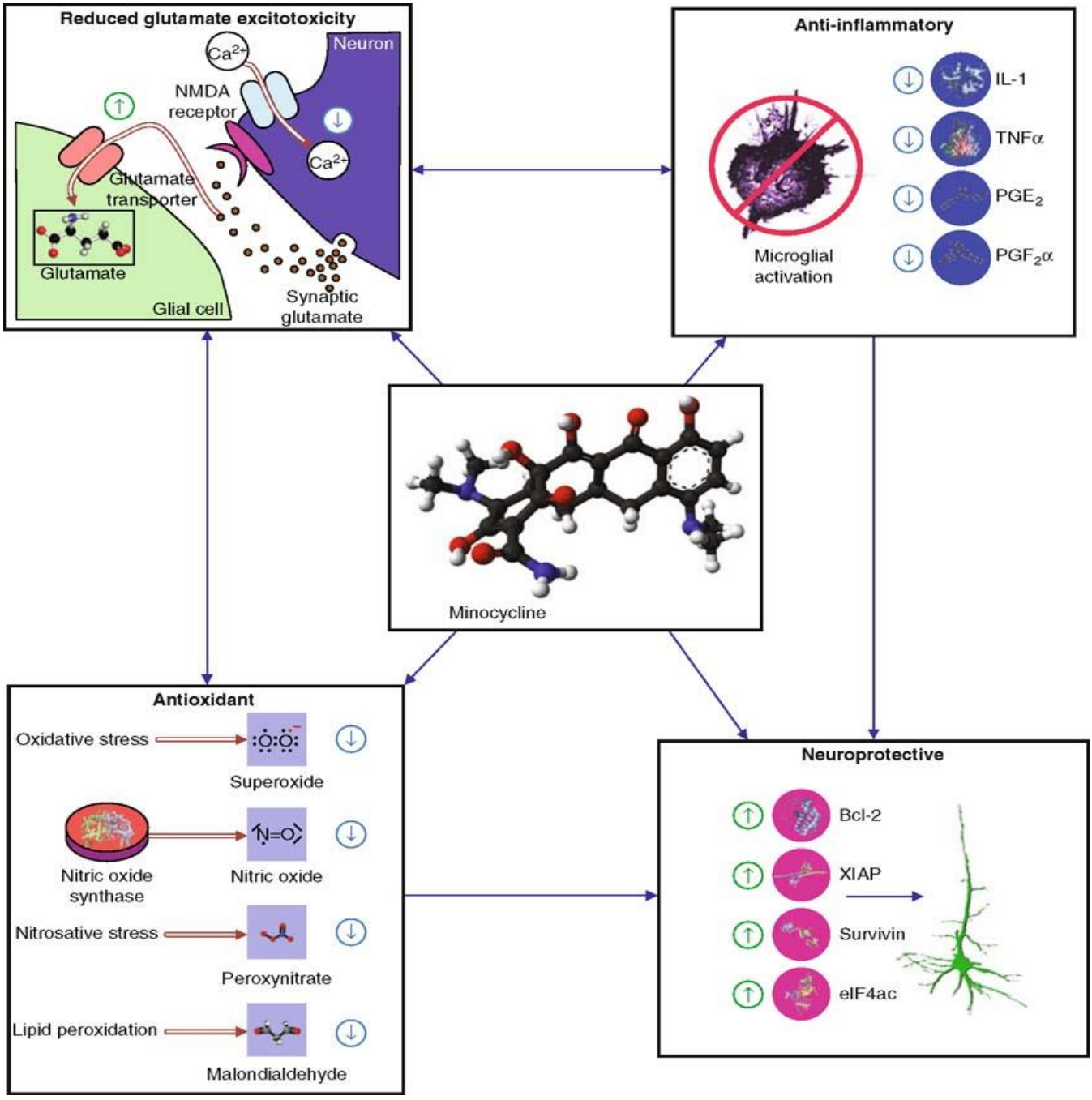

Figure 1.9: Proposed mechanisms of action of minocycline, including reduced glutamate excitotoxicity, inflammation, oxidative stress and augmented neurogenesis, targeted by minocycline. Derived from Dean et al. (2012).

1.10.3 Minocycline and amphetamines

Minocycline readily crosses the blood–brain barrier and its neuro-anti-inflammatory effects significantly impact 5-HT, DA, and glutamate transmission in the brain. In preclinical studies,

minocycline attenuates the development of behavioural sensitization to amphetamines (Kofman et al., 1990, Zhang et al., 2006), as well as the release of dopamine induced by amphetamines in the brain (Zhang et al., 2006). Furthermore, minocycline attenuates the reduction of dopamine transporters (DATs) caused by repeated amphetamine administration in the brains of monkeys (Hashimoto et al., 2007). These inhibitory effects are possibly mediated by minocycline's glutamatergic actions in the brain as minocycline has been shown to block behavioural responses mediated by NMDA-type glutamate receptors in both mice (Fujita et al., 2008) and rats (Levkovitz et al., 2007, Munzar et al., 2002). Minocycline reduces glutamate release in hippocampal neurons of rats (González et al., 2007) and increases phosphorylation and surface expression of $GluR_1$-type AMPA receptor subunits in mouse striatal neurons (Imbesi et al., 2008). In humans, minocycline attenuates the subjective rewarding effects of dextroamphetamine (DAMP), and reduces cortisol levels following DAMP or placebo administration in healthy volunteers (Sofuoglu et al., 2011). It has also been shown to improve responses to the sustained attention to response test (SART) in humans (Sofuoglu et al., 2011), a result supporting its previously demonstrated cognition-enhancing effects in animals (Fujita et al., 2008, Levkovitz et al., 2007, Levkovitz et al., 2010).

Minocycline offers neuroprotection in animal models of MDMA-induced neurotoxicity. Orio et al (2010) demonstrated that a twice daily repeated administration of minocycline over two days (45 mg/kg i.p. day 1, and 90 mg/kg i.p. day 2) prevented MDMA-induced NFκB activation, IL-1β release and microglial activation in the frontal cortex and prevented 5-HT neurotoxicity 7 days later. Similarly, Zhang et al (2006) showed that minocycline (40 mg/kg) attenuated the reduction of 5-HT and DA as well as the density of 5-HTT and DAT in the striatum after the repeated administration of MDMA. They also showed that minocycline attenuated the increase of activated microglia in the hippocampus and striatum (Zhang et al., 2006). Although these studies demonstrated that minocycline administration impacts

microglial activation, pro-inflammatory cytokine release and monoamine release in the brain, they also showed these changes had no significant effect on MDMA-induced hyperthermia. A two-day dosing regimen of minocycline (45 mg/kg first day and 90 mg/kg second day) had no effect on MDMA-induced hyperthermia causing no significant decrease in rat core body temperature (Orio et al., 2010). Similar results were obtained by Zhang et al (2006) who found that MDMA produced a significant hyperthermic response in core body temperature (+2.5 °C) that was not attenuated by minocycline. These results suggest that the neuroprotective effects of minocycline against MDMA-induced neurotoxicity are not due to a reduction in the body temperature that has been previously shown to exacerbate MDMA-induced neurotoxicity (Gordon et al., 1991, Broening et al., 1995, Brown and Kiyatkin, 2004). In contrast, Anderson et al (2011) showed that a 3 day dosing regimen of minocycline (50 mg/kg) was effective in attenuating MDMA-induced hyperthermia in Sprague-Dawley rats, whereas both one and two-day dosing regimens did not achieve this effect (Anderson et al., 2011). They also demonstrated that minocycline had no significant effect on brain or blood concentrations of MDMA (Anderson et al., 2011). These results indicate that minocycline's hyperthermia-attenuating effects are a time-dependent process requiring more than 48 h to achieve maximum effects.

1.11 Research Aims

1.11.1 Optical fibre temperature sensor development

The aim of this work was to develop an optical fibre-based point temperature sensor suitable for use in freely-moving animals. Previous studies investigating MDMA-induced brain hyperthermia have utilised thermocouple electrodes, which lack the advantages provided by light-based sensing. Practical use of previously developed optical fibre fluorescence temperature sensors *in vivo* was limited due to the use of bulk optics, and large benchtop spectrometers for analysis of changes in the optical signal. Other limitations included poor

probe durability, readout instability caused by vibration and environmental factors, as well as long-term measurement errors. In this work many systematic tests were performed to isolate the source of measurement instabilities, before making changes to both the optical configuration and sensor material make-up in accordance with these findings.

1.11.2 Publication 1: "Portable optical fibre probe for in vivo brain temperature measurements" (Biomedical Optics Express, 2016)

The aim of this study was to demonstrate proof-of-principle of a portable rare-earth doped optical fibre point temperature sensor in the brains of freely-moving animals. This work was a direct follow-up to our previous developmental work on an optical fibre point temperature sensor based on rare-earth thermometry (Schartner and Monro, 2014). In this study, brain temperature was recorded in saline treated rats for an extended time period to ensure that the sensor could accurately record brain temperature *in vivo* for the entire experimental duration post-drug administration. Optical fibre brain temperature measurements were also combined with body temperature monitoring using radiotelemetry with the intention of utilising this combined technology in future studies to investigate the thermoregulatory, and physiological effects of MDMA and minocycline in freely-moving rats.

1.11.3 Publication 2: "Improved method for optical fibre temperature probe implantation in brains of free-moving rats" (Journal of Neuroscience Methods, 2019)

There were two primary aims of this study. The first was to develop an improved method for optical fibre sensor implantation in freely-moving animals using conventional microdialysis materials. The second was to determine the acute temperature effects of MDMA in the rat brain using this improved optical fibre probe. This work was an extension of previous probe development efforts that developed an optical fibre point temperature sensor for brain

temperature recording in awake, freely-moving rats. A limitation of the previous method was the high risk of probe breakage prior to and during experimentation, particularly when the animal was administered MDMA, resulting in loss of time and resources spent replacing the sensor. Standard microdialysis probe materials were used in the revised probe structure to allow the implantation and removal of the fibre as a single piece. This was done to permit multiple insertion and removal procedures for each probe as well as high throughput animal experiments. This was also done to make the surgical implantation and handling of the optical fibre sensor as similar as possible to that of conventional microdialysis probes. The improved sensor was tested in MDMA-treated animals at high ambient temperature to investigate the hyperthermic effects of MDMA in the brain.

1.11.4 Publication 3: "Minocycline attenuates 3,4-Methylenedioxymethamphetamine induced brain hyperthermia (Accepted, European Journal of Pharmacology, 2019)

The aims of this study were three-fold. The first was to examine and compare the thermoregulatory and physiological effects of MDMA at both normal and high ambient temperature. The second aim was to examine the thermoregulatory and physiological effects of minocycline in response to MDMA-challenge at high ambient temperature. The third aim was to determine the relationship between brain and body temperature changes induced by minocycline and MDMA. This work using minocycline was an extension of the previous paper that demonstrated that MDMA induced a significant hyperthermic response in the brain at high ambient temperature. Minocycline has been shown to attenuate MDMA-induced hyperthermia in the body. I considered it important to understand its hyperthermia-attenuating effects in the brain, as well as the relationship between brain and body temperature change as the brain is the most temperature-sensitive organ in the body, and the most harmful effects of acute MDMA

administration relate to its modulation of neural activity in temperature regulatory circuits. In addition to this, radiotelemetry was used to measure the effects of minocycline on HR and LMA to gain a better understanding of its potential physiological and pharmacological mechanisms of action.

Chapter 2 – Optical fibre temperature sensor development

2.1 Introduction

Monitoring of physiological parameters such as temperature within the body is a process that requires purpose-built tools in order to achieve accurate and specific monitoring outcomes, especially in areas such as the brain that performs a critical role in controlling body temperature. Currently, experimental brain temperature monitoring *in vivo* is typically performed utilising thermocouple electrodes capable of region-specific brain temperature measurement (Kiyatkin et al., 2016, Kiyatkin et al., 2014, Brown and Kiyatkin, 2004). However, optical fibre sensors present an alternative to many conventional techniques for the real-time *in vivo* monitoring of many physiological parameters. Their small size and inert glass composition make them suitable for minimally invasive implantation in small brain regions, and their ability to provide multiplexed sensing allows for the probing of many different physiological processes within the one system. Despite this, many of the different techniques previously used to perform temperature sensing utilizing optical fibres are unsuitable for region-specific *in vivo* monitoring in the brain due to issues with their resolution (Rao, 1997), long-fibre length requirements (Lee and Nishii, 1998), and sensitivity to changes in environmental conditions (Guan et al., 2006).

As previously discussed in section 1.8.3, one promising alternative method for temperature measurement utilising optical fibres involves rare-earth absorption and fluorescence monitoring. However, previous methods utilising upconversion emission as a temperature indicator have often been based on bulk glass samples (Chen et al., 2015), uniformly-doped optical fibres (Da Silva et al., 2000, Dos Santos et al., 1999) or doped microspheres (Cai and Xu, 2003). While these doped sensors can carry certain advantages, like the previous methods they lack the ability to perform measurements with a high spatial precision limiting

their *in vivo* application where spatially precise measurements are required. This limitation led to the recent development of a high spatial resolution fibre-tip sensor for localised temperature measurement based on rare-earth thermometry (Schartner and Monro, 2014).

The point temperature sensors described here (Schartner and Monro, 2014) were fabricated by briefly immersing the tips of silica multi-mode fibres into Er:Yb co-doped tellurite glass, which greatly minimized the size of the temperature sensitive region of the probe compared to uniformly doped fibres or bulk glass samples. *In vitro* experiments using this probe displayed a good correlation between reference temperatures and the fluorescence ratio of the Er:Yb doped samples for the duration of measurements with the measured change in fluorescence ratio approximated as linear with a short-term resolution of <0.1 °C (Fig. 2.1). However, the long-term accuracy of this sensor was approximated at 0.1-0.3 °C due to stability drift associated with long-term measurements. These results demonstrated a new approach to localised temperature measurement based on a probe at the tip of an optical fibre (Schartner and Monro, 2014). The localised temperature sensitive region in addition to the minimal excitation power requirements of the probe suggested it was suitable for *in vivo* sensing applications due its high spatial resolution and minimized risk of cell damage.

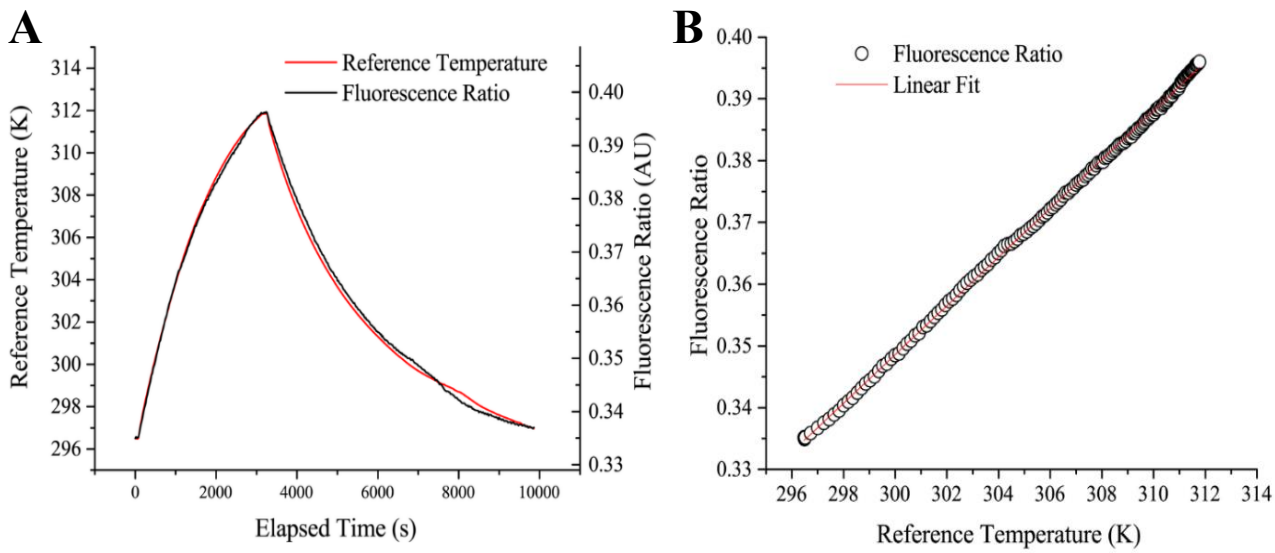

Figure 2.1: A: Erbium ytterbium-doped multi-mode fibre response with a co-located reference resistance temperature detector (RTD) inside an incubator. **B:** Linear regression of fluorescence ratio *vs.* reference temperature for increasing temperature. Derived from Schartner and Monro (2014).

As a part of my honours research, we attempted to utilise this sensor for brain temperature measurement in live animals, however, the transition of this sensor from *in vitro* to *in vivo* sampling presented numerous challenges. Similar to *in vitro* results of the previous study, long-term drift in probe FIR readings, and increasing levels of noise were apparent in the later stages of *in vivo* brain temperature recording (Fig. 2.2). These increased levels of noise and long-term drift resulted in observed brain temperature fluctuations of between approximately 1.5 to 2 °C towards the end of each animal experiment. The unsheathed glass fibres were also extremely susceptible to twisting and breakage during periods of increased animal movement resulting in the loss of the sensor and premature termination of experiments. Prior to breakage, fibre twisting was also seen to cause large observed temperature artefacts as the fibre was bent too close to its critical bend radius resulting in reductions in light transmission to the spectrometer (Fig 2.3).

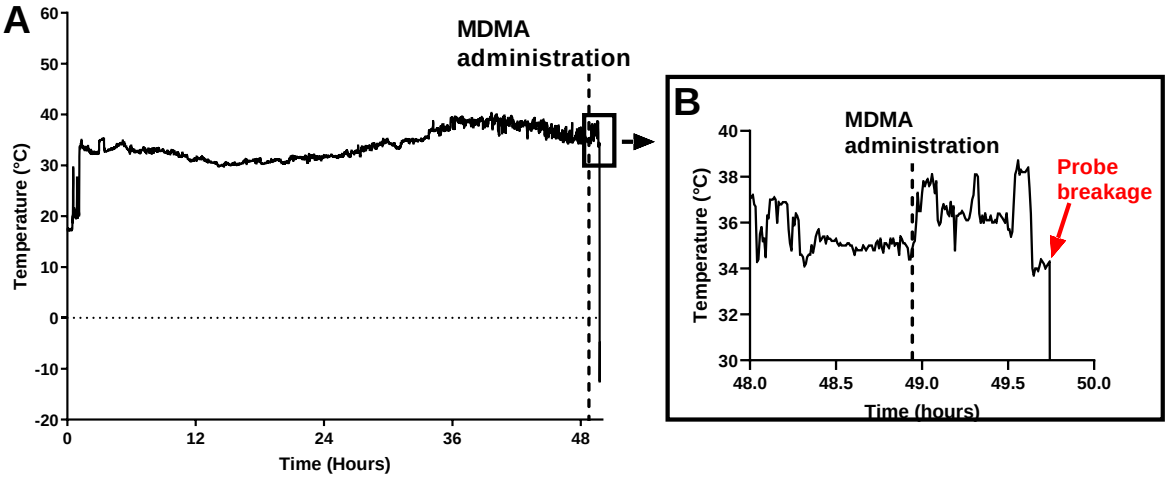

Figure 2.2: A: Brain temperature readout obtained from fibre optic probe implanted in rat brain. Subject was pre-treated with saline during the recovery period mimicking a therapeutic drug pretreatment schedule and received MDMA (10 mg/kg, i.p.) at approximately 49-h. **B:** Final 2 hours of the experiment. Probe breakage occurred approximately 45 min post-MDMA following increased levels of animal movement.

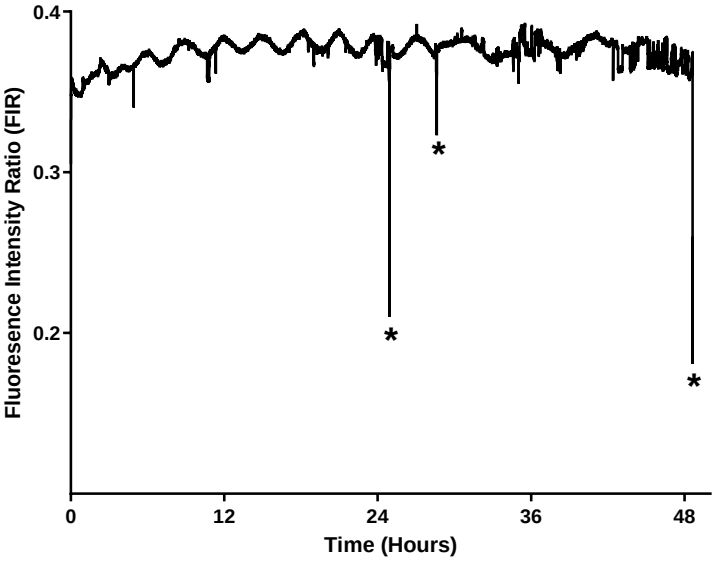

Figure 2.3: FIR readout obtained from fibre optic temperature sensor implanted in rat brain. Subject was pre-treated with saline during the recovery period mimicking a therapeutic drug pretreatment schedule. * depicts time points where the fibre was twisted excessively causing the detector to detect a false FIR drop.

Based on these *in vivo* experiments, the temperature sensor in this configuration was deemed unsuitable for *in vivo* use in freely-moving animals. The dramatic changes in observed temperature caused by animal movement, fibre bending, long-term drift, and increased noise levels, resulted in very low probe stability, well outside of the target resolution of 0.1 °C that

would make it suitable for biological applications. This paired with its low durability and susceptibility to breakage during animal movement made the current fibre structure and optical configuration unsuitable for *in vivo* sampling.

Considering these limitations, the first aim of this PhD project was to further develop the stability and durability of this optical fibre point temperature sensor to increase its suitability for *in vivo* use. We also aimed to adapt the configuration to a more portable setup to facilitate its deployment outside of a conventional optics laboratory. This was achieved through many sequential changes to the probe structure and sensing configuration following the identification of the limiting features of the setup. This step-by-step developmental process is described in detail below.

2.2 Durability improvements

2.2.1 Signal bending-loss – High Numerical Aperture fibre

As mentioned previously, early iterations of the optical fibre temperature sensor suffered drawbacks related to its use in freely-moving animals. Previous *in vivo* experiments demonstrated that probes fabricated with standard single-mode (SM) fibres were susceptible to false FIR changes caused by animal movement-induced fibre bending (Fig. 2.3). Bending modifies the guiding properties of optical fibres causing loss increasingly as the fibre is bent closer to its critical bend radius (Jay, 2010). Light can "leak out" of the fibre as it bends, and as the bend becomes more acute, more light leaks out. In our application, this reduction in signal due to bending expressed itself as a shift in observed temperature. Although the FIR method is usually independent of factors such as bending and power change, this was not exactly the case in our application as the changes we measured were relatively minor and only over a small temperature range. This therefore increased the sensitivity of the temperature sensor to bending losses and changes in power with only a 3-4% change in FIR needed to

amount to a significant 0.5 °C change in observed temperature at 37 °C. This magnitude of temperature discrepancy was well outside of the probes' required resolution of 0.1 °C and unacceptable for biological measurements as even small observed changes in temperature are viewed as significant, especially within the brain. In an attempt to remedy this, we used high numerical aperture fibre during subsequent probe fabrications and tested its ability to reduce the effects of bend-loss in subsequent *in vitro* experiments.

The numerical aperture of an optical fibre is a number that describes the range of angles prior to its critical angle at which incoming light can be totally reflected into the fibre core. If the light exceeds this critical angle outside of its numerical aperture, it undergoes refraction outside of the fibre core and into the cladding. Optical fibres with a high numerical aperture have an increased acceptance angle of light entering the fibre and thus allow the transmission of light at a more acute angle when compared to ordinary multi-mode (MM) or SM fibres and are thus less susceptible to bend-induced signal loss (Harris and Castle, 1986). A standard single mode fibre has a numerical aperture of approximately 0.13. To reduce the effects of bend-loss on our FIR data, we tested probes fabricated with commercially available ultra-high numerical aperture (UHNA) fibre with a NA 0.35. The high numerical aperture optical fibre probe was placed inside an incubator maintained at approximately 39 °C. Light from the laser was transmitted through an unbent fibre to establish control temperature values. The fibre was then bent around a mandrel of 8 to 16 mm in diameter a total of 5 full turns while kept under slight tension to remove slack. Temperature data was recorded from the probe whilst under varying bend intensities (Fig. 2.4).

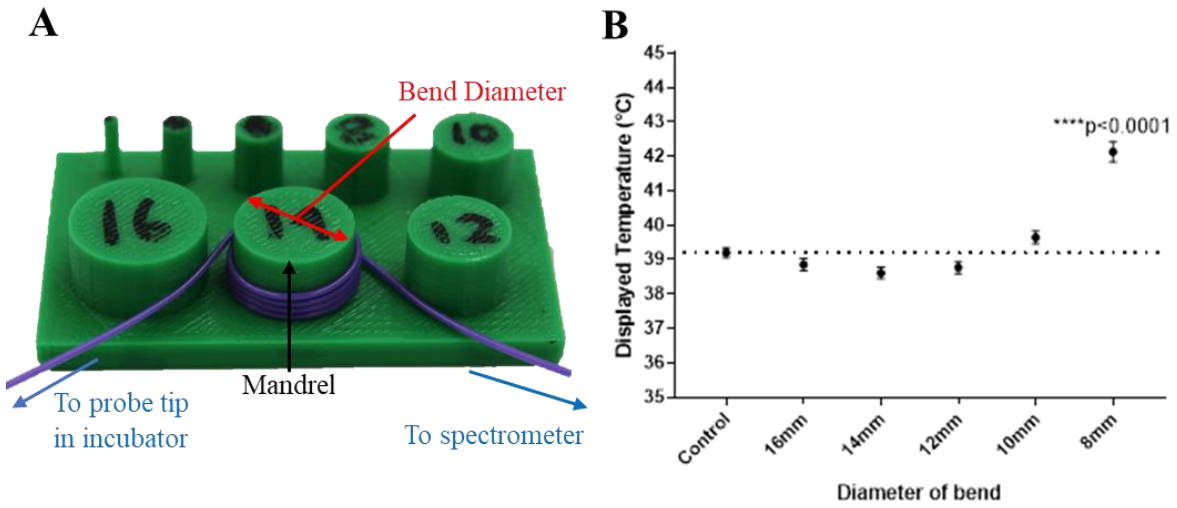

Figure 2.4: A: Photo of the bend-loss measurement setup; the variable (the bend diameter) is indicated in red. **B:** Temperature recorded by optical fibre probe at various bend diameters compared to unbent fibre temperature of 39 °C.

These experiments demonstrated that high numerical aperture fibre had a critical bend radius of approximately 8 mm. Slight changes in observed temperature were observed at bend diameters ranging between 10 to 16 mm however these changes were deemed insignificant. At an 8mm bend diameter however, a significant deviation was present with observed temperatures reaching approximately 42 °C, 3 °C higher than the bath temperature indicating significant bend-loss. Although these results showed a significant change in observed temperature change at an 8 mm bend diameter, this change was significantly reduced compared to previous *in vivo* experiments using SM fibres (Fig. 2.3) that displayed a much higher influence of fibre bending on observed FIR values. Although the use of high numerical aperture fibre dramatically reduced the probes' susceptibility to bend-loss, it did not eliminate it entirely, nor did not remove the greater issue of stability drift over the course of long-term measurements (Fig. 2.5). Considering this, high numerical aperture fibre was unsuitable for use during probe fabrication due to the long recording and recovery associated with our *in vivo* experimental protocol. However, following these experiments subsequent mechanical improvements were made to fabrication materials and methods to increase the probes durability during *in vivo* experimentation, and reduce its susceptibility to coiling caused by increased animal movement.

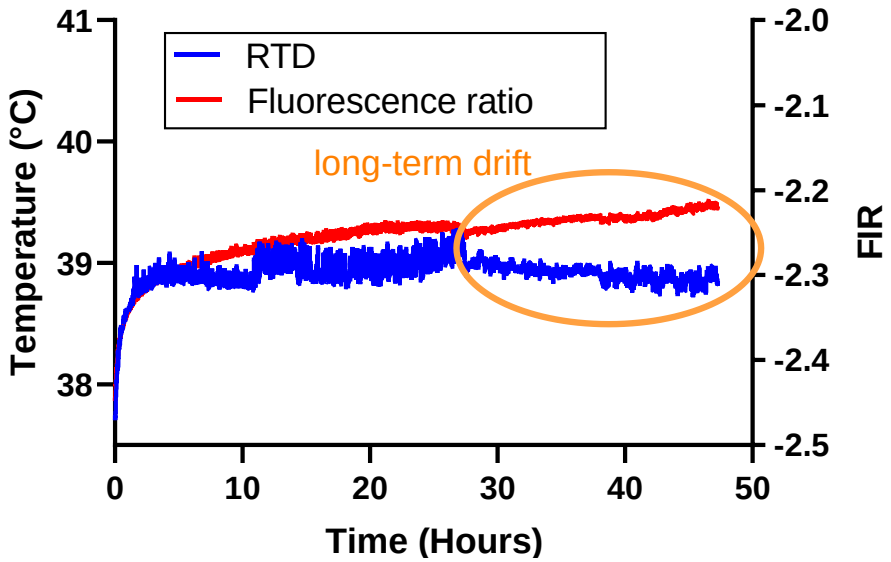

Figure 2.5: UHNA erbium:ytterbium doped optical fibre temperature sensor FIR response with co-located RTD. Probe measurements were performed inside an incubator maintained at a constant temperature.

2.2.2 Animal movement-induced fibre coiling and breakage - Splice procedure

One of the main fabrication procedures altered from the original probe fabrication methods was the probe splicing technique. The original probe fabrication technique used a Fujikura arc splicer FSM-100 (Fujikura Ltd, Tokyo, Japan) to splice the front length of fibre containing the probe tip with a separate fibre length containing the connectorised patch cable to allow easy integration of the probe with the measurement equipment (Fig. 2.6). To fabricate the front portion of this probe, one meter of fibre was cut and the front end of the fibre was inserted into a needle cut to a length of 4 mm, cleaved, and then glued inside the needle body with approximately 2 mm of fibre protruding from the end to act as the probe tip. 15 mm of polymer coating was stripped from the back end of this fibre as well as from a separate fibre length containing the connectorised patch cable. Both stripped portions of the fibres were cleaned with isopropanol and set in a fibre holder so their ends could be cleaved using a high precision cleaver (Fujikura CT-30). The fibre probe was spliced together with the patch cable using the arc splicer and the splice location protected using heat-shrink tubing (Fig. 2.6).

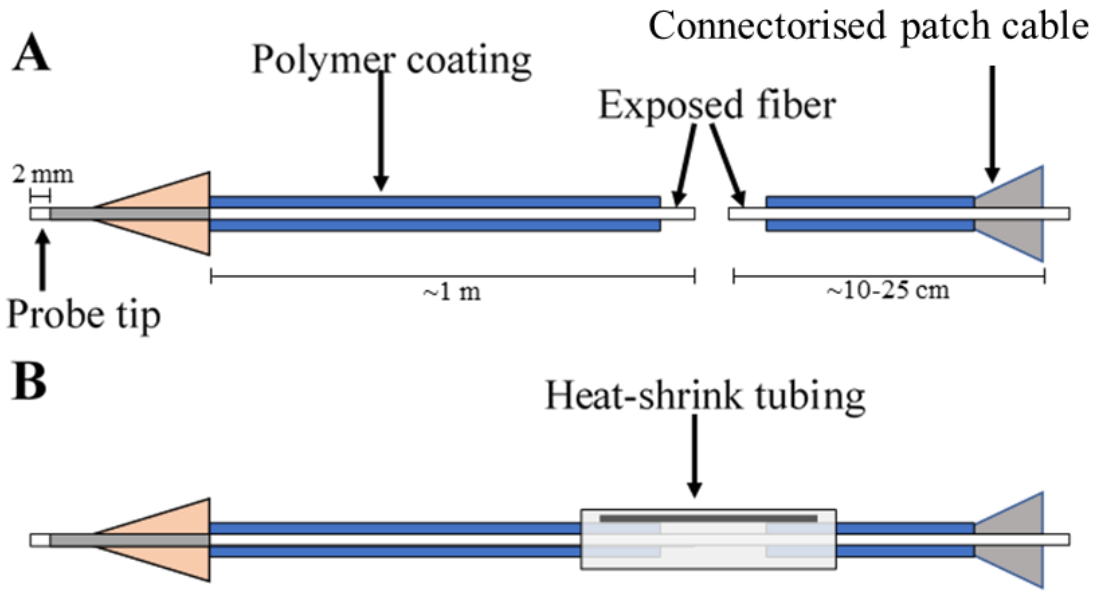

Figure 2.6: Diagram of fibre probe and patch cable fibre. **A.** Pre-splice. **B.** Post-splice.

The arc-splicer automated splice routine calculates the estimated loss from a splice, which in most cases is a negligible value, as seen in Fig, 2.7A. However, in some cases, hotspot bubbles and misalignment occurred during splicing procedures due to contaminated fibre end-faces, poor fibre cleavage, and slippage during end-face heating and fibre push (Fig. 2.7B/C). When this occurred, it often resulted in higher estimated splice loss. This required the splice to be broken, and the splice process repeated until negligible loss values were acquired. This required re-cleaving and re-splicing the fibre which resulted in shorter fibre lengths, and longer fabrication times. A longer fibre lead gives more room for the fibre to coil during animal movement, and thus longer fibre lengths are less susceptible to coiling-induced breakage. Continued re-splicing of the probe often resulted in significantly shorter fibre lengths, and this made the probe much more susceptible to bending and eventually breakage via excessive coiling.

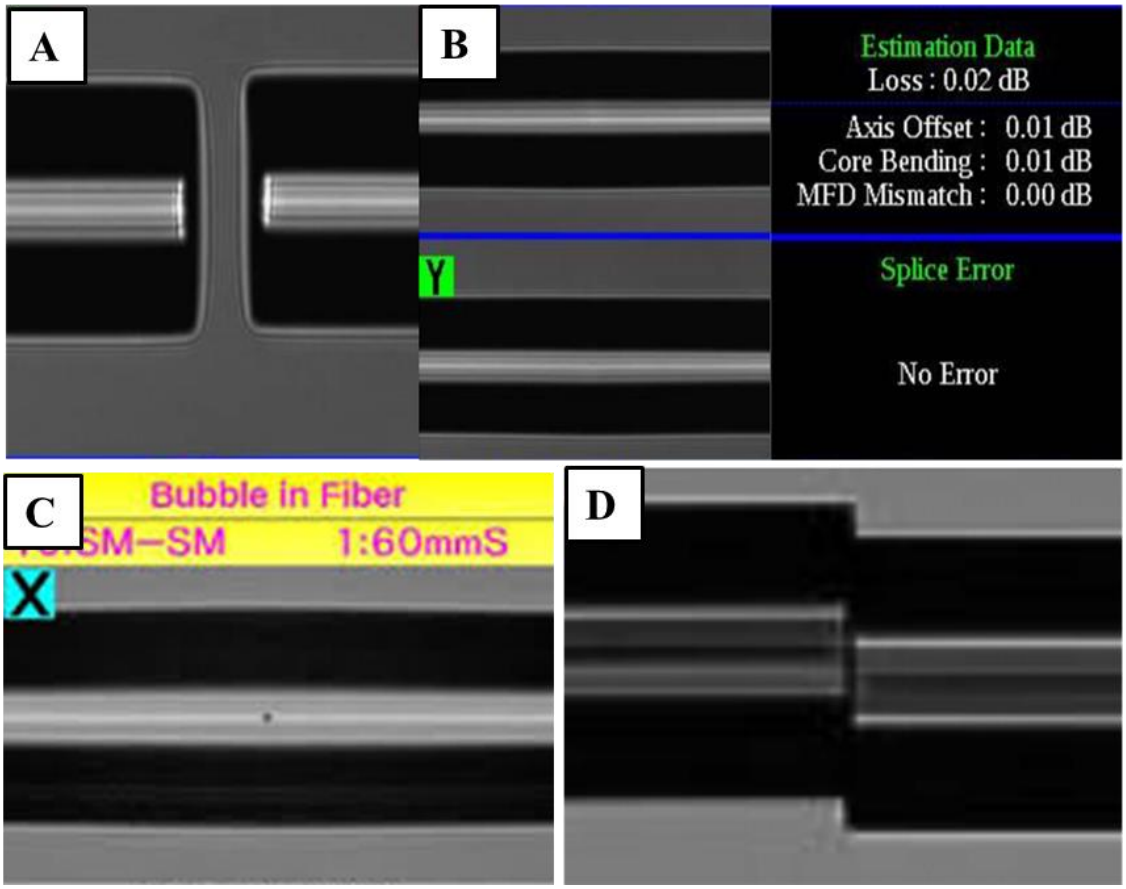

Figure 2.7: A. Arc splicer image of fibre before splicing. **B.** Arc splicer image of fibre after splicing with estimation and error data. **C.** Arc splicer image sowing bubble present at splice location that can occur due to contaminated fibre end-face or poor fibre cleavage. **D.** Misaligned fibre due to slippage during fibre push prior to splicing.

In addition to this, the heat-shrink tubing protecting the exposed splice location was the primary location for fibre twisting and breakage during animal movement (Fig. 2.8). The heat-shrink protector impeded the ability of the fibre to coil during *in vivo* experiments, thus the probe broke on several occasions at either side of tubing protecting the splice location. To remedy this, the temperature sensor was fabricated at the front end of a 2 m length of continuous cable with a more robust 900 μm outer cladding that included the connectorised patch cable. This removed the necessity for splicing that was present in the original temperature sensor fabrication method. The removal of splicing significantly increased the average length each probe which aided its ability to coil during animal movement and removed the splice location

which drastically reduced the probes susceptibility to breakage. The use of this altered probe fabrication method dramatically decreased the number of probe breakages that occurred during follow up *in vivo* trials and allowed for increased experimental throughput.

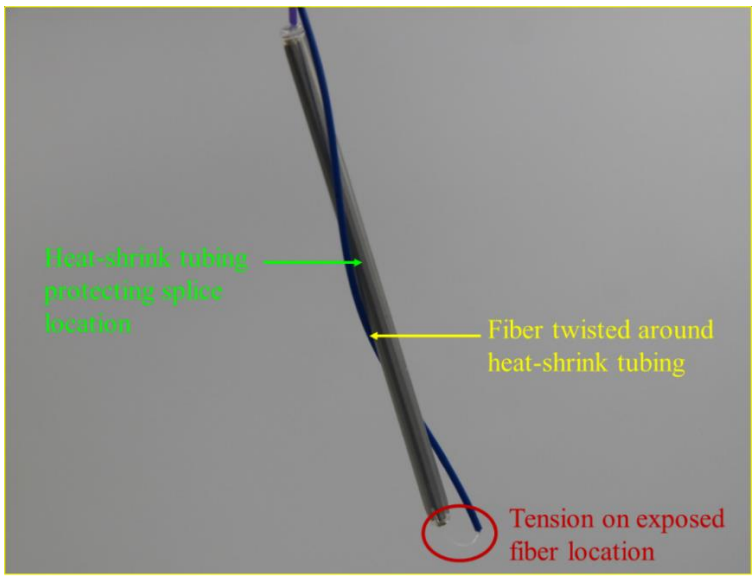

Figure 2.8: Image of optical fibre twisted around heat-shrink tubing protecting the splice location.

2.3 Long-term stability improvements

As mentioned previously, the original optical configurations (Fig. 2.9) were sensitive to environmental changes, and stability drift over the course of long-term measurements, which affected the long-term accuracy of system (Fig 2.10). Several changes were made to the equipment used in the optical set-up to remedy these stability issues. Additional changes were also made in order to reduce the benchtop footprint of the optical setup in the restricted laboratory space and increase its portability. This was mainly achieved by removing any bulk and free-space optical equipment that was present in the original optical configuration, thus reducing the size of the set-up and removing the need for the alignment of any optical components.

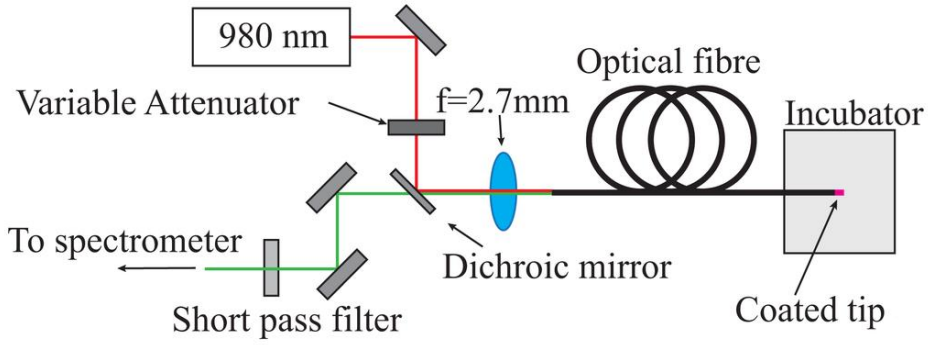

Figure 2.9: Previous bulk optics configuration for optical fibre temperature measurements from Schartner and Monro (2014).

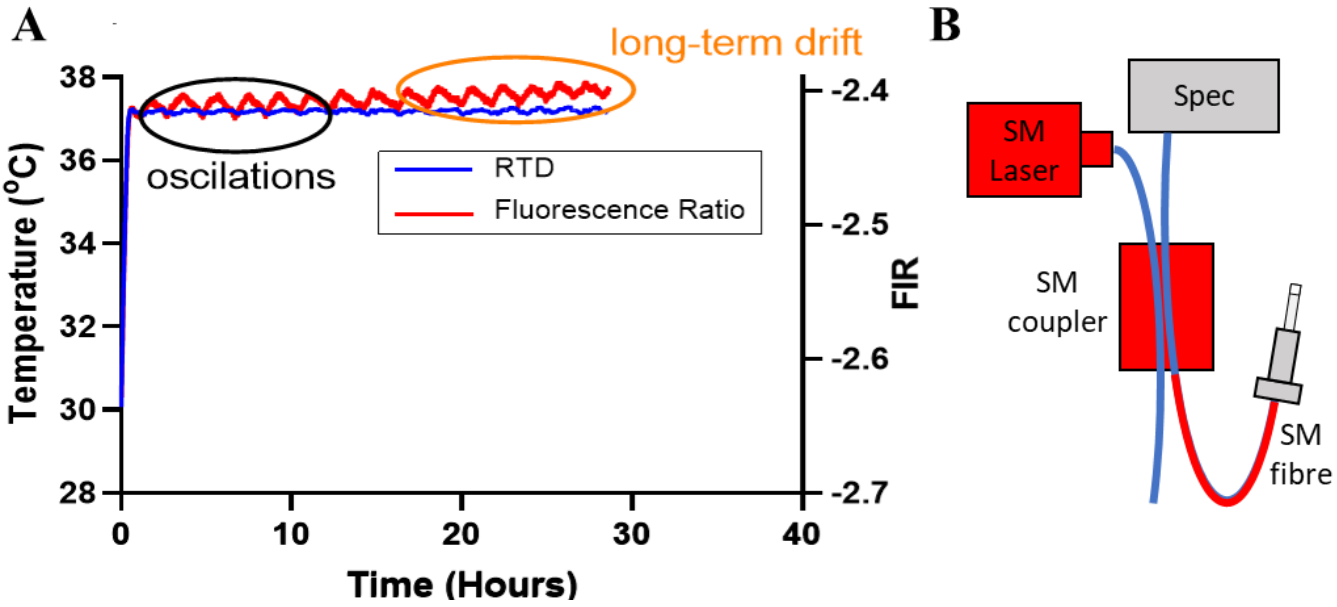

Figure 2.10: A. Erbium:ytterbium doped optical fibre temperature sensor FIR response with co-located RTD. Probe measurements were performed inside an incubator maintained at a constant temperature. Long-term drift of the FIR readings was observed during the later stages of the experiment. Periodic oscillations caused by shifts in lab ambient temperature were also observed throughout the duration of the experiment. **B.** Diagram of components of optical configuration. SM components of the sensing configuration are highlighted in red.

2.3.1 Need for alignment - Short-pass filter

One of the first changes made to the configuration involved the short-pass filter. Like the previous configuration, the output port of the fibre coupler was passed through a short-pass filter to remove the residual pump light. However, in the new set-up this filter was situated inside of a lens tube in order to remove the need for its alignment. As previously mentioned,

many changes were made to the optical configuration to reduce its size, increase its portability, and facilitate its use in a medical research laboratory. The removal of the majority of the bulk optics, and any equipment that required careful alignment was crucial for the probes' deployment in our laboratory, which lacked access to optical tables that would normally enable the alignment of these components with mounting holes and provide a vibration dampening surface (Fig. 2.11).

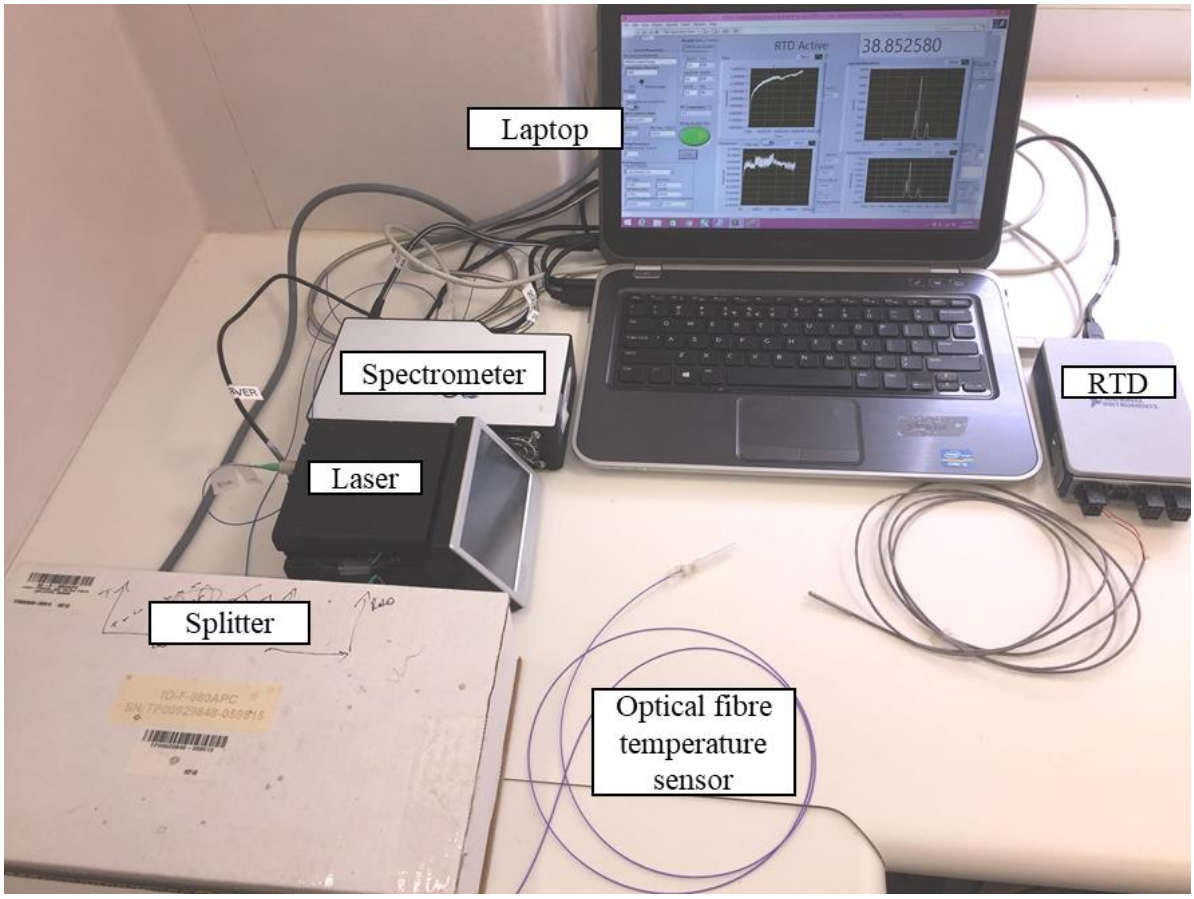

Figure 2.11: Labelled photograph of the components of the portable optical fibre temperature sensing configuration. Removal of most bulk optics and aligned equipment allows the configuration's deployment outside a conventional optics laboratory.

2.3.2 Laser signal variability - Excitation source and isolator

The optical configuration of the original sensor used a 980 nm pigtailed SM laser diode as the source of excitation for the Er:Yb co-doped fibre tips (Schartner and Monro, 2014). The

continued use of a 980 nm laser source and two-photon upconversion in the improved optical configuration was advantageous compared to direct excitation of ions at lower wavelengths as this minimised the potential for local heating at the end face of the fibre tip. This end-face heating may have affected the validity of temperature data gathered and damaged the cells surrounding the probe tip in this area.

Unlike the original configuration, we also introduced an isolator into the system to reduce signal variability from the laser. This significantly reduced back-reflected light and prevented it being coupled back into the laser diode. If this were to occur, it would cause instabilities in signal emission from the laser which could also potentially influence the accuracy of temperature measurements.

Although a 980 nm laser was maintained as the excitation source, initial systematic tests revealed the pigtailed SM diode to be the source of some stability issues with the new portable set-up. *In vitro* tests revealed that ratiometric temperature was susceptible to changes in laboratory ambient temperature despite the probe being located within a temperature-controlled incubator (Fig 2.10). Further tests established that these periodic oscillations caused by ambient temperature changes correlated with changes in laser voltage (Fig 2.12).

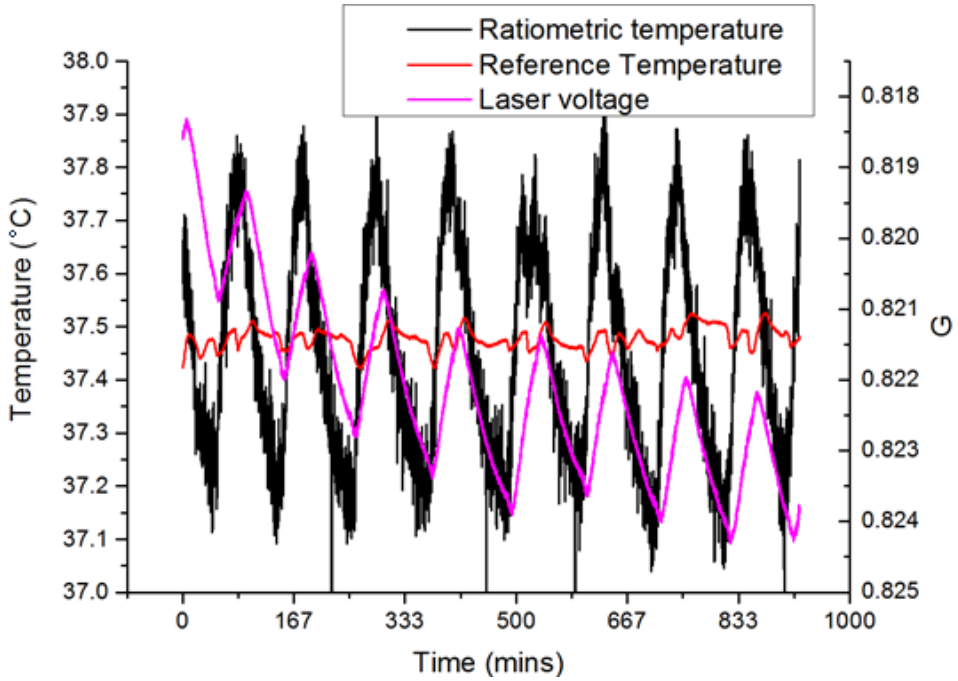

Figure 2.12: SM configuration Erbium:ytterbium doped optical fibre temperature sensor temperature FIR and laser voltage response with co-located RTD. Probe measurements were performed inside an incubator maintained at a constant temperature.

To remedy this issue, the original SM diode was replaced with an equivalent polarisation maintaining (PM) diode and a similar *in vitro* experiment was conducted (Fig. 2.13). Our results showed that the configuration with the PM diode was less susceptible to environmental changes as no fluctuations in probe observed temperature occurred in response to changes in laboratory ambient temperature. However, these results also showed that the PM diode did not improve the long-term stability of the measurements as FIR readings still showed increasing drift away from temperature values towards the end of the experiment This remaining instability of long-term measurements suggested that the cause of instability in the system could be associated with drift in the polarisation of light through the coupler and variance in the returned fluorescence signal over time. Further changes to the system were therefore required to remove these long-term stability issues.

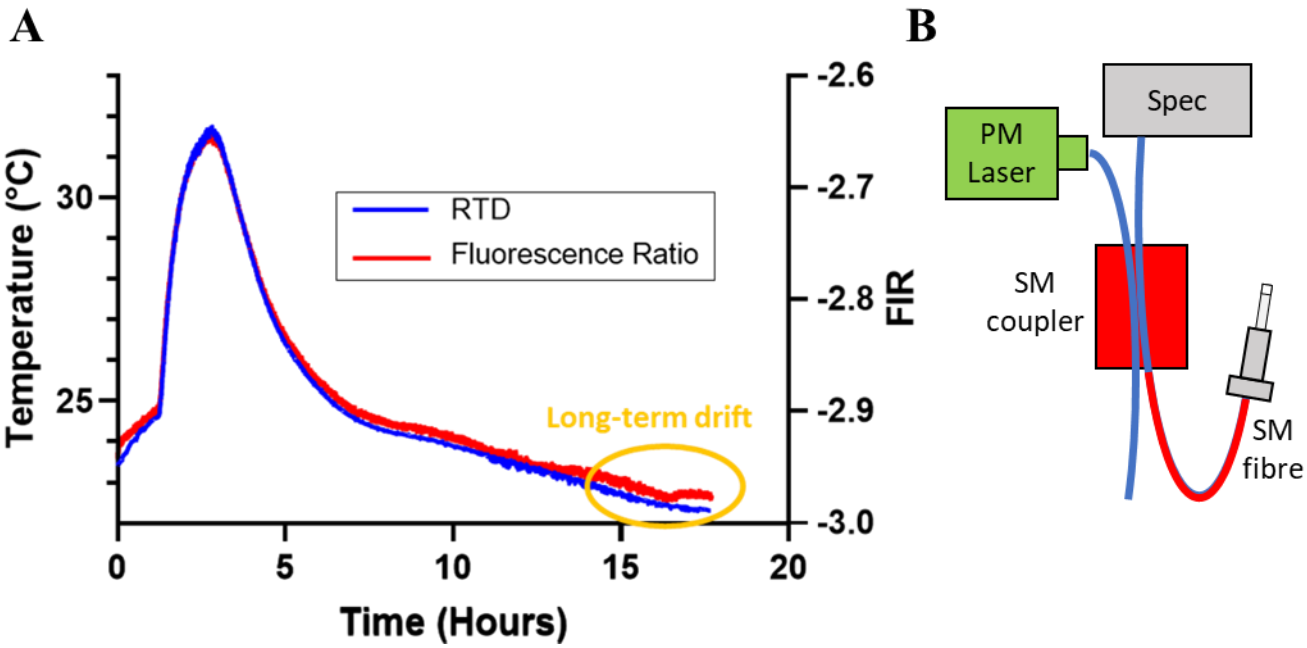

Figure 2.13: A. Optical fibre temperature sensor FIR response with co-located RTD. Probe recording was performed inside an incubator with temperatures cycled from high-low over the duration of the measurements. **B.** Diagram of components of optical configuration. SM components of the sensing configuration are highlighted in red; PM components are highlighted in green.

2.3.3 Long-term stability drift - Coupler changes

In the original probe configuration used by Schartner and Monro (2014), light that passed from the probe tip through the fibre was coupled into a spectrometer for spectral analysis using a SM coupler. The coupler is a key component required for high-precision measurements using fluorescence-based optical fibre sensors. If coupling of laser light, or returned fluorescence signal varies over time, then the collected signal becomes unreliable, which leads to errors in the measurement. The updated portable configuration also used a standard SM coupler, and as we have already shown, measurements conducted with this configuration were affected by long-term stability drift (Fig. 2.10) even when employed with a PM diode (Fig 2.13). To remedy this issue, we experimented with replacing this SM coupler with an equivalent PM fibre coupler. PM fibre is a type of SM optical fibre in which linearly polarized light entering the fibre maintains its polarisation as it propagates through and then exits the fibre. Unlike in standard SM optical fibres, PM fibre prevents crosstalk between vertical and horizontal

polarisation modes travelling within the fibre as a result of bending and random fibre birefringence. This prevents changes to the output polarisation state of light travelling within the fibre over time, and therefore prevents long-term inaccuracies in gathered data. The coupler we tested was a 99:1 PM splitter with the probe connected to 1% output of the splitter. The original configuration used a dichroic mirror for this application (Fig. 2.9); however, this required the configuration to contain a free-space optics sections which required alignment, drifted with changes in environmental temperature, and was non-conducive to the increasing portability of the set-up. Similar to previous *in vitro* tests, the temperature sensor was co-located in a temperature-controlled incubator with an RTD and temperatures recorded for the duration of the experiment (Fig. 2.14). Results of this test demonstrated that use of the PM coupler in addition to the PM diode still did not aid in improving long-term stability of the measurements compared to our previous results using SM couplers. Significant separation was still present between FIR and temperature readings towards later hours of the experiment and this drift equated to observed temperature differences of approximately 1 °C away from real temperature values. This differential was unacceptable for *in vivo* brain temperature measurements and therefore one final change was made to the sensing set-up to ensure the long-term accuracy of the system.

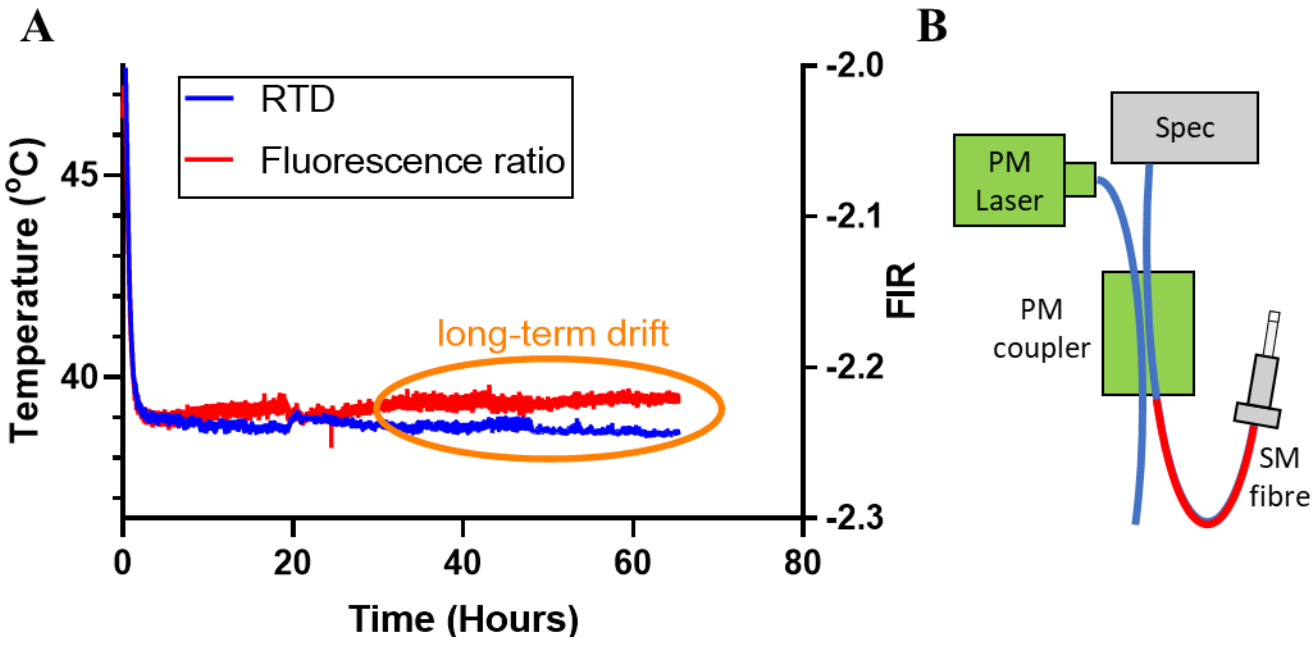

Figure 2.14: A. Optical fibre temperature sensor FIR response with co-located RTD. Probe measurements were performed inside a temperature-controlled incubator. **B.** Diagram of components of optical configuration. SM components of the sensing configuration are highlighted in red; PM components are highlighted in green.

2.3.4 Removing long-term polarisation drift - PM fibre

As mentioned previously, the original probe configuration (Schartner and Monro, 2014) utilised temperature sensors fabricated with multimode fibres to perform temperature measurements i*n vitro*. Although trials using these temperature sensors showed a good correlation between the measured temperature and the fluorescence ratio (Fig. 2.1), a slight separation between FIR readout and measured temperature occurred over the course of long-term measurements. This separation was also observed when using standard SM fibres as previously demonstrated in all of our *in vitro* fibre tests. In principle, use of a PM diode and coupler in this configuration could provide stable long-term measurements and preserve polarisation of light without PM fibre provided the SM fibre displayed a completely symmetrical design free from imperfections with no influence of fibre bending (Gordon and Kogelnik, 2000). However, fibre imperfections permeate nearly all optical fibres making some amount of birefringence unavoidable and this can affect the polarisation state of light along the

fibre length over time and lead to measurement inaccuracies (Gordon and Kogelnik, 2000). Considering stability improvements provided by inclusion of a PM diode and coupler, we decided to switch to an all PM portable configuration, which employed use of PM fibre as opposed to MM or SM fibre during probe fabrication (Fig. 2.15).

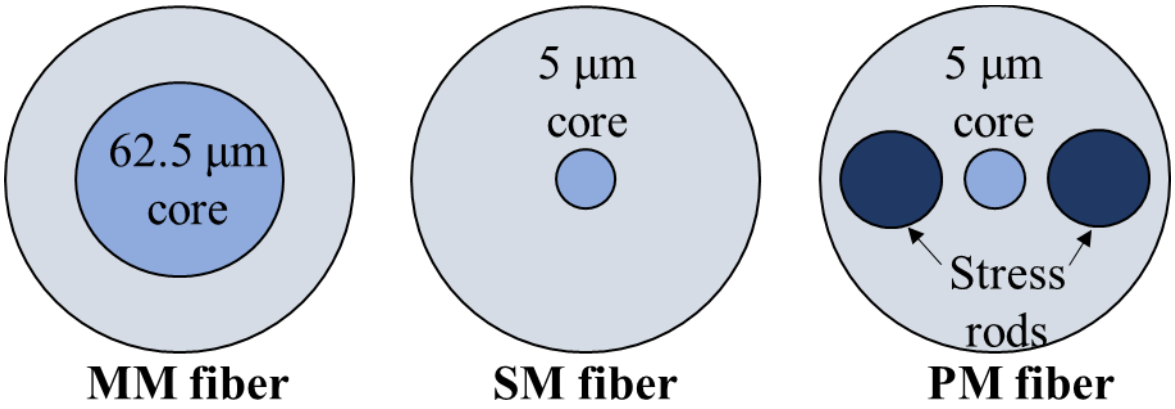

Figure 2.15: Cross-section of 3 different types of optical fibre.

To test the impacts of fabricating temperature sensors using PM fibre, the PM fibre temperature sensor was co-located in a temperature-controlled incubator with an RTD and temperatures recorded for the duration of the experiment (Fig. 2.16).

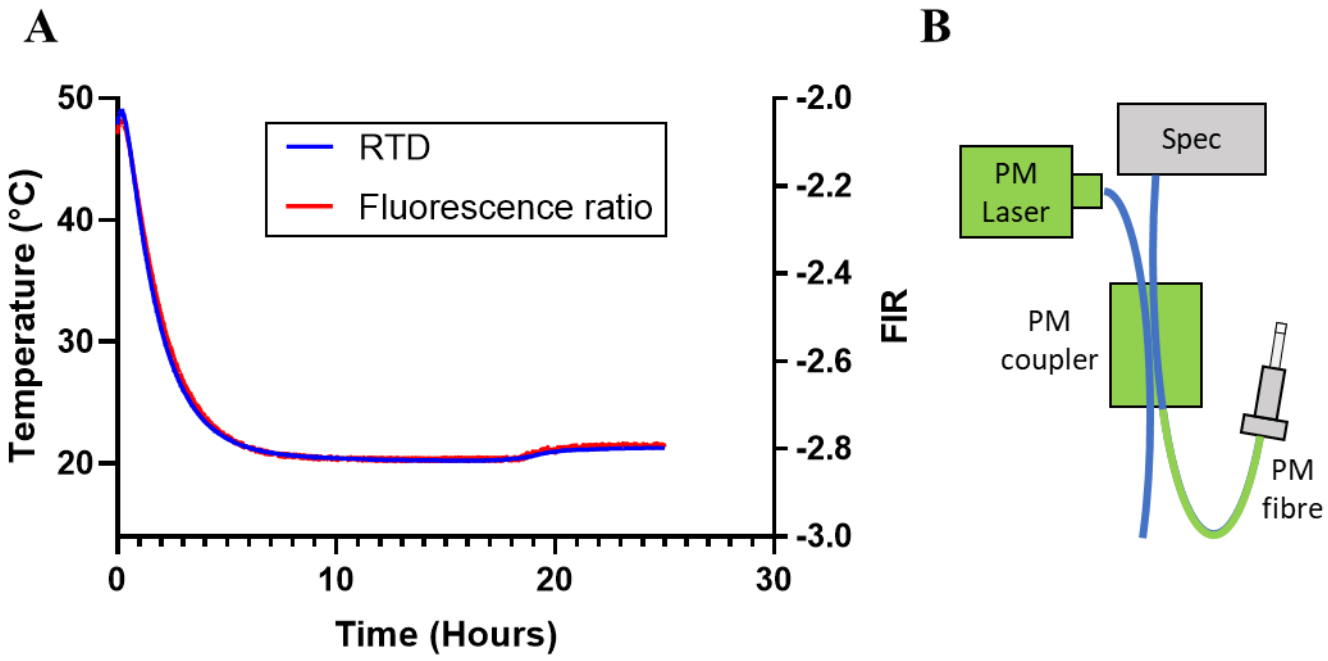

Figure 2.16: A. All PM configuration erbium:ytterbium doped optical fibre temperature sensor FIR response with co-located RTD. Probe measurements were performed inside a temperature-controlled incubator. **B.** Diagram of components of optical configuration. PM components of the sensing configuration are highlighted in green.

Results from this test clearly demonstrated the increased stability in long-term measurements provided by the all-PM configuration compared to previous configurations using MM, UHNA or SM fibre types. At no point during the recording were probe FIR readings significantly separated from recorded RTD temperature, even during later periods of the experiment where stability drift was previously seen to be at its peak. Using the all-PM configuration, the measured change in fluorescence ratio could be approximated as linear over the biologically relevant range with an R^2 of 0.998 (Fig 2.17) with no drift from the reference values occurring over the course of the long-term measurement.

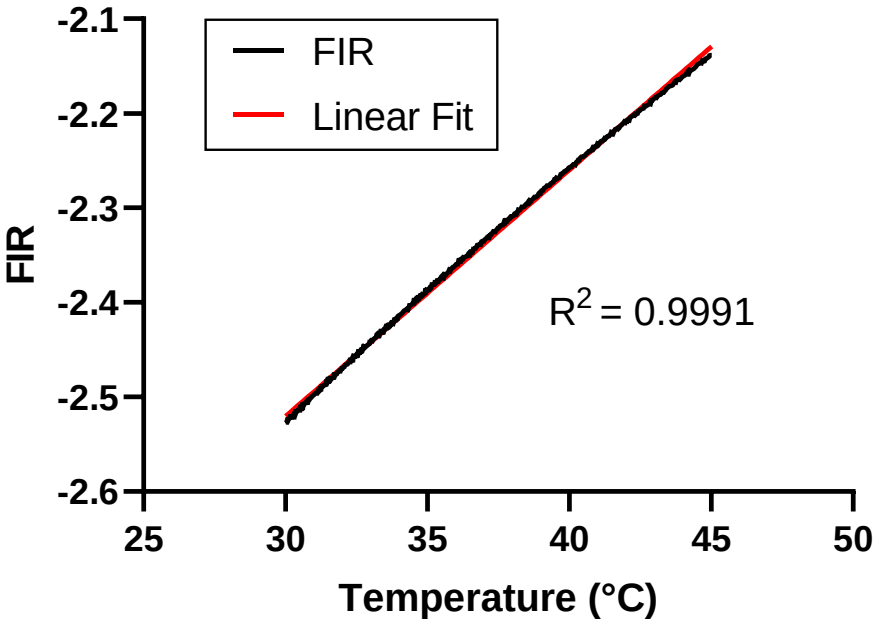

Figure 2.17: Fluorescence ratio *vs.* temperature, R^2 = 0.999 over the biologically relevant range.

2.4 Conclusions

This work has demonstrated that changes made to the original optical fibre temperature sensing configuration and probe fabrication method were successful in improving the probes' durability and readout stability during long-term experiments when deployed in the portable sensing configuration. However, this developmental work in addition to our previous experiments using optical fibre temperature sensors has demonstrated that although advantageous, numerous difficulties exist when trying to deploy these optical systems within a medical research laboratory for *in vivo* sensing applications.

The main issue of previous temperature sensing configurations was their sensitivity to environmental changes, and the measurement instabilities associated with use during long-term experiments. Our *in vitro* experiments demonstrated that the SM diode used in prior temperature sensing configurations was sensitive to changes in ambient temperature resulting in observed temperature artefacts caused by oscillations in laser voltage. In addition to this, they revealed the SM coupler and SM fibre to be a source of long-term term measurement

inaccuracy due to polarisation drift within the fibre. We demonstrated that switching to an all-PM configuration significantly increased long-term stability of FIR recordings and removed its susceptibility to environmental changes compared to configurations using SM equipment or MM fibres. Therefore, the use of PM fibre was a necessity in this application in order to maintain accurate FIR readings for the duration of each experiment.

Probe durability was another issue associated with previous temperature sensing configurations as previous probes were susceptible to temperature artefacts caused by signal bend-loss and breakage during animal movement-induced fibre coiling. This vulnerability was reduced by removing the splice procedure and exposed splice location, which was the site of breakage in many probes, as well as increasing the thickness of the fibres' outer cladding. Removal of the splice procedure significantly increased the average length of each probe, which aided its ability to coil without significant signal loss or probe breakage during *in vivo* experimentation. Although our *in* vitro results also demonstrated that UHNA fibre was effective in reducing effects of fibre bending on signal loss, it was shown to be non-conducive to increasing long-term stability of the configuration, which was only later accomplished using PM fibre. Use of PM fibre in the finalised configuration limited options available for increasing sturdiness of the temperature sensor. This was due to it's incompatibility with much of the commercially available equipment, such as rotation mounts and rotating connectors used to reduce the effects of fibre bending on acquired data. Although this equipment has its own issues associated with its use, such as variations in light transmission of up to 1 dB during fibre rotation that could lead to changes in observed temperature, it is also incompatible with the small 5 μm cores within our PM fibre sensor. Usage of these rotators in our configuration would require use of larger core MM fibres during probe fabrication to ensure their compatibility with our system, which would affect long-term system stability as we've already demonstrated, and also possibly introduce additional issues associated with MM fibres (Mehta et al., 2012). Our work

therefore employed a focus on SM, and later PM fibres, where these potential problems associated with MM fibres and fibre optic rotators were not applicable. Although the final changes made to increase probe durability were relatively minor and purely structural, they significantly increased sturdiness of the fibre without compromising the long-term stability provided by the all-PM configuration.

Although advantageous in many aspects, optical fibre sensors face commercial competition from already well-established sensing technologies, which limits their use in many biomedical studies. To appeal to users accustomed to these traditional sensing methods, optical sensing systems should be more readily available in the forms of complete systems that are suitable for use outside of a conventional optics laboratory. To this end, changes were made to our temperature sensing configuration to comply with these requirements, such as the removal of bulk optics, and the use of equipment that required zero alignment. Not only did this improve the overall robustness of the setup and decrease its benchtop footprint, but also facilitated its deployment within our medical research laboratory where mounting and precision alignment using optical tables was not possible. Our results demonstrated that the finalised probe was able to perform stable long-term measurements *in vitro,* which were in agreeance with concurrent measurements of temperature. Although there were many issues associated with the initial development of this portable optical fibre temperature sensor, we believe the major issues associated with its *in vivo* use were minimised, and that its current form is more suitable for use *in vivo*.

Chapter 3 – Publication 1

Musolino, S., Schartner, E.P., Tsiminis, G., Salem, A., Monro, T.M. and Hutchinson, M.R., 2016. Portable optical fibre probe for in vivo brain temperature measurements. *Biomedical optics express*, *7*(8), pp.3069-3077.

The work performed in this paper aimed at successfully demonstrating proof-of-concept for a portable optical fibre-tip sensor capable of recording brain temperature i*n vivo*. We describe a simple fabrication method that allowed for rapid fabrication of probes with no requirement for post-processing. Coating only the fibre tip as opposed to uniformly doping the fibre allowed for the sensing area to be spatially localized to a thin region directly in front of the core of the fibre. The rationale for this was to minimize the temperature sensitive area of the probe to allow brain thermorecording with a higher spatial precision compared to other optical fibre temperature sensing techniques. We use this probe to perform brain temperature measurements both *in vitro* and *in vivo* utilising a fully portable temperature measurement setup, which does not require alignment of any components.

Our *in vitro* results indicated that the measured fluorescence change from the probe, and temperature change from the RTD could be approximated as linear over the biologically relevant temperature range with high precision. Results were not impacted by systematic errors caused by large ambient temperature fluctuations that were known to impede previous probe configurations and further *in vivo* results confirmed this finding. We also demonstrated repeated brain temperature measurements using this sensor in awake freely-moving rats and showed a good correlation between brain and body temperatures recorded throughout the experiment.

Statement of Authorship

Title of Paper	Portable optical fiber probe for in vivo brain temperature measurements
Publication Status	☑ Published ☐ Accepted for Publication ☐ Submitted for Publication ☐ Unpublished and Unsubmitted w ork w ritten in manuscript style
Publication Details	Biomedical optics express, 7(8), pp.3069-3077. https://doi.org/10.1364/BOE.7.003069

Principal Author

Name of Principal Author (Candidate)	Stefan T Musolino
Contribution to the Paper	Had major input into study design, performed all experimental procedures, statistical analysis, graphical representation of data collected, and wrote and prepared the manuscript for submission.
Overall percentage (%)	80%
Certification:	This paper reports on original research I conducted during the period of my Higher Degree by Research candidature and is not subject to any obligations or contractual agreements with a third party that would constrain its inclusion in this thesis. I am the primary author of this paper.
Signature	Date 22/08/2019

Co-Author Contributions

By signing the Statement of Authorship, each author certifies that:

i. the candidate's stated contribution to the publication is accurate (as detailed above);

ii. permission is granted for the candidate in include the publication in the thesis; and

iii. the sum of all co-author contributions is equal to 100% less the candidate's stated contribution.

Name of Co-Author	Erik P Schartner
Contribution to the Paper	Assisted with study design, statistical analysis, graphical representation of data collected, provided critical review of manuscript drafts prior to submission, and acted as corresponding author.
Signature	Date 22/08/2019

Name of Co-Author	Georgios Tsiminis
Contribution to the Paper	Assisted with development of optical fibre temperature sensing configuration.
Signature	Date 22/08/2019

Please cut and paste additional co-author panels here as required.

Name of Co-Author	Abdallah Salem
Contribution to the Paper	Assisted with study design, statistical analysis, and provided critical review of manuscript drafts prior to submission.
Signature	Date 22/08/2019

Name of Co-Author	Tanya M Monro
Contribution to the Paper	Had major input into the design of the original fibre optic point temperature sensor.
Signature	Date 22/08/2019

Name of Co-Author	Mark R Hutchinson
Contribution to the Paper	Assisted with study design, statistical analysis, and provided critical review of manuscript drafts prior to submission.
Signature	Date 22/08/2019

Research Article | Vol. 7, No. 8 | 1 Aug 2016 | BIOMEDICAL OPTICS EXPRESS 3069

Biomedical Optics EXPRESS

Portable optical fiber probe for *in vivo* brain temperature measurements

STEFAN MUSOLINO,[1,2] ERIK P. SCHARTNER,[1,3,*] GEORGIOS TSIMINIS,[1,2] ABDALLAH SALEM,[2] TANYA M. MONRO,[1,4] AND MARK R. HUTCHINSON[1,2]

[1]*ARC Centre of Excellence for Nanoscale BioPhotonics and Institute for Photonics and Advanced Sensing, Adelaide, SA 5005, Australia*
[2]*School of Medicine, The University of Adelaide, Adelaide, SA 5005, Australia*
[3]*School of Physical Sciences, The University of Adelaide, Adelaide, SA 5005, Australia*
[4]*The University of South Australia, Adelaide, SA 5001, Australia*
[*]*erik.schartner@adelaide.edu.au*

Abstract: This work reports on the development of an optical fiber based probe for *in vivo* measurements of brain temperature. By utilizing a thin layer of rare-earth doped tellurite glass on the tip of a conventional silica optical fiber a robust probe, suitable for long-term *in vivo* measurements of temperature can be fabricated. This probe can be interrogated using a portable optical measurement setup, allowing for measurements to be performed outside of standard optical laboratories.

OCIS codes: (060.2370) Fiber optics sensors; (120.6780) Temperature; (170.6280) Spectroscopy, fluorescence and luminescence; (170.3890) Medical optics instrumentation.

References and links

1. M. W. Dewhirst, B. L. Viglianti, M. Lora-Michiels, M. Hanson, and P. J. Hoopes, "Basic principles of thermal dosimetry and thermal thresholds for tissue damage from hyperthermia," Int. J. Hyperthermia **19**(3), 267–294 (2003).
2. S. J. Schiff and G. G. Somjen, "The effects of temperature on synaptic transmission in hippocampal tissue slices," Brain Res. **345**(2), 279–284 (1985).
3. E. A. Kiyatkin, "Brain temperature homeostasis: physiological fluctuations and pathological shifts," Frontiers Biosci. **15**, 73 (2010).
4. P. L. Brown and E. A. Kiyatkin, "Brain hyperthermia induced by MDMA (ecstasy): modulation by environmental conditions," Eur. J. Neurosci. **20**(1), 51–58 (2004).
5. J. Weis, L. Covaciu, S. Rubertsson, M. Allers, A. Lunderquist, and H. Ahlström, "Noninvasive monitoring of brain temperature during mild hypothermia," Magn. Reson. Imaging **27**(7), 923–932 (2009).
6. K. O. Hill and G. Meltz, "Fiber Bragg grating technology fundamentals and overview," J. Lightwave Technol. **15**(8), 1263–1276 (1997).
7. V. K. Rai, "Temperature sensors and optical sensors," Appl. Phys. B **88**(2), 297–303 (2007).
8. Y.-J. Rao, "In-fibre Bragg grating sensors," Meas. Sci. Technol. **8**(4), 355–375 (1997).
9. J. Feng, M. Ding, J.-L. Kou, F. Xu, and Y.-Q. Lu, "An optical fiber tip micrograting thermometer," IEEE Photonics J. **3**(5), 810–814 (2011).
10. E. P. Schartner, G. Tsiminis, A. François, R. Kostecki, S. C. Warren-Smith, L. V. Nguyen, S. Heng, T. Reynolds, E. Klantsataya, K. J. Rowland, A. D. Abell, H. Ebendorff-Heidepriem, and T. M. Monro, "Taming the Light in Microstructured Optical Fibers for Sensing," Int. J. Appl. Glass Sci. **6**(3), 229–239 (2015).
11. G. Guan, S. Arnold, and V. Otugen, "Temperature measurements using a microoptical sensor based on whispering gallery modes," AIAA J. **44**(10), 2385–2389 (2006).
12. S. Wade, J. Muscat, S. Collins, and G. Baxter, "Nd-doped optical fiber temperature sensor using the fluorescence intensity ratio technique," Rev. Sci. Instrum. **70**(11), 4279 (1999).
13. B. Dong, B. Cao, Y. He, Z. Liu, Z. Li, and Z. Feng, "Temperature Sensing and in Vivo Imaging by Molybdenum Sensitized Visible Upconversion Luminescence of Rare-Earth Oxides," Adv. Mater. **24**(15), 1987–1993 (2012).
14. H. Berthou and C. K. Jörgensen, "Optical-fiber temperature sensor based on upconversion-excited fluorescence," Opt. Lett. **15**(19), 1100–1102 (1990).
15. V. K. Rai, D. Rai, and S. Rai, "Pr^{3+} doped lithium tellurite glass as a temperature sensor," Sens. Actuators A Phys. **128**(1), 14–17 (2006).
16. X. D. Wang, O. S. Wolfbeis, and R. J. Meier, "Luminescent probes and sensors for temperature," Chem. Soc. Rev. **42**(19), 7834–7869 (2013).
17. T.-Y. Sun, D.-Q. Zhang, X.-F. Yu, Y. Xiang, M. Luo, J.-H. Wang, G.-L. Tan, Q.-Q. Wang, and P. K. Chu, "Dual-emitting nanocomposites derived from rare-earth compound nanotubes for ratiometric fluorescence sensing applications," Nanoscale **5**(4), 1629–1637 (2013).
18. J. Jakutis, L. Gomes, C. Amancio, L. Kassab, J. Martinelli, and N. Wetter, "Increased Er^{3+}upconversion in tellurite fibers and glasses by co-doping with Yb^{3+}," Opt. Mater. **33**(1), 107–111 (2010).

#261220 http://dx.doi.org/10.1364/BOE.7.003069
Journal © 2016 Received 16 Mar 2016; revised 10 Jun 2016; accepted 23 Jun 2016; published 20 Jul 2016

Research Article | Vol. 7, No. 8 | 1 Aug 2016 | BIOMEDICAL OPTICS EXPRESS 3070
Biomedical Optics EXPRESS

19. S. Hao, G. Chen, and C. Yang, "Sensing using rare-earth-doped upconversion nanoparticles," Theranostics **3**(5), 331–345 (2013).
20. G. Tsiminis, T. S. Klarić, E. P. Schartner, S. C. Warren-Smith, M. D. Lewis, S. A. Koblar, and T. M. Monro, "Generating and measuring photochemical changes inside the brain using optical fibers: exploring stroke," Biomed. Opt. Express **5**(11), 3975–3980 (2014).
21. P. T. So, C. Y. Dong, B. R. Masters, and K. M. Berland, "Two-photon excitation fluorescence microscopy," Annu. Rev. Biomed. Eng. **2**(1), 399–429 (2000).
22. E. P. Schartner and T. M. Monro, "Fibre Tip Sensors for Localised Temperature Sensing Based on Rare Earth-Doped Glass Coatings," Sensors (Basel) **14**(11), 21693–21701 (2014).
23. X. Feng, T. M. Monro, V. Finazzi, R. C. Moore, K. Frampton, P. Petropoulos, and D. J. Richardson, "Extruded singlemode, high-nonlinearity, tellurite glass holey fibre," Electron. Lett. **41**(15), 835–837 (2005).
24. P. dos Santos, M. De Araujo, A. Gouveia-Neto, J. Medeiros Neto, and A. Sombra, "Optical temperature sensing using upconversion fluorescence emission in Er^{3+} Yb^{3+} codoped chalcogenide glass," Appl. Phys. Lett. **73**(5), 578–580 (1998).
25. S. Bexis, B. D. Phillis, J. Ong, J. M. White, and R. J. Irvine, "Baclofen prevents MDMA-induced rise in core body temperature in rats," Drug Alcohol Depend. **74**(1), 89–96 (2004).
26. G. Paxinos and K. B. Franklin, *The mouse brain in stereotaxic coordinates* (Gulf Professional Publishing, 2004).
27. B. H. Westerink, "Analysis of biogenic amines in microdialysates of the brain," J. Chromatogr. B Biomed. Sci. Appl. **747**(1-2), 21–32 (2000).
28. B. Esteban, E. O'Shea, J. Camarero, V. Sanchez, A. R. Green, and M. I. Colado, "3,4-Methylenedioxymethamphetamine induces monoamine release, but not toxicity, when administered centrally at a concentration occurring following a peripherally injected neurotoxic dose," Psychopharmacology (Berl.) **154**(3), 251–260 (2001).
29. E. O'Shea, I. Escobedo, L. Orio, V. Sanchez, M. Navarro, A. R. Green, and M. I. Colado, "Elevation of ambient room temperature has differential effects on MDMA-induced 5-HT and dopamine release in striatum and nucleus accumbens of rats," Neuropsychopharmacology **30**(7), 1312–1323 (2005).
30. A. Leung, P. M. Shankar, and R. Mutharasan, "A review of fiber-optic biosensors," Sens. Actuators B Chem. **125**(2), 688–703 (2007).

1. Introduction

The brain is the most temperature-sensitive organ in the body [1]. Brain temperature can be influenced by multiple environmental, immunological and toxicological factors, and even small deviations in brain temperature can result in profound functional behavioral impacts, regional cell toxicity within the brain or even neuronal cell death [2]. Preclinical rodent research examining acute thermal insults has relied upon the use of rectal thermometers and/or intraperitoneal telemetry sensor implants. However, when examining thermal insults such as the administration of stimulant drugs (e.g. 3,4-methylenedioxy-methamphetamine; MDMA), whose pharmacology and toxicology impact discrete brain regions deep within complex cellular structures [3], it is important to measure temperature in a localized spatial region within the brain. These requirements make the use of other available techniques impractical. As such, previous spatial resolution of brain temperature had been limited to approximately 125µm [4]. For these complex experiments there is a requirement for a minimally invasive temperature probe, which can record ± 0.1 °C changes within deep brain structures, in a live ambulatory behaving rodent, in a medical science laboratory. Optical fibers have been used as a potential solution for this, with previous work demonstrated using large diameter (0.5 mm) optical fiber probes implanted within a pig brain [5].

Optical fiber temperature sensing has traditionally relied on the interrogation of Bragg gratings inscribed on the core of the fiber to perform measurements by monitoring the shift in the wavelength of light reflected as a result of a temperature change [6]. These fiber sensors however require a significant length of fiber to obtain high efficiency [7, 8], or complex fabrication methods to obtain a sufficient reflection in a small region [9], and generally only show a coarse resolution of 1-2 °C [7, 10]. Alternative methods using resonance effects such as whispering gallery modes can also be used to measure temperature, where the resonant wavelength can be monitored and used to infer temperature [11]. These methods also require very high experimental complexity, both in the fabrication of the resonator as well as the high resolution requirements for signal analysis. In addition, these techniques are also typically cross-sensitive to local refractive index variations, which also present as a shift in the resonant wavelength.

Research Article | Vol. 7, No. 8 | 1 Aug 2016 | BIOMEDICAL OPTICS EXPRESS 3071
Biomedical Optics EXPRESS

In recent years rare-earth thermometry has evolved as a potential solution for small-scale measurements of temperature [12, 13]. This method relies on interrogating rare-earth ions such as erbium [14], neodymium [12] or praseodymium [15] which are doped within a suitable host media. The emission spectrum from two thermally linked energy levels, appearing as two different peaks in the overall emission spectrum of the material, changes its shape as the temperature of the host medium varies [16]. This allows for the temperature to be determined by a ratiometric technique, where the intensity of emission from one band is compared to that from the second band at different temperatures. This results in a calibration of the temperature corresponding to the band ratio that is insensitive to power fluctuations [17]. Co-doping of a sensitizer such as ytterbium allows for greatly enhanced upconversion compared to a material with the same primary ion concentration [13, 18].

Typically rare-earth thermometry technique utilizes upconversion emission, where the relevant spectrum is emitted at a shorter wavelength than the excitation light [19]. This is especially important in an application involving *in vivo* measurements, as alternative optical methods which rely on excitation and collection using UV or visible light can be strongly influenced by background autofluorescence from the surrounding tissue [20]. The use of upconversion emission circumvents background signals, as the only autofluorescence generated is low-efficiency two-photon emission [21].

Our previous work on the fabrication of optical fiber probes using rare-earth doped glass for temperature sensing demonstrated a proof of concept as to the possibility of using fluorescence up conversion in biological/medical applications [22], however practical use of these sensors was limited by the use of bulk optics for coupling into the optical fiber probe, and the use of a large, benchtop spectrometer for analysis of the emitted optical signal.

In this work we build upon the technology developed in our previous paper and demonstrate a fully portable temperature measurement setup based on rare-earth doped glass optical fibers which does not require alignment of any components and can fit on a portable optical breadboard. This setup is deployed to a medical research laboratory to show preliminary results on the use of these optical fiber probes for *in vivo* preclinical measurements of brain temperature.

2. Method

2.1 Probe fabrication

The glass host material chosen was sodium zinc tellurite (ZNT) glass [23], doped with 1 mol% erbium and 9 mol% ytterbium. Co-doping with a sensitizer, in this case ytterbium, allowed for the upconversion efficiency to be significantly increased over doping solely with erbium [18, 24].

Optical fiber probes were fabricated using a previously established method [22]. One meter of polarization maintaining (PM) fiber (Nufern 980XP) was cut, and 15 mm of coating stripped from one end of the fiber. A 25 gauge needle was cut to a length of 4 mm, and any sharp edges rounded off. The fiber was then inserted into the needle, cleaved, and glued inside the needle body with approximately 2 mm of fiber protruding from the end. This fiber tip length was chosen to minimize the impact of fiber implantation on the surrounding microcirculation in tissue.

This fiber was sheathed within a standard 900 µm diameter optical fiber protective sleeve. This step was required as preliminary experiments demonstrated that an uncoated fiber was susceptible to mechanical breakage during the course of the *in vivo* measurements in live ambulatory rats. Testing demonstrated that sheathing the fiber significantly reduced the probability of fiber breakage, even during periods of high locomotion, turning and rearing activity. The sheathed fiber was then spliced using an arc splicer (Fujikura FSM-100) to a connectorized patch cable for easy integration with measurement equipment.

The coating method used to fabricate the sensing region on the fiber tips is shown in Fig. 1. Tellurite glass was used for the fabrication of the tips as the melt temperature used (820 °C) was significantly below the softening point of the silica glass fibers (≈1600 °C) so no

Research Article | Vol. 7, No. 8 | 1 Aug 2016 | BIOMEDICAL OPTICS EXPRESS 3072
Biomedical Optics EXPRESS

deformation of the fibers is observed [22]. The fiber tip was immersed within the molten tellurite glass for a period of approximately one second, before being removed and allowed to cool in ambient atmosphere to room temperature. Probes were stored within a protective case for later use in measurements.

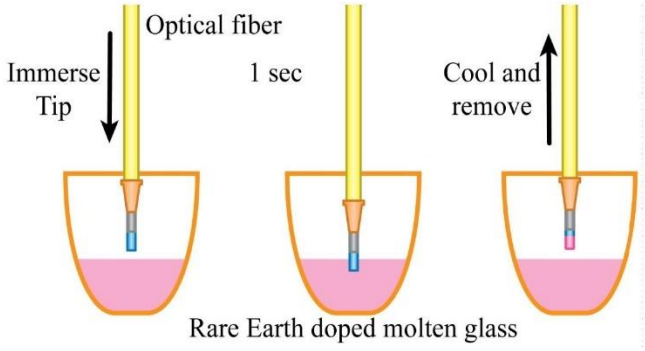

Fig. 1. Method for fabrication of temperature sensitive optical fiber tips. The fibers are cleaved and mounted within needles, and encased within a protective buffer jacket. The assembly is then dipped into erbium:ytterbium doped tellurite glass to rapidly functionalize the tip.

2.2 Optical configuration

Due to the requirement that the temperature probe be used within a medical research laboratory, without access to temperature controlled spaces or vibration-damped tables, the experimental configuration from [22] was found to be unsuitable for this application. Preliminary experiments using a portable breadboard were strongly affected by both vibrations and temperature fluctuations within the measurement space, leading to deviations between the optical probe and reference probe.

The final optical setup is shown in Fig. 2 below. The 980 nm laser source (Thorlabs BF-979-0300) was connected directly to a 99:1 PM splitter (AFW PFC-98-1), with the probe connected to the 1% output of the splitter. This configuration was chosen to minimize the potential for cell damage or local heating at the end face of the probe that could affect the validity of temperature data gathered, while maximizing the returned optical signal through the PM splitter. The output port of the splitter was passed through a short-pass filter (Semrock FF01-842) to remove the residual pump light, before being coupled into a portable spectrometer for spectral analysis (Ocean Optics QE65 Pro).

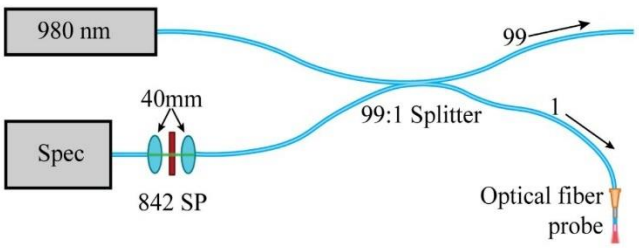

Fig. 2. Optical configuration for experimental setups to minimize the requirement for bulk optics. The short-pass filter is required to prevent backscattered pump light from saturating the detector on the spectrometer.

2.3 Probe calibration

Each probe was individually calibrated to obtain a plot of the expected fluorescence ratio versus the actual temperature. A reference resistance temperature device (RTD, Omega Class

Research Article | Vol. 7, No. 8 | 1 Aug 2016 | BIOMEDICAL OPTICS EXPRESS 3073
Biomedical Optics EXPRESS

A 100 Ω) was utilized during measurements. The RTD was used for calibration during *in vitro* measurements, and for monitoring ambient temperatures during the *in vivo* portion of measurements. For calibration the RTD was co-located within a rats brain submerged in a water bath, with both the probe and RTD temperature cycled using an incubator. The probe was inserted into the brain tissue to better simulate the actual environment that it would experience during *in vivo* trials to ensure that the tissue in close proximity to the optical fiber tip would not influence measurements.

2.4 Animals

Four pathogen-free male Sprague-Dawley rats were used, weighing 270-300 g. All animals were supplied by the Adelaide University Laboratory Animal Services (Adelaide, South Australia). Rats were housed in temperature (18–21 °C) and light-controlled (12 h light/dark cycle; lights on at 0700 h) rooms with standard rodent food and water available *ad libitum*. Ethics approval for this study was given by the University of Adelaide Animal Ethics Committee, and all procedures were in strict accordance with the National Health and Medical Council of Australia Guidelines for the Care and Use of Laboratory Animals.

2.5 Radio telemetry implantation

Rats were anesthetized with chloral hydrate (400 mg/kg i.p.) in 0.9% saline and placed on a water-heated pad (37 °C). Once fully anesthetized, rats were surgically implanted with telemetry devices (Data Sciences International TA11CTA-F40), that measure core body temperature, activity, and ECG, as reported previously [25]. One week recovery from surgery was allowed before rats underwent optic fiber implantation and any drug treatments. A radio receiver, placed under the observation bowl, received information from the implants and transferred it to a computer that recorded the data using the Dataquest LabPro software (Data Sciences International). Radio data was recorded every 2 min over the experimental period using the experimental setup shown in Fig. 3.

2.6 Optical fiber probe implantation

Rats were anesthetized with chloral hydrate (400 mg/kg i.p.) in 0.9% saline and placed on a water-heated pad (37°C). Once fully anesthetized, the animal's head was secured in a stereotaxic frame (Kopf Instruments, Tujunga, CA, USA). After the skull was exposed, the bregma was located and the temperature probe was implanted into the right striatum (A: + 0.2 mm, L: + 3.0 mm, V: −3.5 mm from bregma). All coordinates were referenced from a rat brain atlas [26]. The temperature probe was held in place using dental cement (Vertex, Dentimex BV HJ, Zeist, Netherlands) adhered to the probe casing to form a robust attachment point to the skull. Following temperature probe implantation, rats were given 48 h to recover from surgery. A recovery period of 24 h is considered as satisfactory for microdialysis studies, as neurotransmitter levels are stabilized and interference due to surgery and anesthesia is limited [27–29]. At the end of each experiment animals were humanely killed via anesthetic overdose with chloral hydrate and brains carefully removed and stored in the freezer for future histological analysis in order to validate correct probe placement.

2.7 Drug treatments

Before the experimental day, ambulatory rats were pre-treated with 3 doses of saline (10ml/kg, i.p) over 3 days. On the experimental day, brain and body temperature recording was started at 9am (time −120), and the last saline pre-treatment injection administered at 10.30am (time −30). The temperature recordings taken between time −120 and time 0 were used to establish baseline brain and body temperature levels. At 11am (time 0), rats received the last injection of saline after which both body and brain temperature were recorded for a further 4 h until the end of the experiment. A saline drug treatment schedule was selected for experimentation to ensure low counts of animal locomotor activity (LMA) during the recording period. High LMA counts have the potential to negatively affect optical signal

Research Article | Vol. 7, No. 8 | 1 Aug 2016 | BIOMEDICAL OPTICS EXPRESS 3074
Biomedical Optics EXPRESS

strength due to excess fiber bending and twisting during periods of increased animal movement. National Instruments LabVIEW software was used to simultaneously record both the upconversion emission from the fiber probe, as well as the ambient temperature from the RTD.

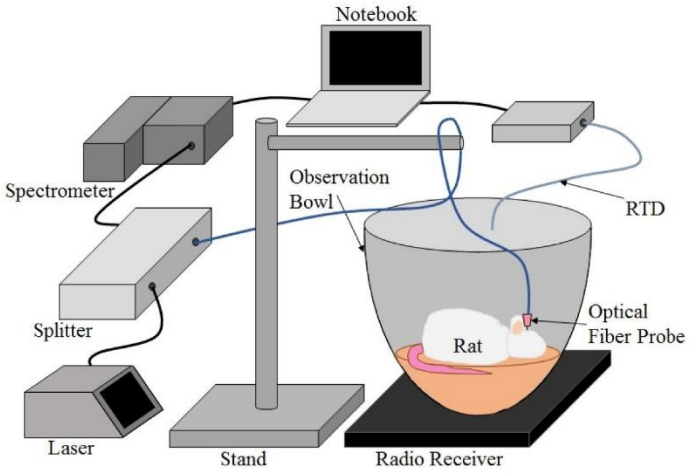

Fig. 3. Experimental set up for *in vivo* measurements to compare brain and body temperature recordings in an ambulatory animal.

3. Results

3.1 In vitro

In vitro results with the fiber probe and co-located RTD are shown in Fig. 4. These demonstrate that the measured change in fluorescence ratio over the relevant biological range can be approximated as linear with an R^2 of 0.9994 over the measured range from 22°C to 51°C, with a sensitivity of $0.00526K^{-1}$ displaying a similar response to the previously published probe that showed a precision of 0.1-0.3 °C [22]. Trials showed that minimal correlation was observed between the environmental temperature, and the temperature recorded from the optical probe even with large (>5 °C) changes in the laboratory temperature over the duration of measurements.

Research Article Vol. 7, No. 8 | 1 Aug 2016 | BIOMEDICAL OPTICS EXPRESS 3075
Biomedical Optics EXPRESS

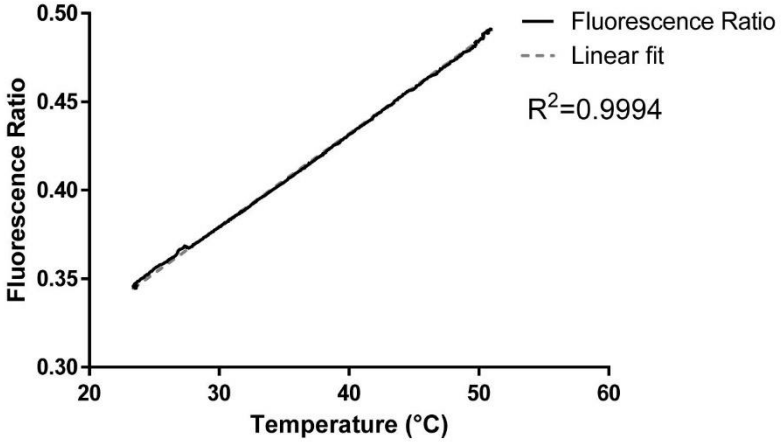

Fig. 4. *In vitro* fluorescence ratio *vs.* reference temperature for increasing temperature, R^2 = 0.9994 and a sensitivity of 0.005258K^{-1}

3.2 In vivo

Results from the implantation of a probe within an ambulatory rat brain is shown in Fig. 5(a) below. Figure 5(a) shows the brain and body temperature measurements gathered from the fiber probe and implanted telemetry device respectively in a saline treated rat, as well as laboratory ambient temperature observed from the RTD. Body, brain, and ambient temperature data are expressed as temperature change from baseline. Figure 5(b) shows the brain temperature measurements, averaged across multiple (n = 4) animals, observed with the fiber probe and body temperature measurements gathered from the implanted telemetry receiver in saline treated rats. Figure 5(b) results are shown as the mean values and standard error across all trials, at six minute intervals.

Research Article | Vol. 7, No. 8 | 1 Aug 2016 | BIOMEDICAL OPTICS EXPRESS 3076
Biomedical Optics EXPRESS

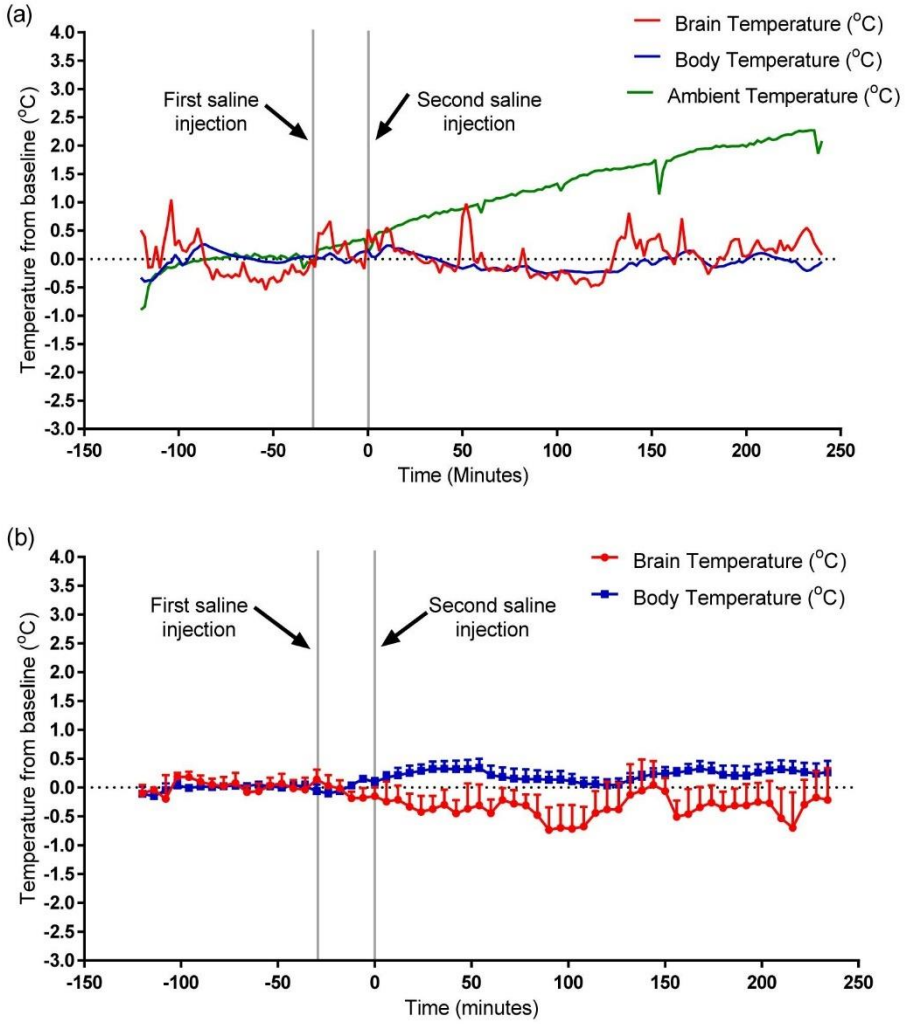

Fig. 5. (a) - *In vivo* results for fluorescence brain temperature probe, implanted body temperature monitor, and RTD ambient temperature monitor for an example saline treated rat (n = 1). Time and temperature are shown relative to the second saline injection time. The brain and ambient temperature are recorded at 10 second intervals and body temperature at 120 second intervals. (b) – *In vivo* results for fluorescence brain temperature probes, and implanted body temperature monitors (n = 4), averaged across all trials at 6 minute intervals. Error bars show the standard error in the mean.

These results demonstrate that the rare-earth doped glass optical fiber sensor is able to measure the temperature within the rat brain over an extended duration, while the rat is free to move within its enclosure. The results in Fig. 5(a) display minimal effects of ambient temperature on optic fiber probe temperature recordings as no systematic trend in the data is observed even from large changes in ambient temperature. Figure 5(b) results display a good correlation between brain and body temperature across the four trials, with both the brain and body temperatures agreeing within the error margin of the experiment.

During preliminary probe trials it was observed that some fluctuations in the overall intensity are seen as the fiber is bent too close to its critical bend radius. Due to the wavelength dependent nature of the bend loss of the fiber, these losses impact the observed

Research Article | Vol. 7, No. 8 | 1 Aug 2016 | BIOMEDICAL OPTICS EXPRESS 3077
Biomedical Optics EXPRESS

fluorescence ratio and the corresponding observed temperature. While in preliminary trials this effect resulted in large (>1 °C) deviations from values with an un-bent fiber, the use of high durability sheathed fibers in this experiment has reduced this, allowing for stable measurements to be performed over the desired time period. Some sharp features of lower amplitude than the preliminary trials were still observed in spectral readings, which are likely due to bending of the fiber, seen as sharp spikes in the brain temperature signal in Fig. 5(a). Further improvements to the robustness of the jacketing, or the use of high numerical aperture (NA) fiber could potentially reduce this further for future trials.

4. Conclusion

We have successfully demonstrated a proof-of-principle measurements for the use of an optical fiber probe to measure temperature *in vivo* based on rare-earth thermometry. The use of the rare-earth coating on the fiber tip allows for the sensing area to be spatially localized to a thin region directly in front of the core of the fiber. Minimizing the temperature sensitive region allows for temperature to be observed at specific locations within the brain. This allows for the probe to be implanted with minimal effect on the local temperature due to the low heat conduction of the silica glass fiber compared to the metal wires within conventional thermocouples. For future measurements if improved spatial resolution is required then the fiber probe can be tapered to reduce the outer diameter, while still allowing the upconversion signal to be collected [30].

The simple fabrication method allows for rapid fabrication of the probes, with no requirement for post-processing after the tips are coated with the tellurite glass.

The use of these probes will allow for temperature to be recorded in an ambulatory animal over an extended period of time post-implantation. Preliminary results demonstrate that the probe can be monitored for a period of at least 48 h with no adverse effects, and due to the physical nature of the sensing method no photobleaching or degradation of the probe signal would be expected for long-duration recordings.

The probe could find applications to perform measurements *in situ* with other sensing elements, such as electrodes, microdialysis probes, and other neural recording equipment. Due to the small size of the fiber tip it could be affixed to an existing sensor, and implanted with an identical method to that used in existing experiments without inducing additional stress or damage. The probe is also suitable for multiplexing with other optical sensors which use visible excitation, as there should be minimal cross-talk between the sensors.

The current experimental procedure made obtaining both optical and reference brain temperature measurements *in vivo* difficult as it was not possible to co-locate the RTD reference measurement in the brain. To address this, future investigations will involve the comparison of brain temperature recorded by the optical fiber probe and a co-located brain implantable thermocouple electrode *in vivo* to more thoroughly assess the accuracy of the optical fiber probe in free-to-move animals. Continued studies will also aim to quantify the effects of fiber curvature on observed fluorescence ratio and temperature readouts of the probe in order to assess its accuracy during periods of high animal activity. Further modifications to the probe design should reduce the effects of bending and vibrations on the temperature readout, and future work will examine the use of more robust outer jacketing and high NA fibers to mitigate the variations induced from these effects.

Future investigations will use this method to assess brain and body temperatures of animals which have been administered either control injections of saline, or injections of 3,4-methylenedioxymethamphetamine (MDMA). Modifications to the experimental protocol during these investigations should allow for the implantation of multiple probes at different spatial positions within the brain. The ability to monitor temperature within different regions of the brain as well as the body should allow for an improved understanding of the hyperthermic effects of stimulant drugs, and the pathways involved in driving the drug-induced hyperthermic response. This information could aid in the development of a pharmacological intervention for acute drug toxicity for use in an emergency room setting.

Research Article | Vol. 7, No. 8 | 1 Aug 2016 | BIOMEDICAL OPTICS EXPRESS 3078
Biomedical Optics EXPRESS

In the future, a fully developed probe could find potential application in human brain temperature monitoring after traumatic brain injury, stroke, or subarachnoid hemorrhage when the brain is extremely sensitive and vulnerable to small deviations in temperature. The probes ability to measure temperature with high temporal and spatial resolution could play a useful role in the multimodal monitoring of patients with severe head trauma in order to prevent secondary injury to the brain. It could also be utilized for tracking hypothermia in infants with neonatal encephalopathy to aid in neuroprotective therapy efforts during the first 72 hours after delivery.

The adaption of the experimental configuration to a completely portable setup with no alignment required allows for the deployment of these probes to spaces outside of conventional optics laboratories, which is an important step towards the use of these probes to examine real-world medical problems.

Acknowledgments

E. Schartner, M. Hutchinson and G. Tsiminis acknowledge financial support from the Australian Research Council (ARC) through the Centre of Excellence for Nanoscale BioPhotonics. E. Schartner and T. Monro would also like to acknowledge financial support from an ARC Linkage funding project. T. Monro acknowledges financial support form an ARC Georgina Sweet Laurate Fellowship. This work was performed in part at the OptoFab node of the Australian National Fabrication Facility utilizing Commonwealth and South Australian State Government funding. The authors would like to acknowledge Prof. Heike Ebendorff-Heidepriem and Dr. Herbert Foo for useful discussions.

Chapter 4 – Publication 2

Musolino, S.T., Schartner, E.P., Hutchinson, M.R. and Salem, A., 2019. Improved method for optical fibre temperature probe implantation in brains of free-moving rats. *Journal of neuroscience methods*, *313*, pp.24-28.

Work performed in this paper aimed at increasing the durability, and reusability of the sensor, as well as its ease of use by developing an improved optical fibre probe fabrication technique utilising conventional microdialysis equipment. This work was a direct extension from the original probe development work performed prior to the previous paper. Standard microdialysis guide cannulas were used in the revised probe structure to facilitate a simplified implantation procedure and allow for the removal of the fibre from the animal post-experiment. This was done to permit multiple insertion and removal procedures for each probe as well as high throughput animal experiments. The rationale for this method optimization was due to the probes' durability issues both pre-experiment, and post-MDMA administration during periods of increased animal movement. Fixing these issues with commercially available equipment such as fibreoptic commutators or short indwelling fibre segments commonly used in optogenetic applications was not possible for our application due to their incompatibility with PM fibre used in the portable configuration. The current study investigated the impacts of these improvements to the probe whilst recording MDMA-induced increases in temperature from the brains of freely-moving rats.

Our results indicated that the new probe structure was easily implanted and extremely durable both pre-experimentation and during sampling *in vivo*. Follow-up *in* vitro experiments confirmed the probe was capable for reuse after removal from the animal. The capability for probe reusability significantly increased experimental workflow and time and resources lost

due to repeated probe fabrication post-experiment. We also showed that rats administered MDMA showed pathological increases in brain temperature, which resulted in the deaths of two animals.

Statement of Authorship

Title of Paper	Improved method for optical fibre temperature probe implantation in brains of free-moving rats.
Publication Status	☑ Published ☐ Accepted for Publication ☐ Submitted for Publication ☐ Unpublished and Unsubmitted w ork w ritten in manuscript style
Publication Details	Journal of neuroscience methods, 313, pp.24-28. https://doi.org/10.1016/j.jneumeth.2018.12.013.

Principal Author

Name of Principal Author (Candidate)	Stefan T Musolino
Contribution to the Paper	Had major input into study design, performed all experimental procedures, statistical analysis, graphical representation of data collected, wrote and prepared the manuscript for submission, and acted as corresponding author.
Overall percentage (%)	90%
Certification:	This paper reports on original research I conducted during the period of my Higher Degree by Research candidature and is not subject to any obligations or contractual agreements with a third party that would constrain its inclusion in this thesis. I am the primary author of this paper.
Signature	Date 22/08/2019

Co-Author Contributions

By signing the Statement of Authorship, each author certifies that:

i. the candidate's stated contribution to the publication is accurate (as detailed above);
ii. permission is granted for the candidate in include the publication in the thesis; and
iii. the sum of all co-author contributions is equal to 100% less the candidate's stated contribution.

Name of Co-Author	Erik P Schartner
Contribution to the Paper	Assisted with study design, statistical analysis, graphical representation of data collected, provided critical review of manuscript drafts prior to submission.
Signature	Date 22/08/2019

Name of Co-Author	Mark R Hutchinson
Contribution to the Paper	Assisted with study design, statistical analysis, and provided critical review of manuscript drafts prior to submission.
Signature	Date 22/08/2019

Please cut and paste additional co-author panels here as required.

Name of Co-Author	Abdallah Salem		
Contribution to the Paper	Assisted with study design, statistical analysis, and provided critical review of manuscript drafts prior to submission.		
Signature		Date	22/08/2019

Journal of Neuroscience Methods 313 (2019) 24–28

Contents lists available at ScienceDirect

Journal of Neuroscience Methods

journal homepage: www.elsevier.com/locate/jneumeth

Improved method for optical fiber temperature probe implantation in brains of free-moving rats

Stefan T. Musolino[a,b,*], Erik P. Schartner[a,c], Mark R. Hutchinson[a,b], Abdallah Salem[b]

[a] ARC Centre of Excellence for Nanoscale BioPhotonics and Institute for Photonics and Advanced Sensing, Adelaide, SA 5005, Australia
[b] Discipline of Pharmacology, Adelaide Medical School, The University of Adelaide, Adelaide, SA 5005, Australia
[c] School of Physical Sciences, The University of Adelaide, Adelaide, SA 5005, Australia

ARTICLE INFO

Keywords:
Stereotaxic operation
In vivo optical fiber sensing
Brain hyperthermia
Rat model

ABSTRACT

Background: The localized monitoring of brain temperature is crucial to the understanding of the mechanisms underlying brain hyperthermia, such as that caused by stimulant drugs. Many animal studies investigating brain hyperthermia have utilized thermocouple electrodes for temperature measurement, however optical fiber sensors have proven to be an attractive alternative to conventional measurement techniques. Despite their advantages, optical fiber sensors in their current form have struggled to find effective use in studies involving free-moving animals.

New method: We have developed an improved optical fiber temperature probe and implantation method suitable for sensing in free-moving animals. By altering the structure of the probe, conventional guide cannulae can be used for stereotaxic implantation thus increasing ease-of-use and probe durability.

Results: The new probe structure was easily implanted and extremely durable both pre-experimentation and during sampling *in vivo*. Probe re-usability also allowed for increased experimental workflow. Rats administered MDMA showed pathological increases in brain temperature.

Comparison with existing method(s): Thermocouples commonly used for temperature measurement in deep brain structures lack the advantages offered by optical fiber sensors. Unlike our improved design, previous optical fiber temperature probes were unable to be removed from the brains of rats without removing the dental cement affixing it to the skull. This made the probe susceptible to breakage and often resulted in the complete loss of the animal from the experiment.

Conclusions: Our fiber temperature probe and revised implantation technique can be easily employed in brain thermorecording using advantageous optical fiber sensors suitable for use in awake free-moving animals.

1. Introduction

Hyperthermia is the most dangerous clinical impact of acute 3,4-methylenedioxymethamphetamine (MDMA, ecstasy) intoxication (Kalant, 2001; Kiyatkin, 2005; Parrott, 2012) and a factor contributing to neurotoxicity (Gordon et al., 1991). It has already been established that an uncontrolled increase in brain temperature can have deleterious effects on neural cells and brain function (Brown and Kiyatkin, 2004), including disruption of the blood-brain barrier. The localized, real-time monitoring of brain temperature while under the influence of drugs such as MDMA is crucial to the understanding of the mechanisms underlying brain hyperthermia, as well as the effects of therapies targeted to alleviate these dangerous clinical symptoms.

Over the last three decades many studies investigating brain hyperthermia have utilized conventional thermocouple electrodes for temperature measurement in deep brain structures (Jiang et al., 1991; Busto et al., 1987; Brown and Kiyatkin, 2004; Kiyatkin et al., 2014). In more recent years however, optical fiber sensors have proven to be an attractive alternative to conventional measurement techniques. They provide unique advantages such as high sensitivity, immunity to electromagnetic interference, small size, robustness, as well as the ability to provide multiplexed sensing (Lee, 2003).

It has previously been shown that emission from rare-earth ions such as erbium (Er^{3+}) (Berthou and Jörgensen, 1990; Dos Santos et al., 1998; Wade et al., 1999), doped within a suitable host medium depends on temperature (Schartner and Monro, 2014). Using this information, optical fiber temperature probes based on erbium:ytterbium co-doped glass have been developed for localized temperature measurements (Schartner and Monro, 2014).

Previous animal studies utilizing optical fiber sensors have been

* Corresponding author at: The University of Adelaide, 30 Frome Rd, Adelaide SA 5000, Australia.
E-mail address: stefan.musolino@adelaide.edu.au (S.T. Musolino).

https://doi.org/10.1016/j.jneumeth.2018.12.013
Received 8 November 2018; Received in revised form 18 December 2018; Accepted 18 December 2018
Available online 19 December 2018
0165-0270/

conducted in animals under general anesthesia (Grant et al., 2001; Chavko et al., 2007; O'Hara et al., 2005; Peterson et al., 1984; Yu et al., 2016). However, it is widely known that general anesthesia causes robust temperature decreases (> 4 °C) in both the brain and in the periphery (Kiyatkin, 2005). Many processes governing neuronal activity are temperature dependent, and even small (1–3 °C) decreases in temperature affect transmitter release and reuptake that can distort the drug-induced neuronal and neurochemical effects of tested drugs (Kiyatkin, 2005, 2010). Ideally, optical fiber sensors used for *in vivo* experiments should be robust enough to withstand experimentation in free-moving animals to remove the influence of general anesthesia on the final experimental results. This motivated us to develop a portable optical fiber temperature sensor for measurement in deep brain structures in free-moving rats (Musolino et al., 2016).

The sensor we developed obtained a temperature resolution of 0.1–0.3 °C over several cycles (Schartner and Monro, 2014) and successfully recorded brain temperature in awake, free-moving rats, however it suffered drawbacks related to the fixation of the optical fiber within a syringe needle to accommodate stereotaxic implantation. The rigid, all-in-one implantation of the fiber fixed inside the needle made the probe susceptible to breakage during the 48 h animal recovery period post stereotaxic implantation. Breakage of the probe in this state resulted in the loss of the sensor, as well as time and resources spent replacing it. Furthermore, it resulted in the loss of the experiment as the remainder of the broken probe remained affixed to the skull and could not be removed without causing excessive damage. Conventional techniques commonly used to prevent such breakages, such as fibreoptic commutators, were found to be incompatible with our probe due to the use of single-mode, polarisation maintaining (PM) fiber to avoid interference effects and increased errors in temperature values caused by animal movement.

In this study, we describe an improved method for optical fiber sensor implantation in free-moving animals. By using a revised probe structure, we have developed a fiber optic temperature probe that can utilize a standard microdialysis guide cannula for stereotaxic implantation to reduce the risk of fiber breakage prior to and during experimentation. The revised probe structure allows the implantation and removal of the fiber as a single piece, allowing for a high level of reproducibility to be obtained from the probe through multiple insertion and removal procedures. The obtained data demonstrates that the optical fiber temperature sensor provides an efficient means of brain temperature recording in awake, MDMA stimulant administered, free-moving rats.

2. Materials and methods

2.1. Probe fabrication

Probes were fabricated using a method described previously using sodium zinc tellurite (ZNT) glass, doped with 1 mol% erbium and 9 mol % ytterbium (Musolino et al., 2016). Co-doping with a sensitizer, in this case ytterbium, allowed for the upconversion efficiency to be significantly increased over doping solely with erbium. Temperature is monitored by observing two emission bands at 524 and 547 nm, with the ratio of these two being correlated to the temperature of the probe.

A 2-meter PM fiber (Nufern 980XP) with connectorized patch cable was used, and 4 mm of coating stripped from the tip of the fiber. A guide cannula (BAS MD-2251, Bioanalytical Systems Inc., West Lafayette, IN, USA) was altered to house the fiber. The metal rod of the guide cannula dummy cap was removed, and the fiber was inserted in its place. The fiber was then cleaved and glued inside of the cap with approximately 15 mm of fiber protruding from the end of the cap, 2 mm of which was tellurite glass coated fiber tip (Fig. 1). This fiber tip length was chosen to minimize the impact of fiber implantation on the surrounding microcirculation in tissue. This fiber was sheathed within a standard 900 µm diameter optical fiber protective sleeve. In these probes only the end-face of the fiber is sensitive to temperature, with the coating that runs on the external surfaces of the fiber having no impact on measurements.

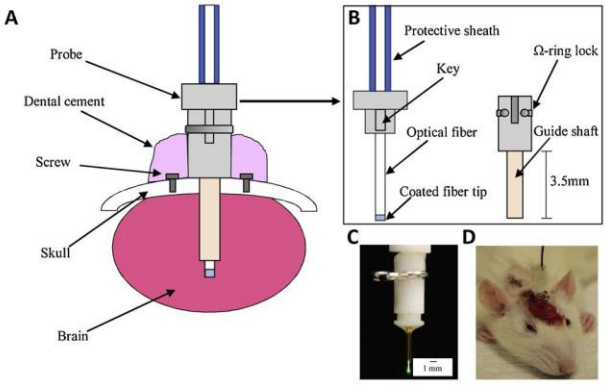

Fig. 1. (A) Surgical implantation of optical fiber temperature sensor. (B) Optical fiber temperature sensor and guide cannula structural components. (C) Photograph of the temperature sensor. (D) Photograph of the implanted sensor located in the striatum of an anaesthetized rat post-surgery.

2.2. Animals

Eight pathogen-free male Sprague-Dawley rats were used, weighing 270–300 g. All animals were supplied by the University of Adelaide Laboratory Animal Services (Adelaide, South Australia). Rats were housed in temperature (18–21 °C) and light-controlled (12 h light/dark cycle; lights on at 0700 h) rooms with standard rodent food and water available *ad libitum*. Ethics approval for this study was given by the University of Adelaide Animal Ethics Committee, and all procedures were in strict accordance with the National Health and Medical Council of Australia Guidelines for the Care and Use of Laboratory Animals.

2.3. Optical fiber guide cannula implantation

Rats were anesthetized with chloral hydrate (400 mg/kg i.p.) in 0.9% saline and placed on a water-heated pad (37 °C). Once fully anesthetized, the animal's head was secured in a stereotaxic frame (Kopf Instruments, Tujunga, CA, USA). After the skull was exposed, the bregma was located and the guide cannula was implanted into the right striatum (A: + 0.2 mm, L: + 3.0 mm, V: − 3.5 mm from bregma). All coordinates were referenced from a rat brain atlas (Paxinos and Franklin, 2004). The guide cannula was held in place using dental cement (Vertex, Dentimex BV HJ, Zeist, Netherlands) to form a robust attachment point to the skull (Fig. 1). Following the surgery, rats were given 48 h to recover. A recovery period of 24 h is considered as satisfactory for microdialysis studies, as neurotransmitter levels are stabilized and interference due to surgery and anesthesia is limited (Westerink, 2000; Esteban et al., 2001; O'Shea et al., 2005). At the end of each experiment animals were humanely killed *via* anesthetic overdose with chloral hydrate and brains carefully removed and stored in the freezer for future histological analysis to validate correct probe placement.

2.4. Drug treatments

Prior to saline (10 ml/kg, i.p) or MDMA (10 mg/kg, i.p) administration at t = 0 on the experimental day, ambulatory rats were pretreated with 3 doses of saline (10 ml/kg, i.p) following a therapeutic drug pre-treatment schedule. On the experimental day, rats were gently restrained as the dummy cap was removed from the guide cannula and the temperature probe inserted into the striatum. Brain temperature recording was started shortly after probe insertion at 9am (time − 120),

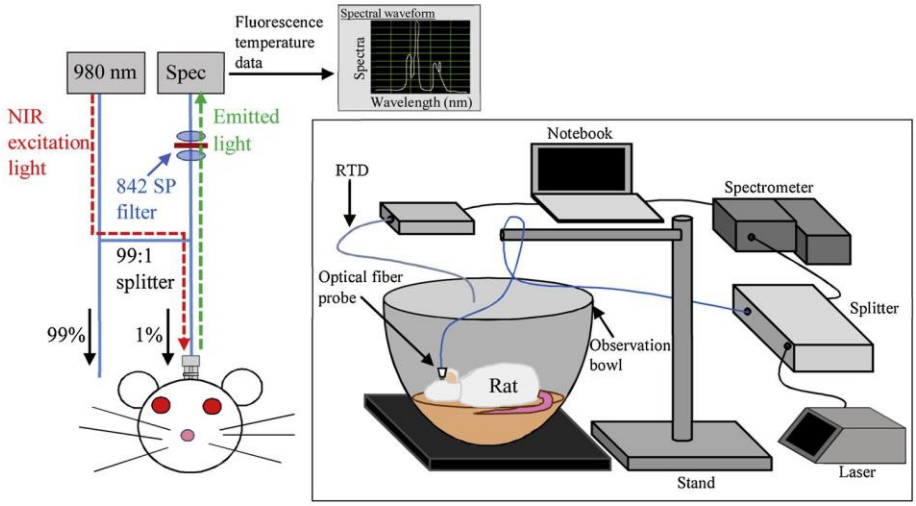

Fig. 2. Experimental setup for *in vivo* temperature measurement using portable optical fiber temperature sensor. A 980-nm wavelength excitation light is used, and the emitted light of 524-nm and 547-nm are acquired with a spectrometer. Adapted with permission from (Musolino et al., 2016), Optical Society of America.

and the last saline pre-treatment injection administered at 10.30am (time −30). The temperature recordings taken between time −120 and time 0 were used to establish baseline brain temperature levels. At 11am (time 0), rats received either saline (10 ml/kg, i.p) or MDMA (10 mg/kg, i.p) after which brain temperature was recorded for a further 4 h until the end of the experiment. A 4 h recording time post-MDMA was chosen as this is a sufficient time period to capture MDMA's peak hyperthermic effects. National Instruments LabVIEW software was used to simultaneously record both the upconversion emission from the fiber probe, as well as the ambient temperature from a resistance temperature detector (RTD) (Fig. 2). A high ambient room temperature of 29 °C was maintained for the duration of the experiment.

2.5. Data analysis

Significant brain temperature differences between control and MDMA-treated groups were evaluated using two-way ANOVA with Bonferroni's post-hoc test. $P < 0.05$ was considered statistically significant.

3. Results

3.1. Post-operation

After the operation, animals recovered quickly and resumed eating and grooming after awakening and were allowed free movement around the observation bowl during the recovery period. All animals were closely monitored over the following 48 h to ensure no damage was done to the guide cannula. Some animals scratched at the guide cannulae area however none were able to remove the guide cannula or open the Ω-ring lock on the guide shaft. The implantation of guide cannulae independent of the sensor ensured no damage was done to the sensor during the recovery period prior to experimentation. Conversely, previous model sensors suffered from twisting and tension along the length of the fiber post-surgery (Fig. 3) and this resulted in probe breakage prior to experimentation on 9 of 15 occasions. Post-experiment, animals were sacrificed, and the temperature probe removed from the guide cannula for later reuse. Guide cannulae were then removed from the skull.

3.2. Probe durability

On the experimental day the temperature probe was inserted

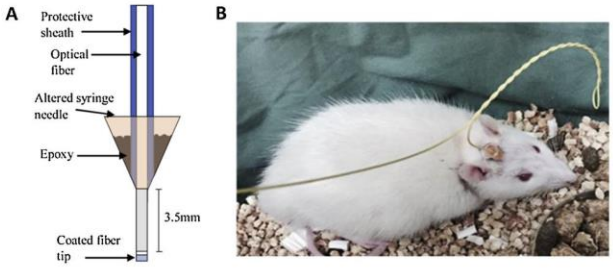

Fig. 3. (A) Previous model temperature sensor structural components. (B) Photograph of previous model temperature sensor implanted within a live rat. Movement of the animal during the overnight recovery period lead to excessive fiber twisting resulting in probe breakage.

successfully through the guide shaft without damaging the probe tip (Fig. 4A). Bending and twisting of the probe was observed throughout MDMA experiments, however this did not result in probe breakage on any occasion. Removed brains displayed only a small hole indicating that animal movement during the experiment resulted in no lateral movement of the probe within the guide shaft (Fig. 4B). Post experiment, *in vitro* probe calibration tests revealed that no significant difference in overall probe signal intensity between pre-implant and post-implant probes, indicating no damage to the sensor occurred during the experiment (Fig. 4C). Post-experiment calibrations also displayed no significant difference in fluorescence intensity ratio (FIR) generated temperature values between pre-implant and post-implant probes, indicating probes were capable of reuse after removal (Fig. 4D).

The separation of temperature sensor from the implant housing allowed for multiple animal implantations per week while requiring only one calibrated sensor for data collection. This facilitated increased experimental throughput on consecutive days due to reduced fiber fabrication time. Previous methods required one calibrated sensor per animal, limiting experimental output due to necessary fiber re-fabrication periods post-experiment. The ability for easy probe removal post-experiment also significantly cut time and resources costs associated with fabricating new sensors for following experiments. This also removed the potential for probe tip damage during cannula removal from the skull following data collection.

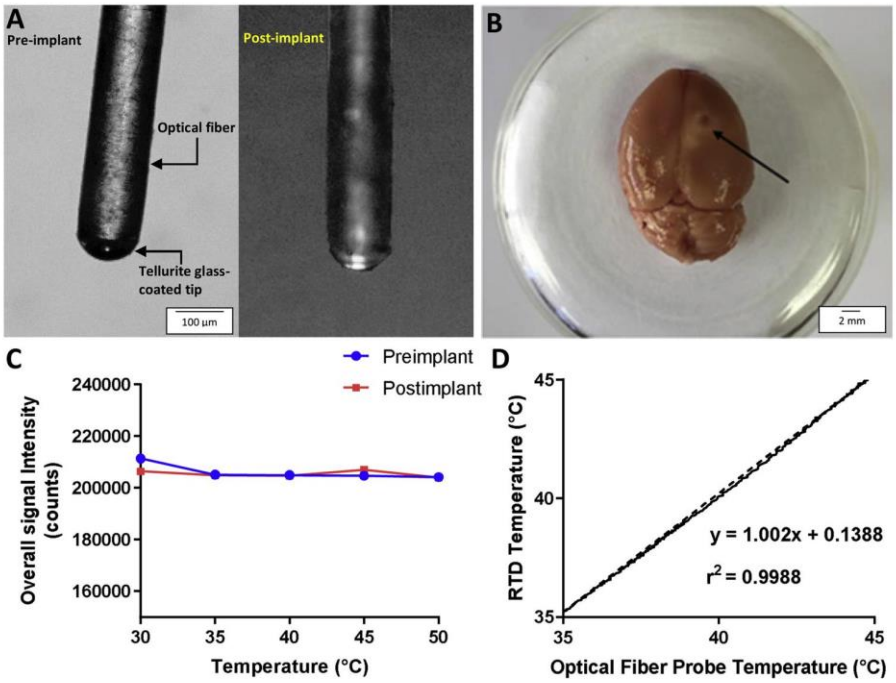

Fig. 4. (A) Microscopic photograph of the temperature sensor and tellurite glass-coated tip pre and post brain implantation. (B) A small hole indicating where the probe was inserted. (C) *In vitro* overall signal intensity results for brain temperature probes pre and post implantation. (D) Linear regression curve of optical fiber temperature probe post-implantation and RTD. Optical fiber probe temperature data expressed utilizing pre-implant calibration values.

3.3. Effect of MDMA at high ambient temperature

Using our improved technique, we found that changes in brain temperature caused by differential drug treatments were clearly identifiable. Fig. 5 shows that when administered at high ambient temperature a saline drug treatment caused no significant increase in striatal brain temperature at any time point compared to baseline temperatures ($p > 0.05$). The mean basal temperature of saline treated rats was 36.34 °C ± 0.13 and this remained steady with no significant fluctuation for the duration of the experiment.

However, MDMA administration at high ambient temperature caused significant increases in striatal brain temperature. Fig. 5 shows that striatal temperature was significantly increased at 30 min post-MDMA administration ($p < 0.0246$) compared to the saline controls ($p > 0.05$), and this peaked at 90 min post-MDMA ($p < 0.0001$). The MDMA-induced elevated striatal temperature was maintained for the majority of the 4-h observation period, however significant temperature differences ceased at 156 min post-MDMA ($p > 0.05$).

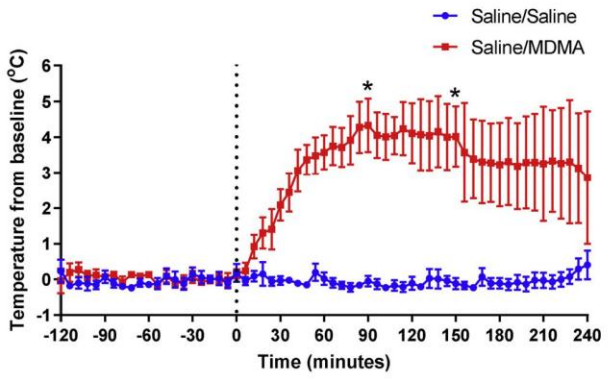

Fig. 5. *In vivo* results for fluorescence brain temperature probes in saline/saline (n = 4) and saline/MDMA treated rats (n = 4) at high ambient temperature (29 °C). Temperature data is presented as temperature change from baseline values and averaged across all trials at 6-minute intervals. Error bars show the standard error in the mean. * indicates where animals died prematurely.

4. Discussion

Until recently, the approaches to measure brain temperature *in vivo* has been limited to thermocouple electrodes, which lack many of the benefits provided by light-based sensing. This led us to develop an optical fiber based temperature probe capable of recording brain temperature within an ambulatory rat (Musolino et al., 2016). Although this sensor achieved localized temperature measurement within deep brain structures, its durability before and during experimentation was not satisfying. Therefore, we developed an improved optical fiber temperature probe with increased durability that utilized a more conventional stereotaxic implantation and insertion technique.

This new optical fiber temperature probe and altered implantation method provided many advantages at all stages of our experiments compared to previously used probe designs. The ease of surgical implantation was greatly increased, as guide cannulae used with the new probe interacted more smoothly with the stereotaxic equipment during surgical implantation compared to the previous probe's altered syringe needle housing. Furthermore, the separation of the sensor from the guide cannula allowed for significantly increased probe durability during the recovery period post-surgery. Many experiments utilizing previous probes ended prematurely due to probe breakage pre-experimentation. Unlike the improved design, previous probes were non-removable from the brain of the rat without first removing the dental cement affixing it to the skull. This made the probe extremely susceptible to breakage when left unattended during overnight recovery. Most probes were either snapped due to excessive twisting caused by animal movement or gnawed through by the animal, resulting in the complete loss of the experiment. New probes were fabricated with the capacity for removal after surgical implantation to remedy this issue. This removability and reusability feature allowed for multiple animal implantations whilst requiring only one temperature probe for all brain thermorecording. This feature drastically reduced the time and resources spent fabricating new sensors after each failed experiment and allowed experiments to take place in parallel increasing experimental workflow.

Using our improved method, we found that a dose of MDMA (10 mg/kg, i.p.) administered at high ambient temperature (29 °C) induced a long and modest hyperthermia in some animals, while others showed extremely high pathological increases in brain temperature values compared to their saline controls. MDMA under these warm conditions was excessively toxic, resulting in lethal over-heating of brain tissue (> 42 °C) in two tested animals. This mortality rate is notable as the commonly accepted LD_{50} for intraperitoneally injected MDMA in the rat is 49 mg/kg (Hardman et al., 1973). The results gathered by our improved probe support previous data that high ambient temperatures exacerbate the MDMA-induced hyperthermic response (Gordon et al., 1991; Malberg and Seiden, 1998; Seiden and Sabol, 1996). It is well known that the brain is the most temperature sensitive organ in the body and even small deviations in temperature can have profound negative impacts within the brain (Schiff and Somjen, 1985), thus an effective means of localized thermometry is required to better assess and understand these impacts.

Optical fiber sensors should compete with more established neural recording techniques such as thermocouple electrodes, however these new sensors do not always appeal to users already accustomed to these mature technologies (Lee, 2003). We have developed a new probe that utilizes an implant procedure identical to that of conventional microdialysis techniques, complete with a fully portable optical setup (Musolino et al., 2016) to accommodate an ease of transition from conventional techniques to the advantageous optical fiber sensing. These fiber sensors also have the potential for multiplexing with other sensors to measure other chemical properties, or for simultaneous imaging and sensing to be done using the same fiber (Li et al., 2018).

Future investigations will use this method of brain thermorecording to assess the therapeutic effects of treatment drugs in animals suffering from acute MDMA intoxication. This improved method of temperature measurement in the brain should allow for an improved understanding of the hyperthermic effects of stimulant drugs, as well as the therapeutic effects of the drugs used to alleviate their dangerous clinical symptoms.

We believe that our novel temperature probe and revised implantation technique can be employed to make brain thermorecording using optical fiber sensors in awake free-moving rats easier, more reliable, and more reproducible in future neurological studies.

Conflicts of interest

None.

Acknowledgements

E. Schartner and M. Hutchinson acknowledge financial support from an ARC Linkage funding project (LP110200736). This work was performed in part at the OptoFab node of the Australian National Fabrication Facility utilizing Commonwealth and South Australian State Government funding.

References

Berthou, H., Jörgensen, C., 1990. Optical-fiber temperature sensor based on upconversion-excited fluorescence. Opt. Lett. 15, 1100–1102.
Brown, P.L., Kiyatkin, E.A., 2004. Brain hyperthermia induced by MDMA (ecstasy): modulation by environmental conditions. Eur. J. Neurosci. 20, 51–58.
Busto, R., Dietrich, W.D., Globus, M.Y.-T., Valdés, I., Scheinberg, P., Ginsberg, M.D., 1987. Small differences in intraischemic brain temperature critically determine the extent of ischemic neuronal injury. J. Cereb. Blood Flow Metab. 7, 729–738.
Chavko, M., Koller, W.A., Prusaczyk, W.K., Mccarron, R.M., 2007. Measurement of blast wave by a miniature fiber optic pressure transducer in the rat brain. J. Neurosci. methods 159, 277–281.
Dos Santos, P., De Araujo, M., Gouveia-Neto, A., Neto, J.M., Sombra, A., 1998. Optical temperature sensing using upconversion fluorescence emission in Er3+/Yb3+-co-doped chalcogenide glass. Appl. Phys. Lett. 73, 578–580.
Esteban, B., O'shea, E., Camarero, J., Sanchez, V., Green, A.R., Colado, M.I., 2001. 3, 4-Methylenedioxymethamphetamine induces monoamine release, but not toxicity, when administered centrally at a concentration occurring following a peripherally injected neurotoxic dose. Psychopharmacology 154, 251–260.
Gordon, C.J., Watkinson, W.P., O'callaghan, J.P., Miller, D.B., 1991. Effects of 3,4-methylenedioxymethamphetamine on autonomic thermoregulatory responses of the rat. Pharmacol. Biochem. Behav. 38, 339–344.
Grant, S.A., Bettencourt, K., Krulevitch, P., Hamilton, J., Glass, R., 2001. In vitro and in vivo measurements of fiber optic and electrochemical sensors to monitor brain tissue pH. Sens. Actuators B: Chem. 72, 174–179.
Hardman, H.F., Haavik, C.O., Seevers, M.H., 1973. Relationship of the structure of mescaline and seven analogs to toxicity and behavior in five species of laboratory animals. Toxicol. Appl. Pharmacol. 25, 299–309.
Jiang, J.Y., Lyeth, B.G., Clifton, G.L., Jenkins, L.W., Hamm, R.J., Hayes, R.L., 1991. Relationship between body and brain temperature in traumatically brain-injured rodents. J. Neurosurg. 74, 492–496.
Kalant, H., 2001. The pharmacology and toxicology of "ecstasy" (MDMA) and related drugs. Canad. Med. Assoc. J. 165, 917–928.
Kiyatkin, E.A., 2005. Brain hyperthermia as physiological and pathological phenomena. Brain Res. Rev. 50, 27–56.
Kiyatkin, E.A., 2010. Brain temperature homeostasis: physiological fluctuations and Pathological Shifts. Front. Biosci. : J. Virtual Lib. 15, 73–92.
Kiyatkin, E.A., Kim, A.H., Wakabayashi, K.T., Baumann, M.H., Shaham, Y., 2014. Critical role of peripheral vasoconstriction in fatal brain hyperthermia induced by MDMA (Ecstasy) under conditions that mimic human drug use. J. Neurosci. 34, 7754–7762.
Lee, B., 2003. Review of the present status of optical fiber sensors. Opt. Fiber Technol. 9, 57–79.
Li, J., Schartner, E., Musolino, S., Quirk, B.C., Kirk, R.W., Ebendorff-Heidepriem, H., Mclaughlin, R.A., 2018. Miniaturized single-fiber-based needle probe for combined imaging and sensing in deep tissue. Opt. Lett. 43, 1682–1685.
Malberg, J.E., Seiden, L.S., 1998. Small changes in ambient temperature cause large changes in 3,4-methylenedioxymethamphetamine (MDMA)-induced serotonin neurotoxicity and core body temperature in the rat. J. Neurosci. 18, 5086–5094.
Musolino, S., Schartner, E.P., Tsiminis, G., Salem, A., Monro, T.M., Hutchinson, M.R., 2016. Portable optical fiber probe for in vivo brain temperature measurements. Biomed. Opt. Express 7, 3069–3077.
O'hara, J.A., Hou, H., Demidenko, E., Springett, R.J., Khan, N., SwarTZ, H.M., 2005. Simultaneous measurement of rat brain cortex PtO2 using EPR oximetry and a fluorescence fiber-optic sensor during normoxia and hyperoxia. Physiol. Meas. 26, 203.
O'shea, E., Escobedo, I., Orio, L., Sanchez, V., Navarro, M., Green, A.R., Colado, M.I., 2005. Elevation of ambient room temperature has differential effects on MDMA-induced 5-HT and dopamine release in striatum and nucleus accumbens of rats. Neuropsychopharmacology 30, 1312–1323.
Parrott, A., 2012. MDMA and temperature: a review of the thermal effects of 'Ecstasy'in humans. Drug Alcohol Depend. 121, 1–9.
Paxinos, G., Franklin, K.B., 2004. The Mouse Brain in Stereotaxic Coordinates. Gulf Professional Publishing.
Peterson, J.I., Fitzgerald, R.V., Buckhold, D.K., 1984. Fiber-optic probe for in vivo measurement of oxygen partial pressure. Anal. Chem. 56, 62–67.
Schartner, E., Monro, T., 2014. Fibre tip sensors for localised temperature sensing based on rare earth-doped glass coatings. Sensors 14, 21693.
Schiff, S.J., Somjen, G.G., 1985. The effects of temperature on synaptic transmission in hippocampal tissue slices. Brain Res. 345, 279–284.
Seiden, L.S., Sabol, K.E., 1996. Methamphetamine and methylenedioxymethamphetamine neurotoxicity: possible mechanisms of cell destruction. NIDA Res. Monogr. 163, 251–276.
Wade, S., Muscat, J., Collins, S., Baxter, G., 1999. Nd3+-doped optical fiber temperature sensor using the fluorescence intensity ratio technique. Rev. Sci. Instrum. 70, 4279–4282.
Westerink, B.H., 2000. Analysis of biogenic amines in microdialysates of the brain. J. Chromatogr. B: Biomed. Sci. Appl. 747, 21–32.
Yu, L., Wu, Y., Dunn, J.F., Murari, K., 2016. In-vivo monitoring of tissue oxygen saturation in deep brain structures using a single fiber optical system. Biomed. Opt. Express 7, 4685–4694.

Chapter 5 – Publication 3

Musolino, S.T., Schartner, E.P., Hutchinson, M.R. and Salem, A., 2019. Minocycline attenuates 3,4-methylenedioxymethamphetamine-induced hyperthermia in the rat brain. *European Journal of Pharmacology*, *858*, pp. 172495.

This paper shifts in focus to the first two papers. The previous papers focused mainly on initial optical fibre probe proof-of-concept, and further improvements to the original method. The aim of the current study was to use this optimised method of brain thermorecording to investigate the effects of the tetracycline drug minocycline on MDMA-induced increases in brain temperature, and the relationship between MDMA-induced temperature change in the brain when compared to the body. The current study compared the brain and body temperature changes occurring post-MDMA administration at both normal and high ambient temperature, as well as minocycline's hyperthermia attenuating effects in the brain and body. Concurrent measures of HR, and LMA were also undertaken to examine drug effects on these physiological parameters, as well as to better understand the physiological and pharmacological mechanisms underlying minocycline's' attenuation of MDMA-induced hyperthermia. Rationale for this investigation was based on lack of previous information regarding minocycline's hyperthermia-attenuating effects in the brain, as well as lack of knowledge regarding MDMA-induced brain hyperthermia in general.

Our study indicated that the temperature effects of MDMA occur more rapidly and to a greater extent in the brain when compared to the body. Brain temperatures dropped more suddenly and to lower levels when compared to body when MDMA was administered at normal ambient temperature. A similar trend was also apparent at high ambient temperature with significantly faster and more pronounced temperature elevations in the brain when compared to the

periphery. These rapid increases in temperature resulted in two fatalities when brain temperatures reached ~43 °C. HR and LMA were also significantly elevated post-MDMA. A three-day minocycline pretreatment attenuated MDMA-induced hyperthermia in the brain as well as in the body, and prevented all fatalities resulting from MDMA administration at high ambient temperature. We also found that minocycline attenuated MDMA-induced increases in LMA, and lowered baseline HR levels prior to MDMA administration.

Statement of Authorship

Title of Paper	Minocycline attenuates 3,4-methylenedioxymethamphetamine-induced hyperthermia in the rat brain.
Publication Status	☑ Published ☐ Accepted for Publication ☐ Submitted for Publication ☐ Unpublished and Unsubmitted w ork w ritten in manuscript style
Publication Details	European Journal of Pharmacology, 858, pp. 172495. https://doi.org/10.1016/j.ejphar.2019.172495

Principal Author

Name of Principal Author (Candidate)	Stefan T Musolino
Contribution to the Paper	Had major input into study design, performed all experimental procedures, statistical analysis, graphical representation of data collected, wrote and prepared the manuscript for submission, and acted as corresponding author.
Overall percentage (%)	90%
Certification:	This paper reports on original research I conducted during the period of my Higher Degree by Research candidature and is not subject to any obligations or contractual agreements with a third party that would constrain its inclusion in this thesis. I am the primary author of this paper.
Signature	Date 22/08/2019

Co-Author Contributions

By signing the Statement of Authorship, each author certifies that:

i. the candidate's stated contribution to the publication is accurate (as detailed above);

ii. permission is granted for the candidate in include the publication in the thesis; and

iii. the sum of all co-author contributions is equal to 100% less the candidate's stated contribution.

Name of Co-Author	Erik P Schartner
Contribution to the Paper	Assisted with study design, statistical analysis, graphical representation of data collected, provided critical review of manuscript drafts prior to submission.
Signature	Date 22/08/2019

Name of Co-Author	Mark R Hutchinson
Contribution to the Paper	Assisted with study design, statistical analysis, and provided critical review of manuscript drafts prior to submission.
Signature	Date 22/08/2019

Please cut and paste additional co-author panels here as required.

Name of Co-Author	Abdallah Salem		
Contribution to the Paper	Assisted with study design, statistical analysis, and provided critical review of manuscript drafts prior to submission.		
Signature		Date	22/08/2019

European Journal of Pharmacology 858 (2019) 172495

Contents lists available at ScienceDirect

European Journal of Pharmacology

journal homepage: www.elsevier.com/locate/ejphar

Full length article

Minocycline attenuates 3,4-methylenedioxymethamphetamine-induced hyperthermia in the rat brain

Stefan T. Musolino[a,b,*], Erik P. Schartner[a,c], Mark R. Hutchinson[a,b], Abdallah Salem[b]

[a] ARC Centre of Excellence for Nanoscale BioPhotonics and Institute for Photonics and Advanced Sensing, Adelaide, SA, 5005, Australia
[b] Discipline of Pharmacology, Adelaide Medical School, The University of Adelaide, Adelaide, SA, 5005, Australia
[c] School of Physical Sciences, The University of Adelaide, Adelaide, SA, 5005, Australia

ARTICLE INFO

Keywords:
3,4-Methylenedioxymethamphetamine
Minocycline
Hyperthermia
Brain temperature
Radiotelemetry
Warm environment

ABSTRACT

Hyperthermia is most dangerous clinical symptom of acute MDMA administration, and a key factor related to potentially life-threatening MDMA-induced complications. MDMA induces a consistently faster onset of brain hyperthermia when compared to a delayed and moderate hyperthermia in the body, and the most harmful effects of MDMA are related to its modulation of neural functions. The primary focus of this study was to investigate the effects of minocycline, a centrally acting tetracycline derivative on MDMA-induced brain hyperthermia at high ambient temperature. However, we also simultaneously recorded body temperature, heart rate, and locomotor activity changes, allowing us to gain a better understanding of the mechanisms underlying the MDMA-induced hyperthermic response. We also investigated the effects of MDMA at normal ambient temperature to provide further evidence as to the importance of environmental factors on the intensity of MDMA's temperature effects. At normal ambient temperature, MDMA (10 mg/kg, i.p.) induced a significant brain and body hypothermia for the first 90 min following drug administration, and significantly increased heart rate and locomotor activity compared to saline controls. At high ambient temperature however, MDMA (10 mg/kg, i.p.) induced a robust and extended brain and body hyperthermia, as well as significantly increased heart rate and locomotor activity. A 3-day minocycline (50 mg/kg, i.p.) pre-treatment significantly attenuated MDMA-induced increases in brain temperature, body temperature, heart rate, and locomotor activity. Our findings indicate that minocycline is more effective in attenuating the exacerbated MDMA-induced hyperthermic response in the brain compared to the body at high ambient temperature.

1. Introduction

3,4-methylenedioxymethamphetamine (MDMA, Ecstasy) is a drug of abuse used frequently by young people in a recreational setting, particularly at warm, crowded dance venues (Kalant, 2001; Green et al., 2003). It's been well documented that prolonged use of MDMA and its administration in high doses can be fatal in humans (Garcıa-Repetto et al., 2003; Walubo and Seger, 1999) and leads to neurotoxicity in serotonin (5-HT) and dopamine (DA) systems in the brains of animals (Green et al., 2003; Orio et al., 2010; Jensen et al., 1993; O'hearn et al., 1988; Ricaurte et al., 2002; Colado et al., 2001; Müller et al., 2019).

In addition to long-term neurotoxic effects, MDMA has also been shown to induce an acute hyperthermic response in animals which has been identified as the most dangerous clinical symptom of acute MDMA administration and a key factor related to life-threatening MDMA-induced complications such as rhabdomyolysis, renal failure, hyponatremia, haemodilution, disseminated intravascular coagulation and brain oedema (Kalant, 2001; Green et al., 2004; Stanley et al., 2007; Anderson et al., 2011). The patterns of this MDMA-induced hyperthermic response in the body are well-known (Mechan et al., 2001; Colado et al., 1993; Broening et al., 1995; Dafters, 1994; Stanley et al., 2007; Malberg and Seiden, 1998), however, the accompanying changes in brain temperature and how they relate to the progression of hyperthermia in the body are not as well understood. Previous research has established that brain hyperthermia has deleterious effects on neural cells and brain functioning including disruption of the blood-brain barrier (Kiyatkin et al., 2007; Kiyatkin and Sharma, 2009a, 2009b). Considering the temperature dependence of many psychochemical processes governing neural activity and neuronal cell health, brain hyperthermia may be a key factor for potentiating the toxic effects of MDMA in the brain.

Despite the potential danger MDMA administration poses, the

* Corresponding author. ARC Centre of Excellence for Nanoscale BioPhotonics and Institute for Photonics and Advanced Sensing, Adelaide, SA, 5005, Australia.
E-mail address: stefan.musolino@adelaide.edu.au (S.T. Musolino).

https://doi.org/10.1016/j.ejphar.2019.172495
Received 12 April 2019; Received in revised form 21 June 2019; Accepted 21 June 2019
Available online 22 June 2019

emergency room strategies to treat these serious heath complications are limited. Current emergency techniques to counteract MDMA-induced hyperthermia include simple whole body cooling techniques, fluid and electrolyte replacement therapies, anaesthesia, and the muscle relaxant dantrolene in extreme cases of hyperpyrexia (Hall and Henry, 2006; Grunau et al., 2010). Considering these limited options, there is a pressing need for effective pharmacotherapy used to treat MDMA-induced hyperthermia in a clinical setting.

The semi-synthetic tetracycline derivative minocycline is an antibiotic drug with unique ability to cross the blood brain barrier and possesses potent anti-inflammatory and neuroprotective properties thought to be a result of its ability to inhibit microglial activation and the ensuing release of cytotoxic substances (Stirling et al., 2005; Domercq and Matute, 2004; Yrjanheikki et al., 1998; Yrjänheikki et al., 1999; Chen et al., 2000; Wang et al., 2003; Du et al., 2001; Zhu et al., 2002). In addition to this, minocycline has been shown to attenuate long-term MDMA-induced 5-HT and DA neurotoxicity (Zhang et al., 2006; Orio et al., 2010) as well as acute MDMA-induced body hyperthermia in animals (Anderson et al., 2011). Although minocycline has been seen to attenuate MDMA-induced hyperthermia in the body, its exact effects on the temperature of the brain post-MDMA administration are currently unknown.

Previous research has revealed that drugs acting centrally display superior effectiveness in reversing MDMA-induced hyperthermia compared to drugs acting in the periphery (Kiyatkin et al., 2016). Minocycline can readily cross the blood-brain barrier, regardless of dose and route of administration (Barza et al., 1975; Fagan et al., 2004) and thus, in this study we used brain thermorecording to assess the effectiveness of minocycline in reversing MDMA-induced hyperthermia in the brain at high ambient temperature. We also investigated MDMA's temperature effects at normal ambient temperature and employed radiotelemetry techniques to assess drug-induced changes in core body temperature, heart rate and locomotor activity to gain a better understanding of the mechanisms underlying MDMA-induced hyperthermia and their modulation by environmental conditions.

2. Materials and methods

2.1. Animals

24 pathogen-free male Sprague-Dawley rats were used, weighing 270–300 g. All animals were supplied by the University of Adelaide Laboratory Animal Services (Adelaide, South Australia). Rats were housed in temperature (18–21 °C) and light-controlled (12 h light/dark cycle; lights on at 0700 h) rooms with standard rodent food and water available *ad libitum*. Ethics approval for this study was given by the University of Adelaide Animal Ethics Committee, and all procedures were in strict accordance with the National Health and Medical Council of Australia Guidelines for the Care and Use of Laboratory Animals.

2.2. Drug treatments

Minocycline hydrochloride (Sigma-Aldrich, St. Louis, USA) was dissolved in 0.9% saline solution. Minocycline (50 mg/kg) or vehicle was injected intraperitoneally (i.p.) in a volume of 10 ml/kg once a day, three days prior to the experiment. This pre-treatment dosing regimen of minocycline was selected because similar dosing regimens inhibited immune response to lipopolysaccharide challenge in mice (O'connor et al., 2009), and was shown to attenuate MDMA-induced body hyperthermia in rats (Anderson et al., 2011). MDMA (Australian Government Analytical Laboratories, Sydney Australia) was dissolved in 0.9% saline solution. MDMA (10 mg/kg) was injected i.p. in a volume of 10 ml/kg. This dose of MDMA was selected because at this dose the drug was shown to consistently produce hyperthermia in rats (Stanley et al., 2007) and result in similar plasma concentrations of the drug that had been reported in human cases of hyperthermia (Colado et al., 1995; Chu et al., 1996).

2.3. Measurement of body temperature, heart rate, and locomotor activity by radiotelemetry

Rats were anesthetized with chloral hydrate (400 mg/kg i.p.) in 0.9% saline and placed on a water-heated pad (37 °C). Once fully anesthetized, rats were surgically implanted with telemetry devices (Data Sciences International TA11CTA-F40), that measure core body temperature, locomotor activity, and ECG, as reported previously (Bexis et al., 2004; Musolino et al., 2016). One-week recovery from surgery was allowed before rats underwent any drug treatments. A radio receiver, placed under the observation bowl, received information from the implants and transferred it to a computer that recorded the data using the Dataquest LabPro software (Data Sciences International).

2.4. Measurement of brain temperature by optical fiber temperature sensor

Rats were anesthetized with chloral hydrate (400 mg/kg i.p.) in 0.9% saline and placed on a water-heated pad (37 °C). Once fully anesthetized, the animal's head was secured in a stereotaxic frame (Kopf Instruments, Tujunga, CA, USA). After the skull was exposed, the bregma was located and the guide cannula with dummy cap was implanted into the right striatum (A: +0.2 mm, L: +3.0 mm, V: 3.5 mm from bregma) as described previously (Musolino et al., 2019). All coordinates were referenced from a rat brain atlas (Paxinos and Watson, 1998). The striatum was chosen as it has previously been implicated in the MDMA-induced hyperthermic response as well as the behavioral changes induced by MDMA (Malberg and Seiden, 1998; Dafters and Lynch, 1998; Shankaran and Gudelsky, 1999; Mechan et al., 2002). The guide cannula was held in place using dental cement (Vertex, Dentimex BV HJ, Zeist, Netherlands) to form a robust attachment point to the skull. Following the surgery, rats were given 48 h to recover. A recovery period of 24 h is considered as satisfactory for microdialysis studies, as neurotransmitter levels are stabilized and interference due to surgery and anaesthesia is limited (Westerink, 2000; Esteban et al., 2001, O'shea et al., 2005).

2.5. Experimental protocol

On the experiment day, rats were gently restrained as the dummy cap was removed from the guide cannula and the optical fiber temperature sensor inserted into the striatum after which brain temperature and telemetry recording was started (t = −120 min). The recordings taken between time −120 and time 0 were used to establish baseline brain and body temperature levels. At t = 0, rats received MDMA (10 mg/kg) after which recordings continued for a further 4 h until the end of the experiment. National Instruments LabVIEW software was used to simultaneously record both the upconversion emission from the fiber probe, as well as the ambient temperature from a resistance temperature detector (RTD). Radio data from the telemetry implant was recorded every 2 min over the experimental period. For Experiment 1, experiments occurred at normal ambient temperature (23 °C). For Experiment 2, a high ambient room temperature (29 °C) was maintained for the duration of the experiments. At the end of each experiment animals were humanely killed via anesthetic overdose with chloral hydrate and brains carefully removed and stored in the freezer for future biochemical analysis.

2.6. Data analysis

To analyze the effects of treatments during the experiments, mean values for brain temperature, body temperature, heart rate, and locomotor activity were calculated for the time periods -30-0, 0–30, 30–60, 60–90, 90–120, 120–180, and 180–240 and analyzed between each of the four treatment groups. Significant differences between groups were

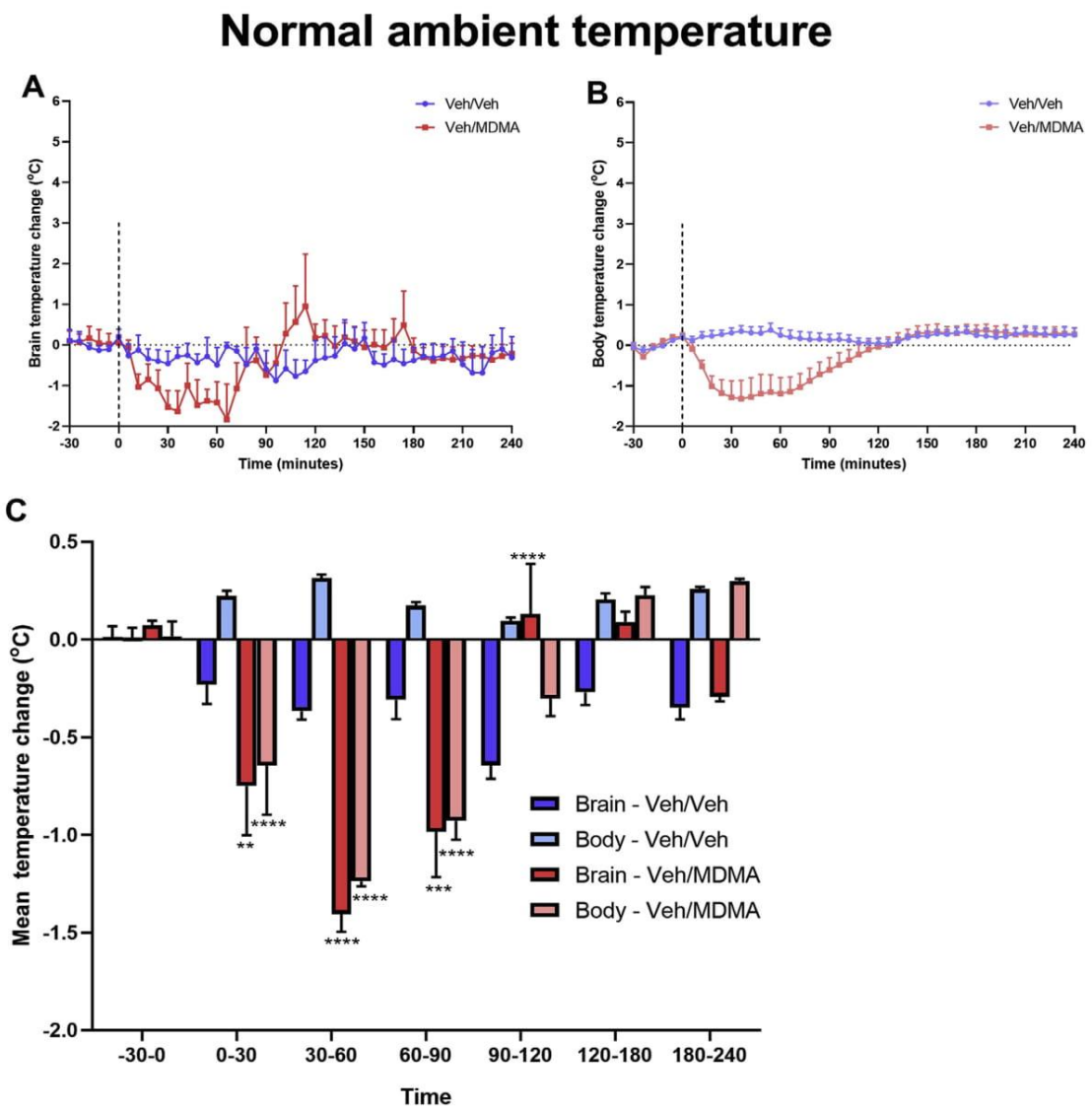

Fig. 1. Temperature effects of MDMA (10 mg/kg, i.p.) at normal ambient temperature. **(A)** Brain temperature change. **(B)** Body temperature change. Temperature data is presented as temperature change from baseline values and averaged across all trials at 6-min intervals (n = 4 per group). **(C)** Mean brain and body temperature change for different time periods for the corresponding line graphs. The * indicates significant difference from Veh/Veh (*$P < 0.05$, **$P < 0.01$, ***$P < 0.001$, ****$P < 0.0001$). Error bars show the standard error in the mean.

evaluated using two-way ANOVA with Bonferroni's post-hoc test. $P < 0.05$ was considered statistically significant.

3. Results

3.1. Effects of MDMA on brain and body temperature at normal ambient temperature

When administered at normal ambient temperature (23 °C), MDMA (10 mg/kg, i.p.) induced a moderate hypothermia in both the brain (~1 °C) and body (~0.9 °C) for the first 90 min post drug administration (Fig. 1). Basal temperatures were lower in the brain (36.9 ± 0.18 °C) compared to the body (37.2 ± 0.08 °C). Following MDMA administration, brain temperature was significantly decreased for the time periods 0–30 min (−0.75 ± 0.25, $P = 0.006$), 30–60 min (−1.4 ± 0.09 °C, $P < 0.0001$) and 60–90 min (−0.98 ± 0.23 °C, $P = 0.0002$) with an average temperature of 35.9 ± 0.56 °C for the first 90 min (Fig. 1C). A significant increase in temperature occurred during time period 90–120 min ($P < 0.0001$) before falling and then stabilizing for the remainder of the experiment (Fig. 1C). Body temperature was also significantly reduced following MDMA administration for time periods 0–30 min (−0.65 ± 0.25 °C, $P < 0.0001$), 30–60 min (−0.12 ± 0.27 °C, $P < 0.0001$) and 60–90 min (−0.93 ± 0.97 °C, $P < 0.0001$) with an average temperature of 36.6 ± 0.45 °C for approximately 90 min before returning to baseline levels and stabilizing for the remainder of the experiment (Fig. 1C).

3.2. Effects of MDMA on heart rate at normal ambient temperature

Two-way ANOVA analysis revealed significant differences between the two treatment groups at normal ambient temperature. Veh/MDMA rats had a significantly higher baseline heart rate (386 ± 6 bpm, $P < 0.0001$) when compared to veh/veh (346 ± 3 bpm) (Fig. 2). The administration of MDMA (10 mg/kg, i.p.) at normal ambient

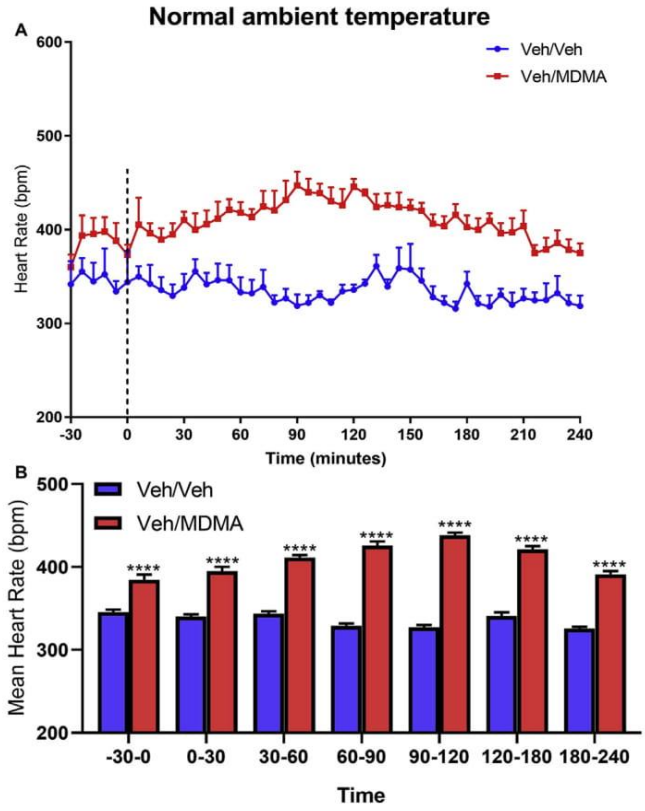

Fig. 2. (A) Effects of MDMA-induced increases in heart rate at normal ambient temperature. Data have been averaged across all trials at 6-min intervals (n = 4 per group). **(B)** Mean heart rate results at different time periods for the corresponding line graph. The * indicates significant difference from Veh/Veh (*P < 0.05, **P < 0.01, ***P < 0.001, ****P < 0.0001). Error bars show the standard error in the mean.

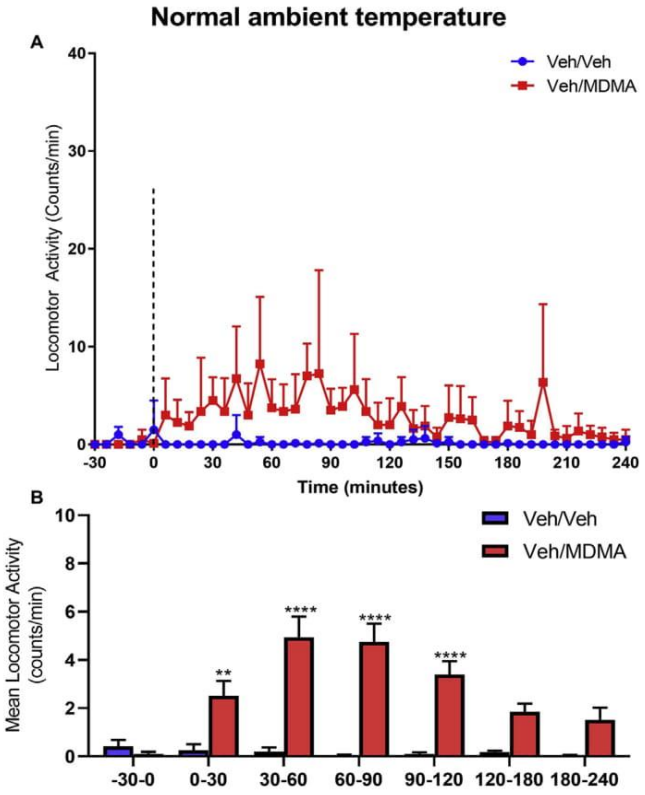

Fig. 3. (A) Effects of MDMA-induced increases in locomotor at normal ambient temperature. Data have been averaged across all trials at 6-min intervals (n = 4 per group). **(B)** Mean locomotor activity results at different time periods for the corresponding line graph. The * indicates significant difference from Veh/Veh (*P < 0.05, **P < 0.01, **P < 0.001, ****P < 0.0001). Error bars show the standard error in the mean. Y- axis scale has been maintained at 40 to allow comparisons between LMA graphs.

temperature caused heart rate to remain significantly increased at all time periods (P < 0.0001) (Fig. 2B). Mean heart rate following drug administration in MDMA treated rats was 411 ± 3 bpm, significantly increased compared to 334 bpm ± 2 bpm in saline controls.

3.3. Effects of MDMA on locomotor activity at normal ambient temperature

Two-way ANOVA analysis revealed significant differences between the two treatment groups. There was no significant difference in baseline locomotor activity between the two groups (P > 0.05). The administration of MDMA (10 mg/kg, i.p.) at normal ambient temperature significantly increased locomotor activity during the time periods 0–30 min (2.5 ± 0.61 counts/min, P = 0.003), 30–60 min (4.9 ± 0.86 counts/min, P < 0.0001), 60–90 min (4.8 ± 0.75 counts/min, P < 0.0001), and 90–120 min (3.4 ± 0.55, P < 0.0001) (Fig. 3B). Mean locomotor activity following drug administration in MDMA treated rats was 2.8 ± 0.33 counts/min, significantly increased compared to 0.14 ± 0.05 counts/min in saline controls.

3.4. Effects of MDMA on brain and body temperature at high ambient temperature

When given at high ambient temperature (29 °C), MDMA (10 mg/kg, i.p.) induced a robust hyperthermia in both the brain (+3.5 ± 0.51 °C) and body (+2.8 ± 0.96 °C) with temperatures remaining elevated above 40 °C for the duration of the experiment (Fig. 4). Basal temperatures were slightly higher in the body (37.2 ± 0.08 °C) when compared with the brain (36.4 ± 0.23 °C). The administration of MDMA (10 mg/kg, i.p.) at high ambient temperature produced significant brain hyperthermia for all time periods; 0–30 min (+1.0 ± 0.30 °C, P < 0.0001), 30–60 min (+3.0 ± 0.25 °C, P < 0.0001), 60–90 min (+3.9 ± 0.13 °C, P < 0.0001), 90–120 min (+4.1 ± 0.05 °C, P < 0.0001), 120–180 min (+3.7 ± 0.12 °C, P < 0.0001), 180–240 min (+3.2 ± 0.04 °C, P < 0.0001) (Fig. 4C). Body temperatures were also significantly increased for all time periods following MDMA administration; 0–30 min (+0.74 ± 0.19 °C, P = 0.0008), 30–60 min (+2.4 ± 0.25, P < 0.0001), 60–90 min (+3.5 ± 0.12 °C, P < 0.0001), 90–120 min (+3.5 ± 0.09 °C, P < 0.0001), 120–180 min (+3.3 ± 0.08 °C, P < 0.0001), 180–240 min (+3.0 ± 0.10 °C, P < 0.0001) (Fig. 4C). The brain saw significantly higher temperature increases when compared to the body at time 30–60 min (+0.59 °C, P < 0.0001), 60–90 min (+0.45 °C, P = 0.0063), and 90–120 min (+0.64 °C, P < 0.0001) (Fig. 4C). The effects of MDMA were varied among the four individuals. All rats showed a robust brain and body hyperthermia post-MDMA, however two rats displayed lethal hyperthermic responses with brain temperatures reaching +6.3 °C and +5.7 °C higher than baseline levels, and body temperatures reaching maximums of +6.0 °C and +4.7 °C respectively (Fig. 5). Both rats died following extended hyperthermia with their brain temperatures reaching > 43 °C. Although both rats died, there was a large time difference between MDMA administration and time of death with one rat dying at 90 min while the other died at 150 min (Fig. 5). The initial onset of hyperthermia differed between the brain and the body of MDMA-treated animals. Animals

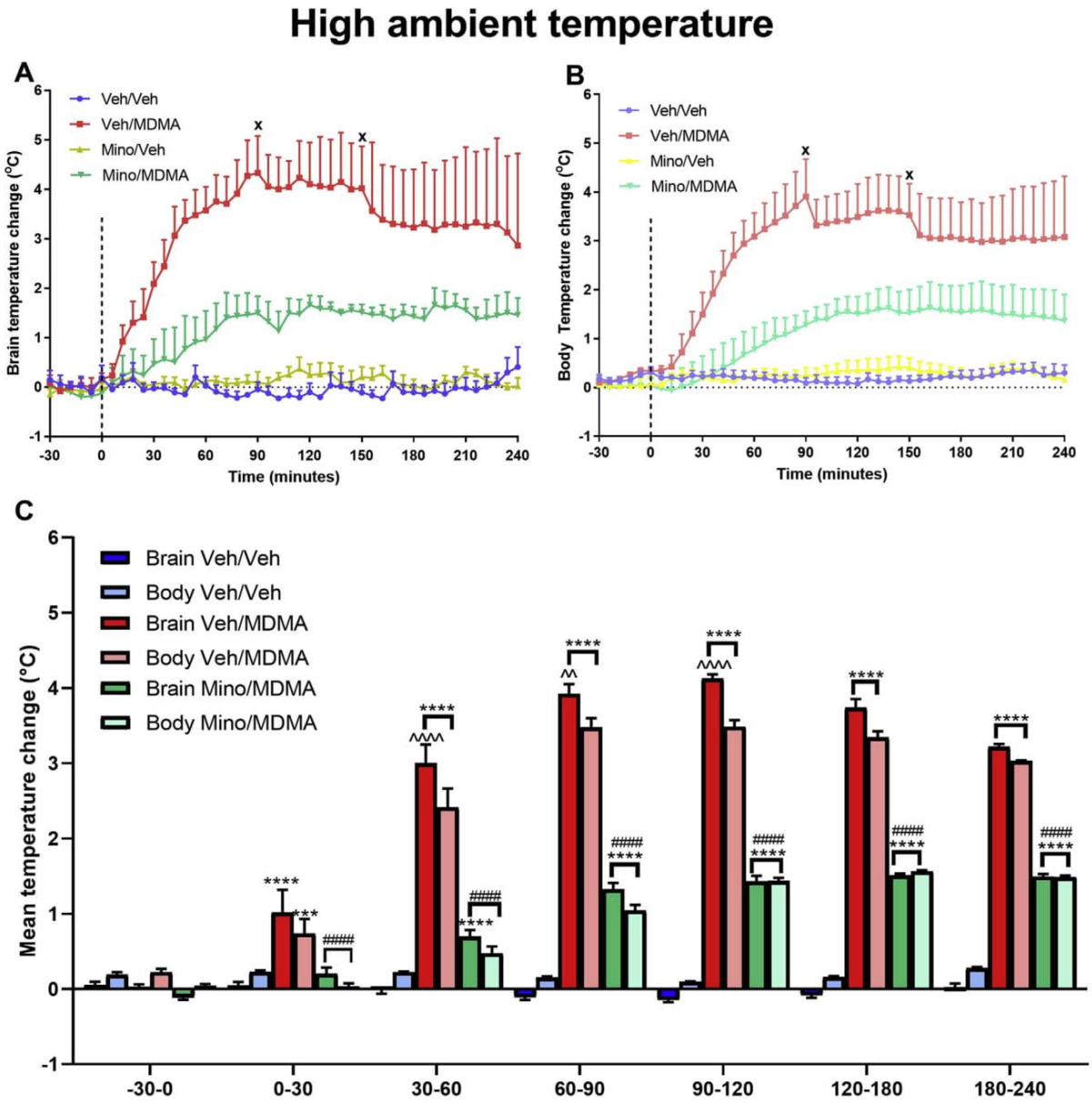

Fig. 4. Temperature effects of MDMA (10 mg/kg, i.p.) and minocycline (50 mg/kg, i.p.) at high ambient temperature. **(A)** Brain temperature change. **(B)** Body temperature change. Temperature data is presented as temperature change from baseline values and averaged across all trials at 6-min intervals (n = 4 per group). X indicates where animals died prematurely. **(C)** Mean brain and body temperature change for different time periods. The * indicates significant difference from Veh/Veh, the # indicates significant difference from Veh/MDMA, the ^ indicates significant difference from body temperature (*$P < 0.05$, **$P < 0.01$, ***$P < 0.001$, ****$P < 0.0001$). No significant difference was found between the control groups veh/veh and mino/veh, therefore mino/veh data has been excluded to improve graph readability. Error bars show the standard error in the mean.

displayed significant brain hyperthermia approximately 12 min post-MDMA administration ($P < 0.01$). This was delayed in the body where no significant increase in temperature was recorded until 24 min post-MDMA ($P = 0.0003$).

3.5. Effects of minocycline on MDMA-induced brain and body hyperthermia at high ambient temperature

Two-way ANOVA analysis revealed significant differences in groups pre-treated with minocycline (50 mg/kg, i.p.) at high ambient temperature. Minocycline pre-treatment was shown to have no significant effect on baseline temperature levels pre-MDMA ($P > 0.05$). MDMA-induced brain hyperthermia was significantly attenuated by minocycline (50 mg/kg, i.p.) at all time periods; 0–30 min (+0.2 ± 0.08 °C, $P < 0.0001$), 30–60 min (+0.7 ± 0.09 °C, $P < 0.0001$), 60–90 min (+1.3 ± 0.09 °C, $P < 0.0001$), 90–120 min (+1.4 ± 0.07 °C, $P < 0.0001$), 120–180 min (+1.5 ± 0.03 °C, $P < 0.0001$), 180–240 min (+1.5 ± 0.03 °C, $P < 0.0001$) (Fig. 4). Average brain temperature for the duration post-MDMA administration was 37.1 ± 0.6 °C MDMA-induced increases in body temperature were also significantly attenuated for all time periods; 0–30 min (+0.04 ± 0.04 °C, $P = 0.0028$), 30–60 min (+0.47 ± 0.09 °C, $P < 0.0001$), 60–90 min (+1.0 ± 0.08 °C, $P < 0.0001$), 90–120 min (+1.4 ± 0.04 °C, $P < 0.0001$), 120–180 min (+1.6 ± 0.01 °C,

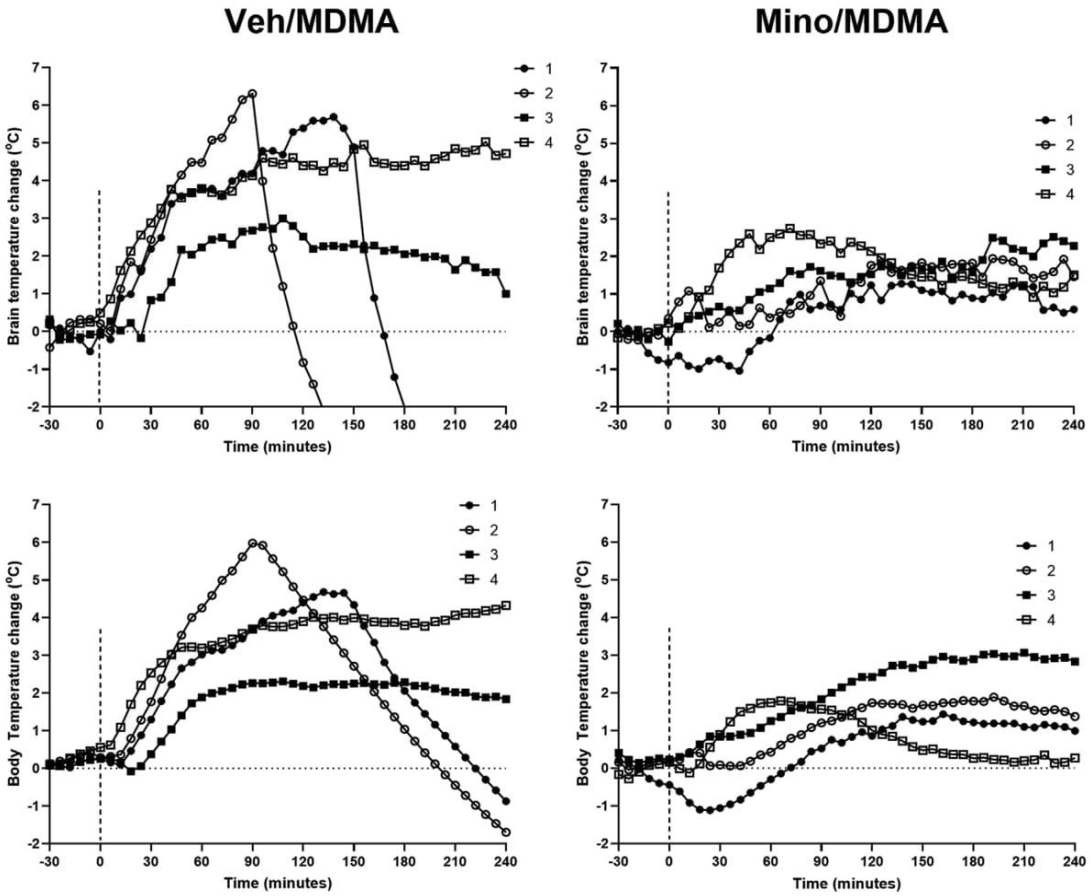

Fig. 5. Individual changes in brain and body temperature induced by MDMA (10 mg/kg, i.p.) and minocycline (50 mg/kg, i.p.) administered at high ambient temperature. Veh/MDMA caused premature death in 2 of 4 individuals after brain temperatures reached > 43 °C.

$P < 0.0001$), 180–240 min (+1.5 ± 0.02 °C, $P < 0.0001$) (Fig. 4). Average body temperature for the duration post-MDMA administration was 37.8 ± 0.6 °C. There was no significant difference between brain and body temperature in minocycline pre-treated animals at any time point ($P > 0.05$). Temperature responses varied amongst individuals pre-treated with minocycline post-MDMA administration. Maximum temperature increases from baseline varied between +1.3 and +2.7 °C and +1.4 to +3.1 °C in the brain and body respectively, however this was significantly reduced compared to saline pre-treated animals at +3.0 to +6.3 °C in the brain and +2.3 to +6.0 °C in the body. These reduced temperature increases did not result in premature death in any of the individuals (Fig. 5).

3.6. Effects of MDMA and minocycline on heart rate at high ambient temperature

Two-way ANOVA analysis revealed significant differences among the four treatment groups at high ambient temperature. Basal heart rate was significantly lower in mino/veh (310 ± 4 bpm, $P < 0.0001$) and veh/MDMA (315 ± 4 bpm, $P = 0.0003$) groups compared to veh/veh (345 ± 3 bpm). (Fig. 6). The administration of MDMA (10 mg/kg, i.p.) at high ambient temperature significantly increased heart rate during time periods 30–60 min (410 ± 10 bpm, $P < 0.0001$), 60–90 min (445 ± 11 bpm, $P < 0.0001$), 90–120 min (477 ± 6 bpm, $P < 0.0001$), 120–180 min (465 ± 8 bpm, $P < 0.0001$), and 180–240 min (446 ± 3 bpm, $P < 0.0001$) (Fig. 6). Minocycline alone significantly reduced heart rate compared to veh/veh during time periods 0–30 min ($P < 0.0001$), 30–60 min ($P < 0.0001$), 90–120 min ($P = 0.0068$), 120–180 min ($P < 0.0001$), and 180–240 min ($P = 0.0085$). Minocycline was effective in significantly reducing MDMA-induced increases in heart rate at high ambient temperature. Mean heart rate in minocycline pre-treated rats was significantly reduced during all time periods post-MDMA; 0–30 min (326 ± 5 bpm, $P = 0.0093$), 30–60 min (345 ± 3 bpm, $P < 0.0001$), 60–90 min (362 ± 3 bpm, $P < 0.0001$), 90–120 min (362 ± 1 bpm, $P < 0.0001$), 120–180 min (365 ± 2 bpm, $P < 0.0001$), and 180–240 (355 ± 3 bpm, $P < 0.0001$) compared to veh/MDMA (Fig. 6).

3.7. Effects of MDMA and minocycline on locomotor activity at high ambient temperature

Two-way ANOVA analysis revealed significant differences among the four treatment groups at high ambient temperature. There was no significant difference in basal locomotor activity between any drug treatment groups ($P > 0.05$). (Fig. 7). The administration of MDMA (10 mg/kg, i.p.) at high ambient temperature significantly increased locomotor activity during time periods 30–60 min (6.8 ± 1.4 counts/min, $P < 0.0001$), 60–90 min (5.8 ± 1.4 counts/min, $P < 0.0001$), and 90–120 min (7.0 ± 2.2 counts/min, $P < 0.0001$) (Fig. 7). Minocycline alone had no significant effect on locomotor activity compared to veh/veh ($P > 0.05$). A three-day pre-treatment of minocycline (50 mg/kg, i.p.) significantly reduced MDMA-induced increases in locomotor activity at high ambient temperature. Mean locomotor activity in minocycline pre-treated rats was significantly reduced during time periods 30–60 min (2.4 ± 0.6 counts/min, $P < 0.0001$), 60–90 min

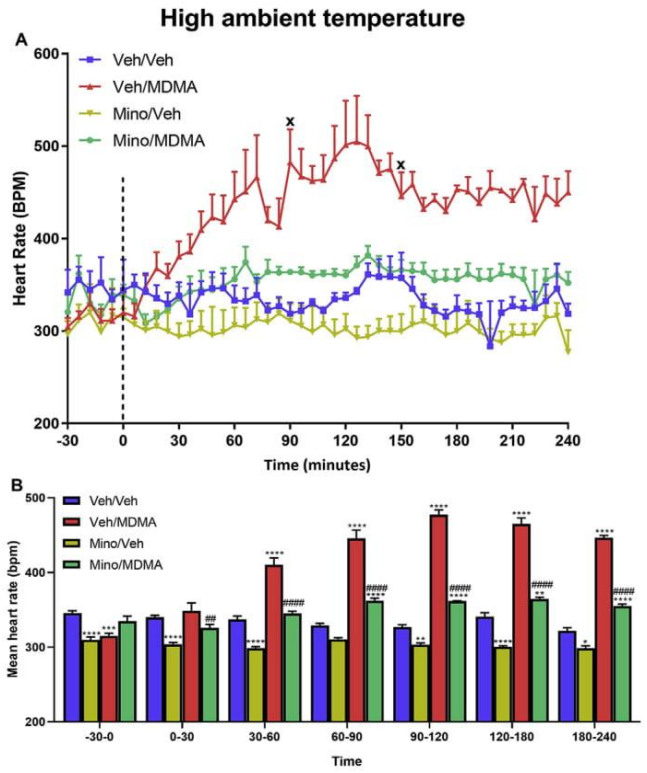

Fig. 6. (A) Effects of minocycline on MDMA-induced increases in heart rate at high ambient temperature. Data have been averaged across all trials at 6-min intervals (n = 4 per group). X indicates where animals died prematurely. **(B)** Mean heart rate results at different time periods for the corresponding line graph. The * indicates significant difference from Veh/Veh, the # indicates significant difference from Veh/MDMA (*P < 0.05, **P < 0.01, ***P < 0.001, ****P < 0.0001). Error bars show the standard error in the mean.

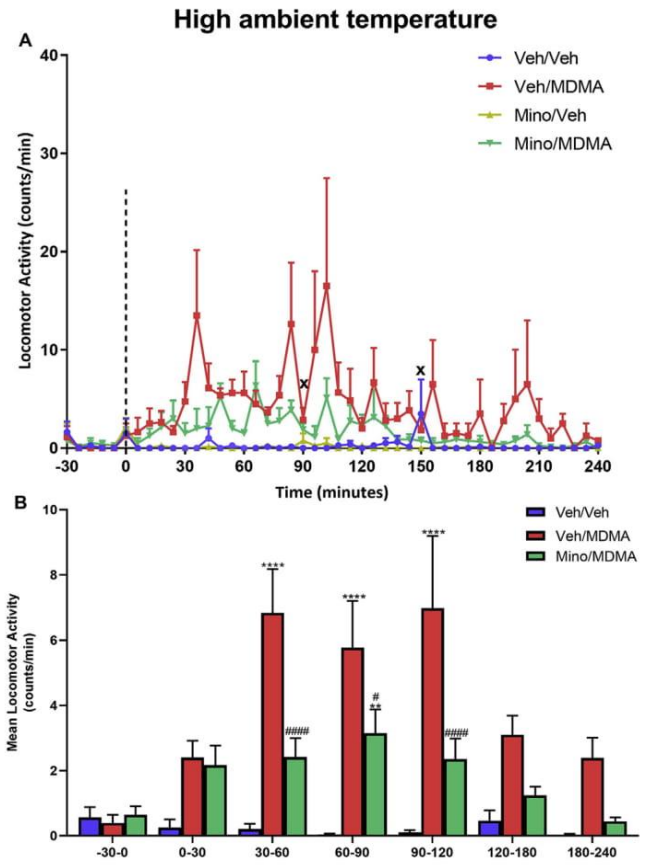

Fig. 7. (A) Effects of minocycline (50 mg/kg, i.p.) on MDMA-induced increases in locomotor activity at high ambient temperature. Data have been averaged across all trials at 6-min intervals (n = 4 per group). X indicates where animals died prematurely. **(B)** Mean locomotor activity results at different time periods for the corresponding line graph. The * indicates significant difference from Veh/Veh, the # indicates significant difference from Veh/MDMA (*P < 0.05, **P < 0.01, **P < 0.001, ****P < 0.0001). No significant difference was found between the control groups veh/veh and mino/veh, therefore mino/veh data has been excluded. to improve graph readability. Error bars show the standard error in the mean.

(3.2 ± 0.74 counts/min, P = 0.037), 90–120 min (2.4 ± 0.6 counts/min, P < 0.0001) compared to veh/MDMA (Fig. 7).

4. Discussion

The major finding of the present study is that a three-day pre-treatment with minocycline significantly attenuated MDMA-induced brain hyperthermia at high ambient temperature and prevented fatalities related to severe hyperthermia. Although dose is the most important factor determining drug toxicity, the MDMA-induced hyperthermic response can be exacerbated under several environmental conditions including high ambient temperature. At normal ambient temperature we found that MDMA produced an initial hypothermic response in the brain and body which returned to baseline levels at approximately 90 min post-MDMA. Conversely, at high ambient temperature we found the same dose of MDMA produced a robust and extended hyperthermic response that was significantly stronger in the brain and eventually resulted in the death of two out of four animals. These varying temperature responses under differing environmental conditions are consistent with those described previously (Daws et al., 2000; Malberg and Seiden, 1998; Brown and Kiyatkin, 2004; Gordon et al., 1991).

Acute MDMA administration produces a significant release of 5-HT and DA in the brain, both of which have been linked to the development of hyperthermia (Stone et al., 1986; Malberg and Seiden, 1998; Colado et al., 1999; Sabol and Seiden, 1998; Gordon et al., 1991; Stanley et al., 2007). This monoamine release post drug administration has been revealed to be temperature dependent, with low ambient temperatures associated with decreased 5-HT and DA levels and hypothermia (Bowyer et al., 1992), and high ambient temperatures associated with increased concentrations and hyperthermia (Clausing et al., 1996; Tao et al., 2015). A high ambient temperature also impairs the body's ability to dissipate heat to the external environment, resulting in higher temperatures than would normally be observed (Brown and Kiyatkin, 2004). It is likely that the mechanisms of MDMA-induced heat accumulation in conjunction with impaired mechanisms of heat loss exacerbated by high ambient temperatures resulted in pathological brain and body over-heating and the hyperthermic death of two animals. This 50% mortality rate is of note as the accepted LD_{50} for MDMA administration in the rat is 49 mg/kg (Hardman et al., 1973) further highlighting the importance of environmental factors on acute MDMA toxicity. This is relevant to human drug consumption as this warm environment is typical of a night club setting where MDMA and other stimulant drugs are often administered.

The two key physiological mechanisms underlying MDMA-induced brain hyperthermia are thought to involve increased intra-brain heat production caused by metabolic neural activation, and heat retention due to peripheral vasoconstriction (Kiyatkin, 2010; Kiyatkin et al., 2014). Brain temperatures have previously been shown to increase at a

faster rate and to higher levels than that seen in the body following MDMA administration (Brown and Kiyatkin, 2004), thus this increase in intra-brain heat generation is thought to be the primary cause of brain hyperthermia and a key factor in a delayed and weaker hyperthermia in the body. Our results are synonymous with these findings and support this hypothesis. At both normal and high ambient temperature, the brain showed a more intense temperature change in response to MDMA when compared to the body, however, significant differences in the brain-body differential were only apparent when administered at high ambient temperature. Brain temperatures were significantly elevated compared to the body between 30 and 120 min following MDMA administration. These results are clinically relevant and suggest that core temperature monitoring in a hospital setting may not provide accurate feedback as to the full intensity of the MDMA-induced hyperthermic response. Thus, pharmacotherapies aimed at alleviating the adverse temperature effects of MDMA should have action within the brain where these effects are most potent.

In addition to acute monoamine release, is also well documented MDMA administration induces microglial activation and the subsequent release of pro-inflammatory cytokines such as IL-6, IL-1β, and TNF-α. These cytokines are known to contribute to the hyperthermic response in response to MDMA (Orio et al., 2004) as well as other exogenous pyrogens (Klir et al., 1994; Luheshi et al., 1997, 1999). Minocycline reduces MDMA-induced microglial activation and inhibits IL-1β release in the brain in a region-specific manner (Zhang et al., 2006; Orio et al., 2010). In addition to this, it has also been shown to affect 5-HT and DA systems of neurotransmission with minocycline attenuating depletion of these monoamines induced by multiple administrations of MDMA (Zhang et al., 2006) as well as preventing the MDMA-induced reduction of 5-HT uptake sites in the frontal cortex (Orio et al., 2010). Interestingly however, both studies found that the effects of minocycline on these neuronal and neuroinflammatory pathways were not accompanied by the attenuation of MDMA-induced hyperthermia in the body. Contrary to these findings, we found that not only does minocycline attenuate MDMA-induced hyperthermia in both the brain and body, but that it does so at high ambient temperature at which the temperature effects of MDMA are strongly exacerbated. Minocycline (50 mg/kg) strongly reduced increases in brain and body temperature at all time periods following MDMA-administration at high ambient temperature and significantly reduced brain-body temperature differentials during peak hyperthermia compared to saline controls. This is consistent with the central action of minocycline and suggests that minocycline causes a significant reduction in intra-brain heat production by decreasing MDMA-induced metabolic brain activation (Kiyatkin et al., 2016). This attenuation of pathological brain and body tissue over-heating was shown to prevent premature hyperthermic death in all individuals pre-treated with minocycline. This survival rate is quite high considering the increased toxicity of MDMA when administered under these deleterious environmental conditions.

The discrepancies in minocycline's temperature effects compared to previous literature could be explained by a few key factors. Firstly, our study employed a three-day minocycline pre-treatment schedule compared to 24 h by Orio et al. (2010) and 30 min prior to MDMA by Zhang et al. (2006). Our group has previously shown that both one and two-day pre-treatment periods with minocycline were ineffective in attenuating MDMA-induced body hyperthermia (Anderson et al., 2011) indicating that minocycline's hyperthermia-attenuating effects are a time-dependent process requiring more than 48 h to achieve maximum effects. Animal and species differences may also contribute to these discrepancies. There are marked differences in the way differing rat strains and mice handle MDMA challenge. Dark Agouti rats used by Orio et al. (2010) are much more susceptible to MDMA-induced neurotoxicity with a single dose of MDMA (10–15 mg/kg) producing up to 50% reduction in cerebral 5-HT (Colado et al., 1995; O'shea et al., 1998) compared to Sprague-Dawley rats which require repeated doses of up to 20 mg/kg MDMA to achieve similar losses (Colado et al., 1993; Shankaran and Gudelsky, 1999). Mice used by Zhang et al. (2006) produce a significantly different response to MDMA when compared to rats as the MDMA challenge predominantly affects the 5-HT system in rats and the DA system in mice (Logan et al., 1988; Sharma and Ali, 2008). D_1 receptors play a key role in MDMA-induced hyperthermia (Mechan et al., 2002) and as such it is likely that the greater impact on the DA neurons that occurs in mice contributes to a stronger and more resilient hyperthermic response that may have overwhelmed any protective effects of minocycline. These factors in combination with differing doses of MDMA used by Orio et al. (2010) (12.5 mg/kg, i.p.), and Zhang et al. (2006) (3 × 10 mg/kg, i.p.), may have contributed to the reduced effectiveness of minocycline in attenuating MDMA-induced hyperthermia.

MDMA-induced tachycardia and hyperlocomotion were also significantly attenuated by minocycline at high ambient temperature. These results are consistent with its effects on monoamine and neuro anti-inflammatory pathways in the brain. MDMA produces cardiac stimulation and tachycardia in rats which has been associated with sympathomimetic activation and actions on descending central and peripheral 5-HT pathways (Fitzgerald and Reid, 1994; Al-Sahli et al., 2001; Lester et al., 2000, O'cain et al., 2000). It has also been reported to dose-dependently produce hyperlocomotion linked to activation of a variety of 5-HT receptors, interactions between 5-HT and DA, as well as agonistic action at α_{2A}-adrenoreceptors (Bankson and Cunningham, 2001; Cole and Sumnall, 2003; Lähdesmäki et al., 2003; Bexis and Docherty, 2006). Our results are consistent with these findings and show that MDMA (10 mg/kg) administered at high ambient temperature significantly increased heart rate and locomotor activity when compared to saline controls. Tachycardia induced by MDMA at high ambient temperature was significantly attenuated by a three-day pre-treatment with minocycline. The mechanisms by which minocycline attenuates this increase in heart rate caused by MDMA are currently unknown. However, pro-inflammatory cytokine release in the CNS is known to modify sympathetic neuronal outflow and play a role in cardiovascular regulation (Kannan et al., 1996; Kimura et al., 1993; Ufnal et al., 2005). It is likely that minocycline's inhibition of MDMA-induced microglial activation and pro-inflammatory cytokine release, in conjunction with a reduction in MDMA-induced central monoamine release contributed to reductions in heart rate following drug administration. MDMA-induced hyperlocomotion was also significantly attenuated by a three-day pre-treatment with minocycline. This response may be explained in some part by minocycline's reduction of MDMA-induced 5-HT and DA release in the brain that has previously been linked to hyperlocomotion (Cole and Sumnall, 2003). However, minocycline has also been shown to cause an inhibition of glutaminergic system activation both *in vitro* (González et al., 2007; Tikka and Koistinaho, 2001) and *in vivo* (González et al., 2007; Zhang et al., 2007) which has previously been shown to result in significant decreases in locomotor activity (Zhang et al., 2007).

To the best of our knowledge, this study is the first to assess the effectiveness of minocycline in attenuating MDMA-induced brain and body hyperthermia at high ambient temperature, whilst also observing its physiological effects in free-moving animals. It is also the first to investigate minocycline's temperature effects in the brain using optical fiber sensing technology. The aim of this study was to determine the potential usefulness of targeting MDMA-induced neuroinflammation as a treatment for acute MDMA-induced hyperthermia in the brain. Further work will be necessary to determine whether these results can be replicated using interventional drugs as well as to establish dose-response relationships for these potential therapeutic substances. A better understanding of the mechanisms underlying the MDMA-induced hyperthermic response is crucial for the future development of an effective pharmacological intervention used to treat MDMA-induced hyperthermia in an emergency room setting.

In conclusion, our data indicates that minocycline is effective in attenuating the exacerbated MDMA-induced hyperthermic response in

the brain and body at high ambient temperature.

Acknowledgements

E. Schartner and M. Hutchinson acknowledge financial support from the Australian Research Council through the Centre of Excellence for Nanoscale BioPhotonics (CE140100003). E. Schartner would also like to acknowledge financial support from an ARC Linkage funding project (LP110200736). This work was performed in part at the OptoFab node of the Australian National Fabrication Facility utilizing Commonwealth and South Australian State Government funding.

References

Al-Sahli, W., Ahmad, H., Kheradmand, F., Connolly, C., Docherty, J.R., 2001. Effects of methylenedioxymethamphetamine on noradrenaline-evoked contractions of rat right ventricle and small mesenteric artery. Eur. J. Pharmacol. 422, 169–174.

Anderson, P., Hutchinson, M., Irvine, R., Salem, A., 2011. Attenuating glial activation with minocycline reduces the hyperthermic response to 3, 4-methylenedioxymethamphetamine (MDMA) in the rat. Open Addict. J. 4.

Bankson, M.G., Cunningham, K.A., 2001. 3, 4-Methylenedioxymethamphetamine (MDMA) as a unique model of serotonin receptor function and serotonin-dopamine interactions. J. Pharmacol. Exp. Ther. 297, 846–852.

Barza, M., Brown, R.B., Shanks, C., Gamble, C., Weinstein, L., 1975. Relation between lipophilicity and pharmacological behavior of minocycline, doxycycline, tetracycline, and oxytetracycline in dogs. Antimicrob. Agents Chemother. 8, 713–720.

Bexis, S., Docherty, J.R., 2006. Effects of MDMA, MDA and MDEA on blood pressure, heart rate, locomotor activity and body temperature in the rat involve α-adrenoceptors. Br. J. Pharmacol. 147, 926–934.

Bexis, S., Phillis, B.D., Ong, J., White, J.M., Irvine, R.J., 2004. Baclofen prevents MDMA-induced rise in core body temperature in rats. Drug Alcohol Depend. 74, 89–96.

Bowyer, J., Tank, A., Newport, G., Slikker, W., Ali, S., Holson, R., 1992. The influence of environmental temperature on the transient effects of methamphetamine on dopamine levels and dopamine release in rat striatum. J. Pharmacol. Exp. Ther. 260, 817–824.

Broening, H.W., Bowyer, J.F., Slikker JR., W., 1995. Age-dependent sensitivity of rats to the long-term effects of the serotonergic neurotoxicant (+/-)-3,4-methylenedioxymethamphetamine (MDMA) correlates with the magnitude of the MDMA-induced thermal response. J. Pharmacol. Exp. Ther. 275, 325–333.

Brown, P.L., Kiyatkin, E.A., 2004. Brain hyperthermia induced by MDMA (ecstasy): modulation by environmental conditions. Eur. J. Neurosci. 20, 51–58.

Chen, M., Ona, V.O., Li, M., Ferrante, R.J., Fink, K.B., Zhu, S., Bian, J., Guo, L., Farrell, L.A., Hersch, S.M., 2000. Minocycline inhibits caspase-1 and caspase-3 expression and delays mortality in a transgenic mouse model of Huntington disease. Nat. Med. 6, 797.

Chu, T., Kumagai, Y., Distefano, E.W., Cho, A.K., 1996. Disposition of methylenedioxymethamphetamine and three metabolites in the brains of different rat strains and their possible roles in acute serotonin depletion. Biochem. Pharmacol. 51, 789–796.

Clausing, P., Bloom, D., Newport, G., Holson, R., Slikker, W., Bowyer, J., 1996. Individual differencs in dopamine release but not rotational behavior correlate with extracellular amphetamine levels in caudate putament in unlesioned rats. Psychopharmacology 127, 187–194.

Colado, M., Murray, T., Green, A., 1993. 5-HT loss in rat brain following 3, 4-methylenedioxymethamphetamine (MDMA), p-chloroamphetamine and fenfluramine administration and effects of chlormethiazole and dizocilpine. Br. J. Pharmacol. 108, 583–589.

Colado, M., O'shea, E., Granados, R., Esteban, B., Martin, A., Green, A., 1999. Studies on the role of dopamine in the degeneration of 5-HT nerve endings in the brain of Dark Agouti rats following 3, 4-methylenedioxymethamphetamine (MDMA or 'ecstasy') administration. Br. J. Pharmacol. 126, 911–924.

Colado, M.I., Camarero, J., Mechan, A.O., Sanchez, V., Esteban, B., Elliott, J.M., Green, A.R., 2001. A study of the mechanisms involved in the neurotoxic action of 3, 4-methylenedioxymethamphetamine (MDMA,'ecstasy') on dopamine neurones in mouse brain. Br. J. Pharmacol. 134, 1711–1723.

Colado, M.I., Williams, J.L., Green, A.R., 1995. The hyperthermic and neurotoxic effects of 'Ecstasy' (MDMA) and 3,4 methylenedioxyamphetamine (MDA) in the Dark Agouti (DA) rat, a model of the CYP2D6 poor metabolizer phenotype. Br. J. Pharmacol. 115, 1281–1289.

Cole, J.C., Sumnall, H.R., 2003. The pre-clinical behavioural pharmacology of 3, 4-methylenedioxymethamphetamine (MDMA). Neurosci. Biobehav. Rev. 27, 199–217.

Dafters, R.I., 1994. Effect of ambient temperature on hyperthermia and hyperkinesis induced by 3, 4-methylenedioxymethamphetamine (MDMA or "ecstasy") in rats. Psychopharmacology 114, 505–508.

Dafters, R.I., Lynch, E., 1998. Persistent loss of thermoregulation in the rat induced by 3, 4-methylenedioxymethamphetamine (MDMA or "Ecstasy") but not by fenfluramine. Psychopharmacology 138, 207–212.

Daws, L.C., Irvine, R.J., Callaghan, P.D., Toop, N.P., White, J.M., Bochner, F., 2000. Differential behavioural and neurochemical effects of para-methoxyamphetamine and 3, 4-methylenedioxymethamphetamine in the rat. Prog. Neuro Psychopharmacol. Biol. Psychiatr. 24, 955–977.

Domercq, M., Matute, C., 2004. Neuroprotection by tetracyclines. Trends Pharmacol. Sci. 25, 609–612.

Du, Y., Ma, Z., Lin, S., Dodel, R.C., Gao, F., Bales, K.R., Triarhou, L.C., Chernet, E., Perry, K.W., Nelson, D.L., 2001. Minocycline prevents nigrostriatal dopaminergic neurodegeneration in the MPTP model of Parkinson's disease. Proc. Natl. Acad. Sci. Unit. States Am. 98, 14669–14674.

Esteban, B., O'shea, E., Camarero, J., Sanchez, V., Green, A.R., Colado, M.I., 2001. 3, 4-Methylenedioxymethamphetamine induces monoamine release, but not toxicity, when administered centrally at a concentration occurring following a peripherally injected neurotoxic dose. Psychopharmacology 154, 251–260.

Fagan, S.C., Edwards, D.J., Borlongan, C.V., Xu, L., Arora, A., Feuerstein, G., Hess, D.C., 2004. Optimal delivery of minocycline to the brain: implication for human studies of acute neuroprotection. Exp. Neurol. 186, 248–251.

Fitzgerald, J., Reid, J., 1994. Sympathomimetic actions of methylenedioxymethamphetamine in rat and rabbit isolated cardiovascular tissues. J. Pharm. Pharmacol. 46, 826–832.

Garcıa-Repetto, R., Moreno, E., Soriano, T., Jurado, C., Gimenez, M., Menendez, M., 2003. Tissue concentrations of MDMA and its metabolite MDA in three fatal cases of overdose. Forensic Sci. Int. 135, 110–114.

González, J.C., Egea, J., Del Carmen Godino, M., Fernandez-Gomez, F.J., Sánchez-Prieto, J., Gandía, L., García, A.G., Jordán, J., Hernández-Guijo, J.M., 2007. Neuroprotectant minocycline depresses glutamatergic neurotransmission and Ca2+ signalling in hippocampal neurons. Eur. J. Neurosci. 26, 2481–2495.

Gordon, C.J., Watkinson, W.P., O'callaghan, J.P., Miller, D.B., 1991. Effects of 3,4-methylenedioxymethamphetamine on autonomic thermoregulatory responses of the rat. Pharmacol. Biochem. Behav. 38, 339–344.

Green, A.R., Mechan, A.O., Elliott, J.M., O'shea, E., Colado, M.I., 2003. The pharmacology and clinical pharmacology of 3,4-methylenedioxymethamphetamine (MDMA, "ecstasy"). Pharmacol. Rev. 55, 463–508.

Green, A.R., O'shea, E., Colado, M.I., 2004. A review of the mechanisms involved in the acute MDMA (ecstasy)-induced hyperthermic response. Eur. J. Pharmacol. 500, 3–13.

Grunau, B.E., Wiens, M.O., Brubacher, J.R., 2010. Dantrolene in the treatment of MDMA-related hyperpyrexia: a systematic review. Can. J. Emerg. Med. 12, 435–442.

Hall, A., Henry, J., 2006. Acute toxic effects of 'Ecstasy'(MDMA) and related compounds: overview of pathophysiology and clinical management. Br. J. Addict.: Br. J. Anaesth. 96, 678–685.

Hardman, H.F., Haavik, C.O., Seevers, M.H., 1973. Relationship of the structure of mescaline and seven analogs to toxicity and behavior in five species of laboratory animals. Toxicol. Appl. Pharmacol. 25, 299–309.

Jensen, K.F., Olin, J., Haykal-Coates, N., O'callaghan, J., Miller, D.B., De Olmos, J.S., 1993. Mapping toxicant-induced nervous system damage with a cupric silver stain: a quantitative analysis of neural degeneration induced by 3, 4-methylenedioxymethamphetamine. NIDA Res. Monogr. 136, 133–149.

Kalant, H., 2001. The pharmacology and toxicology of "ecstasy" (MDMA) and related drugs. Can. Med. Assoc. J. 165, 917–928.

Kannan, H., Tanaka, Y., Kunitake, T., Ueta, Y., Hayashida, Y., Yamashita, H., 1996. Activation of sympathetic outflow by recombinant human interleukin-1 beta in conscious rats. Am. J. Physiol. Regul. Integr. Comp. Physiol. 270, R479–R485.

Kimura, T., Yamamoto, T., Ota, K., Shoji, M., Inoue, M., Sato, K., Ohta, M., Funyu, T., Yoshinaga, K., 1993. Central effects of interleukin-1 on blood pressure, thermogenesis, and the release of vasopressin, ACTH, and atrial natriuretic peptide. Ann. N. Y. Acad. Sci. 689, 330–345.

Kiyatkin, E.A., 2010. BRAIN TEMPERATURE HOMEOSTASIS: PHYSIOLOGICAL FLUCTUATIONS AND PATHOLOGICAL SHIFTS. Front. Biosci. : J. Vis. Lit. 15, 73–92.

Kiyatkin, E.A., Brown, P.L., Sharma, H.S., 2007. Brain edema and breakdown of the blood–brain barrier during methamphetamine intoxication: critical role of brain hyperthermia. Eur. J. Neurosci. 26, 1242–1253.

Kiyatkin, E.A., Kim, A.H., Wakabayashi, K.T., Baumann, M.H., Shaham, Y., 2014. Critical role of peripheral vasoconstriction in fatal brain hyperthermia induced by MDMA (Ecstasy) under conditions that mimic human drug use. J. Neurosci. 34, 7754–7762.

Kiyatkin, E.A., Ren, S., Wakabayashi, K.T., Baumann, M.H., Shaham, Y., 2016. Clinically relevant pharmacological strategies that reverse MDMA-induced brain hyperthermia potentiated by social interaction. Neuropsychopharmacology 41, 549–559.

Kiyatkin, E.A., Sharma, H.S., 2009a. Acute methamphetamine intoxication: brain hyperthermia, blood–brain barrier, brain edema, and morphological cell abnormalities. Int. Rev. Neurobiol. 88, 65–100.

Kiyatkin, E.A., Sharma, H.S., 2009b. Permeability of the blood–brain barrier depends on brain temperature. Neuroscience 161, 926–939.

Klir, J.J., Mcclellan, J.L., Kluger, M.J., 1994. Interleukin-1 beta causes the increase in anterior hypothalamic interleukin-6 during LPS-induced fever in rats. Am. J. Physiol. Regul. Integr. Comp. Physiol. 266, R1845–R1848.

Lähdesmäki, J., Sallinen, J., Macdonald, E., Sirviö, J., Scheinin, M., 2003. α2-Adrenergic drug effects on brain monoamines, locomotion, and body temperature are largely abolished in mice lacking the α2A-adrenoceptor subtype. Neuropharmacology 44, 882–892.

Lester, S.J., Baggott, M., Welm, S., Schiller, N.B., Jones, R.T., Foster, E., Mendelson, J., 2000. Cardiovascular effects of 3, 4-methylenedioxymethamphetamine: a double-blind, placebo-controlled trial. Ann. Intern. Med. 133, 969–973.

Logan, B.J., Laverty, R., Sanderson, W.D., Yee, Y.B., 1988. Differences between rats and mice in MDMA (methylenedioxymethylamphetamine) neurotoxicity. Eur. J. Pharmacol. 152, 227–234.

Luheshi, G., Stefferl, A., Turnbull, A., Dascombe, M., Brouwer, S., Hopkins, S., Rothwell, N., 1997. Febrile response to tissue inflammation involves both peripheral and brain IL-1 and TNF-alpha in the rat. Am. J. Physiol. Regul. Integr. Comp. Physiol. 272, R862–R868.

Luheshi, G.N., Gardner, J.D., Rushforth, D.A., Loudon, A.S., Rothwell, N.J., 1999. Leptin actions on food intake and body temperature are mediated by IL-1. Proc. Natl. Acad.

Sci. Unit. States Am. 96, 7047–7052.
Malberg, J.E., Seiden, L.S., 1998. Small changes in ambient temperature cause large changes in 3, 4-methylenedioxymethamphetamine (MDMA)-induced serotonin neurotoxicity and core body temperature in the rat. J. Neurosci. 18, 5086–5094.
Mechan, A.O., Esteban, B., O'shea, E., Elliott, J.M., Colado, M.I., Green, A.R., 2002. The pharmacology of the acute hyperthermic response that follows administration of 3, 4-methylenedioxymethamphetamine (MDMA,'ecstasy') to rats. Br. J. Pharmacol. 135, 170–180.
Mechan, A.O., O'shea, E., Elliott, M.J., Colado, M., Green, R.A., 2001. A neurotoxic dose of 3, 4-methylenedioxymethamphetamine (MDMA; ecstasy) to rats results in a long term defect in thermoregulation. Psychopharmacology 155, 413–418.
Müller, F., Brändle, R., Liechti, M.E., Borgwardt, S., 2019. Neuroimaging of chronic MDMA ("ecstasy") effects: a meta-analysis. Neurosci. Biobehav. Rev. 96, 10–20.
Musolino, S., Schartner, E.P., Tsiminis, G., Salem, A., Monro, T.M., Hutchinson, M.R., 2016. Portable optical fiber probe for in vivo brain temperature measurements. Biomed. Opt. Express 7, 3069–3077.
Musolino, S.T., Schartner, E.P., Hutchinson, M.R., Salem, A., 2019. Improved method for optical fiber temperature probe implantation in brains of free-moving rats. J. Neurosci. Methods 313, 24–28.
O'cain, P.A., Hletko, S.B., Ogden, B.A., Varner, K.J., 2000. Cardiovascular and sympathetic responses and reflex changes elicited by MDMA. Physiol. Behav. 70, 141–148.
O'connor, J.C., Lawson, M.A., Andre, C., Moreau, M., Lestage, J., Castanon, N., Kelley, K.W., Dantzer, R., 2009. Lipopolysaccharide-induced depressive-like behavior is mediated by indoleamine 2,3-dioxygenase activation in mice. Mol. Psychiatry 14, 511–522.
O'hearn, E., Battaglia, G., De Souza, E., Kuhar, M., Molliver, M., 1988. Methylenedioxyamphetamine (MDA) and methylenedioxymethamphetamine (MDMA) cause selective ablation of serotonergic axon terminals in forebrain: immunocytochemical evidence for neurotoxicity. J. Neurosci. 8, 2788–2803.
O'shea, E., Escobedo, I., Orio, L., Sanchez, V., Navarro, M., Green, A.R., Colado, M.I., 2005. Elevation of ambient room temperature has differential effects on MDMA-induced 5-HT and dopamine release in striatum and nucleus accumbens of rats. Neuropsychopharmacology 30, 1312–1323.
O'shea, E., Granados, R., Esteban, B., Colado, M., Green, A., 1998. The relationship between the degree of neurodegeneration of rat brain 5-HT nerve terminals and the dose and frequency of administration of MDMA (ecstasy'). Neuropharmacology 37, 919–926.
Orio, L., Llopis, N., Torres, E., Izco, M., O'shea, E., Colado, M.I., 2010. A study on the mechanisms by which minocycline protects against MDMA ('ecstasy')-induced neurotoxicity of 5-HT cortical neurons. Neurotox. Res. 18, 187–199.
Orio, L., O'shea, E., Sanchez, V., Pradillo, J.M., Escobedo, I., Camarero, J., Moro, M.A., Green, A.R., Colado, M.I., 2004. 3, 4-Methylenedioxymethamphetamine increases interleukin-1β levels and activates microglia in rat brain: studies on the relationship with acute hyperthermia and 5-HT depletion. J. Neurochem. 89, 1445–1453.
Paxinos, G., Watson, C., 1998. The Rat Brain Atlas in Stereotaxic Coordinates. Academic, San Diego.
Ricaurte, G.A., Yuan, J., Hatzidimitriou, G., CORD, B.J., MCCANN, U.D., 2002. Severe dopaminergic neurotoxicity in primates after a common recreational dose regimen of MDMA (" ecstasy"). Science 297, 2260–2263.
Sabol, K.E., Seiden, L.S., 1998. Reserpine attenuates D-amphetamine and MDMA-induced transmitter release in vivo: a consideration of dose, core temperature and dopamine synthesis. Brain Res. 806, 69–78.
Shankaran, M., Gudelsky, G.A., 1999. A neurotoxic regimen of MDMA suppresses behavioral, thermal and neurochemical responses to subsequent MDMA administration. Psychopharmacology 147, 66–72.
Sharma, H.S., Ali, S.F., 2008. Acute administration of 3, 4-methylenedioxymethamphetamine induces profound hyperthermia, blood–brain barrier disruption, brain edema formation, and cell injury: an experimental study in rats and mice using biochemical and morphologic approaches. Ann. N. Y. Acad. Sci. 1139, 242–258.
Stanley, N., Salem, A., Irvine, R.J., 2007. The effects of co-administration of 3,4-methylenedioxymethamphetamine ("ecstasy") or para-methoxyamphetamine and moclobemide at elevated ambient temperatures on striatal 5-HT, body temperature and behavior in rats. Neuroscience 146, 321–329.
Stirling, D.P., Koochesfahani, K.M., Steeves, J.D., Tetzlaff, W., 2005. Minocycline as a neuroprotective agent. Neuroscientist 11, 308–322.
Stone, D.M., Stahl, D.C., Hanson, G.R., Gibb, J.W., 1986. The effects of 3, 4-methylenedioxymethamphetamine (MDMA) and 3, 4-methylenedioxyamphetamine (MDA) on monoaminergic systems in the rat brain. Eur. J. Pharmacol. 128, 41–48.
Tao, R., Shokry, I.M., Callanan, J.J., Adams, H.D., MA, Z., 2015. Mechanisms and environmental factors that underlying the intensification of 3, 4-methylenedioxymethamphetamine (MDMA, Ecstasy)-induced serotonin syndrome in rats. Psychopharmacology 232, 1245–1260.
Tikka, T.M., Koistinaho, J.E., 2001. Minocycline provides neuroprotection against N-methyl-D-aspartate neurotoxicity by inhibiting microglia. J. Immunol. 166, 7527–7533.
Ufnal, M., Żera, T., Szczepańska-Sadowska, E., 2005. Blockade of angiotensin II AT1 receptors inhibits pressor action of centrally administered interleukin-1β in Sprague Dawley rats. Neuropeptides 39, 581–585.
Walubo, A., Seger, D., 1999. Fatal multi-organ failure after suicidal overdose with MDMA,Ecstasy': case report and review of the literature. Hum. Exp. Toxicol. 18, 119–125.
Wang, X., Zhu, S., Drozda, M., Zhang, W., Stavrovskaya, I.G., Cattaneo, E., Ferrante, R.J., Kristal, B.S., Friedlander, R.M., 2003. Minocycline inhibits caspase-independent and-dependent mitochondrial cell death pathways in models of Huntington's disease. Proc. Natl. Acad. Sci. Unit. States Am. 100, 10483–10487.
Westerink, B.H., 2000. Analysis of biogenic amines in microdialysates of the brain. J. Chromatogr. B Biomed. Sci. Appl. 747, 21–32.
Yrjanheikki, J., Keinanen, R., Pellikka, M., Hokfelt, T., Koistinaho, J., 1998. Tetracyclines inhibit microglial activation and are neuroprotective in global brain ischemia. Proc. Natl. Acad. Sci. U. S. A. 95, 15769–15774.
Yrjänheikki, J., Tikka, T., Keinänen, R., Goldsteins, G., Chan, P.H., Koistinaho, J., 1999. A tetracycline derivative, minocycline, reduces inflammation and protects against focal cerebral ischemia with a wide therapeutic window. Proc. Natl. Acad. Sci. Unit. States Am. 96, 13496–13500.
Zhang, L., Kitaichi, K., Fujimoto, Y., Nakayama, H., Shimizu, E., Iyo, M., Hashimoto, K., 2006. Protective effects of minocycline on behavioral changes and neurotoxicity in mice after administration of methamphetamine. Prog. Neuro Psychopharmacol. Biol. Psychiatr. 30, 1381–1393.
Zhang, L., Shirayama, Y., Iyo, M., Hashimoto, K., 2007. Minocycline attenuates hyperlocomotion and prepulse inhibition deficits in mice after administration of the NMDA receptor antagonist dizocilpine. Neuropsychopharmacology 32, 2004.
Zhu, S., Stavrovskaya, I.G., Drozda, M., Kim, B.Y., Ona, V., Li, M., Sarang, S., Liu, A.S., Hartley, D.M., Gullans, S., 2002. Minocycline inhibits cytochrome c release and delays progression of amyotrophic lateral sclerosis in mice. Nature 417, 74.

Chapter 6 – General Discussion

Portable optical fibre probe development

The focus of our work concerning fibre optic probe development aimed at optimising optical fibre temperature sensor configuration, which required addressing many issues related to its long-term stability and *in vivo* durability. This goal was achieved by using an all-PM optical configuration, and altering the probes' structure we were successful in developing a portable optical temperature sensor capable of specific and reliable long-term temperature measurements in the brains of freely-moving rats. Continued development of the sensor further optimised fabrication and implantation procedures allowing for increased ease of use, lower costs, and higher throughput animal experiments.

Although optical fibre sensors have found increasing use in modern medical applications (Yin and Ruffin, 2006), and have been substantially researched and improved upon since the first generations of optical fibre sensors were commercialised, they have yet to find the commercial success and widespread use that optical fibres have found in other applications, such as communications. One possible reason for this is likely associated with the numerous difficulties in employing these sensors within *in vivo* studies as we have demonstrated within our own initial developmental work. Despite these difficulties, many sensors have been successfully tested *in vivo* measuring pH (Grant et al., 2001), temperature (Samset et al., 2001), pressure (Poeggel et al., 2015), strain (Dziuda et al., 2012), as well as a variety of other parameters. However, in many animal studies, these optical fibre sensors have been used to perform *in vivo* measurements in animals under anaesthesia (Grant et al., 2001, O'Hara et al., 2005, Chavko et al., 2007, Peterson et al., 1984, Yu et al., 2016). This is likely due to the mechanical strength of the fibres being insufficient to withstand strain caused by animal movement (Schena et al., 2016). As seen in our developmental work, animal movement and fibre coiling can affect

optical signal transmission within the probe that can lead to measurement inaccuracies, which can be limited using anaesthesia. However, anaesthesia is also known to alter core temperature, neuronal activity, and behavioural response in animals (Kiyatkin, 2005, Kiyatkin, 2010), which may produce confounding effects on data gathered by the optical sensors used in these studies. Similar *in* vivo studies have reported limitations regarding animals needing to remain tethered to fibres post-implantation, with extra care required to prevent damage to fibre tips during long-term measurements (Cui et al., 2014). Other studies reviewing the current state of optical fibres in biomedical studies and the healthcare industry have attributed their lacking use to deficiencies in well-designed sensors for their specific applications (Vincent et al., 2014), and a lack of standardised protocols capable of producing repeatable and reproducible results *in vivo* (Chiavaioli et al., 2017). In contrast to this, the numerous structural changes made to our optical sensor, and the optimisations made to the probe implant and handling procedures have minimised the effects of these limitations in our temperature sensing application. The finalised probe is durable enough to withstand use in active rats administered MDMA without breakage or significant periods of signal loss, and provide stable long-term measurements of brain temperature. In addition to this, the improved guide cannula probe housing allows for probe separation from the animal post-implant, probe re-use, and repeatable measurements requiring only one calibration, while also maintaining the simple implant and handling procedures of conventional microdialysis techniques.

Although there can be many limitations associated with the deployment of optical fibres *in vivo*, we believe that their potential advantages far outweigh the initial drawbacks related to their implementation. New optimisations are constantly being made to optical fibre sensors for not only traditional sensing parameters such as temperature, strain, and pressure, but also for new applications such as chemical sensing (Wang et al., 2016, Schartner et al., 2016) and biosensing (Long et al., 2014, Singh and Gupta, 2013, Coscelli et al., 2009). My development

and validation of the optical fibre point temperature sensor within a portable system provided a suitable means for investigating temperature change within the brain whilst maintaining the advantages provided by optical fibre sensing. Future development of this sensor could aid in providing a method that enables the multiplexed, real-time *in vivo* sensing of physical, chemical, and biological parameters within one system, which would far exceed capabilities of the equivalent conventional temperature monitoring techniques.

Thermoregulatory effects of MDMA

The second component of this study successfully applied the portable optical fibre temperature sensor to investigate MDMA's thermoregulatory effects in the brain and the relationnship to temperature changes in the body. We showed that MDMA at 10 mg/kg increases brain and body temperature when given to male SD rats at high ambient temperature (29 ^{o}C). Conversely, at normal ambient temperature (22 ^{o}C) the same dose of MDMA induced a significant hypothermic response. In both cases, these temperature changes occurred more rapidly, and to a greater extent in the brain when compared to the body.

Our results demonstrated contrasting temperature responses to MDMA under differing environmental conditions. These findings are synonymous with previous literature showing that the magnitude of MDMA-induced hyperthermia is greatly influenced by ambient temperature (Gordon et al., 1991, Mechan et al., 2002, Malberg et al., 1996, Malberg and Seiden, 1998). The two key physiological mechanisms underlying MDMA-induced hyperthermia are increased metabolic rate and increased peripheral vasoconstriction (Brown and Kiyatkin, 2004). MDMA-induced increases in metabolism results in increased heat production while MDMA-induced peripheral vasoconstriction impairs the body's ability to dissipate this excess heat. This leads to increased heat accumulation in the body and hyperthermia. High ambient temperatures are known to significantly increase metabolic rate

and heat production in rats compared to lower ambient temperatures (Gordon et al., 1991), thus leading to a significantly amplified hyperthermic response (Malberg and Seiden, 1998, Brown and Kiyatkin, 2004, Mechan et al., 2002). As mentioned previously, MDMA-induced hyperthermia has been linked to the release, and inhibition of uptake of monoamines such as 5-HT, DA, and NA following MDMA administration (Stone et al., 1986, Gordon et al., 1991, Green et al., 2003, Stanley et al., 2007). Extracellular levels of these neurotransmitters are also ambient temperature dependent as past studies have shown significant decreases in neurotransmitter activity in response to MDMA administered at low ambient temperatures (Bowyer et al., 1992) compared to administration at high ambient temperatures (Clausing et al., 1996, Tao et al., 2015). Our results support these findings and suggest that modulation of physiological and pharmacological actions of MDMA by high ambient temperature greatly increases the severity of MDMA-induced hyperthermia in response to a modest dose of MDMA. This was further reflected by the death of two of four animals administered MDMA at high ambient temperature, with body temperatures in excess of 43 °C. This finding is concerning as the accepted LD_{50} for MDMA administration in the rat is 49 mg/kg (i.p.) (Hardman et al., 1973), almost five times higher than the dose used in our studies. In contrast, the administration of same-dose MDMA at normal ambient temperature did not result in premature death of any animals. These findings have significant implications for instances of human drug use as these harmful high-ambient temperature conditions are typical of settings where stimulant drugs such as MDMA are taken. Potentiation of drug effects by detrimental environmental conditions pose a serious problem to unaware drug users as relatively modest doses of MDMA taken under these conditions may result in severe adverse effects and in rare cases even death.

Our results also demonstrate that administration of MDMA at high ambient temperature elicited a significant temperature increase in both the brain and the body. However, brain

temperatures rose more quickly and to a higher degree compared to the periphery. Striatal temperatures were significantly elevated approximately 12 minutes post-MDMA administration, compared to 24 minutes in the body. The brain-body temperature differential was also significant during peak hyperthermia with brain temperatures approximately 0.6 °C higher on average than those in the body. Although current literature surrounding MDMA-induced hyperthermia in the brain is limited, our results are comparable with previous reports. Brain temperatures have been shown to increase faster, and to greater elevations than those in the body (+0.4 - 0.8 °C) (Kiyatkin et al., 2002, Brown and Kiyatkin, 2004). These results are not surprising as the brain is responsible for 20% of the body's oxygen consumption and has significantly higher metabolic rates compared to the rest of the body (Bélanger et al., 2011). Activation of neurons is energy intensive and the majority of this energy is spent re-establishing membrane potentials after neurotransmitter release (Richie, 1973). Most of the energy used to maintain constant neural activity is eventually transformed into heat (Richie, 1973, Bélanger et al., 2011), thus increased neural activity and neurotransmitter release in the brain induced by MDMA (Gordon et al., 1991, Mechan et al., 2002, Freezer et al., 2005, Stanley et al., 2007) is likely to contribute to increased heat production and eventually hyperthermia. This is relevant to humans as core temperature is a key vital sign and is often monitored in a clinical setting, however, our results suggest that it does not give an adequate reflection as to the severity of MDMA-induced temperature effects in the brain. Although the monitoring of brain temperature in humans has undergone great strides in the past few decades, identifying differences between brain and core body temperature in patients undergoing neurosurgery (Mellergard and Nordström, 1990, Mellergård, 1995, Rossi et al., 2001, Soukup et al., 2002), these techniques are impractical in an acute emergency room setting. Additional studies performing brain and body temperature measurements in animals, or in humans during neurosurgery could aid in developing a formula for extrapolating brain temperature information

from core body temperature readings. However, this would require many more neuroscience studies adopting brain temperature recording techniques within their protocols before this could be achieved. Nevertheless, the increased magnitude of MDMA-induced hyperthermia in the brain must be taken into consideration in a clinical setting, and therapeutic interventions should ideally exert their cooling effects in the brain accordingly.

Minocycline's effects on MDMA-induced hyperthermia

The primary aim of our work concerning minocycline was to investigate its hyperthermia-attenuating effects in the brain at high ambient temperature. We also used radiotelemetry to further examine the extent of its temperature effects in the periphery. Our results demonstrated that a three-day pretreatment with minocycline (50 mg/kg) significantly attenuated MDMA-induced hyperthermia in both brain and body. MDMA-induced temperature increases in the brain and body were attenuated for all time periods following drug administration and average peak temperature increases reached only +1.5 °C from baseline, significantly reduced compared to saline/MDMA treated groups of over +4 °C. Brain-body temperature differentials during MDMA's peak of action were non-significant, consistent with minocycline's central action.

There are only a few studies detailing minocycline's effects in regard to MDMA-induced hyperthermia and the protective properties that we have demonstrated are not consistent with those reported previously. It is known that an increase in IL-1β concentration, a pro-inflammatory cytokine and pyrogen, is involved in the development of hyperthermia following MDMA administration (Orio et al., 2004, O'Shea et al., 2005). Release of IL-1β is also associated with increased activity of nuclear factor kappaB (NF-κB), an inducible transcription factor with a key role in regulation of genes involved in inflammatory and immune responses, and a contributor to a cyclical mechanism of continued IL-1β release (Orio et al., 2004, Ahn

and Aggarwal, 2005, Nadjar et al., 2005). Minocycline is known to attenuate the increased expression of intracellular cysteine protease caspase-1 (Yrjänheikki et al., 1998, Chen et al., 2000, Mievis et al., 2007), an enzyme which acts to process inactive pro-IL-1β into its mature state (Thornberry et al., 1992). It has also been shown to attenuate MDMA-induced NF-κB DNA binding in a region specific manner (Orio et al., 2010). In addition to this, minocycline region-specifically attenuates loss of 5-HTT related to reductions in IL-1β and NF-κB signalling in these regions (Orio et al., 2010), and attenuates 5-HT and DA loss, as well as microglial activation in response to MDMA (Zhang et al., 2006). Although monoamine release, microglial activation, and subsequent release of pro-inflammatory cytokines are known to play a role in development of hyperthermia in response to MDMA (Stone et al., 1986, Gordon et al., 1991, Malberg and Seiden, 1998, Stanley et al., 2007, Orio et al., 2004, O'Shea et al., 2005), previous studies show that minocycline's action within monoamine and neuroinflammatory systems does not correspond with attenuation of acute hyperthermia in the body (Zhang et al., 2006, Orio et al., 2010). In contrast to these findings, prior work in our lab showed that a three-day pretreatment with minocycline (50 mg/kg) was sufficient to attenuate MDMA-induced hyperthermia at normal ambient temperature (Anderson et al., 2011). Our results are consistent with this and go one step further to demonstrate that minocycline is also effective in attenuating the exacerbated MDMA-induced hyperthermic response in both the brain and body at high ambient temperature. Discrepancies between results from our lab and those of others may have resulted, at least in part, from methodological differences, including a higher dose of MDMA, a lower dose of minocycline, and differences in animal species and strain (Zhang et al., 2006, Orio et al., 2010). However, they might best be explained by the reduced minocycline pretreatment time period used, one to two days, compared to our three-day pretreatment period. We found that a three-day minocycline pretreatment period not only attenuates modest (10 mg/kg, i.p.) MDMA-induced hyperthermia at normal ambient temperature, but also attenuates

exacerbated and possibly deadly hyperthermia at high ambient temperature. These results highlight the time-dependent nature of minocycline's hyperthermia-attenuating mechanisms of action. Our results may also provide some insight into actions of minocycline within different regions of the brain. There is known heterogeneity in the release of IL-1β in the brain in response to MDMA, specifically in the hypothalamus (Tringali et al., 1996, Tringali et al., 1997, Lindberg et al., 2004, O'Shea et al., 2005). Release of IL-1β is thought to be a consequence of MDMA-induced hyperthermia rather than its cause, based on its delayed peak concentrations compared to the rapid onset of hyperthermia, and the absence of its release when hyperthermia is abolished (Orio et al., 2004, O'Shea et al., 2005). A reduction in MDMA-induced IL-1β release by minocycline in brain areas such as the midbrain (Anderson, unpublished data) and frontal cortex (Orio et al., 2010) could reflect increased hypothermic action in these brain areas, possibly through the attenuation of acute monoamine release. This is in contrast to the hypothalamus where insignificant decreases in IL-1β signalling in response to shorter minocycline pretreatment periods, and no attenuation of hyperthermia has been reported (Orio et al., 2010). This suggests a three-day minocycline pretreatment period is required to achieve significant attenuation of acute MDMA-induced increases in extracellular monoamines, and subsequent release of IL-1β in the hypothalamus that plays a key role in development of hyperthermia in the brain and body. This idea is further supported by the fact that the hypothalamus is known to possess a readily available pool of mature IL-1β available for release, that originates in neurons (Lindberg et al., 2004), with release mediated by dopamine (Tringali et al., 1996, Tringali et al., 1997). However, further studies examining multiple brain regions, and using both microdialysis and IL-1β assays would be required to test this hypothesis.

Hyperthermia is known to exacerbate long-term MDMA-induced 5-HT and DA neurotoxicity (Gordon et al., 1991, Broening et al., 1995, Malberg and Seiden, 1998, Brown and Kiyatkin,

2004, O'Shea et al., 2005) thus, our results support the hypothesis that minocycline's neuroprotective effects are linked to its ability to attenuate acute hyperthermia. Attenuation of pathological brain and body tissue over-heating by minocycline was shown to prevent premature hyperthermic death in all animals administered MDMA. This survival rate is significant considering the increased danger MDMA poses when taken under deleterious high-ambient temperature conditions (Brown and Kiyatkin, 2004). This also supports the hypothesis that drugs acting centrally to prevent brain hyperthermia such as minocycline are more effective in attenuating MDMA-induced hyperthermia compared to those acting in the periphery as previously demonstrated (Kiyatkin et al., 2016). These findings are relevant clinically considering the limited therapeutic techniques currently in use for treatment of acute drug-induced hyperthermia in humans, none of which involve pharmacotherapies that exhibit direct cooling effects in the brain (Kiyatkin et al., 2016). Considering this, future pharmacotherapies and clinical techniques aimed at alleviating the adverse temperature effects of MDMA should ideally have action within the brain where we have demonstrated these effects are most severe.

MDMA-induced Heart Rate and Locomotor Activity changes

In addition to brain and body temperature, HR and LMA were measured during all *in vivo* MDMA and minocycline experiments. Most data were consistent with existing literature reporting the individual effects of these drugs on HR and LMA (Jaehne et al., 2008, Liechti and Vollenweider, 2000, Orio et al., 2010, Badon et al., 2002, Bankson and Cunningham, 2001, Baumann et al., 2008, Zhang et al., 2007). However, there is no literature currently available that investigates the cardiovascular and behavioural effects of minocycline in the context of MDMA-induced hyperthermia. Inclusion of these measures in our studies gave added insight into potential pharmacological mechanisms underlying the attenuation of MDMA-induced hyperthermia by minocycline that warrants further discussion.

In our third paper, we demonstrated that acute MDMA administration significantly increased HR at high ambient temperature, a result consistent with existing literature (Dafters, 1994, Bexis and Docherty, 2006, Green et al., 2003, Jaehne et al., 2008). Delayed increases in HR were also observed at normal ambient temperature post-MDMA, however, these were significantly reduced compared to high ambient temperature administration. Cardiovascular physiology is important in mammals when adapting to changes in ambient temperature (Jaehne et al., 2008). While core temperatures are being maintained, cardiovascular changes in response to cold ambient temperatures are closely related to mechanisms of heat production in rats, which increase in parallel with HR (Chambers et al., 2000). Similarly, in non-human primates, disruption of the pre-optic anterior hypothalamus by direct cooling has been linked to increases in HR and core temperature, while direct warming has been linked to lower HR and decreases in core temperature (Morishima and Gale, 1972). Changes in HR and other cardiovascular parameters may therefore give an indirect indication of heat production and disrupted autonomic thermoregulation. This suggests that higher HR observed in animals treated at high ambient temperature could be related to their higher brain and core body temperatures. However, reduced but significant HR increases also occurred in rats exhibiting brain and body hypothermia when administered MDMA at normal ambient temperature, which does not fit with this hypothesis (Jaehne et al., 2008). This suggests that MDMA's effects on HR may occur independently from its effects on brain and body temperatures.

The effect of MDMA on cardiovascular parameters such as HR and blood pressure are comparable to other sympathomimetic agents such as amphetamine (O'Cain et al., 2000) and cocaine (Branch and Knuepfer, 1992) whose mechanisms of cardiac stimulation involve both central and peripheral sympathetic components. (Schindler, 1996). Existing literature indicates that the adrenergic system is the primary mediator underlying the cardiovascular effects of MDMA. Administration of β-adrenoreceptor antagonists have been shown to block MDMA-

induced increases in HR (Hysek et al., 2010, Schindler et al., 2014), and both α_1- and α_2-adrenoreceptor antagonists are known to reduce the duration of MDMAs cardiovascular effects (O'Cain et al., 2000, Vandeputte and Docherty, 2002) and in some cases completely reverse them (McDaid and Docherty, 2001). NA uptake blockers are also known to reduce blood pressure and HR elevations following MDMA administration in humans, indicating that the NA transporter is involved in this mechanism (Hysek et al., 2011). In addition to this, central monoamine systems are known to contribute to the cardiovascular effects of MDMA (Liechti and Vollenweider, 2000, Liechti et al., 2001). Agonist activity of MDMA at 5-HT_2 receptors is known to contribute to cardiovascular stimulation (McDaid and Docherty, 2001) while inhibition of 5-HT uptake by selective serotonin reuptake inhibitors (SSRI) attenuates this stimulation induced by MDMA (Liechti and Vollenweider, 2000). Dopamine receptor blockade is known to reduce the subjective effects of MDMA in humans, however this does not alter the drugs' cardiovascular effects (Liechti et al., 2000a, Liechti et al., 2001). Pro-inflammatory cytokine release in the CNS is also known to modify sympathetic neuronal outflow, which plays a key role in the regulation of cardiovascular function (Kannan et al., 1996, Kimura et al., 1993, Ufnal et al., 2005, Liechti and Vollenweider, 2000). As mentioned previously, minocycline is known to attenuate MDMA-induced 5-HT neurotoxicity (Zhang et al., 2006, Orio et al., 2010), and the maturation and release of pro-inflammatory cytokines (Yrjänheikki et al., 1998, Chen et al., 2000). Furthermore, it has been shown to offer cardiac protection via reduction in markers of oxidative stress (Salameh et al., 2015), which are known to be increased following MDMA administration (Song et al., 2010). Although not quantified in our studies, it is likely that minocycline's inhibition of MDMA-induced microglial activation and pro-inflammatory cytokine release, in conjunction with its direct reduction in MDMA-induced central monoamine release contributed to its hypothermic effects in the brain and body, reflected in our study by the reduction in cardiac stimulation following acute MDMA

administration. These inhibitory cardiovascular effects may also indicate that minocycline also has a mechanism of action at peripheral α- and β-adrenoreceptors, as well as activity at the NA transporter that are involved in regulation of cardiovascular activity. Furthermore, the reduction of baseline HR pre-MDMA administration by minocycline may indicate that it reduces baseline monoamine activity levels in the brain, and may also directly accumulate in cardiac tissue to reduce cardiac stimulation (Romero-Perez et al., 2008). However, further ligand-receptor binding studies would be required to test these hypotheses.

In addition to its cardiovascular effects, our results show that MDMA administration causes significant increases in LMA that were also impacted by minocycline. LMA was significantly elevated for approximately 2 h post-MDMA administration at both normal and high ambient temperatures before activity levels decreased nearing the end of the experiment. The increase in activity post-MDMA agrees with previous literature demonstrating MDMA-induced increases in locomotion (Bankson and Cunningham, 2001, Bankson and Cunningham, 2002, Baumann et al., 2008). Like MDMA's effects on HR, these changes in LMA occurred independently from increases in brain and body temperature. These results are in-line with previous literature reporting that abolishment of hyperthermia by low ambient temperatures had no effect on MDMA-induced hyperkinesis (Dafters, 1994). This dissociation indicates that MDMA-induced heat production via hyperlocomotion is not a major factor determining the magnitude of the hyperthermic response.

Increased locomotion induced by MDMA is thought to primarily involve an increase in dopaminergic activity (Baumann et al., 2008). However, drug-induced hyperlocomotion is also accompanied by behavioural features of serotonin syndrome (Spanos and Yamamoto, 1989, Colado et al., 1993), and drug actions at both the 5-HTT and 5-HT receptors have also been implicated in this response (Bankson and Cunningham, 2001, Bankson and Cunningham, 2002). Furthermore, glutaminergic system activation is known to produce hyperlocomotion,

and the inhibitory activity of minocycline at glutamate receptors has been demonstrated to reduce baseline LMA as well as amphetamine-induced increases in LMA (González et al., 2007, Zhang et al., 2007, Tikka and Koistinaho, 2001). Our results demonstrate that pretreatment with minocycline significantly attenuated MDMA-induced increases in locomotion at high ambient temperature. Although not quantified in our studies, our results support the hypothesis that minocycline's attenuation of MDMA-induced brain and body hyperthermia involves both the direct and indirect inhibition of acute DA (Zhang et al., 2007) and 5-HT release (Orio et al., 2010), as well as the reversal MDMA-induced monoamine reuptake impairment, as explained by the drugs attenuation of MDMA-induced increases in LMA. However, future studies examining acute neurotransmitter and pro-inflammatory cytokine release, metabolism, and reuptake would be required to confirm these hypothesis.

Future directions

The most important aspect that should be expanded upon in the future is the combination and multiplexing of this temperature probe with other optical sensors and sensing equipment. One of the main advantages of optical fibre sensors for biomedical monitoring applications in the CNS is their ability to provide for multiplexed sensing using one implanted probe. This limits potential stress or tissue damage that would accompany implantation of multiple different sensors for monitoring of multiple parameters. Due to the relatively small size of our fibre-tip sensor, it can be easily combined with existing sensors, or multiplexed with other compatible optical sensors. For example, we have already successfully demonstrated successful multiplexing of this sensor with an optical coherence tomography imaging sensor for simultaneous brain temperature sensing and structural imaging (Li et al., 2018) (see Appendix 1). Another promising option for multiplexing would be the previously demonstrated optical fibre immunosensor for localized detection of IL-1β (Zhang et al., 2019). *Ex vivo* results using this sensor demonstrated a significant correlation with commercial IL-1β ELISA kits, and

successfully carried out localized measurement of IL-1β in anesthetized rats. The combination of these two sensors in future studies could allow simultaneous monitoring of MDMA-induced brain temperature change, and IL-1β release *in vivo* without the need for conventional and time-consuming IL-1β immunoassays. The combination of optical fibre sensors with other neurochemical assays such as microdialysis, as well as other recording techniques such as radiotelemetry monitoring could lead to a powerful armamentarium of approaches that provide a comprehensive view of the physiological and pharmacological effects of acute MDMA administration, and to assess pharmacological interventions aimed at attenuating the resulting hyperthermic response.

Ideally future MDMA studies using this temperature sensor would include examining a variety of other factors to further the results and better understand MDMA-induced hyperthermia. One important aspect of this thesis to build on includes examination of MDMA co-administration with other drugs that may prevent the adverse thermoregulatory effects of MDMA. This includes any drug with action on central 5-HT, DA, and NA systems, as well as noradrenergic transmission in the periphery such as receptor agonists, antagonists, selective reuptake inhibitors, transporter blockers, and drugs that prevent neurotransmitter breakdown such as MAO inhibitors. Examination of drugs with central anti-inflammatory properties similar to minocycline should also be included in this investigation. Previous studies with these types of drugs have demonstrated attenuation of hyperthermia owing to modulation of neurotransmitter activity (Malberg et al., 1996, Mechan et al., 2002, Blessing et al., 2003) and neuroinflammation (Porceddu et al., 2016) following MDMA administration. Investigation of these drugs would lead to a more complete understanding of the mechanisms underlying MDMA-induced hyperthermia, and the priority pathways in which future pharmacological interventions should target to achieve adequate attenuation of this dangerous clinical symptom in an acute setting.

Other options for furthering results presented in this thesis include examining drug administration schedules, conditions of drug administration, and MDMA administration with other stimulant drugs. For example, in the last paper, we attempted to simulate conditions typical of human drug administration by administering single-dose MDMA at high ambient temperature and investigating the therapeutic effects of minocycline under these deleterious environmental conditions. However, this one change to conditions under which the drug was administered may be too simplistic when attempting to simulate human drug use. Other factors such as social interaction, water consumption, repeated dosing, and co-administration with other drugs are also typical of human drug use and have been shown to further exacerbate MDMA-induced hyperthermia and contribute to the drug's adverse effects (Dafters, 1995, Brown and Kiyatkin, 2004, Stanley et al., 2007). Inclusion of these factors during future *in vivo* sampling would yield results more relatable to human use. The efficacy of potential pharmacological interventions for attenuation of acute MDMA-induced hyperthermia in humans could then be better evaluated.

Conclusions

I have demonstrated an optical fibre point temperature sensor capable of performing *in vivo* temperature measurements in the brains of freely-moving, MDMA-treated rats. The improved temperature probe utilised equipment commonly found in other neurochemical assays to enable ease of use and handling, and to help facilitate its translation into medical laboratories where these optical sensors could provide many advantages over current monitoring technologies. Using this sensor, I demonstrated that, at high ambient temperature, MDMA induced a significantly more rapid and intense hyperthermic response in the brain when compared to the body, and was much more lethal than expected under these conditions based on its accepted LD_{50}. I subsequently demonstrated that pretreatment of animals with the tetracycline drug minocycline was effective in attenuating MDMA-induced hyperthermia in both the brain and

body, and prevented the fatalities caused by administration of MDMA at high ambient temperature. Minocycline's attenuating effects on MDMA-induced increases in HR and LMA provided some insight into its mechanisms of actions within neuronal and neuroinflammatory pathways in the brain, however subsequent studies should employ further quantification of monoamine levels and neuroinflammation to validate these findings. The current state of research surrounding MDMA makes it clear that pharmacology of the hyperthermic response is not fully understood. Further work is needed regarding the thermoregulatory effects of MDMA in the brain, and the central effects of potential therapeutics in order to better understand mechanisms underlying acute hyperthermia, and the best pathways to target for the effective treatment of MDMA-induced hyperthermia. Continued advancement of optical fibre sensing technology for physical, chemical, and biological monitoring *in vivo* is likely to provide a promising means for better understanding these complex pharmacological pathways in future investigations.

References

ACQUAS, E., MARROCU, P., PISANU, A., CADONI, C., ZERNIG, G., SARIA, A. & DI CHIARA, G. 2001. Intravenous administration of ecstasy (3, 4-methylendioxymethamphetamine) enhances cortical and striatal acetylcholine release in vivo. *European journal of pharmacology,* 418**,** 207-211.

ADDANKI, S., AMIRI, I. & YUPAPIN, P. 2018. Review of optical fibers-introduction and applications in fiber lasers. *Results in Physics,* 10**,** 743-750.

AHN, K. S. & AGGARWAL, B. B. 2005. Transcription factor NF-κB: a sensor for smoke and stress signals. *Annals of the new York Academy of Sciences,* 1056**,** 218-233.

AHUJA, M., BISHNOI, M. & CHOPRA, K. 2008. Protective effect of minocycline, a semi-synthetic second-generation tetracycline against 3-nitropropionic acid (3-NP)-induced neurotoxicity. *Toxicology,* 244**,** 111-122.

AL-SAHLI, W., AHMAD, H., KHERADMAND, F., CONNOLLY, C. & DOCHERTY, J. R. 2001. Effects of methylenedioxymethamphetamine on noradrenaline-evoked contractions of rat right ventricle and small mesenteric artery. *European journal of pharmacology,* 422**,** 169-174.

ANDERSON, G., BRAUN, G., BRAUN, U., NICHOLS, D. E. & SHULGIN, A. T. 1978. Absolute configuration and psychotomimetic activity. *NIDA Res Monogr,* 22**,** 8-15.

ANDERSON, P., HUTCHINSON, M., IRVINE, R. & SALEM, A. 2011. Attenuating glial activation with minocycline reduces the hyperthermic response to 3, 4-methylenedioxymethamphetamine (MDMA) in the rat. *The Open Addiction Journal,* 4.

AUGOUSTI, A., GRATTAN, K. & PALMER, A. 1988. Visible-LED pumped fiber-optic temperature sensor. *IEEE transactions on instrumentation and measurement,* 37**,** 470-472.

AULAKH, C., HILL, J., WOZNIAK, K. & MURPHY, D. L. 1988. Fenfluramine-induced suppression of food intake and locomotor activity is differentially altered by the selective type A monoamine oxidase inhibitor clorgyline. *Psychopharmacology,* 95**,** 313-317.

AUSTRALIAN INSTITUTE OF HEALTH AND WELFARE 2017. National Drug Strategy Household Survey 2016: Detailed Findings. Canberra: AIHW.

BADON, L. A., HICKS, A., LORD, K., OGDEN, B. A., MELEG-SMITH, S. & VARNER, K. J. 2002. Changes in cardiovascular responsiveness and cardiotoxicity elicited during binge administration of Ecstasy. *Journal of Pharmacology and Experimental Therapeutics,* 302**,** 898-907.

BAE, D. D., BROWN, P. L. & KIYATKIN, E. A. 2007. Procedure of rectal temperature measurement affects brain, muscle, skin, and body temperatures and modulates the effects of intravenous cocaine. *Brain research,* 1154**,** 61-70.

BANERJEE, R. K. & DASGUPTA, S. 2010. Characterization methods of high-intensity focused ultrasound-induced thermal field. *Advances in Heat Transfer.* Elsevier.

BANKSON, M. G. & CUNNINGHAM, K. A. 2001. 3, 4-Methylenedioxymethamphetamine (MDMA) as a unique model of serotonin receptor function and serotonin-dopamine interactions. *Journal of Pharmacology and Experimental Therapeutics,* 297**,** 846-852.

BANKSON, M. G. & CUNNINGHAM, K. A. 2002. Pharmacological studies of the acute effects of (+)-3, 4-methylenedioxymethamphetamine on locomotor activity: role of 5-HT1B/1D and 5-HT2 receptors. *Neuropsychopharmacology,* 26**,** 40-52.

BATTAGLIA, G., YEH, S. & DE SOUZA, E. B. 1988. MDMA-induced neurotoxicity: parameters of degeneration and recovery of brain serotonin neurons. *Pharmacology Biochemistry and Behavior,* 29**,** 269-274.

BAUMANN, M. H., CLARK, R. D. & ROTHMAN, R. B. 2008. Locomotor stimulation produced by 3, 4-methylenedioxymethamphetamine (MDMA) is correlated with dialysate levels of serotonin and dopamine in rat brain. *Pharmacology Biochemistry and Behavior,* 90**,** 208-217.

BAUMANN, M. H., ZOLKOWSKA, D., KIM, I., SCHEIDWEILER, K. B., ROTHMAN, R. B. & HUESTIS, M. A. 2009. Effects of dose and route of administration on pharmacokinetics of (±)-3, 4-methylenedioxymethamphetamine in the rat. *Drug Metabolism and Disposition,* 37**,** 2163-2170.

BAYLEN, C. A. & ROSENBERG, H. 2006. A review of the acute subjective effects of MDMA/ecstasy. *Addiction,* 101**,** 933-947.

BEARDSLEY, P. M., BALSTER, R. L. & HARRIS, L. S. 1986. Self-administration of methylenedioxymethamphetamine (MDMA) by rhesus monkeys. *Drug and alcohol dependence,* 18**,** 149-157.

BÉLANGER, M., ALLAMAN, I. & MAGISTRETTI, P. J. 2011. Brain energy metabolism: focus on astrocyte-neuron metabolic cooperation. *Cell metabolism,* 14**,** 724-738.

BERGER, U. V., GU, X. F. & AZMITIA, E. C. 1992. The substituted amphetamines 3, 4-methylenedioxymethamphetamine, methamphetamine, p-chloroamphetamine and fenfluramine induce 5-hydroxytryptamine release via a common mechanism blocked by fluoxetine and cocaine. *European journal of pharmacology,* 215**,** 153-160.

BERTHOU, H. & JÖRGENSEN, C. 1990. Optical-fiber temperature sensor based on upconversion-excited fluorescence. *Optics letters,* 15**,** 1100-1102.

BEXIS, S. & DOCHERTY, J. R. 2005. Role of α2A-adrenoceptors in the effects of MDMA on body temperature in the mouse. *British journal of pharmacology,* 146**,** 1-6.

BEXIS, S. & DOCHERTY, J. R. 2006. Effects of MDMA, MDA and MDEA on blood pressure, heart rate, locomotor activity and body temperature in the rat involve α-adrenoceptors. *British journal of pharmacology,* 147**,** 926-934.

BEXIS, S., PHILLIS, B. D., ONG, J., WHITE, J. M. & IRVINE, R. J. 2004. Baclofen prevents MDMA-induced rise in core body temperature in rats. *Drug and Alcohol Dependence,* 74**,** 89-96.

BHATIA, V. 1999. Applications of long-period gratings to single and multi-parameter sensing. *Optics express,* 4**,** 457-466.

BLESSING, W., SEAMAN, B., PEDERSEN, N. & OOTSUKA, Y. 2003. Clozapine reverses hyperthermia and sympathetically mediated cutaneous vasoconstriction induced by 3, 4-methylenedioxymethamphetamine (ecstasy) in rabbits and rats. *Journal of Neuroscience,* 23**,** 6385-6391.

BLESSING, W. W. & SEAMAN, B. 2003. 5-Hydroxytryptamine2A receptors regulate sympathetic nerves constricting the cutaneous vascular bed in rabbits and rats. *Neuroscience,* 117**,** 939-948.

BOGAARDS, J., BERTRAND, M., JACKSON, P., OUDSHOORN, M., WEAVER, R., VAN BLADEREN, P. & WALTHER, B. 2000. Determining the best animal model for human cytochrome P450 activities: a comparison of mouse, rat, rabbit, dog, micropig, monkey and man. *Xenobiotica,* 30**,** 1131-1152.

BORA, F., YıLMAZ, F. & BORA, T. 2016. Ecstasy (MDMA) and its effects on kidneys and their treatment: a review. *Iranian journal of basic medical sciences,* 19**,** 1151.

BOWYER, J., TANK, A., NEWPORT, G., SLIKKER, W., ALI, S. & HOLSON, R. 1992. The influence of environmental temperature on the transient effects of methamphetamine on dopamine levels and dopamine release in rat striatum. *Journal of Pharmacology and Experimental Therapeutics,* 260**,** 817-824.

BOWYER, J. F., YOUNG, J. F., SLIKKER JR, W., ITZAK, Y., MAYORGA, A., NEWPORT, G. D., ALI, S. F., FREDERICK, D. L. & PAULE, M. G. 2003. Plasma levels of parent compound and metabolites after doses of either d-fenfluramine or d-3, 4-methylenedioxymethamphetamine (MDMA) that produce long-term serotonergic alterations. *Neurotoxicology,* 24**,** 379-390.

BRANCH, C. A. & KNUEPFER, M. M. 1992. Adrenergic mechanisms underlying cardiac and vascular responses to cocaine in conscious rats. *Journal of Pharmacology and Experimental Therapeutics,* 263**,** 742-751.

BROENING, H. W., BOWYER, J. F. & SLIKKER, W., JR. 1995. Age-dependent sensitivity of rats to the long-term effects of the serotonergic neurotoxicant (+/-)-3,4-methylenedioxymethamphetamine (MDMA) correlates with the magnitude of the MDMA-induced thermal response. *J Pharmacol Exp Ther,* 275**,** 325-33.

BROGDEN, R., SPEIGHT, T. & AVERY, G. 1975. Minocycline: a review of its antibacterial and pharmacokinetic properties and therapeutic use. *Drugs,* 9**,** 251-291.

BROWN, P. L. & KIYATKIN, E. A. 2004. Brain hyperthermia induced by MDMA (ecstasy): modulation by environmental conditions. *Eur J Neurosci,* 20**,** 51-8.

BURNS, N., OLVERMAN, H., KELLY, P. & WILLIAMS, B. 1996. Effects of ecstasy on aldosterone secretion in the rat in vivo and in vitro. *Endocrine research,* 22**,** 601-606.

BYARD, R., GILBERT, J., JAMES, R. & LOKAN, R. 1998. Amphetamine derivative fatalities in South Australia-is" Ecstasy" the culprit? *The American journal of forensic medicine and pathology,* 19**,** 261-265.

CAI, Z. & XU, H. 2003. Point temperature sensor based on green upconversion emission in an Er: ZBLALiP microsphere. *Sensors and Actuators A: Physical,* 108**,** 187-192.

CALDICOTT, D. G., EDWARDS, N. A., KRUYS, A., KIRKBRIDE, K. P., SIMS, D. N., BYARD, R. W., PRIOR, M. & J. IRVINE, R. 2003. Dancing with "death": p-methoxyamphetamine overdose and its acute management. *Journal of Toxicology: Clinical Toxicology,* 41**,** 143-154.

CALLAGHAN, P. D., FARRAND, K., SALEM, A., HUGHES, P., DAWS, L. C. & IRVINE, R. J. 2006. Repeated administration of the substituted amphetamine p-methoxyamphetamine produces reductions in cortical 5-HT transporter binding but not 5-HT content, unlike 3, 4-methylenedioxyamethamphetamine. *European journal of pharmacology,* 546**,** 74-81.

CALLAWAY, C. W., WING, L. L. & GEYER, M. A. 1990. Serotonin release contributes to the locomotor stimulant effects of 3, 4-methylenedioxymethamphetamine in rats. *Journal of Pharmacology and Experimental Therapeutics,* 254**,** 456-464.

CANNON, D. M., KEENAN, A. K., GUIRY, P. J., BUON, C., BAIRD, A. W. & MCBEAN, G. J. 2001. In vitro neuronal and vascular responses to 5-HT in rats chronically exposed to MDMA. *British journal of pharmacology,* 134**,** 1455-1460.

CAPELA, J. P., CARMO, H., REMIÃO, F., BASTOS, M. L., MEISEL, A. & CARVALHO, F. 2009. Molecular and cellular mechanisms of ecstasy-induced neurotoxicity: an overview. *Molecular neurobiology,* 39**,** 210-271.

CHAMBERS, J., WILLIAMS, T., NAKAMURA, A., HENDERSON, R., OVERTON, J. & RASHOTTE, M. 2000. Cardiovascular and metabolic responses of hypertensive and normotensive rats to one week of cold exposure. *American Journal of Physiology-Regulatory, Integrative and Comparative Physiology,* 279**,** R1486-R1494.

CHAVKO, M., KOLLER, W. A., PRUSACZYK, W. K. & MCCARRON, R. M. 2007. Measurement of blast wave by a miniature fiber optic pressure transducer in the rat brain. *Journal of neuroscience methods,* 159**,** 277-281.

CHEN, D., WAN, Z., ZHOU, Y. & JI, Z. 2015. Cr3+-doped gallium-based transparent bulk glass ceramics for optical temperature sensing. *Journal of the European Ceramic Society,* 35**,** 4211-4216.

CHEN, M., ONA, V. O., LI, M., FERRANTE, R. J., FINK, K. B., ZHU, S., BIAN, J., GUO, L., FARRELL, L. A. & HERSCH, S. M. 2000. Minocycline inhibits caspase-1 and caspase-3 expression and delays mortality in a transgenic mouse model of Huntington disease. *Nature medicine,* 6**,** 797.

CHIAVAIOLI, F., GOUVEIA, C., JORGE, P. & BALDINI, F. 2017. Towards a uniform metrological assessment of grating-based optical fiber sensors: From refractometers to biosensors. *Biosensors,* 7**,** 23.

CHRISTENSEN, D. Fiberoptic temperature sensing for biomedical applications. Optical Fibers in Medicine III, 1988. International Society for Optics and Photonics, 108-114.

CHU, T., KUMAGAI, Y., DISTEFANO, E. W. & CHO, A. K. 1996. Disposition of methylenedioxymethamphetamine and three metabolites in the brains of different rat strains and their possible roles in acute serotonin depletion. *Biochem Pharmacol,* 51**,** 789-96.

CLAUSING, P., BLOOM, D., NEWPORT, G., HOLSON, R., SLIKKER, W. & BOWYER, J. 1996. Individual differencs in dopamine release but not rotational behavior correlate with extracellular amphetamine levels in caudate putament in unlesioned rats. *Psychopharmacology,* 127**,** 187-194.

CLEMENS, K. J., VAN NIEUWENHUYZEN, P. S., LI, K. M., CORNISH, J. L., HUNT, G. E. & MCGREGOR, I. S. 2004. MDMA ("ecstasy"), methamphetamine and their combination: long-term changes in social interaction and neurochemistry in the rat. *Psychopharmacology,* 173**,** 318-325.

CLEMENT, J. G., MILLS, P. & BROCKWAY, B. 1989. Use of telemetry to record body temperature and activity in mice. *Journal of pharmacological methods,* 21**,** 129-140.

COLADO, M., MURRAY, T. & GREEN, A. 1993. 5-HT loss in rat brain following 3, 4-methylenedioxymethamphetamine (MDMA), p-chloroamphetamine and fenfluramine administration and effects of chlormethiazole and dizocilpine. *British journal of pharmacology,* 108**,** 583-589.

COLADO, M. I., WILLIAMS, J. L. & GREEN, A. R. 1995. The hyperthermic and neurotoxic effects of 'Ecstasy' (MDMA) and 3,4 methylenedioxyamphetamine (MDA) in the Dark Agouti (DA) rat, a model of the CYP2D6 poor metabolizer phenotype. *Br J Pharmacol,* 115**,** 1281-9.

COLE, J. C., BAILEY, M., SUMNALL, H. R., WAGSTAFF, G. F. & KING, L. A. 2002. The content of ecstasy tablets: implications for the study of their long-term effects. *Addiction,* 97**,** 1531-1536.

COLE, J. C. & SUMNALL, H. R. 2003. The pre-clinical behavioural pharmacology of 3, 4-methylenedioxymethamphetamine (MDMA). *Neuroscience & Biobehavioral Reviews,* 27**,** 199-217.

CONCHEIRO, M., BAUMANN, M. H., SCHEIDWEILER, K. B., ROTHMAN, R. B., MARRONE, G. F. & HUESTIS, M. A. 2014. Nonlinear pharmacokinetics of (±) 3, 4-methylenedioxymethamphetamine (MDMA) and its pharmacodynamic consequences in the rat. *Drug Metabolism and Disposition,* 42**,** 119-125.

CONNOR, T. J., KELLY, J. P., MCGEE, M. & LEONARD, B. E. 2000. Methylenedioxymethamphetamine (MDMA; Ecstasy) suppresses IL-1β and TNF-α secretion following an in vivo lipopolysaccharide challenge. *Life Sciences,* 67**,** 1601-1612.

CONNOR, T. J., MCNAMARA, M. G., FINN, D., CURRID, A., O'MALLEY, M., REDMOND, A. M., KELLY, J. P. & LEONARD, B. E. 1998. Acute 3, 4-methylenedioxymethamphetamine (MDMA) administration produces a rapid and sustained suppression of immune function in the rat. *Immunopharmacology,* 38**,** 253-260.

CONNOR, T. J., MCNAMARA, M. G., KELLY, J. P. & LEONARD, B. E. 1999. 3, 4-methylenedioxymethamphetamine (MDMA; Ecstasy) administration produces dose-dependent neurochemical, endocrine and immune changes in the rat. *Human Psychopharmacology: Clinical and Experimental,* 14**,** 95-104.

CORREIA, R., JAMES, S., LEE, S., MORGAN, S. & KORPOSH, S. 2018. Biomedical application of optical fibre sensors. *Journal of Optics,* 20**,** 073003.

COSCELLI, E., SOZZI, M., POLI, F., PASSARO, D., CUCINOTTA, A., SELLERI, S., CORRADINI, R. & MARCHELLI, R. 2009. Toward a highly specific DNA biosensor: PNA-modified suspended-core photonic crystal fibers. *IEEE Journal of selected topics in quantum electronics,* 16**,** 967-972.

CUI, G., JUN, S. B., JIN, X., LUO, G., PHAM, M. D., LOVINGER, D. M., VOGEL, S. S. & COSTA, R. M. 2014. Deep brain optical measurements of cell type–specific neural activity in behaving mice. *Nature protocols,* 9**,** 1213.

CULSHAW, B. & DAKIN, J. Optical fiber sensors: Systems and applications. Volume 2. Optical Fiber Sensors: Systems and Applications. Volume 2, 1989.

DA SILVA, C., DE ARAUJO, M., GOUVEIA, E. & GOUVEIA-NETO, A. 2000. Thermal effect on multiphonon-assisted anti-Stokes excited upconversion fluorescence emission in Yb3+-sensitized Er3+-doped optical fiber. *Applied Physics B,* 70**,** 185-188.

DAFTERS, R. I. 1994. Effect of ambient temperature on hyperthermia and hyperkinesis induced by 3, 4-methylenedioxymethamphetamine (MDMA or "ecstasy") in rats. *Psychopharmacology,* 114**,** 505-508.

DAFTERS, R. I. 1995. Hyperthermia following MDMA administration in rats: effects of ambient temperature, water consumption, and chronic dosing. *Physiology & behavior,* 58**,** 877-882.

DAFTERS, R. I. & LYNCH, E. 1998. Persistent loss of thermoregulation in the rat induced by 3, 4-methylenedioxymethamphetamine (MDMA or "Ecstasy") but not by fenfluramine. *Psychopharmacology,* 138**,** 207-212.

DARVESH, A. S., SHANKARAN, M. & GUDELSKY, G. A. 2002. 3, 4-Methylenedioxymethamphetamine produces glycogenolysis and increases the extracellular concentration of glucose in the rat brain. *Journal of Pharmacology and Experimental Therapeutics,* 301**,** 138-144.

DAVISON, D. & PARROTT, A. 1997. Ecstasy (MDMA) in recreational users: self-reported psychological and physiological effects. *Human Psychopharmacology Clinical and Experimental,* 12**,** 221-226.

DAWS, L. C., IRVINE, R. J., CALLAGHAN, P. D., TOOP, N. P., WHITE, J. M. & BOCHNER, F. 2000. Differential behavioural and neurochemical effects of para-methoxyamphetamine and 3, 4-methylenedioxymethamphetamine in the rat. *Progress in Neuro-Psychopharmacology and Biological Psychiatry,* 24**,** 955-977.

DE LA TORRE, R. & FARRÉ, M. 2004. Neurotoxicity of MDMA (ecstasy): the limitations of scaling from animals to humans. *Trends in pharmacological sciences,* 25**,** 505-508.

DE LA TORRE, R., FARRE, M., ORTUNO, J., MAS, M., BRENNEISEN, R., ROSET, P., SEGURA, J. & CAMI, J. 2000. Non-linear pharmacokinetics of MDMA ('ecstasy') in humans. *British journal of clinical pharmacology,* 49**,** 104-109.

DE LA TORRE, R., FARRÉ, M., ROSET, P. N., PIZARRO, N., ABANADES, S., SEGURA, M., SEGURA, J. & CAMÍ, J. 2004. Human pharmacology of MDMA: pharmacokinetics, metabolism, and disposition. *Therapeutic drug monitoring,* 26**,** 137-144.

DEAN, O. M., DATA-FRANCO, J., GIORLANDO, F. & BERK, M. 2012. Minocycline. *CNS drugs,* 26**,** 391-401.

DEGENHARDT, L., BRUNO, R. & TOPP, L. 2010. Is ecstasy a drug of dependence? *Drug and alcohol dependence,* 107**,** 1-10.

DESIRENA, H., DE LA ROSA, E., SHULZGEN, A., SHABET, S. & PEYGHAMBARIAN, N. 2008. Er3+ and Yb3+ concentration effect in the spectroscopic properties and energy transfer in Yb3+/Er3+ codoped tellurite glasses. *Journal of Physics D: Applied Physics,* 41**,** 095102.

DILSAVER, S. C., MAJCHRZAK, M. J. & ALESSI, N. E. 1990. Telemetric measurement of core temperature in pharmacological research: validity and reliability.

DINARELLO, C. A., CANNON, J. G. & WOLFF, S. M. 1988. New concepts on the pathogenesis of fever. *Reviews of infectious diseases***,** 168-189.

DOCHERTY, J. & GREEN, A. 2010. The role of monoamines in the changes in body temperature induced by 3, 4-methylenedioxymethamphetamine (MDMA, ecstasy) and its derivatives. *British journal of pharmacology,* 160**,** 1029-1044.

DOS SANTOS, P., DE ARAUJO, M., GOUVEIA-NETO, A., NETO, J. M. & SOMBRA, A. 1998. Optical temperature sensing using upconversion fluorescence emission in Er3+/Yb3+-codoped chalcogenide glass. *Applied physics letters,* 73**,** 578-580.

DOS SANTOS, P., DE ARAUJO, M., GOUVEIA-NETO, A., NETO, J. M. & SOMBRA, A. 1999. Optical thermometry through infrared excited upconversion fluorescence emission in Er/sup 3+/-and Er/sup 3+/-Yb/sup 3+/-doped chalcogenide glasses. *IEEE Journal of Quantum Electronics,* 35**,** 395-399.

DU, Y., MA, Z., LIN, S., DODEL, R. C., GAO, F., BALES, K. R., TRIARHOU, L. C., CHERNET, E., PERRY, K. W. & NELSON, D. L. 2001. Minocycline prevents nigrostriatal dopaminergic neurodegeneration in the MPTP model of Parkinson's disease. *Proceedings of the National Academy of Sciences,* 98**,** 14669-14674.

DZIUDA, Ł., KREJ, M. & SKIBNIEWSKI, F. W. 2013. Fiber Bragg grating strain sensor incorporated to monitor patient vital signs during MRI. *IEEE Sensors Journal,* 13**,** 4986-4991.

DZIUDA, L., SKIBNIEWSKI, F. W., KREJ, M. & LEWANDOWSKI, J. 2012. Monitoring respiration and cardiac activity using fiber Bragg grating-based sensor. *IEEE Transactions on Biomedical Engineering,* 59**,** 1934-1942.

FAJKUS, M., NEDOMA, J., MARTINEK, R., VASINEK, V., NAZERAN, H. & SISKA, P. 2017. A non-invasive multichannel hybrid fiber-optic sensor system for vital sign monitoring. *Sensors,* 17**,** 111.

FALK, E. M., COOK, V. J., NICHOLS, D. E. & SPRAGUE, J. E. 2002. An antisense oligonucleotide targeted at MAO-B attenuates rat striatal serotonergic neurotoxicity induced by MDMA. *Pharmacology Biochemistry and Behavior,* 72**,** 617-622.

FANTEGROSSI, W. E., GODLEWSKI, T., KARABENICK, R. L., STEPHENS, J. M., ULLRICH, T., RICE, K. C. & WOODS, J. H. 2003. Pharmacological characterization of the effects of 3, 4-methylenedioxymethamphetamine (" ecstasy") and its enantiomers on lethality, core temperature, and locomotor activity in singly housed and crowded mice. *Psychopharmacology,* 166**,** 202-211.

FELDBERG, W. & SAXENA, P. 1975. Prostaglandins, endotoxin and lipid A on body temperature in rats. *The Journal of physiology,* 249**,** 601-615.

FISCHER, H., ZERNIG, G., SCHATZ, D., HUMPEL, C. & SARIA, A. 2000. MDMA (‘ecstasy’) enhances basal acetylcholine release in brain slices of the rat striatum. *European Journal of Neuroscience,* 12**,** 1385-1390.

FITZGERALD, J. & REID, J. 1994. Sympathomimetic actions of methylenedioxymethamphetamine in rat and rabbit isolated cardiovascular tissues. *Journal of pharmacy and pharmacology,* 46**,** 826-832.

FITZGERALD, J. L. & REID, J. J. 1993. Interactions of methylenedioxymethamphetamine with monoamine transmitter release mechanisms in rat brain slices. *Naunyn-Schmiedeberg's archives of pharmacology,* 347**,** 313-323.

FORSLING, M. L., FALLON, J. K., SHAH, D., TILBROOK, G. S., COWAN, D. A., KICMAN, A. T. & HUTT, A. J. 2002. The effect of 3, 4-methylenedioxymethamphetamine (MDMA,? ecstasy?) and its metabolites on neurohypophysial hormone release from the isolated rat hypothalamus. *British journal of pharmacology,* 135**,** 649-656.

FOX, H., PARROTT, A. & TURNER, J. 2001. Ecstasy use: cognitive deficits related to dosage rather than self-reported problematic use of the drug. *Journal of psychopharmacology,* 15**,** 273-281.

FRANKEL, H. M. 1959. Effects of restraint on rats exposed to high temperature. *Journal of applied physiology,* 14**,** 997-999.

FREEZER, A., SALEM, A. & IRVINE, R. J. 2005. Effects of 3, 4-methylenedioxymethamphetamine (MDMA,'Ecstasy') and para-methoxyamphetamine on striatal 5-HT when co-administered with moclobemide. *Brain research,* 1041**,** 48-55.

FREUDENMANN, R. W., ÖXLER, F. & BERNSCHNEIDER-REIF, S. 2006. The origin of MDMA (ecstasy) revisited: the true story reconstructed from the original documents. *Addiction,* 101**,** 1241-1245.

FUJITA, Y., ISHIMA, T., KUNITACHI, S., HAGIWARA, H., ZHANG, L., IYO, M. & HASHIMOTO, K. 2008. Phencyclidine-induced cognitive deficits in mice are improved by subsequent subchronic administration of the antibiotic drug minocycline. *Progress in Neuro-Psychopharmacology and Biological Psychiatry,* 32**,** 336-339.

GARRIDO-MESA, N., ZARZUELO, A. & GÁLVEZ, J. 2013. Minocycline: far beyond an antibiotic. *British journal of pharmacology,* 169**,** 337-352.

GEGOUT-POTTIE, P., PHILIPPE, L., SIMONIN, M.-A., GUINGAMP, C., GILLET, P., NETTER, P. & TERLAIN, B. 1999. Biotelemetry: an original approach to experimental models of inflammation. *Inflammation Research,* 48**,** 417-424.

GOLD, L. H., HUBNER, C. B. & KOOB, G. F. 1989. A role for the mesolimbic dopamine system in the psychostimulant actions of MDMA. *Psychopharmacology,* 99**,** 40-47.

GONZÁLEZ, J. C., EGEA, J., DEL CARMEN GODINO, M., FERNANDEZ-GOMEZ, F. J., SÁNCHEZ-PRIETO, J., GANDÍA, L., GARCÍA, A. G., JORDÁN, J. & HERNÁNDEZ-GUIJO, J. M. 2007. Neuroprotectant minocycline depresses glutamatergic neurotransmission and Ca2+ signalling in hippocampal neurons. *European Journal of Neuroscience,* 26**,** 2481-2495.

GOODWIN, G. M. & GREEN, A. R. 1985. A behavioural and biochemical study in mice and rats of putative selective agonists and antagonists for 5-HT1 and 5-HT2 receptors. *British journal of pharmacology,* 84**,** 743-753.

GORDON, C. J. 1990. Thermal biology of the laboratory rat. *Physiology & behavior,* 47**,** 963-991.

GORDON, C. J., WATKINSON, W. P., O'CALLAGHAN, J. P. & MILLER, D. B. 1991. Effects of 3,4-methylenedioxymethamphetamine on autonomic thermoregulatory responses of the rat. *Pharmacol Biochem Behav,* 38**,** 339-44.

GORDON, J. & KOGELNIK, H. 2000. PMD fundamentals: Polarization mode dispersion in optical fibers. *Proceedings of the National Academy of Sciences,* 97**,** 4541-4550.

GOWING, L. R., HENRY-EDWARDS, S. M., IRVINE, R. J. & ALI, R. L. 2002. The health effects of ecstasy: a literature review. *Drug and Alcohol Review,* 21**,** 53-63.

GRAHAME-SMITH, D. 1971a. Inhibitory effect of chlorpromazine on the syndrome of hyperactivity produced by l-tryptophan or 5-methoxy-N, N-dimethyltryptamine in rats treated with a monoamine oxidase inhibitor. *British journal of pharmacology,* 43**,** 856-864.

GRAHAME-SMITH, D. 1971b. Studies in vivo on the relationship between brain tryptophan, brain 5-HT synthesis and hyperactivity in rats treated with a monoamine oxidase inhibitor and L-tryptophan. *Journal of Neurochemistry,* 18**,** 1053-1066.

GRATTAN, K., PALMER, A. & WILSON, C. 1987. A miniaturised microcomputer-based neodymium'decay-time'temperature sensor. *Journal of Physics E: Scientific Instruments,* 20**,** 1201.

GRATTAN, K. T. & MEGGITT, B. T. 1995. *Optical fiber sensor technology*, Springer.
GREEN, A. R., MECHAN, A. O., ELLIOTT, J. M., O'SHEA, E. & COLADO, M. I. 2003. The pharmacology and clinical pharmacology of 3,4-methylenedioxymethamphetamine (MDMA, "ecstasy"). *Pharmacol Rev,* 55**,** 463-508.

GREEN, A. R., O'SHEA, E. & COLADO, M. I. 2004. A review of the mechanisms involved in the acute MDMA (ecstasy)-induced hyperthermic response. *Eur J Pharmacol,* 500**,** 3-13.

GRUNAU, B. E., WIENS, M. O. & BRUBACHER, J. R. 2010. Dantrolene in the treatment of MDMA-related hyperpyrexia: a systematic review. *Canadian Journal of Emergency Medicine,* 12**,** 435-442.

GUAN, G., ARNOLD, S. & OTUGEN, M. 2006. Temperature measurements using a microoptical sensor based on whispering gallery modes. *AIAA journal,* 44**,** 2385.

GUIOL, C., LEDOUSSAL, C. & SURGE, J.-M. 1992. A radiotelemetry system for chronic measurement of blood pressure and heart rate in the unrestrained rat validation of the method. *Journal of pharmacological and toxicological methods,* 28**,** 99-105.

HALL, A. & HENRY, J. 2006. Acute toxic effects of 'Ecstasy'(MDMA) and related compounds: overview of pathophysiology and clinical management. *BJA: British Journal of Anaesthesia,* 96**,** 678-685.

HALPERN, J. H., POPE, H. G., SHERWOOD, A. R., BARRY, S., HUDSON, J. I. & YURGELUN-TODD, D. 2004. Residual neuropsychological effects of illicit 3, 4-methylenedioxymethamphetamine (MDMA) in individuals with minimal exposure to other drugs. *Drug and alcohol dependence,* 75**,** 135-147.

HALPERN, P., MOSKOVICH, J., AVRAHAMI, B., BENTUR, Y., SOFFER, D. & PELEG, K. 2011. Morbidity associated with MDMA (ecstasy) abuse: a survey of emergency department admissions. *Human & experimental toxicology,* 30**,** 259-266.

HARDMAN, H. F., HAAVIK, C. O. & SEEVERS, M. H. 1973. Relationship of the structure of mescaline and seven analogs to toxicity and behavior in five species of laboratory animals. *Toxicology and applied Pharmacology,* 25**,** 299-309.

HARRIS, A. & CASTLE, P. 1986. Bend loss measurements on high numerical aperture single-mode fibers as a function of wavelength and bend radius. *Journal of Lightwave technology,* 4**,** 34-40.

HASHIMOTO, K., TSUKADA, H., NISHIYAMA, S., FUKUMOTO, D., KAKIUCHI, T. & IYO, M. 2007. Protective Effects of Minocycline on the Reduction of Dopamine Transporters in the Striatum After Administration of Methamphetamine: A Positron Emission Tomography Study in Conscious Monkeys. *Biological Psychiatry,* 61**,** 577-581.

HATZIDIMITRIOU, G., MCCANN, U. D. & RICAURTE, G. A. 1999. Altered serotonin innervation patterns in the forebrain of monkeys treated with (±) 3, 4-methylenedioxymethamphetamine seven years previously: factors influencing abnormal recovery. *Journal of Neuroscience,* 19**,** 5096-5107.

HOCKER, G. 1979. Fiber-optic sensing of pressure and temperature. *Applied optics,* 18**,** 1445-1448.

HOMSI, S., FEDERICO, F., CROCI, N., PALMIER, B., PLOTKINE, M., MARCHAND-LEROUX, C. & JAFARIAN-TEHRANI, M. 2009. Minocycline effects on cerebral edema: relations with inflammatory and oxidative stress markers following traumatic brain injury in mice. *Brain research,* 1291**,** 122-132.

HOUSE, R. V., THOMAS, P. T. & BHARGAVA, H. N. 1995. Selective modulation of immune function resulting from in vitro exposure to methylenedioxymethamphetamine (Ecstasy). *Toxicology,* 96**,** 59-69.

HYSEK, C., SCHMID, Y., RICKLI, A., SIMMLER, L., DONZELLI, M., GROUZMANN, E. & LIECHTI, M. 2012. Carvedilol inhibits the cardiostimulant and thermogenic effects of MDMA in humans. *British journal of pharmacology,* 166**,** 2277-2288.

HYSEK, C., VOLLENWEIDER, F. & LIECHTI, M. 2010. Effects of a β-blocker on the cardiovascular response to MDMA (Ecstasy). *Emergency medicine journal,* 27**,** 586-589.

HYSEK, C. M., FINK, A. E., SIMMLER, L. D., DONZELLI, M., GROUZMANN, E. & LIECHTI, M. E. 2013a. α1-adrenergic receptors contribute to the acute effects of 3, 4-methylenedioxymethamphetamine in humans. *Journal of clinical psychopharmacology,* 33**,** 658-666.

HYSEK, C. M., SCHMID, Y., RICKLI, A. & LIECHTI, M. E. 2013b. Carvedilol inhibits the cardiostimulant and thermogenic effects of MDMA in humans: lost in translation. *British journal of pharmacology,* 170**,** 1273-1275.

HYSEK, C. M., SIMMLER, L. D., INEICHEN, M., GROUZMANN, E., HOENER, M. C., BRENNEISEN, R., HUWYLER, J. & LIECHTI, M. E. 2011. The Norepinephrine Transporter Inhibitor Reboxetine Reduces Stimulant Effects of MDMA ("Ecstasy") in Humans. *Clinical Pharmacology & Therapeutics,* 90**,** 246-255.

IMBESI, M., UZ, T., MANEV, R., SHARMA, R. P. & MANEV, H. 2008. Minocycline increases phosphorylation and membrane insertion of neuronal GluR1 receptors. *Neuroscience letters,* 447**,** 134-137.

IRVINE, R. J., KEANE, M., FELGATE, P., MCCANN, U. D., CALLAGHAN, P. D. & WHITE, J. M. 2006. Plasma drug concentrations and physiological measures in 'dance party'participants. *Neuropsychopharmacology,* 31**,** 424.

IRVINE, R. J., WHITE, J. & CHAN, R. 1997. The influence of restraint on blood pressure in the rat. *Journal of pharmacological and toxicological methods,* 38**,** 157-162.

JAEHNE, E. J., MAJUMDER, I., SALEM, A. & IRVINE, R. J. 2011. Increased effects of 3, 4-methylenedioxymethamphetamine (ecstasy) in a rat model of depression. *Addiction biology,* 16**,** 7-19.

JAEHNE, E. J., SALEM, A. & IRVINE, R. J. 2005. Effects of 3,4-methylenedioxymethamphetamine and related amphetamines on autonomic and behavioral thermoregulation. *Pharmacol Biochem Behav,* 81**,** 485-96.

JAEHNE, E. J., SALEM, A. & IRVINE, R. J. 2008. The effect of long-term repeated exposure to 3, 4-methylenedioxymethamphetamine on cardiovascular and thermoregulatory changes. *Psychopharmacology,* 201**,** 161-170.

JAKUTIS, J., GOMES, L., AMANCIO, C., KASSAB, L., MARTINELLI, J. & WETTER, N. 2010. Increased Er 3+ upconversion in tellurite fibers and glasses by co-doping with Yb 3+. *Optical Materials,* 33**,** 107-111.

JAY, J. A. 2010. An overview of macrobending and microbending of optical fibers. *White paper of Corning***,** 1-21.

JOHNSTON, L. D., O'MALLEY, P. M., BACHMAN, J. G. & SCHULENBERG, J. E. 2007. Monitoring the Future: National Survey Results on Drug Use, 1975-2006. Volume I: Secondary School Students. NIH Publication No. 07-6205. *National Institute on Drug Abuse (NIDA).*

KAMIEN, J. B., JOHANSON, C. E., SCHUSTER, C. R. & WOOLVERTON, W. L. 1986. The effects of (±)-methylenedioxymethamphetamine and (±)-methylenedioxyamphetamine in monkeys trained to discriminate (+)-amphetamine from saline. *Drug and alcohol dependence,* 18**,** 139-147.

KANNAN, H., TANAKA, Y., KUNITAKE, T., UETA, Y., HAYASHIDA, Y. & YAMASHITA, H. 1996. Activation of sympathetic outflow by recombinant human interleukin-1 beta in conscious rats. *American Journal of Physiology-Regulatory, Integrative and Comparative Physiology,* 270**,** R479-R485.

KEHNE, J., KETTELER, H., MCCLOSKEY, T., SULLIVAN, C., DUDLEY, M. & SCHMIDT, C. 1996. Effects of the selective 5-HT 2A receptor antagonist MDL 100,907 on MDMA-induced locomotor stimulation in rats. *Neuropsychopharmacology,* 15**,** 116.

KIELIAN, T., ESEN, N., LIU, S., PHULWANI, N. K., SYED, M. M., PHILLIPS, N., NISHINA, K., CHEUNG, A. L., SCHWARTZMAN, J. D. & RUHE, J. J. 2007. Minocycline modulates neuroinflammation independently of its antimicrobial activity in Staphylococcus aureus-induced brain abscess. *The American journal of pathology,* 171**,** 1199-1214.

KIM, B. J., KIM, M.-J., PARK, J.-M., LEE, S.-H., KIM, Y.-J., RYU, S., KIM, Y. H. & YOON, B.-W. 2009. Reduced neurogenesis after suppressed inflammation by minocycline in transient cerebral ischemia in rat. *Journal of the neurological sciences,* 279**,** 70-75.

KIM, S.-S., KONG, P.-J., KIM, B.-S., SHEEN, D.-H., NAM, S.-Y. & CHUN, W. 2004. Inhibitory action of minocycline on lipopolysaccharide-lnduced release of nitric oxide and prostaglandin E2 in BV2 microglial cells. *Archives of pharmacal research,* 27**,** 314-318.

KIMURA, T., YAMAMOTO, T., OTA, K., SHOJI, M., INOUE, M., SATO, K., OHTA, M., FUNYU, T. & YOSHINAGA, K. 1993. Central effects of interleukin-1 on blood pressure, thermogenesis, and the release of vasopressin, ACTH, and atrial natriuretic peptide. *Annals of the New York Academy of Sciences,* 689**,** 330-345.

KIYATKIN, E. A. 2005. Brain hyperthermia as physiological and pathological phenomena. *Brain research reviews,* 50**,** 27-56.

KIYATKIN, E. A. 2010. BRAIN TEMPERATURE HOMEOSTASIS: PHYSIOLOGICAL FLUCTUATIONS AND PATHOLOGICAL SHIFTS. *Frontiers in bioscience : a journal and virtual library,* 15**,** 73-92.

KIYATKIN, E. A. 2013. The hidden side of drug action: brain temperature changes induced by neuroactive drugs. *Psychopharmacology (Berl),* 225**,** 765-80.

KIYATKIN, E. A., BROWN, P. L. & SHARMA, H. S. 2007. Brain edema and breakdown of the blood–brain barrier during methamphetamine intoxication: critical role of brain hyperthermia. *European Journal of Neuroscience,* 26**,** 1242-1253.

KIYATKIN, E. A., BROWN, P. L. & WISE, R. A. 2002. Brain temperature fluctuation: a reflection of functional neural activation. *European Journal of Neuroscience,* 16**,** 164-168.

KIYATKIN, E. A., KIM, A. H., WAKABAYASHI, K. T., BAUMANN, M. H. & SHAHAM, Y. 2014. Critical role of peripheral vasoconstriction in fatal brain hyperthermia induced by MDMA (Ecstasy) under conditions that mimic human drug use. *J Neurosci,* 34**,** 7754-62.

KIYATKIN, E. A., REN, S., WAKABAYASHI, K. T., BAUMANN, M. H. & SHAHAM, Y. 2016. Clinically Relevant Pharmacological Strategies That Reverse MDMA-Induced Brain Hyperthermia Potentiated by Social Interaction. *Neuropsychopharmacology,* 41**,** 549-559.

KIYATKIN, E. A. & SHARMA, H. S. 2009. Acute methamphetamine intoxication: brain hyperthermia, blood–brain barrier, brain edema, and morphological cell abnormalities. *International review of neurobiology,* 88**,** 65-100.

KLEIN, N. C. & CUNHA, B. A. 1995. Tetracyclines. *Medical Clinics of North America,* 79**,** 789-801.

KLIR, J. J., MCCLELLAN, J. L. & KLUGER, M. J. 1994. Interleukin-1 beta causes the increase in anterior hypothalamic interleukin-6 during LPS-induced fever in rats. *American Journal of Physiology-Regulatory, Integrative and Comparative Physiology,* 266**,** R1845-R1848.

KOFMAN, O., KLEIN, E., NEWMAN, M., HAMBURGER, R., KIMCHI, O., NIR, T., SHIMON, H. & BELMAKER, R. 1990. Inhibition by antibiotic tetracyclines of rat cortical noradrenergic adenylate cyclase and amphetamine-induced hyperactivity. *Pharmacology Biochemistry and Behavior,* 37**,** 417-424.

KUHN, D. M. & GEDDES, T. J. 2000. Molecular footprints of neurotoxic amphetamine action. *Annals of the New York Academy of Sciences,* 914**,** 92-103.

LANGE, R. A., CIGARROA, R. G., FLORES, E. D., MCBRIDE, W., KIM, A. S., WELLS, P. J., BEDOTTO, J. B., DANZIGER, R. S. & HILLIS, L. D. 1990. Potentiation of cocaine-induced coronary vasoconstriction by beta-adrenergic blockade. *Annals of Internal Medicine,* 112**,** 897-903.

LAVELLE, A., HONNER, V. & DOCHERTY, J. 1999. Investigation of the prejunctional α2-adrenoceptor mediated actions of MDMA in rat atrium and vas deferens. *British journal of pharmacology,* 128**,** 975-980.

LEE, B. 2003. Review of the present status of optical fiber sensors. *Optical fiber technology,* 9**,** 57-79.

LEE, B. & NISHII, J. 1998. Self-interference of long-period fibre grating and its application as temperature sensor. *Electronics Letters,* 34**,** 2059-2060.

LEMUNYAN, C. D., WHITE, W., NYBERG, E. & CHRISTIAN, J. J. 1959. Design of a miniature radio transmitter for use in animal studies. *The Journal of Wildlife Management,* 23**,** 107-110.

LEONARDI, E. T. K. & AZMITIA, E. C. 1994. MDMA (ecstasy) inhibition of MAO type A and type B: comparisons with fenfluramine and fluoxetine (Prozac). *Neuropsychopharmacology,* 10**,** 231-238.

LEVKOVITZ, Y., LEVI, U., BRAW, Y. & COHEN, H. 2007. Minocycline, a second-generation tetracycline, as a neuroprotective agent in an animal model of schizophrenia. *Brain research,* 1154**,** 154-162.

LEVKOVITZ, Y., MENDLOVICH, S., RIWKES, S., BRAW, Y., LEVKOVITCH-VERBIN, H., GAL, G., FENNIG, S., TREVES, I. & KRON, S. 2010. A double-blind, randomized study of minocycline for the treatment of negative and cognitive symptoms in early-phase schizophrenia. *Journal of Clinical Psychiatry,* 71**,** 138.

LI, I.-H., SHIH, J.-H., CHENG-TSUNG, L., CHIU, C.-H. & MA, K.-H. 2019. Exploring the effects of methimazole against MDMA-induced hyperthermia and serotonergic neurotoxicity in rats using small animal PET. *Journal of Nuclear Medicine,* 60**,** 1308-1308.

LI, J., SCHARTNER, E., MUSOLINO, S., QUIRK, B. C., KIRK, R. W., EBENDORFF-HEIDEPRIEM, H. & MCLAUGHLIN, R. A. 2018. Miniaturized single-fiber-based needle probe for combined imaging and sensing in deep tissue. *Optics Letters,* 43**,** 1682-1685.

LIECHTI, M. E., BAUMANN, C., GAMMA, A. & VOLLENWEIDER, F. X. 2000a. Acute Psychological Effects of 3,4-Methylenedioxymethamphetamine (MDMA, [ldquo]Ecstasy[rdquo]) are Attenuated by the Serotonin Uptake Inhibitor Citalopram. *Neuropsychopharmacology,* 22**,** 513-521.

LIECHTI, M. E., GEYER, M. A., HELL, D. & VOLLENWEIDER, F. X. 2001. Effects of MDMA (ecstasy) on prepulse inhibition and habituation of startle in humans after pretreatment with citalopram, haloperidol, or ketanserin. *Neuropsychopharmacology,* 24**,** 240.

LIECHTI, M. E., SAUR, M. R., GAMMA, A., HELL, D. & VOLLENWEIDER, F. X. 2000b. Psychological and physiological effects of MDMA ("Ecstasy") after pretreatment with the 5-HT 2 antagonist ketanserin in healthy humans. *Neuropsychopharmacology,* 23**,** 396.

LIECHTI, M. E. & VOLLENWEIDER, F. X. 2000. The serotonin uptake inhibitor citalopram reduces acute cardiovascular and vegetative effects of 3, 4-methylenedioxymethamphetamine ('Ecstasy') in healthy volunteers. *Journal of Psychopharmacology,* 14**,** 269-274.

LINDBERG, C., ERIKSSON, C., VAN DAM, A.-M., WINBLAD, B. & SCHULTZBERG, M. 2004. Neuronal expression of caspase-1 immunoreactivity in the rat central nervous system. *Journal of neuroimmunology,* 146**,** 99-113.

LONG, F., ZHU, A., ZHOU, X., WANG, H., ZHAO, Z., LIU, L. & SHI, H. 2014. Highly sensitive and selective optofluidics-based immunosensor for rapid assessment of Bisphenol A leaching risk. *Biosensors and Bioelectronics,* 55**,** 19-25.

LUHESHI, G., STEFFERL, A., TURNBULL, A., DASCOMBE, M., BROUWER, S., HOPKINS, S. & ROTHWELL, N. 1997. Febrile response to tissue inflammation involves both peripheral and brain IL-1 and TNF-alpha in the rat. *American Journal of Physiology-Regulatory, Integrative and Comparative Physiology,* 272**,** R862-R868.

LUHESHI, G. N., GARDNER, J. D., RUSHFORTH, D. A., LOUDON, A. S. & ROTHWELL, N. J. 1999. Leptin actions on food intake and body temperature are mediated by IL-1. *Proceedings of the National Academy of Sciences,* 96**,** 7047-7052.

LYLES, J. & CADET, J. L. 2003. Methylenedioxymethamphetamine (MDMA, Ecstasy) neurotoxicity: cellular and molecular mechanisms. *Brain Research Reviews,* 42**,** 155-168.

MACIEL, G., DES MENEZES, L., GOMES, A., DE ARAUJO, C. B., MESSADDEQ, Y., FLOREZ, A. & AEGERTER, A. 1995. Temperature sensor based on frequency upconversion in Er/sup 3+/-doped fluoroindate glass. *IEEE Photonics Technology Letters,* 7**,** 1474-1476.

MALBERG, J. E., SABOL, K. E. & SEIDEN, L. S. 1996. Co-administration of MDMA with drugs that protect against MDMA neurotoxicity produces different effects on body temperature in the rat. *J Pharmacol Exp Ther,* 278**,** 258-67.

MALBERG, J. E. & SEIDEN, L. S. 1998. Small changes in ambient temperature cause large changes in 3, 4-methylenedioxymethamphetamine (MDMA)-induced serotonin neurotoxicity and core body temperature in the rat. *Journal of Neuroscience,* 18**,** 5086-5094.

MANNS, F., MILNE, P. J., GONZALEZ-CIRRE, X., DENHAM, D. B., PAREL, J. M. & ROBINSON, D. S. 1998. In situ temperature measurements with thermocouple probes during laser interstitial thermotherapy (LITT): quantification and correction of a measurement artifact. *Lasers in Surgery and Medicine: The Official Journal of the American Society for Laser Medicine and Surgery,* 23**,** 94-103.

MARTIN, G. E. & PAPP, N. L. 1979. Effect on core temperature of restraint after peripherally and centrally injected morphine in the Sprague-Dawley rat. *Pharmacology Biochemistry and Behavior,* 10**,** 313-315.

MAURER, H. H., BICKEBOELLER-FRIEDRICH, J., KRAEMER, T. & PETERS, F. T. 2000. Toxicokinetics and analytical toxicology of amphetamine-derived designer drugs ('Ecstasy'). *Toxicology letters,* 112**,** 133-142.

MCCANN, U. D., SLATE, S. O. & RICAURTE, G. A. 1996. Adverse reactions with 3, 4-methylenedioxymethamphetamine (MDMA;'ecstasy'). *Drug Safety,* 15**,** 107-115.

MCCANN, U. D., SZABO, Z., SCHEFFEL, U., DANNALS, R. & RICAURTE, G. 1998. Positron emission tomographic evidence of toxic effect of MDMA ("Ecstasy") on brain serotonin neurons in human beings. *The Lancet,* 352**,** 1433-1437.

MCDAID, J. & DOCHERTY, J. R. 2001. Vascular actions of MDMA involve α1 and α2-adrenoceptors in the anaesthetized rat. *British journal of pharmacology,* 133**,** 429-437.

MECHAN, A. O., ESTEBAN, B., O'SHEA, E., ELLIOTT, J. M., COLADO, M. I. & GREEN, A. R. 2002. The pharmacology of the acute hyperthermic response that follows administration of 3, 4-methylenedioxymethamphetamine (MDMA,'ecstasy') to rats. *British journal of pharmacology,* 135**,** 170-180.

MEHTA, D. S., NAIK, D. N., SINGH, R. K. & TAKEDA, M. 2012. Laser speckle reduction by multimode optical fiber bundle with combined temporal, spatial, and angular diversity. *Applied optics,* 51**,** 1894-1904.

MELLERGÅRD, P. 1995. Intracerebral temperature in neurosurgical patients: intracerebral temperature gradients and relationships to consciousness level. *Surgical neurology,* 43**,** 91-95.

MELLERGARD, P. & NORDSTRÖM, C.-H. 1990. Epidural temperature and possible intracerebral temperature gradients in man. *British journal of neurosurgery,* 4**,** 31-38.

MIEVIS, S., LEVIVIER, M., COMMUNI, D., VASSART, G., BROTCHI, J., LEDENT, C. & BLUM, D. 2007. Lack of minocycline efficiency in genetic models of Huntington's disease. *Neuromolecular medicine,* 9**,** 47-54.

MIGNANI, A. G. & BALDINI, F. 1996. Biomedical sensors using optical fibres. *Reports on Progress in Physics,* 59**,** 1.

MILLER, G. M. 2011. The emerging role of trace amine-associated receptor 1 in the functional regulation of monoamine transporters and dopaminergic activity. *Journal of neurochemistry,* 116**,** 164-176.

MOREFIELD, K. M., KEANE, M., FELGATE, P., WHITE, J. M. & IRVINE, R. J. 2011. Pill content, dose and resulting plasma concentrations of 3, 4-methylendioxymethamphetamine (MDMA) in recreational 'ecstasy'users. *Addiction,* 106**,** 1293-1300.

MORISHIMA, M. & GALE, C. 1972. Relationship of blood pressure and heart rate to body temperature in baboons. *American Journal of Physiology-Legacy Content,* 223**,** 387-395.

MUNZAR, P., LI, H., NICHOLSON, K. L., WILEY, J. L. & BALSTER, R. L. 2002. Enhancement of the discriminative stimulus effects of phencyclidine by the tetracycline antibiotics doxycycline and minocycline in rats. *Psychopharmacology,* 160**,** 331-336.

MURPHY, J. E., FLYNN, J. J., CANNON, D. M., GUIRY, P. J., MCCORMACK, P., BAIRD, A. W., MCBEAN, G. J. & KEENAN, A. K. 2002. In vitro neuronal and vascular responses to 5-hydroxytryptamine: modulation by 4-methylthioamphetamine, 4-methylthiomethamphetamine and 3, 4-methylenedioxymethamphetamine. *European journal of pharmacology,* 444**,** 61-67.

NADJAR, A., TRIDON, V., MAY, M. J., GHOSH, S., DANTZER, R., AMÉDÉE, T. & PARNET, P. 2005. NFκB activates in vivo the synthesis of inducible Cox-2 in the brain. *Journal of Cerebral Blood Flow & Metabolism,* 25**,** 1047-1059.

NASH, J. F., MELTZER, H. & GUDELSKY, G. A. 1988. Elevation of serum prolactin and corticosterone concentrations in the rat after the administration of 3, 4-methylenedioxymethamphetamine. *Journal of pharmacology and experimental therapeutics,* 245**,** 873-879.

NISHISAWA, S., MZENGEZA, S. & DIKSIC, M. 1999. Acute effects of 3, 4-methylenedioxymethamphetamine on brain serotonin synthesis in the dog studied by positron emission tomography. *Neurochemistry international,* 34**,** 33-40.

NYBO, L., SECHER, N. H. & NIELSEN, B. 2002. Inadequate heat release from the human brain during prolonged exercise with hyperthermia. *The Journal of physiology,* 545**,** 697-704.

O'CAIN, P. A., HLETKO, S. B., OGDEN, B. A. & VARNER, K. J. 2000. Cardiovascular and sympathetic responses and reflex changes elicited by MDMA. *Physiology & behavior,* 70**,** 141-148.

O'HARA, J. A., HOU, H., DEMIDENKO, E., SPRINGETT, R. J., KHAN, N. & SWARTZ, H. M. 2005. Simultaneous measurement of rat brain cortex PtO2 using EPR oximetry and a fluorescence fiber-optic sensor during normoxia and hyperoxia. *Physiological measurement,* 26**,** 203.

O'HEARN, E., BATTAGLIA, G., DE SOUZA, E., KUHAR, M. & MOLLIVER, M. 1988. Methylenedioxyamphetamine (MDA) and methylenedioxymethamphetamine (MDMA) cause selective ablation of serotonergic axon terminals in forebrain: immunocytochemical evidence for neurotoxicity. *Journal of Neuroscience,* 8**,** 2788-2803.

O'SHEA, E., ESCOBEDO, I., ORIO, L., SANCHEZ, V., NAVARRO, M., GREEN, A. R. & COLADO, M. I. 2005. Elevation of Ambient Room Temperature has Differential Effects on MDMA-Induced 5-HT and Dopamine Release in Striatum and Nucleus Accumbens of Rats. *Neuropsychopharmacology,* 30**,** 1312-1323.

O'SHEA, E., SANCHEZ, V., ORIO, L., ESCOBEDO, I., GREEN, A. R. & COLADO, M. I. 2005. 3,4-Methylenedioxymethamphetamine increases pro-interleukin-1β production and caspase-1 protease activity in frontal cortex, but not in hypothalamus, of Dark Agouti rats: Role of interleukin-1β in neurotoxicity. *Neuroscience,* 135**,** 1095-1105.

OOTSUKA, Y. & BLESSING, W. W. 2003. 5-Hydroxytryptamine 1A receptors inhibit cold-induced sympathetically mediated cutaneous vasoconstriction in rabbits. *The Journal of physiology,* 552**,** 303-314.

ORIO, L., LLOPIS, N., TORRES, E., IZCO, M., O'SHEA, E. & COLADO, M. I. 2010. A study on the mechanisms by which minocycline protects against MDMA ('ecstasy')-induced neurotoxicity of 5-HT cortical neurons. *Neurotox Res,* 18**,** 187-99.

ORIO, L., O'SHEA, E., SANCHEZ, V., PRADILLO, J. M., ESCOBEDO, I., CAMARERO, J., MORO, M. A., GREEN, A. R. & COLADO, M. I. 2004. 3, 4-Methylenedioxymethamphetamine increases interleukin-1β levels and activates microglia in rat brain: studies on the relationship with acute hyperthermia and 5-HT depletion. *Journal of neurochemistry,* 89**,** 1445-1453.

PARROTT, A. 2004. Is ecstasy MDMA? A review of the proportion of ecstasy tablets containing MDMA, their dosage levels, and the changing perceptions of purity. *Psychopharmacology,* 173**,** 234-241.

PARROTT, A. C. 2001. Human psychopharmacology of Ecstasy (MDMA): a review of 15 years of empirical research. *Human Psychopharmacology: Clinical and Experimental,* 16**,** 557-577.

PARROTT, A. C. & LASKY, J. 1998. Ecstasy (MDMA) effects upon mood and cognition: before, during and after a Saturday night dance. *Psychopharmacology,* 139**,** 261-268.

PARTILLA, J. S., DEMPSEY, A. G., NAGPAL, A. S., BLOUGH, B. E., BAUMANN, M. H. & ROTHMAN, R. B. 2006. Interaction of amphetamines and related compounds at the vesicular monoamine transporter. *Journal of Pharmacology and Experimental Therapeutics,* 319**,** 237-246.

PEDERSEN, N. & BLESSING, W. 2001. Cutaneous vasoconstriction contributes to hyperthermia induced by 3, 4-methylenedioxymethamphetamine (ecstasy) in conscious rabbits. *Journal of Neuroscience,* 21**,** 8648-8654.

PETERSON, J. I., FITZGERALD, R. V. & BUCKHOLD, D. K. 1984. Fiber-optic probe for in vivo measurement of oxygen partial pressure. *Analytical chemistry,* 56**,** 62-67.

POEGGEL, S., TOSI, D., DURAIBABU, D., LEEN, G., MCGRATH, D. & LEWIS, E. 2015. Optical fibre pressure sensors in medical applications. *Sensors,* 15**,** 17115-17148.
POOLE, S. & STEPHENSON, J. 1977. Core temperature: some shortcomings of rectal temperature measurements. *Physiology & behavior,* 18**,** 203-205.

PORCEDDU, P. F., ISHOLA, I. O., CONTU, L. & MORELLI, M. 2016. Metformin prevented dopaminergic neurotoxicity induced by 3, 4-methylenedioxymethamphetamine administration. *Neurotoxicity research,* 30**,** 101-109.

POWELL, J. A. 1974. A simple two-fiber optical displacement sensor. *Review of Scientific Instruments,* 45**,** 302-303.

QUATE, L., MCBEAN, D. E., RITCHIE, I. M., OLVERMAN, H. J. & KELLY, P. A. 2004. Acute methylenedioxymethamphetamine administration: effects on local cerebral blood flow and glucose utilisation in the Dark Agouti rat. *Psychopharmacology,* 173**,** 287-295.

QUEDNOW, B. B., JESSEN, F., KÜHN, K.-U., MAIER, W., DAUM, I. & WAGNER, M. 2006. Memory deficits in abstinent MDMA (ecstasy) users: neuropsychological evidence of frontal dysfunction. *Journal of Psychopharmacology,* 20**,** 373-384.

QUEDNOW, B. B., KÜHN, K.-U., HOPPE, C., WESTHEIDE, J., MAIER, W., DAUM, I. & WAGNER, M. 2007. Elevated impulsivity and impaired decision-making cognition in heavy users of MDMA ("Ecstasy"). *Psychopharmacology,* 189**,** 517-530.

RAI, V. K. 2007. Temperature sensors and optical sensors. *Applied Physics B,* 88**,** 297-303.
RAI, V. K. & RAI, A. 2007. Temperature sensing behavior of Eu 3+ doped tellurite and calibo glasses. *Applied Physics B,* 86**,** 333-335.

RAI, V. K., RAI, D. & RAI, S. 2006. Pr3+ doped lithium tellurite glass as a temperature sensor. *Sensors and Actuators A: Physical,* 128**,** 14-17.

RAJAMANI, K., LEONG, S., LAVELLE, A. & DOCHERTY, J. R. 2001. Prejunctional actions of methylenedioxymethamphetamine in vas deferens from wild-type and α2A/D-adrenoceptor knockout mice. *European journal of pharmacology,* 423**,** 223-228.

RAO, Y.-J. 1997. In-fibre Bragg grating sensors. *Measurement science and technology,* 8**,** 355.

RENEMAN, L., BOOIJ, J., HABRAKEN, J., DE BRUIN, K., HATZIDIMITRIOU, G., DEN HEETEN, G. J. & RICAURTE, G. A. 2002a. Validity of [123I] β-CIT SPECT in detecting MDMA-induced serotonergic neurotoxicity. *Synapse,* 46**,** 199-205.

RENEMAN, L., BOOIJ, J., LAVALAYE, J., DE BRUIN, K., REITSMA, J. B., GUNNING, B. W., DEN HEETEN, G. J. & VAN DEN BRINK, W. 2002b. Use of amphetamine by recreational users of ecstasy (MDMA) is associated with reduced striatal dopamine transporter densities: a [123 I] β-CIT SPECT study–preliminary report. *Psychopharmacology,* 159**,** 335-340.

RICHIE, J. 1973. Energetic aspects of nerve conduction: the relationships between heat production, electrical activity and metabolism. *Progress in biophysics and molecular biology,* 26**,** 147-187.

RIDGE, E. A., PACHHAIN, S., CHOUDHURY, S. R., BODNAR, S. R., LARSEN, R. A., PHUNTUMART, V. & SPRAGUE, J. E. 2019. The influence of the host microbiome on 3, 4-methylenedioxymethamphetamine (MDMA)-induced hyperthermia and vice versa. *Scientific reports,* 9**,** 4313.

RIVENS, I., SHAW, A., CIVALE, J. & MORRIS, H. 2007. Treatment monitoring and thermometry for therapeutic focused ultrasound. *International journal of hyperthermia,* 23**,** 121-139.

ROBINSON, T. E. & BECKER, J. B. 1986. Enduring changes in brain and behavior produced by chronic amphetamine administration: a review and evaluation of animal models of amphetamine psychosis. *Brain research reviews,* 11**,** 157-198.

RODSIRI, R., SPICER, C., GREEN, A. R., MARSDEN, C. A. & FONE, K. C. 2011. Acute concomitant effects of MDMA binge dosing on extracellular 5-HT, locomotion and body temperature and the long-term effect on novel object discrimination in rats. *Psychopharmacology,* 213**,** 365-376.

ROMERO-PEREZ, D., FRICOVSKY, E., YAMASAKI, K. G., GRIFFIN, M., BARRAZA-HIDALGO, M., DILLMANN, W. & VILLARREAL, F. 2008. Cardiac uptake of minocycline and mechanisms for in vivo cardioprotection. *Journal of the American College of Cardiology,* 52**,** 1086-1094.

ROSSI, S., ZANIER, E. R., MAURI, I., COLUMBO, A. & STOCCHETTI, N. 2001. Brain temperature, body core temperature, and intracranial pressure in acute cerebral damage. *Journal of Neurology, Neurosurgery & Psychiatry,* 71**,** 448-454.

ROTHMAN, R. B., BAUMANN, M. H., DERSCH, C. M., ROMERO, D. V., RICE, K. C., CARROLL, F. I. & PARTILLA, J. S. 2001. Amphetamine-type central nervous system stimulants release norepinephrine more potently than they release dopamine and serotonin. *Synapse,* 39**,** 32-41.

RUBENSON, D., GRIFFIN, J. C., ANDREW, F., CLAUDE, J., REITZ, B., KNUTTI, J., BILLINGHAM, M. & HARRISON, D. C. 1984. Telemetry of electrophysiologic variables from conscious dogs: system design, validation, and serial studies. *American heart journal,* 107**,** 90-96.

RUSYNIAK, D. E. & SPRAGUE, J. E. 2005. Toxin-induced hyperthermic syndromes. *Medical Clinics,* 89**,** 1277-1296.

RUSYNIAK, M. D. DANIEL E., BANKS, P. D. MATTHEW L., MILLS, P. D. EDWARD M. & SPRAGUE, P. D. JON E. 2004. Dantrolene Use in 3,4-Methylenedioxymethamphetamine ("Ecstasy")–Mediated Hyperthermia. *Anesthesiology,* 101**,** 263-263.

SACCOMANDI, P., SCHENA, E. & SILVESTRI, S. 2013. Techniques for temperature monitoring during laser-induced thermotherapy: an overview. *International Journal of Hyperthermia,* 29**,** 609-619.

SALAMEH, A., HALLING, M., SEIDEL, T. & DHEIN, S. 2015. Effects of minocycline on parameters of cardiovascular recovery after cardioplegic arrest in a rabbit Langendorff heart model. *Clinical and Experimental Pharmacology and Physiology,* 42**,** 1258-1265.

SAMSET, E., MALA, T., EDWIN, B., GLADHAUG, I., SØREIDE, O. & FOSSE, E. 2001. Validation of estimated 3D temperature maps during hepatic cryo surgery. *Magnetic resonance imaging,* 19**,** 715-721.

SCHARTNER, E. & MONRO, T. 2014. Fibre Tip Sensors for Localised Temperature Sensing Based on Rare Earth-Doped Glass Coatings. *Sensors,* 14**,** 21693.

SCHARTNER, E. P., HENDERSON, M. R., PURDEY, M., MONRO, T. M., GILL, P. & CALLEN, D. F. A portable optical fiber pH probe for cancer margin detection. 2016 IEEE Photonics Conference (IPC), 2016. IEEE, 1-2.

SCHENA, E., TOSI, D., SACCOMANDI, P., LEWIS, E. & KIM, T. 2016. Fiber optic sensors for temperature monitoring during thermal treatments: an overview. *Sensors,* 16**,** 1144.

SCHINDLER, C. 1996. Cocaine and cardiovascular toxicity. *Addiction biology,* 1**,** 31-47.

SCHINDLER, C. W., THORNDIKE, E. B., BLOUGH, B. E., TELLA, S. R., GOLDBERG, S. R. & BAUMANN, M. H. 2014. Effects of 3, 4-methylenedioxymethamphetamine (MDMA) and its main metabolites on cardiovascular function in conscious rats. *British journal of pharmacology,* 171**,** 83-91.

SCHMID, C. J. & KEHNE, J. H. 1990. Neurotoxicity of MDMA: neurochemical effects. *Annals of the New York Academy of Sciences,* 600**,** 665-680.

SCHMIDT, C. J., ABBATE, G. M., BLACK, C. K. & TAYLOR, V. L. 1990. Selective 5-hydroxytryptamine2 receptor antagonists protect against the neurotoxicity of methylenedioxymethamphetamine in rats. *Journal of Pharmacology and Experimental Therapeutics,* 255**,** 478-483.

SCHMIDT, C. J., WU, L. & LOVENBERG, W. 1986. Methylenedioxymethamphetamine: a potentially neurotoxic amphetamine analogue. *European journal of pharmacology,* 124**,** 175-178.

SELKER, J. S., THÉVENAZ, L., HUWALD, H., MALLET, A., LUXEMBURG, W., VAN DE GIESEN, N., STEJSKAL, M., ZEMAN, J., WESTHOFF, M. & PARLANGE, M. B. 2006. Distributed fiber-optic temperature sensing for hydrologic systems. *Water Resources Research,* 42.

SESSLER, D. I. 1997. Mild perioperative hypothermia. *New England Journal of Medicine,* 336**,** 1730-1737.

SHANKARAN, M. & GUDELSKY, G. A. 1999. A neurotoxic regimen of MDMA suppresses behavioral, thermal and neurochemical responses to subsequent MDMA administration. *Psychopharmacology,* 147**,** 66-72.

SHEEM, S. & GIALLORENZI, T. 1979. Polarization effects on single-mode optical fiber sensors. *Applied Physics Letters,* 35**,** 914-917.

SILVA BASTOS, L. F., PINHEIRO DE OLIVEIRA, A. C., MAGNUS SCHLACHETZKI, J. C. & FIEBICH, B. L. 2011. Minocycline reduces prostaglandin E synthase expression and 8-isoprostane formation in LPS-activated primary rat microglia. *Immunopharmacology and immunotoxicology,* 33**,** 576-580.

SIMON, H. B. 1993. Hyperthermia. *New England Journal of Medicine,* 329**,** 483-487.

SINGH, S. & GUPTA, B. D. 2013. Fabrication and characterization of a surface plasmon resonance based fiber optic sensor using gel entrapment technique for the detection of low glucose concentration. *Sensors and Actuators B: Chemical,* 177**,** 589-595.

SOFUOGLU, M., MOONEY, M., KOSTEN, T., WATERS, A. & HASHIMOTO, K. 2011. Minocycline attenuates subjective rewarding effects of dextroamphetamine in humans. *Psychopharmacology,* 213**,** 61-68.

SOFUOGLU, M., POLING, J., HILL, K. & KOSTEN, T. 2009. Atomoxetine attenuates dextroamphetamine effects in humans. *The American journal of drug and alcohol abuse,* 35**,** 412-416.

SONG, B.-J., MOON, K.-H., V UPRETI, V., D EDDINGTON, N. & J LEE, I. 2010. Mechanisms of MDMA (ecstasy)-induced oxidative stress, mitochondrial dysfunction, and organ damage. *Current pharmaceutical biotechnology,* 11**,** 434-443.

SOUKUP, J., ZAUNER, A., DOPPENBERG, E. M., MENZEL, M., GILMAN, C., YOUNG, H. F. & BULLOCK, R. 2002. The importance of brain temperature in patients after severe head injury: relationship to intracranial pressure, cerebral perfusion pressure, cerebral blood flow, and outcome. *Journal of neurotrauma,* 19**,** 559-571.

SPANOS, L. J. & YAMAMOTO, B. K. 1989. Acute and subchronic effects of methylenedioxymethamphetamine [(±) MDMA] on locomotion and serotonin syndrome behavior in the rat. *Pharmacology Biochemistry and Behavior,* 32**,** 835-840.

STANLEY, N., SALEM, A. & IRVINE, R. J. 2007. The effects of co-administration of 3,4-methylenedioxymethamphetamine ("ecstasy") or para-methoxyamphetamine and moclobemide at elevated ambient temperatures on striatal 5-HT, body temperature and behavior in rats. *Neuroscience,* 146**,** 321-9.

STIRLING, D. P., KHODARAHMI, K., LIU, J., MCPHAIL, L. T., MCBRIDE, C. B., STEEVES, J. D., RAMER, M. S. & TETZLAFF, W. 2004. Minocycline treatment reduces delayed oligodendrocyte death, attenuates axonal dieback, and improves functional outcome after spinal cord injury. *Journal of Neuroscience,* 24**,** 2182-2190.

STONE, D. M., JOHNSON, M., HANSON, G. R. & GIBB, J. W. 1988. Role of endogenous dopamine in the central serotonergic deficits induced by 3, 4-methylenedioxymethamphetamine. *Journal of Pharmacology and Experimental Therapeutics,* 247**,** 79-87.

STONE, D. M., STAHL, D. C., HANSON, G. R. & GIBB, J. W. 1986. The effects of 3, 4-methylenedioxymethamphetamine (MDMA) and 3, 4-methylenedioxyamphetamine (MDA) on monoaminergic systems in the rat brain. *European journal of pharmacology,* 128**,** 41-48.

STONER, H. 1971. Effect of injury on shivering thermogenesis in the rat. *The Journal of physiology,* 214**,** 599-615.

STROTE, J., LEE, J. E. & WECHSLER, H. 2002. Increasing MDMA use among college students: results of a national survey. *Journal of adolescent health,* 30**,** 64-72.

STUERENBURG, H., PETERSEN, K., BÄUMER, T., ROSENKRANZ, M., BUHMANN, C. & THOMASIUS, R. 2002. Plasma concentrations of 5-HT, 5-HIAA, norepinephrine, epinephrine and dopamine in ecstasy users. *Neuro endocrinology letters,* 23**,** 259-261.

SU, H., IORDACHITA, I. I., TOKUDA, J., HATA, N., LIU, X., SEIFABADI, R., XU, S., WOOD, B. & FISCHER, G. S. 2017. Fiber-optic force sensors for MRI-guided interventions and rehabilitation: a review. *IEEE sensors journal,* 17**,** 1952-1963.

SUN-EDELSTEIN, C., TEPPER, S. J. & SHAPIRO, R. E. 2008. Drug-induced serotonin syndrome: a review. *Expert opinion on drug safety,* 7**,** 587-596.

TAO, R., SHOKRY, I. M., CALLANAN, J. J., ADAMS, H. D. & MA, Z. 2015. Mechanisms and environmental factors that underlying the intensification of 3, 4-methylenedioxymethamphetamine (MDMA, Ecstasy)-induced serotonin syndrome in rats. *Psychopharmacology,* 232**,** 1245-1260.

TAYLOR, E. W. & CARDIMONA, D. A. 2008. *Nanophotonics and Macrophotonics for Space Environments VII.*

TEUNISSEN, L., DE HAAN, A., DE KONING, J., CLAIRBOIS, H. & DAANEN, H. 2011. Limitations of temperature measurement in the aural canal with an ear mould integrated sensor. *Physiological measurement,* 32**,** 1403.

THORNBERRY, N. A., BULL, H. G., CALAYCAY, J. R., CHAPMAN, K. T., HOWARD, A. D., KOSTURA, M. J., MILLER, D. K., MOLINEAUX, S. M., WEIDNER, J. R. & AUNINS, J. 1992. A novel heterodimeric cysteine protease is required for interleukin-1βprocessing in monocytes. *Nature,* 356**,** 768.

TIKKA, T. M. & KOISTINAHO, J. E. 2001. Minocycline provides neuroprotection against N-methyl-D-aspartate neurotoxicity by inhibiting microglia. *The Journal of Immunology,* 166**,** 7527-7533.

TORRES, E., GUTIERREZ-LOPEZ, M. D., BORCEL, E., PERAILE, I., MAYADO, A., O'SHEA, E. & COLADO, M. I. 2010. Evidence that MDMA ('ecstasy') increases cannabinoid CB2 receptor expression in microglial cells: role in the neuroinflammatory response in rat brain. *Journal of neurochemistry,* 113**,** 67-78.

TOSI, D., POEGGEL, S., IORDACHITA, I. & SCHENA, E. 2018. Fiber optic sensors for biomedical applications. *Opto-Mechanical Fiber Optic Sensors.* Elsevier.
TOSI, D., SACCOMANDI, P., SCHENA, E., DURAIBABU, D., POEGGEL, S., LEEN, G. & LEWIS, E. 2016. Intra-tissue pressure measurement in ex vivo liver undergoing laser ablation with fiber-optic Fabry-Perot probe. *Sensors,* 16**,** 544.

TRINGALI, G., MANCUSO, C., MIRTELLA, A., POZZOLI, G., PARENTE, L., PREZIOSI, P. & NAVARRA, P. 1996. Evidence for the neuronal origin of immunoreactive interleukin-1β released by rat hypothalamic explants. *Neuroscience letters,* 219**,** 143-146.

TRINGALI, G., MIRTELLA, A., MANCUSO, C., GUERRIERO, G., PREZIOSI, P. & NAVARRA, P. 1997. THE RELEASE OF IMMUNOREACTIVE INTERLEUKIN-1B FROM RAT HYPOTHALAMIC EXPLANTS IS MODULATED BY NEUROTRANSMITTERS AND CORTICOTROPIN-RELEASING HORMONE. *Pharmacological research,* 36**,** 269-273.

UFNAL, M., ŻERA, T. & SZCZEPAŃSKA-SADOWSKA, E. 2005. Blockade of angiotensin II AT1 receptors inhibits pressor action of centrally administered interleukin-1β in Sprague Dawley rats. *Neuropeptides,* 39**,** 581-585.

UNITED NATIONS 2018. World Drug Report 2018. New York: United Nations Office on Drugs and Crime.

VAN DEN BUUSE, M. 1994. Circadian rhythms of blood pressure, heart rate, and locomotor activity in spontaneously hypertensive rats as measured with radio-telemetry. *Physiology & Behavior,* 55**,** 783-787.

VANDEPUTTE, C. & DOCHERTY, J. R. 2002. Vascular actions of 3, 4-methylenedioxymethamphetamine in α2A/D-adrenoceptor knockout mice. *European journal of pharmacology,* 457**,** 45-49.

VERRICO, C. D., LYNCH, L., FAHEY, M. A., FRYER, A.-K., MILLER, G. M. & MADRAS, B. K. 2008. MDMA-induced impairment in primates: antagonism by a selective norepinephrine or serotonin, but not by a dopamine/norepinephrine transport inhibitor. *Journal of psychopharmacology,* 22**,** 187-202.

VINCENT, C. J., LI, Y. & BLANDFORD, A. 2014. Integration of human factors and ergonomics during medical device design and development: It's all about communication. *Applied ergonomics,* 45**,** 413-419.

WADE, S., MUSCAT, J., COLLINS, S. & BAXTER, G. 1999. Nd3+-doped optical fiber temperature sensor using the fluorescence intensity ratio technique. *Review of scientific instruments,* 70**,** 4279-4282.

WADE, S. A., COLLINS, S. F. & BAXTER, G. W. 2003. Fluorescence intensity ratio technique for optical fiber point temperature sensing. *Journal of Applied physics,* 94**,** 4743-4756.

WANG, T., YASUKOCHI, W., KORPOSH, S., JAMES, S. W., TATAM, R. P. & LEE, S.-W. 2016. A long period grating optical fiber sensor with nano-assembled porphyrin layers for detecting ammonia gas. *Sensors and Actuators B: Chemical,* 228**,** 573-580.

WANG, X., BAUMANN, M. H., XU, H. & ROTHMAN, R. B. 2004. 3, 4-methylenedioxymethamphetamine (MDMA) administration to rats decreases brain tissue serotonin but not serotonin transporter protein and glial fibrillary acidic protein. *Synapse,* 53**,** 240-248.

WANG, X., ZHU, S., DROZDA, M., ZHANG, W., STAVROVSKAYA, I. G., CATTANEO, E., FERRANTE, R. J., KRISTAL, B. S. & FRIEDLANDER, R. M. 2003. Minocycline inhibits caspase-independent and-dependent mitochondrial cell death pathways in models of Huntington's disease. *Proceedings of the National Academy of Sciences,* 100**,** 10483-10487.

WEBB, D. J., HATHAWAY, M., JACKSON, D. A., JONES, S., ZHANG, L. & BENNION, I. 2000. First in-vivo trials of a fiber Bragg grating based temperature profiling system. *Journal of biomedical optics,* 5**,** 45-51.

WILLIAMSON, S., GOSSOP, M., POWIS, B., GRIFFITHS, P., FOUNTAIN, J. & STRANG, J. 1997. Adverse effects of stimulant drugs in a community sample of drug users. *Drug and alcohol dependence,* 44**,** 87-94.

WOLFF, K., TSAPAKIS, E., WINSTOCK, A., HARTLEY, D., HOLT, D., FORSLING, M. & AITCHISON, K. J. 2006. Vasopressin and oxytocin secretion in response to the consumption of ecstasy in a clubbing population. *Journal of Psychopharmacology,* 20**,** 400-410.

YAMAMOTO, B. K. & SPANOS, L. J. 1988. The acute effects of methylenedioxymethamphetamine on dopamine release in the awake-behaving rat. *Eur J Pharmacol,* 148**,** 195-203.

YIN, S. & RUFFIN, P. 2006. Fiber optic sensors. *Wiley Encyclopedia of Biomedical Engineering*.

YONG, V. W., WELLS, J., GIULIANI, F., CASHA, S., POWER, C. & METZ, L. M. 2004. The promise of minocycline in neurology. *The Lancet Neurology,* 3**,** 744-751.

YOO, W.-J., JANG, K.-W., SEO, J.-K., HEO, J.-Y., MOON, J.-S., PARK, J.-Y. & LEE, B.-S. 2010. Development of respiration sensors using plastic optical fiber for respiratory monitoring inside MRI system. *Journal of the Optical Society of Korea,* 14**,** 235-239.

YRJÄNHEIKKI, J., KEINÄNEN, R., PELLIKKA, M., HÖKFELT, T. & KOISTINAHO, J. 1998. Tetracyclines inhibit microglial activation and are neuroprotective in global brain ischemia. *Proceedings of the National Academy of Sciences,* 95**,** 15769-15774.

YU, L., WU, Y., DUNN, J. F. & MURARI, K. 2016. In-vivo monitoring of tissue oxygen saturation in deep brain structures using a single fiber optical system. *Biomedical Optics Express,* 7**,** 4685-4694.

YUAN, J., CALLAHAN, B. T., MCCANN, U. D. & RICAURTE, G. A. 2001. Evidence against an essential role of endogenous brain dopamine in methamphetamine-induced dopaminergic neurotoxicity. *Journal of neurochemistry,* 77**,** 1338-1347.

YUAN, J., CORD, B. J., MCCANN, U. D., CALLAHAN, B. T. & RICAURTE, G. A. 2002. Effect of depleting vesicular and cytoplasmic dopamine on methylenedioxymethamphetamine neurotoxicity. *Journal of neurochemistry,* 80**,** 960-969.

ZHANG, K., ARMAN, A., ANWER, A. G., HUTCHINSON, M. R. & GOLDYS, E. M. 2019. An optical fiber based immunosensor for localized detection of IL-1β in rat spinal cord. *Sensors and Actuators B: Chemical,* 282**,** 122-129.

ZHANG, L., KITAICHI, K., FUJIMOTO, Y., NAKAYAMA, H., SHIMIZU, E., IYO, M. & HASHIMOTO, K. 2006. Protective effects of minocycline on behavioral changes and neurotoxicity in mice after administration of methamphetamine. *Progress in Neuro-Psychopharmacology and Biological Psychiatry,* 30**,** 1381-1393.

ZHANG, L., SHIRAYAMA, Y., IYO, M. & HASHIMOTO, K. 2007. Minocycline attenuates hyperlocomotion and prepulse inhibition deficits in mice after administration of the NMDA receptor antagonist dizocilpine. *Neuropsychopharmacology,* 32**,** 2004.

Appendix 1

Li, J., Schartner, E., **Musolino, S.,** Quirk, B.C., Kirk, R.W., Ebendorff-Heidepriem, H. and McLaughlin, R.A., 2018. Miniaturized single-fiber-based needle probe for combined imaging and sensing in deep tissue. *Optics letters*, *43*(8), pp.1682-1685.

Statement of Authorship

Title of Paper	Miniaturized single-fiber-based needle probe for combined imaging and sensing in deep tissue.
Publication Status	☑ Published ☐ Accepted for Publication ☐ Submitted for Publication ☐ Unpublished and Unsubmitted work written in manuscript style
Publication Details	Optics letters, 43(8), pp.1682-1685. https://doi.org/10.1364/OL.43.0016825

Principal Author

Name of Principal Author (Candidate)	Stefan T Musolino		
Contribution to the Paper	Assisted with experimental procedures and functionalisation of probe tip.		
Overall percentage (%)	5%		
Certification:	This paper reports on original research I conducted during the period of my Higher Degree by Research candidature and is not subject to any obligations or contractual agreements with a third party that would constrain its inclusion in this thesis. I am the primary author of this paper.		
Signature		Date	22/08/2019

Co-Author Contributions

By signing the Statement of Authorship, each author certifies that:

i. the candidate's stated contribution to the publication is accurate (as detailed above);

ii. permission is granted for the candidate in include the publication in the thesis; and

iii. the sum of all co-author contributions is equal to 100% less the candidate's stated contribution.

Name of Co-Author	Jiawen Li		
Contribution to the Paper	Primary contributor to study design, imaging measurments, experimental trials, statistical analysis, and preparation of manuscript.		
Signature		Date	22/08/2019

Name of Co-Author	Erik P Schartner		
Contribution to the Paper	Assisted with study design, coating trials, experimental trials, statistical analysis, softwarre interfacing and critical review of manuscript.		
Signature		Date	22/08/2019

Please cut and paste additional co-author panels here as required.

Name of Co-Author	Bryden C Quirk		
Contribution to the Paper	Assisted with imaging probe assembly methods.		
Signature		Date	22/08/2019

Name of Co-Author	Rodney W Kirk		
Contribution to the Paper	Assisted with data processing of images and software interfacing.		
Signature		Date	22/08/2019

Name of Co-Author	Heike Ebendorff-Heidepriem		
Contribution to the Paper	Provided advice concerning methods and probe coating requirments, and assisted with critical review of manuscript.		
Signature		Date	22/08/2019

Name of Co-Author	Robert A McLaughlin		
Contribution to the Paper	Provided advice on imaging experiments and assisted with critical review of manuscript.		
Signature		Date	22/08/2019

1682 Vol. 43, No. 8 / 15 April 2018 / Optics Letters Letter

Optics Letters

Miniaturized single-fiber-based needle probe for combined imaging and sensing in deep tissue

Jiawen Li,[1,2,3,*] Erik Schartner,[1,2,4] Stefan Musolino,[1,2,3] Bryden C. Quirk,[1,2,3] Rodney W. Kirk,[1,2,3] Heike Ebendorff-Heidepriem,[1,2,4] and Robert A. McLaughlin[1,2,3]

[1]Australian Research Council Centre of Excellence for Nanoscale BioPhotonics, University of Adelaide, Adelaide, SA, Australia
[2]Institute for Photonics and Advanced Sensing, University of Adelaide, Adelaide, SA, Australia
[3]Adelaide Medical School, The University of Adelaide, Adelaide, SA, Australia
[4]School of Physical Sciences, The University of Adelaide, Adelaide, SA, Australia
*Corresponding author: jiawen.li01@adelaide.edu.au

Received 23 February 2018; accepted 8 March 2018; posted 12 March 2018 (Doc. ID 323306); published 6 April 2018

The ability to visualize structure while simultaneously measuring chemical or physical properties of a biological tissue has the potential to improve our understanding of complex biological processes. We report the first miniaturized single-fiber-based imaging + sensing probe capable of simultaneous optical coherence tomography (OCT) imaging and temperature sensing. An OCT lens is fabricated at the distal end of a double-clad fiber, including a thin layer of rare-earth-doped tellurite glass to enable temperature measurements. The high refractive index of the tellurite glass enables a common-path interferometer configuration for OCT, allowing easy exchange of probes for biomedical applications. The simultaneous imaging + sensing capability is demonstrated on rat brains.

OCIS codes: (170.0170) Medical optics and biotechnology; (060.2370) Fiber optics sensors; (060.2350) Fiber optics imaging; (170.4500) Optical coherence tomography; (280.4788) Optical sensing and sensors.

https://doi.org/10.1364/OL.43.001682

Miniaturized fiber-optic imaging probes, such as those based on optical coherence tomography (OCT), enable us to image deep inside the body with micrometer-scale resolution and have demonstrated utility in a wide range of biomedical applications [1,2]. However, these OCT fiber imaging probes are limited to acquiring structural information and lack the capability to sense functional information that would be desirable for advancing the fundamental understanding of complex biological processes [3–5]. In parallel, a wide range of optical sensing techniques have been developed in nonimaging applications, providing insight into physiologically important parameters such as temperature [4], pH [5], metal ions [3], hydrogen peroxide [6] or other small molecules [7]. However, current fiber sensing approaches do not provide information about the local tissue structure, rendering them subject to measurement artifacts because of structural heterogeneity or misplacement of the fiber sensing probe. For example, previous work has demonstrated a portable configuration of a fiber-optic sensing probe to monitor local temperature changes in rat brains [4], with the probe inserted into an anatomical region of interest (ROI) relative to a standardized rat brain atlas. This semiblind procedure is done without intraoperative imaging guidance and is subject to intersubject variations due to anatomical differences between animals [8]. In this paper, we propose a novel multimodal imaging + sensing fiber-optic probe that provides additional insight over imaging alone and mitigates many potential measurement artifacts present in unguided sensing.

Earlier work has demonstrated integrated OCT + fluorescence fiber-optic probes [9–12]. Cell-specific or disease-specific fluorophores are introduced for specific labeling of tissue, providing molecular contrast. We build upon this work but utilize the fluorescence signal for fluorescence-based fiber sensing by incorporating a functionalized fluorescent coating on the distal tip of the fiber [13,14]. These sensing approaches can be utilized to detect the presence of specific molecules [6,7], as well as a wide range of physiological parameters, such as temperature and ion concentration [3–5].

In a previous example of imaging + sensing, Michael *et al.* [14] made a fiber-bundle-based imaging probe comprising several thousand fiber cores and coated with a pH-sensitive film. The device enabled reflectance microscopy imaging and sensing for acid release during fertilization of eggs. The technique demonstrated the potential of such a combined approach but lacked the depth differentiation of tissue that is possible by utilizing an OCT probe as the imaging component.

Here we have developed, for the first time, a single-fiber-based imaging + sensing probe that can provide colocalized OCT tissue visualization and measurement of temperature in deep tissue. We describe the design and fabrication of the imaging + sensing probe and demonstrate its performance on *ex vivo* rat brain samples.

The fabrication of the sensing and imaging elements used here has been previously explored as two distinct probes [15,16], with these being combined here into a single,

0146-9592/18/081682-04 Journal © 2018 Optical Society of America

multifunctional probe. As shown in Fig. 1(a), the probe consists of a 35 cm length of double-clad fiber (DCF, with a 125 μm cladding diameter, DCF13, Thorlabs Inc., USA), terminated with a microlens to focus the OCT light beam that is transmitted through the core of the DCF. The microlens is constructed by splicing 190 μm of no-core fiber (NCF, 125 μm cladding diameter, POFC, Taiwan) to the distal end of the DCF, to expand the OCT light beam from the core. This was then dipped in a rare-earth-doped tellurite glass melt to form a curved, focusing element terminating the fiber, as shown in Fig. 1(b). Using microscopic images of the distal tip of the fiber, we manually measured the radius of the focusing element of four probes to be 78 ± 1 μm. To fabricate reproducible optics, we found it important to control for temperature of the glass melt (815°C) and time between removing the glass melt from the oven and performing the dip-coating (5 s) [17]. The output beam from the probe, shown in Fig. 1(c), has a working distance of 335 μm in water (146 μm in air due to the larger refractive index difference between air and tellurite). The simulation result was obtained by setting the radius of curvature for the tellurite portion of the probe as

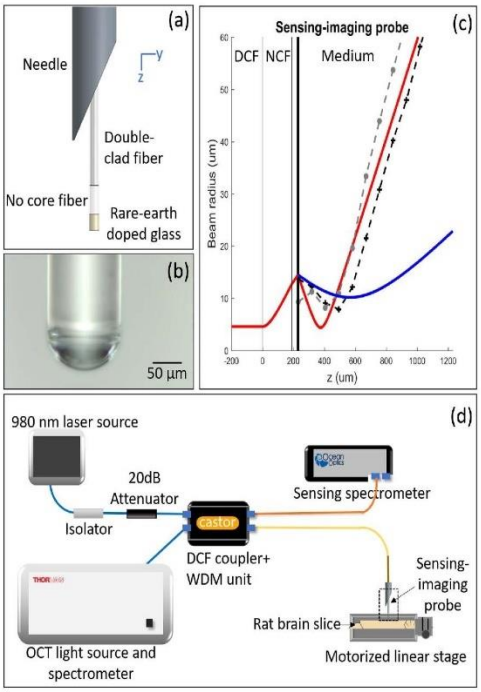

Fig. 1. (a) Schematic design of the tip of the imaging + sensing probe; (b) microscopic photo of the tip of the probe, showing the curved tellurite focusing element; (c) simulated and measured beam diameters of the imaging + sensing probe; (d) schematic of the entire system. In (c), the solid black vertical line denotes the interface between tellurite and the external medium (air or water); red and blue curves represent the simulated beam propagation in air and in water, respectively; black and gray dotted curves represent the measured beam diameters in the *x* and *y* axes, respectively, which were obtained in air; *z*: physical distance; DCF: double-clad fiber; NCF: no-core fiber. In (d), note the dashed box drawn around the imaging probe in the bottom right. This corresponds to the zoomed schematic view shown in (a). Blue line: single-mode fiber; orange line: multimode fiber; light orange line: double-clad fiber.

78 μm and the thickness as 40 μm, which are averaged values measured across four probes. The beam profile was measured in air with a CMOS camera-based beam profiler (WinCamD-XHR-1310, DataRay Inc., USA) using an OCT light source (SLD1325, Thorlabs Inc., USA). To increase the robustness of the fiber probe and avoid breakage during animal experiments, the optical assembly was protected inside a modified 25-gauge needle (outer diameter 520 μm) [4], leaving approximately 2 mm of bare fiber protruding from the distal end of the needle for sensing.

Temperature sensitivity is incorporated into the probe through dipping the end of the assembled OCT probe into a molten glass doped with erbium and ytterbium, using a method reported previously for standard single-mode fibers [15]. The populations of two thermally linked energy states of the erbium ions change depending on the environmental temperature, with the temperature then determined by monitoring the ratio of two emission bands (524 and 547 nm), which is insensitive to fluctuations of the excitation intensity [18,19]. This rare-earth thermometry technique utilizes upconversion as the pumping mechanism, using a near infrared source that minimizes autofluorescence emissions typically seen in biological samples [15].

For this project, tellurite glass was used for the fabrication of the temperature sensitive region, as it has low phonon energy and can accommodate the high rare-earth doping concentrations that allow for efficient upconversion generation [20]. Additionally, it possesses the low melting temperature (815°C) required to avoid deformation of the silica glass during the dipping process and has a high refractive index to increase the backreflection at the fiber/tellurite interface that is used to generate a common-path OCT signal [14]. This common-path configuration has the advantage of minimizing issues of dispersion or polarization mismatch, often seen in dual-arm OCT configurations, and avoiding the need to carefully match the optical pathlengths of separate sample and reference arms. In practice, this allows quick and easy interchange of the imaging + sensing probes during experiments.

The integrated system is shown in Fig. 1(c). In the sensing subsystem, a compact 980 nm laser (BF-970-0300, Thorlabs, USA) and a portable spectrometer (QE65 Pro, Ocean Optics, USA) were used for excitation of the doped fiber tips and to spectrally analyze the upconversion emission for temperature measurement, respectively. Due to the strong fluorescence signal that can be collected via the probe, the laser was attenuated by 20 dB, with a transmitted power through the probe of less than 0.5 mW. To minimize backscattered 980 nm pump incident on the spectrometer, a dichroic-coated collection filter (800 nm SP, Omega Filters, USA) was used to avoid the need for bulk optics seen in previous work [15]. In the imaging subsystem, the light source (nominal wavelength: 1300 nm) and the spectrometer of a commercially available OCT system (Telesto III, Thorlabs, USA) were utilized. The exposure time to obtain each A-scan was set as 13.1 μs during tissue experiments. These two subsystems were integrated using a customized DCF coupler module (Castor Optics, Canada), comprising a wavelength division multiplexer (WDM) and a double-clad fiber coupler (DCFC). In the DCF-based dual-function probe, the single mode core of the DCF carries the OCT signal to and from the sample, and also the fluorescence excitation light for temperature sensing. Emitted fluorescence is

1684 Vol. 43, No. 8 / 15 April 2018 / Optics Letters Letter

collected within the inner cladding of the DCF. The WDM combines the OCT light and the 980 nm laser source, while DCFC separates the detected signals in the core (for imaging) and inner cladding (for sensing), and couples them into the OCT system and sensing spectrometer, respectively.

A temperature calibration plot for the probe [Fig. 2(a)] was obtained by placing it in a water bath with a resistance temperature detector (RTD, 100 Ω Class A, Omega Engineering, USA) positioned within 1 mm of the probe [4]. Custom LabView software was used to simultaneously record the reference temperature obtained by the RTD and the emission spectra from the probe. The emission spectra were then used to calculate fluorescence ratios at two wavelength bands as described in Ref. [15], generating a calibration curve modeled with a second order polynomial ($R^2 = 0.999$). A small change in the observed fluorescence ratio was seen if the OCT source was turned on or off, and as a result all temperature measurements were performed with the OCT scans running.

To demonstrate usage of the probe for simultaneous temperature sensing and imaging within tissue, we conducted an experiment in an intact, *ex vivo* rat brain. To test across the range of biologically relevant temperatures, the brain and RTD were submerged in a warm water bath and slowly cooled to room temperature [Fig. 2(b)]. As the probe was inserted into the rat brain, motion-mode (M-mode) images of OCT A-scans versus time and temperature measurements were obtained concurrently. Figure 2(c) is an M-mode image recorded as the tip of the probe penetrates the rat brain, allowing visualization of vessel structures before entering a region of highly scattering, solid tissue. Figure 2(d) shows temperature readings, extending from initial insertion until the brain had cooled to room temperature. The time point at which Fig. 2(c) was acquired is indicated by the vertical red line on Fig. 2(d). Once the probe had been positioned at the ROI, no notable change was observed in the OCT M-mode image.

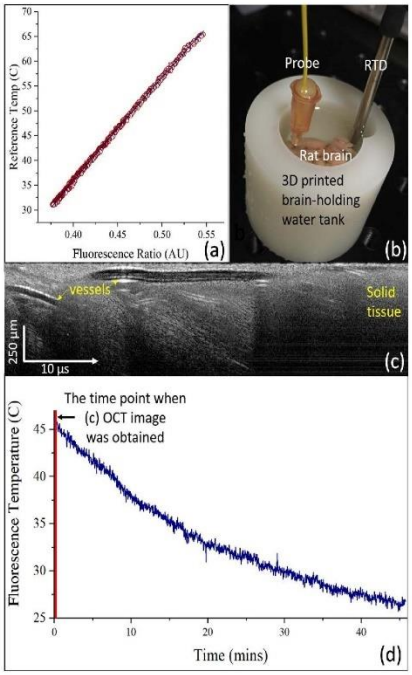

Fig. 2. (a) Fluorescence ratio versus reference temperature for increasing temperature, $R^2 = 0.999$; (b) photo showing the setup for *ex vivo* rat brain experiment; (c) M-mode structural OCT image during probe insertion; (d) rat brain temperature measurements obtained by the imaging + sensing probe. The red vertical line in (d) indicates when the OCT image (c) was obtained.

To assess the imaging + sensing probe's capability to differentiate brain tissue types and provide image guidance, we imaged a dissected rat brain, mounting the probe on a two-dimensional linear stage and scanning it over the tissue sample as shown in Fig. 1(c). This setup allowed us to obtain co-registered histology for validation of structures visualized in the OCT. Figure 3 shows a representative *en face* OCT image with matching hematoxylin and eosin (H&E) histology. The striated appearance of the dark-and-bright region indicated the location of the striatum. Anterior commissure, which comprises a bundle of nerve fibers (white matter), appeared as a large oval-shaped region of low backscatter (dark gray) in the OCT image and is clearly differentiated from the surrounding septal area.

In this paper, we have presented a forward-facing imaging probe. Such a probe has the potential to allow tissue differentiation mechanisms such as estimation of the attenuation coefficient [21–23] and differentiation of solid tissue from blood vessels through speckle decorrelation [24]. However, side-viewing configurations are also possible, enabling the acquisition of a B-scan on insertion of the probe and providing visualization of tissue microstructure. Such a configuration can be realized by terminating the no-core fiber in the focusing optics with an angle-polished and metal-coated surface, such as that presented by Lorenser *et al.* [25].

In addition to temperature sensing, the imaging + sensing probe design reported in this study has the potential to be utilized with a range of other fluorescence-based sensing techniques, particularly those that are realized by a single-fiber-based tip sensor design [5,6,13].

In conclusion, we have demonstrated the first single-fiber-based OCT imaging + sensing probe. This probe can simultaneously image tissue microarchitecture and measure local temperature. The design not only enables the precise placement of fiber sensors but also provides structural information to complement the functional measurements of the fiber sensor. Incorporating this combined probe into a needle enabled

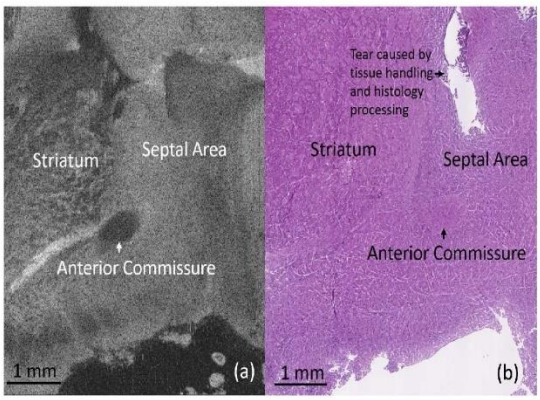

Fig. 3. (a) *En face* OCT image obtained in a rat brain. Visible structures include the striatum, anterior commissure, and septal area, consistent with (b), which show colocated H&E histology.

measurements to be acquired in deep tissue, well beyond the depth penetration of a superficial optical signal. Measurements in rat brains demonstrated the practical use of this novel probe in a biological sample.

Funding. Australian Research Council (ARC) (CE140100003, DP150104660, LP110200736); The University of Adelaide; South Australian Government Department of State Development (Premier's Research and Industry Fund grant).

Acknowledgment. We would like to thank Prof. Mark Hutchinson and Ms. Vicky Staikopoulos for their technical support in rat brain atlas, and Ms. Kathryn Batra for her assistance in histology processing. The authors would like to also acknowledge Castor Optics (Canada) for spending time and efforts in customizing the DCF coupler + WDM unit. This work was performed in part at the OptoFab node of the Australian National Fabrication Facility utilizing Australian Commonwealth and South Australian State Government funding.

REFERENCES

1. E. A. Swanson and J. G. Fujimoto, Biomed. Opt. Express **8**, 1638 (2017).
2. M. J. Gora, M. J. Suter, G. J. Tearney, and X. Li, Biomed. Opt. Express **8**, 2405 (2017).
3. G. Cui, S. B. Jun, X. Jin, G. Luo, M. D. Pham, D. M. Lovinger, S. S. Vogel, and R. M. Costa, Nat. Protoc. **9**, 1213 (2014).
4. S. Musolino, E. P. Schartner, G. Tsiminis, A. Salem, T. M. Monro, and M. R. Hutchinson, Biomed. Opt. Express **7**, 3069 (2016).
5. E. P. Schartner, M. R. Henderson, M. Purdey, D. Dhatrak, T. M. Monro, P. G. Gill, and D. F. Callen, Cancer Res. **76**, 6795 (2016).
6. M. S. Purdey, J. G. Thompson, T. M. Monro, A. D. Abell, and E. P. Schartner, Sensors **15**, 31904 (2015).
7. X.-D. Wang and O. S. Wolfbeis, Anal. Chem. **88**, 203 (2015).
8. N. Kovačević, J. T. Henderson, E. Chan, N. Lifshitz, J. Bishop, A. C. Evans, R. M. Henkelman, and X. J. Chen, Cereb. Cortex **15**, 639 (2004).
9. H. Yoo, J. W. Kim, M. Shishkov, E. Namati, T. Morse, R. Shubochkin, J. R. McCarthy, V. Ntziachristos, B. E. Bouma, F. A. Jaffer, and G. J. Tearney, Nat. Med. **17**, 1680 (2011).
10. S. Liang, A. Saidi, J. Jing, G. Liu, J. Li, J. Zhang, C. Sun, J. Narula, and Z. Chen, J. Biomed. Opt. **17**, 0705011 (2012).
11. L. Scolaro, D. Lorenser, W.-J. Madore, R. W. Kirk, A. S. Kramer, G. C. Yeoh, N. Godbout, D. D. Sampson, C. Boudoux, and R. A. McLaughlin, Biomed. Opt. Express **6**, 1767 (2015).
12. H. Pahlevaninezhad, A. M. D. Lee, G. Hohert, S. Lam, T. Shaipanich, E.-L. Beaudoin, C. MacAulay, C. Boudoux, and P. Lane, Opt. Lett. **41**, 3209 (2016).
13. W. Tan, Z.-Y. Shi, S. Smith, D. Birnbaum, and R. Kopelman, Science **258**, 778 (1992).
14. K. L. Michael and D. R. Walt, Anal. Biochem. **273**, 168 (1999)
15. E. P. Schartner and T. M. Monro, Sensors **14**, 21693 (2014).
16. R. A. McLaughlin, D. Lorenser, and D. D. Sampson, *Handbook of Coherent-Domain Optical Methods* (Springer, 2013), pp. 1065–1102.
17. N. M. Parikh, J. Am. Ceram. Soc. **41**, 18 (1958).
18. S. A. Wade, J. C. Muscat, S. F. Collins, and G. W. Baxter, Rev. Sci. Instrum. **70**, 4279 (1999).
19. V. Kumar Rai, Appl. Phys. B **88**, 297 (2007).
20. F. Vetrone, J.-C. Boyer, J. A. Capobianco, A. Speghini, and M. Bettinelli, Appl. Phys Lett. **80**, 1752 (2002).
21. R. A. McLaughlin, L. Scolaro, P. Robbins, C. Saunders, S. L. Jacques, and D. D. Sampson, J. Biomed. Opt. **15**, 046029 (2010).
22. C. Xu, J. M. Schmitt, S. G. Carlier, and R. Virmani, J. Biomed. Opt. **13**, 034003 (2008).
23. F. J. van der Meer, D. J. Faber, D. M. B. Sassoon, M. C. Aalders, G. Pasterkamp, and T. G. van Leeuwen, IEEE Trans. Med. Imag. **24**, 1369 (2005).
24. N. Uribe-Patarroyo, M. Villiger, and B. E. Bouma, Opt. Express **22**, 24411 (2014).
25. D. Lorenser, X. Yang, R. W. Kirk, B. C. Quirk, R. A. McLaughlin, and D. D. Sampson, Opt. Lett. **36**, 3894 (2011).